Thermodynamics of Quantum Devices

Thesis submitted for the degree of
"Doctor of Philosophy"

By

Amikam Levy

Submitted to the Senate of the Hebrew University of Jerusalem

November 2016 CE

This work was carried out under the supervision of:

Prof. Ronnie Kosloff

Acknowledgments

First of all, I thank Ronnie Kosloff for his unlimited support and his willingness to share his wisdom and extensive knowledge, both scientific and personal.

I am grateful to my collaborators Robert Alicki, Lajos Diosi and Raam Uzdin with whom I had the opportunity to work and to learn from. I also like to thank my colleagues Matteo Lostaglio, Luis A. Correa, David Gelbwaser, Karen Hovhannisyan, Armen Allahverdyan, Peter Salamon and Gershon Kurizki for fruitful and stimulating discussions.

I thank Ronnie's former and current group members; in particular I would like to thank Erik Torrontegui, Morag Am-Shallem, Ido Schaefer and Yair Rezek for hours of consultations and brainstorming. Spacial thanks to Tova Feldmann for inspiring and encouraging me along the years.

For the daily moral support I am thankful for my classmates Nitzan Livneh, Kobi Cohen, Yael Cytter, Liel Sapir, Barak Hirshberg, Shahar Sukenik, Daniel Palhan, Jenya Papeer, Avner Gross and Jayanth Thrissur.

Last but not least, I am grateful to my loving family and parents Lilian and Moty Levy who backed me all these years.

Abstract

This thesis aims at revealing the role of thermodynamics in the quantum regime by the study of thermodynamical aspects of quantum devices. For more than a century, thermodynamics is considered as one of the pillars of physics. The theory is concerned with energetic and entropic processes in the macroscopic regime under a set of constraints. With only few variables, systems at equilibrium can be fully characterized thermodynamically. Conversely, quantum theory is concerned with the dynamics and properties of microscopic systems at the atomic length scale. Based on few postulates the theory predicts the full dynamics of the system, also far from equilibrium. The field of quantum thermodynamics aims to reveal the intimate relationship between thermodynamics and quantum mechanics.

The study of quantum thermal machines is the platform employed to explore the field of quantum thermodynamics. These can be quantum engines, quantum refrigerators and quantum energy storage devices. All these devices describe quantum systems operating out of equilibrium. This is achieved by coupling the system to a number of reservoirs which can be passive or active. To analyze the dynamics of the quantum devices, tools from the theory of open quantum systems, quantum monitoring and quantum feedback control are employed. Linking thermodynamics and quantum mechanics is achieved by relating quantum features such as discreet energy levels, quantum correlations and quantum coherence with the efficiency, the energy currents and the entropy production of the devices. This reveals both fundamentally and technologically novel aspects of quantum mechanics and thermodynamics.

From the fundamental aspect we examine the laws of thermodynamics and their manifestations in the quantum regime and provide a coherent framework to describe both theories on a common ground. We establish a description of energy transport between two heat reservoirs through a quantum network. The description reveals a common flaw in the literature in setting models of energy transport using the master equation techniques. The description suggested is shown to be consistent with the second law of thermodynamics and reveals the global nature of quantum mechanics. We propose definitions for thermodynamic properties such as power and heat currents in complex quantum systems and provide proofs for the fulfillment of the laws of thermodynamics. These systems can be simultaneously coupled to thermal

reservoirs and driven strongly by a periodic field or even subject to monitoring and feedback control.

A dynamical formulation of the third law of thermodynamics is proposed with the purpose of quantifying the optimal cooling speed towards absolute zero temperature. This formulation is shown to be superior to other formulations of this law; suggesting a solution to a longstanding problem. In this context we also observe the universality of the cooling speed scaling with temperature for different quantum refrigerator types when attaining absolute zero temperature.

Additional aspects of this thesis are to reveal novel resources and protocols to drive thermodynamical processes in the quantum regime. These will have significant implications on future quantum technologies. We introduce the innovative concept of the quantum absorption refrigerator. This device exploits noise or a heat source to drive a cooling process. It operates in an autonomous manner that does not require an active control of the device. Specifically, we consider Gaussian and Poisson noise and relate it to weak quantum measurements. Using this model we also study the third law of thermodynamics.

In this thesis, we also apply for the first time quantum monitoring and feedback control protocols to regulate thermal devices. In particular, we show that using these techniques we can increase the charging efficiency of quantum energy storage device and stabilize the destructive fluctuations. A balance between information gained from monitoring the device and information fed back to the device is found to maximize the charging efficiency.

The role of coherence in thermodynamics is also revealed. It is shown that in the small action regime, which corresponds to a quantum regime, coherent work extraction is considerably stronger than the stochastic (classical) one. This also implies that coherence can be considered as a resource to drive thermodynamic processes. Moreover, in this regime of operation, different types of thermal machines exhibit similar thermodynamic properties. The models considered in this thesis are analytically tractable, allowing a deeper insight into the mechanism of the quantum devices and their relation to thermodynamics.

A Letter of Contribution

All of the work on this PhD thesis was done by Amikam Levy as the main contributor, under the supervision of Prof. Ronnie Kosloff. In particular, the following holds:

- The study introduced in chapter 3, *The local approach to quantum transport may violate the second law of thermodynamics*, was performed by Amikam Levy under the supervision of Prof. Ronnie Kosloff.
- The study introduced in chapter 4, *Quantum Absorption Refrigerators*, was performed by Amikam Levy under the supervision of Prof. Ronnie Kosloff.
- The study introduced in chapter 5, *Quantum refrigerators and the third law of thermodynamics*, was performed in collaboration with Robert Alicki from Gdańsk University. Nevertheless, Amikam Levy is the main contributor and author of this work, under the supervision of Prof. Ronnie Kosloff.
- The study introduced in chapter 6, *Quantum flywheel*, was performed in collaboration with Lajos Diosi from Wigner Research Center for Physics. Nevertheless, Amikam Levy is the main contributor and author of this work, under the supervision of Prof. Ronnie Kosloff.

Contents

Chapter 1

Introduction and outline

Physical realism is what motivates scientists to formulate laws which are obeyed by physical objects under certain circumstances in space and time, and that are believed to be mind-independent. These laws are deduced from empirical observations and typically require an additional step of idealization. The laws of thermodynamics exhibit clearly how simple intuition leads scientists to formulate physical laws. Thermodynamics was developed as a physical theory almost two hundred years ago with the pioneering work of Carnot on the efficiency of a hypothetical heat engine. Using concepts such as temperature, energy and entropy, macroscopic systems are characterized thermodynamically. With the establishment of statistical mechanics, a statistical interpretation of the laws of thermodynamics was introduced and a satisfactory connection between thermodynamics and the microscopic description was achieved.

Quantum mechanics was initiated in the early 20^{th} century with the work of Planck on black body radiation and the explanation of Einstein of the photoelectric effect. The postulates of quantum mechanics are also inferred from empirical observations. These are significantly less intuitive than those of thermodynamics. To the best of our knowledge, quantum mechanics gives the most accurate predictions on the behavior of physical objects in space and time. Since both theories are currently deeply rooted in physics, it calls into question what is the relationship between the two. The field of quantum thermodynamics attempts to explore this relationship.

Although thermodynamics and quantum mechanics are founded on different sets of axioms, the initiation of quantum mechanics was achieved thanks to consistency with thermodynamics. This is the first indication of the delicate relationship between the two theories. Quantum thermodynamics admits a dichotomous relationship between quantum mechanics and thermodynamics. On the one hand, thermodynamics plays the role of the bouncer that sets physical restrictions on quantum models. This typically occurs when approximations are held in the quantum description of open systems. Then, consistency with the laws of thermodynamics can

reveal flaws in the model assumptions which are not necessarily linked directly to thermodynamics [Levy 2012a, Levy 2014]. On the other hand, the framework applied to study novel thermodynamic features in the microscopic world are those of quantum mechanics.

This apparent paradoxical behavior can be settled by refining the objectives of the quantum thermodynamics study. Since our current observations are compatible with the laws of thermodynamics, it is desirable to apply these constraints to the quantum regime in order to acquire a realistic consistent quantum description of Nature. This by no means suggests that attempts of challenging these laws should not be considered. It only implies that without strong evidence of a violation of these laws, theoretical or empirical, consistency with thermodynamics is essential in setting realistic quantum models. The other aspect of quantum thermodynamics is studying thermodynamic processes of small ensembles, much smaller than the thermodynamic ensemble. In this regime, a new insight on the role of quantum features in energetic and entropic processes can be observed. This aspect has both fundamental and technological implications.

Some of the primary questions in the field are: To what extent do the paradigms and laws of thermodynamics apply in the quantum domain? Do quantum effects such as quantum correlations and coherence play a significant role in thermodynamic processes? Can we use quantum features as resources to drive thermodynamic processes? What are the requirements of theory to describe quantum mechanics and thermodynamics on a common ground? To treat these issues, one needs to construct an appropriate mathematical and physical framework. This thesis addresses the field of quantum thermodynamics by studying quantum thermal machines that operate far from thermal equilibrium and where quantum effects still exist. Extreme care has been taken to choose models which can be analyzed from first principles.

Forty years ago, the study of Gedanken quantum thermal machines emerged [Scovil 1959, Alicki 1979, Kosloff 1984]. Today, scientists are constructing these in laboratories worldwide [Baugh 2005, Pekola 2007, Fornieri 2015, Thierschmann 2015, Roßnagel 2016]. Quantum heat engines, quantum refrigerators and quantum energy storage devices are examples of such quantum thermal machines. These are the natural candidates to approach the study of quantum thermodynamics as they unite basic properties of quantum mechanics with those of nonequilibrium thermodynamics.

Using this platform, we can treat fundamental issues such as: The proper definitions of heat and work in the quantum regime; the manifestation of the laws of thermodynamics in the microscopic world; the emergence of thermodynamic friction and the manifestation of power-efficiency trade-off; and also the role of quantum effects on thermodynamic processes. From a practical standpoint, such models can

provide a frame for studying energy transport and quantum effects in biological systems, such as in photosynthesis process. It is relevant for optimizing the performance of photoelectric devices driven by solar photons. Introducing novel cooling mechanism and revealing the limitations on the cooling process, and studying the quantum nature of molecular rotors.

The methodology employed to study quantum thermal machines is the theory of open quantum systems. In the theoretical background chapter, 2, we briefly review the roles of the theory of open quantum systems that are relevant to this thesis. In addition, we introduce concepts from the theory of quantum measurement and feedback control which are essential for chapter 6. Finally, we integrate these mathematical tools in the context of the theory of quantum thermodynamics.

Chapter 3 [Levy 2014] intends to point out a common flaw in setting quantum models of energy transport that is repeated in dozens of papers, and to show how this omission should be corrected. We present a quantum thermodynamic analysis of heat transport between two thermal reservoirs through a quantum network as a case study. In the literature a local description of a quantum network coupled to multiple reservoirs is common. In this description, the coupling between a reservoir and each subsystem of the network is modeled by a local Lindblad generator (see section 2.1.3). The interaction between the network subsystems is manifested only through the unitary part of the evolution and does not affect directly the dissipation part. If the inter-coupling between the subsystems are weak this description seems reasonable. Nevertheless, we show that even in the weak inter-coupling limit this approach may lead to a violation of the second law of thermodynamics.

We further show that a global approach that accounts for the inter-coupling in the derivation of the Lindblad equation is always consistent with the second law. This is an immediate consequence of the Spohn inequality (see section 2.3.2). Lindblad dynamics is an axiomatic powerful description of open quantum systems. Nevertheless, it will not necessarily result in a physical consistent picture. Thermodynamic study uncovers the global nature of quantum mechanics and the necessity of a microscopic derivation of the master equation. It provides physical testing tools for approximations and assumptions carried out on the dynamics of quantum system (see also appendix A [Levy 2012a], for example in the context of the third law).

In chapter 4 [Levy 2012c], the concept of heat and noise assisted cooling which we termed the quantum absorption refrigerator is introduced. The aim is to extract heat from a system using a noise source or a thermal source instead of an externally controlled field in order to drive the cooling process. This type of quantum thermal machine belongs to the class of continuous and autonomous machines that benefit from the advantage that no constant manipulation and control of the quantum system is required. We further study the limitations on the cooling process, thus

we present the optimal scaling of the heat current from the reservoir being cooled with temperature as we approach the absolute zero temperature. We treat both Gaussian and Poisson white noise as the resources driving the cooling process. We then relate this to a thermal source at the high temperature limit and to monitoring (continuously measuring) some observables of the quantum system. This work implies that noise which is typically considered as a harmful process can serve as a thermodynamic resource for obtaining a more ordered (cooler) system. Additional new results can be found in the review paper [Kosloff, R. and Levy, A. 2014] and in [Correa 2014b].

Chapter 5 [Levy 2012b] introduces a study of the third law of thermodynamics and refining it from a dynamical standpoint. Previous studies regarding quantum refrigerators and the quest for absolute zero temperature [Kosloff 2000, Rezek 2008, Rezek 2009, Levy 2012c] concentrated on the Nernst's heat theorem (see section 2.3.2). This statement sets limitations on the scaling of the heat current from the reservoir being cooled with temperature as we approach the absolute zero. In this chapter we study the implications of the unattainability principle and restate the third law in its dynamical form. This formulation enables us to quantify the third law in terms of a characteristic exponent for the cooling process. The characteristic exponent describes the scaling of the rate of temperature change with temperature itself. Different studies investigating the relation between the two formulations, led to different answers regarding which, and if at all, one of these formulations imply the other [Landsberg 1956, Belgiorno 2003a, Belgiorno 2003b]. Our formulation of this law is shown to be more restrictive than the Nernst's heat theorem as it imposes limitations on the spectral density and the dispersion dynamics of the reservoir.

We then examine this exponent for different types of quantum refrigerators. Thus gaining a deeper insight on the role of each component of the device. Specifically, we consider different cooling substances, the standard harmonic oscillator reservoir, and the ideal Bose and Fermi gas. The working medium is either a two coupled two-level system or harmonic oscillators, and the work source is treated as a very hot thermal reservoir or a periodically external field. For a quantum refrigerator driven by a strong periodic field Floquet's theory is employed to derive the master equation and the proper definitions for heat and work are presented. These definitions are shown to be compatible with the second law of thermodynamics. Universal behavior of the final scaling near the absolute zero is obtained. The characteristic exponent does not depend on the dimension of the substance being cooled, nor does on the type of refrigerator, absorption or periodically driven refrigerator. Different medium, i.e. harmonic oscillators and TLS's also produce the same scaling.

Storing useful work and extracting it on demand will have a significant impact on future quantum technologies. In chapter 6 [Levy 2016], we present the novel concept

of the quantum flywheel (a quantum energy storing device) as an integral part of quantum heat machines. Generally, when a work repository is quantized it may be subject to entropy increase and reduction in charging efficiency. This "problematic feature" is absent when a classical approximation for the external field is made. In this work we confront this difficulty, going beyond the standard classical scenario. For the particular work repository realized by a quantum harmonic oscillator, quantum and thermal fluctuations dominate the dynamics leading to divergence of the thermodynamic properties of the flywheel. For the first time, tools from quantum measurement and feedback control are utilized to overcome these fluctuations and to regulate quantum heat machines. This merging between the different fields also raises new fundamental questions about the definitions of work and heat in quantum stochastic feedback systems.

Recent studies in quantum thermodynamics [Uzdin 2015, Perarnau-Llobet 2015] have shown that quantum properties enhance work extraction. Any realization of quantum heat machines as part of future technology requires regulation by measurement. However, measurement is known to collapse the state of the system and demolish these quantum features, thus making regulation impossible. Therefore, we suggest that weak quantum measurements and feedback control play an integral part of future advances in the study of quantum heat machines. We further show that a particular balance between information gained by monitoring the system and information fed back to the system maximizes the charging efficiency and minimizes the entropy production of the flywheel. Despite its complexity the model is analytically solvable, and can be decomposed to its basic components, gaining insight into the operation of the quantum flywheel. The model studied is applicable to a variety of experimental setup systems such as QED cavities, nanomechanical oscillators, trapped particles, and superconducting circuits. In the conclusion, chapter 7, we discuss this in detail.

Appendix A [Levy 2012a], presents an example of how the formulation and quantification of the third law of thermodynamics introduced in [Levy 2012b] reveals flaws in setting quantum models.

In appendix B we present joint work with Raam Uzdin [Uzdin 2015]. In this work, we introduce quantum thermodynamic signatures in the operation of quantum thermal devices. Specifically, it is shown that in the small action regime with respect to $\hbar$ different types of quantum engines (two stroke, four stroke and continuous engines) are thermodynamically equivalent. That is, after a complete cycle, power, heat and efficiency are the same for all types of engines. This behavior is traced back to the role of coherence in quantum thermal devices that becomes dominant in the small action regime. Furthermore, it is shown that for small action a quantum engine outperforms a stochastic (classic) one. The coherent work extraction is considerably

stronger than the stochastic work extraction mechanism. This enables us to derive a power bound for stochastic engines that constitutes a quantum-thermodynamics signature. This means that for a given set of thermal resources and thermodynamic measurements (for example, measurement of the power output of an engine) one can determine if the device exploits coherence in its operation. This finding implies that coherence can be used as a resource to drive thermodynamic processes. Presently, these predictions are being examined in the laboratory.

The study of thermodynamics of quantum devices is mainly concentrated in a regime where the quantum system is coupled weakly to the thermal reservoirs. This is important for having a clear thermodynamic interpretation of heat and work, see section discussion in 2.3.2. In appendix C [Uzdin 2016], we treat the strong coupling limit using the idea of heat exchangers. These are mediating particles that can interact strongly with the quantum system and then thermalize via a secondary thermal reservoir. This setup enables us to extend the equivalence of different types of thermal machines presented in appendix B to the non-Markovian regime. It is shown that this regime introduces a higher degree of equivalence that cannot be achieved in the Markovian one. We further study the charging process of a quantum battery, and obtain the condition for energy transfer without increasing the entropy of the battery. In the strong coupling limit it is also possible to super-charge the battery. Which means that the energy of the battery increases while its entropy decreases at the same time.

In appendix D we introduce the useful Liouville space representation of open quantum systems and the KMS condition. Appendix E presents additional information on stochastic differential equations that was not included in the theoretical background. In appendix F we summarize properties of entropy and relative entropy, and in appendix G the list of publications is shown. Finally, additional novel results on thermodynamics of quantum devices can be found in the review article [Kosloff, R. and Levy, A. 2014]. Form length considerations, this review article is not displayed in the thesis.

Chapter 2

Theoretical background

2.1 The theory of open quantum systems

Quantum mechanics is a probabilistic theory describing the dynamics of microscopic systems. The core of the theory is concerned with *closed* systems. The state of a closed (isolated) quantum system follows a *unitary evolution* given by the solution of the Schrödinger equation for pure states, and in the more general case, the solution of the von Neumann equation that embodies the dynamics of mixed states. The unitary evolution is represented by the linear unitary operator $\hat{U}$ which form a continuous time translation symmetry group. The knowledge of the state of a closed quantum system at some time t' allows to predict the state and the measurement outcome at any given time t.

An open quantum system $\mathcal{S}$ is a quantum system that interacts with another system $\mathcal{R}$. Typically system $\mathcal{S}$ is the system we are interested in. It is considered to be small with respect to the system $\mathcal{R}$ and has a well defined structure. System $\mathcal{R}$ is often referred to as the environment or the reservoir. Under additional thermodynamic equilibrium conditions it is referred to as a heat bath[1]. For example, $\mathcal{R}$ can represent phonons in a crystal, a gas of particles or a beam of photons. The joint system $\mathcal{S} \vee \mathcal{R}$ is closed and the knowledge about subsystem $\mathcal{S}$ can in principle be retrieved from the dynamics of $\mathcal{S} \vee \mathcal{R}$. Since the $\mathcal{S} \vee \mathcal{R}$ can be very large, it is impossible to solve the evolution equation of the joint state. Many techniques were developed to overcome this issue [Breuer 2002, Weiss 1998, Alicki 1987]. The idea behind most of these techniques is to ignore parts of the environment $\mathcal{R}$ that are assumed to have negligible effects on the evolution of the subsystem $\mathcal{S}$. Then, the effect of the environment $\mathcal{R}$ on the subsystem $\mathcal{S}$ can be characterized to some approximation by a comparably small number of parameters such as temperature, spectral density and correlation functions of the environment. The dynamics of the

[1] In most cases of practical interest these conditions are fulfilled.

open system $\mathcal{S}$ becomes non-unitary and thermodynamic irreversibility emerges. In this section we mainly concentrate on the reduced dynamics of the open systems which are described by Markovian master equations.

2.1.1 Density operator description

Quantum mechanics of isolated system corresponding to maximal knowledge about the state of the system is described by pure states. These states can be identified with normalized vectors $\{|\psi_i\rangle\}$ in Hilbert space $\mathcal{H}$. To treat the dynamics of an open system or of a subsystem belonging to a bigger isolated system, concepts from statistical mechanics are applied. Randomness and incomplete information about system $\mathcal{S}$ is reflected in the density operator description for mixed states (sometimes referred as to the density matrix).

The incomplete information interpretation has two different aspects. The first is the ensemble aspect where the system is found in a statistical mixture of pure states. The experiment is performed repeatedly on the ensemble to obtain an averaged outcome of the measurement. Because of fluctuations the ensemble is composed of pure states with different weights. This statistical nature is embodied in the density operator formalism. The second aspect results from splitting of the total Hilbert space into sub-spaces. By tracing out parts of the total system in order to obtain the reduced description of the subsystem, information that is stored in quantum correlations is lost. For example, if we start with a pure entangled bipartite state $|\psi\rangle \in \mathcal{H}_1 \otimes \mathcal{H}_2$, then by tracing out one of the subsystems, the other one becomes a mixed state.

Another standpoint for the density operator relies on the complexity of the environment and the random phase postulate. We assume that the Hamiltonian of the joint system $\mathcal{S} \vee \mathcal{R}$ is time independent and non-degenerate. This state can be written as,

$$|\Psi(t)\rangle = \sum_{i,j} c_{i,j}(t)\, |\psi_i\rangle \otimes |\phi_j\rangle \in \mathcal{H}_{S\vee R},$$

with the coefficients $c_{i,j} = \langle\psi_i\phi_j|\Psi\rangle$, and the states $|\psi_i\rangle \in \mathcal{H}_S$ and $|\phi_j\rangle \in \mathcal{H}_R$. The operator $\hat{A}$ represents an observable of the system $\mathcal{S}$, and the expectation value is given by,

$$\left\langle \hat{A} \right\rangle = \langle\Psi|\, \hat{A} \otimes \hat{I}\, |\Psi\rangle = \sum_{i,j} c_i^*(t) c_j(t)\, \langle\psi_i|\, \hat{A}\, |\psi_j\rangle\,, \quad \text{with } c_i(t) = \sum_j c_{i,j}(t)\, |\phi_j\rangle\,.$$

In actual experiments the average of many identical recurrences is taken over a time interval τ and are not instantaneously in time. This time interval is much shorter than the resolving time of the measurement apparatus, but long compared to the

fluctuations time scale of the environment, such that the random phase postulate holds. It is postulated that the phases are averaged to zero on the time interval τ (indicated by an over-line),

$$\overline{c_i^*(t)c_j(t)} = \lambda_i \delta_{ij}, \text{ such that } \sum_i \lambda_i = 1.$$

The expectation value of the operator $\hat{A}$ is then given by,

$$\left\langle \hat{A} \right\rangle = \sum_i \lambda_i \left\langle \psi_i \right| \hat{A} \left| \psi_i \right\rangle .$$

The time average can be interpreted as an average with respect to a stationary mixed state.

The density operator can now be identified as a non-negative trace class operator of trace one belonging to Banach space $\mathcal{T}(\mathcal{H})$ of operators acting on the Hilbert space $\mathcal{H}$. The states defined by the density operator form a convex set with the pure stats as the extreme points. According to the spectral theorem the density operator can be represented in a diagonal form,

$$\hat{\rho} = \sum_i \lambda_i \left| \psi_i \right\rangle \left\langle \psi_i \right| , \tag{2.1}$$

such that $\sum_i \lambda_i = 1$ and $\lambda_i \geq 0$. The density operator corresponds to a pure state if and only if it is a rank one projector. Mixing of the density operator is quantified by the purity function, defined as,

$$P = \mathrm{Tr}\left(\hat{\rho}^2\right) \leq 1. \tag{2.2}$$

Here, $\mathrm{Tr}\left(\cdot\right)$ is denoted the trace operation, and equality holds if and only if the state $\hat{\rho}$ is a pure state. Other measures for mixing (information) will be discussed in section 2.3.

Dynamics:

The dynamics of the density operator of isolated systems is described by the von-Neumann equation [von Neumann 1955]:

$$\frac{d\hat{\rho}}{dt} = -i \left[\hat{H}, \hat{\rho} \right] . \tag{2.3}$$

Here $\hat{H}$ is the Hamiltonian and the generator of the dynamics, and $[\cdot,\cdot]$ stands for the commutator. The formal solution of Eq.(2.3) is given by,

$$\hat{\rho}(t) = \mathcal{U}(t,0)\hat{\rho}(0), \quad \text{with } \mathcal{U}(t,0) \cdot \stackrel{\text{def}}{=} \hat{U}(t,0) \cdot \hat{U}^{\dagger}(t,0), \tag{2.4}$$

and

$$\hat{U}(t,0) = \mathtt{T} \exp\left[-i \int_0^t \hat{H}(s) ds\right]. \tag{2.5}$$

Here $\mathtt{T}$ stands for the time ordering operator, and without loss of generality we take the initial time to zero.

Observables:

In quantum mechanics an observable is a physically measured quantity represented by linear self-adjoint operators. The set of all linear bounded operators[2] equipped with the operator norm $\|\cdot\|_\infty$ is a Banach space $\mathcal{B}(\mathcal{H})$. The average of the observable A is given by,

$$\left\langle \hat{A} \right\rangle = \mathrm{Tr}\left(\hat{\rho}\hat{A}\right). \tag{2.6}$$

For any linear bounded map Λ on $\mathcal{T}(\mathcal{H})$ there exists a dual map Λ^* on $\mathcal{B}(\mathcal{H})$ such that[3],

$$\mathrm{Tr}\left((\Lambda\hat{\rho})\hat{A}\right) = \mathrm{Tr}\left(\hat{\rho}(\Lambda^*\hat{A})\right), \quad \forall \ \hat{\rho} \in \mathcal{T}(\mathcal{H}) \text{ and } \hat{A} \in \mathcal{B}(\mathcal{H}). \tag{2.7}$$

It is now clear that the equation of motion for the operators (the Heisenberg equation) is the adjoint of the von-Neumann equation,

$$\frac{d\hat{A}}{dt} = i\left[\hat{H}, \hat{A}\right] + \frac{\partial \hat{A}}{\partial t}, \tag{2.8}$$

where the partial derivative is added in case the operator $\hat{A}$ does explicitly depend on time. The solution of Eq.(2.8) is given $\hat{A}(t) = \mathcal{U}^{\dagger}(t,0)\hat{A}(0)$.

2.1.2 Open Quantum System: Reduced Description

As discussed in section 2.1, in most practical cases we are interested in the reduced dynamics of the subsystem $\mathcal{S}$ under the influence of reservoir $\mathcal{R}$. The Hilbert space of the joint system is given by the tensor product of the system and reservoir Hilbert spaces, $\mathcal{H}_{S\vee R} = \mathcal{H}_S \otimes \mathcal{H}_R$. The total Hamiltonian of $\mathcal{S} \vee \mathcal{R}$ can be taken to be of the form:

$$\hat{H}_{tot} = \hat{H}_S \otimes \hat{I}_R + \hat{I}_S \otimes \hat{H}_R + \hat{H}_{SR}. \tag{2.9}$$

[2]Unbounded observables are treated as limits of sequences of bounded ones, see also the discussion in [Alicki 2001].

[3]In the special case of closed dynamics $\Lambda = \mathcal{U}$ and $\Lambda^* = \mathcal{U}^{\dagger}$.

Here $\hat{H}_S$ and $\hat{H}_R$ are the self Hamiltonians of the system and the reservoir, respectively, and $\hat{H}_{SR}$ is the Hamiltonian describing the interaction between the two systems. The joint states $\hat{\rho}(t) \in \mathcal{H}_{S\vee R}$ follow the von-Neumann Eq.(2.3) with the Hamiltonian $\hat{H}_{tot}$ (see Eq.(2.9)). The reduced dynamics of $\mathcal{S}$ denoted by $\hat{\rho}_S(t)$ is given by taking the partial trace over the reservoir,

$$\hat{\rho}_S(t) = \Lambda(t,0)\hat{\rho}_S(0) \stackrel{\text{def}}{=} \mathrm{Tr}_R\left(\hat{U}(t,0)\hat{\rho}(0)\hat{U}^\dagger(t,0)\right). \tag{2.10}$$

The map $\Lambda(t)$ describes the state change of the reduced system $\mathcal{S}$ and maps the space $\mathcal{T}(\mathcal{H}_S)$ into itself,

$$\Lambda(t) : \mathcal{T}(\mathcal{H}_S) \to \mathcal{T}(\mathcal{H}_S). \tag{2.11}$$

A crucial assumption to obtain a completely positive dynamical map is that the initial state is a tensor product $\hat{\rho}(0) = \hat{\rho}_S(0) \otimes \hat{\rho}_R$, and the reservoir state $\hat{\rho}_R$ is a fixed reference state[4]. Working in the orthonormal diagonal basis of $\{\phi_j\}$ of the reservoir $\hat{\rho}_R = \sum_j \lambda_j |\phi_j\rangle \langle\phi_j|$, we can then express the propagator as,

$$\hat{U}(t,0) = \sum_{ij} \hat{V}_{ij}(t,0) \otimes |\phi_i\rangle \langle\phi_i|, \tag{2.12}$$

where $\hat{V}_{ij}$ are operators acting on the reduced system $\mathcal{S}$. Eq.(2.10) can now be expressed as,

$$\Lambda(t)\hat{\rho}_S(0) = \sum_n \hat{K}_n \hat{\rho}_S(0) \hat{K}_n^\dagger, \tag{2.13}$$

where we have defined $\hat{K}_n \stackrel{\text{def}}{=} \sqrt{\lambda_j}\hat{V}_{ij}(t,0)$, and relation $\sum_n \hat{K}_n\hat{K}_n^\dagger = \hat{I}_S$ holds.

The operators $\hat{K}_n$ are also known as the Kraus operators [Kraus 1971], and Eq.(2.13) is the most general form of a completely positive dynamical maps[5] describing irreversible time evolution of an open system. It can also be shown that for every such $\{\hat{K}_n\}$ there exist a unitary operator $\hat{U}$ acting on $\mathcal{H}_S \otimes \mathcal{H}_R$ [Alicki 2001].

Complete positivity:

A positive map Λ is a map between C*-algebras that maps a linear positive operator $\hat{A}$ into a linear positive operator $\Lambda(\hat{A}) = \tilde{A}$,

$$\Lambda : \hat{A} \to \tilde{A}. \tag{2.14}$$

It is assumed to be unity preserving if $\Lambda(\hat{I}) \to \hat{I}$. Complete positivity (CP) imposes more restrictive demands on the map Λ than positivity do. The idea is that the CP

[4]This assumption implies that the state of the reservoir does not change significantly during the evolution.

[5]Generally, the term dynamical maps refers to completely positive maps.

map preserves positivity with respect to tensor product operation[6]. If map Λ acts on $\mathcal{T}(\mathcal{H}_S)$ then CP implies that the trivial extension $\Lambda \otimes id$ maps positive operators from the extended space into positive operators,

$$\Lambda \otimes id : \hat{A} \otimes \hat{B} \rightarrow \tilde{A} \otimes \hat{B} \tag{2.15}$$

Here, id denotes the identity map of some auxiliary space and $\hat{B}$ is an operator belonging to that space. Physically, CP maps are essential for the description of open quantum systems. A dynamical map of a quantum system should allow the probabilistic interpretation of the density operator also when it is coupled to a reservoir. In composed classical systems positivity is a sufficient requirement from reduced maps. This is not true in the quantum case where existence of entangled states leads to the requirement of CP maps. A known example that makes use of positive but not of CP maps is the Peres-Horodeccki criterion for two quantum system to be separable [Peres 1996, Horodecki 1996]. The criterion relies on the fact the the partial transpose operation is a positive map but not a CP one. Then the eigenvalues of the composite density operator become negative if the states are entangled[7].

2.1.3 Quantum Dynamical Semigroups

The map defined by Eq.(2.13) represent a map for a fixed time $t \geq 0$. In order to describe the time evolution of an open system we define the one-parameter family $\{\Lambda(t), t \geq 0\}$ of dynamical maps. Generally, this family of maps satisfies a complicated integro-differential equation. However, in many physical scenarios the class of dynamical semigroups provide a good approximation of the evolution, that now becomes Markovian. Physically, the Markovian approximation is justified when the reservoir correlation functions decay faster then the intrinsic time scale of the system. Therefore, any information that transfers from the system to the environment is lost, leading to a "no-memory" effect. We elaborate on the validity of the approximation in the following section.

The term *semigroup* implies that the time evolution forms a family of maps which does not form a full group. It lacks the negative range of the parameter t, which implies that the inverse property required from a group is missing. Physically, this property is the manifestation of irreversible dynamics which allows us to distinguish the future from the past. To summarize, the quantum dynamical semigroup is a continuous one-parameter family of maps $\{\Lambda(t), t \geq 0\}$ which satisfy the properties:

[6] The tensor product of two positive maps is not necessarily positive.

[7] Generally, the criterion is only a necessary condition. The exception is for the case of a dimension lower then 6D where it is also sufficient.

1. $\Lambda(0) = I$.

2. $\Lambda(t)$ is completely positive and trace preserving.

3. $\Lambda(t)\Lambda(s) = \Lambda(t+s)$ $t, s \geq 0$ semigroup (Markovian) property.

4. $\lim_{t\to 0}\|\Lambda(t)x - x\| = 0$ $\forall x \in \mathcal{B}$ strongly continuous property.

5. $\|\Lambda(t)\| \leq 1$ contraction semigroup property.

Based on the mathematical properties (1-5) it is possible to define the generator of the semigroup $\mathcal{L}$ such that,

$$\frac{d}{dt}\hat{\rho}_S = \mathcal{L}\hat{\rho}_S \tag{2.16}$$

Lindblad and separately Gorini, Kossakowski and Sudarshan introduced the most general structure of the generator $\mathcal{L}$ of the dynamical semigroup [Lindblad 1976, Gorini 1976a]. The Markovian master equation known as the LGKS equation or as the Lindblad equation takes the form[8],

$$\frac{d}{dt}\hat{\rho}_S = \mathcal{L}\hat{\rho}_S \stackrel{\text{def}}{=} -i[\hat{H}, \hat{\rho}_S] + \sum_j \hat{V}_j\hat{\rho}_S\hat{V}_j^\dagger + \frac{1}{2}\left\{\hat{V}_j^\dagger\hat{V}_j, \hat{\rho}_S\right\}. \tag{2.17}$$

Here $\{\cdot,\cdot\}$ is the anticommutator, the $\hat{V}_j$ are bounded operators[9] acting on $\mathcal{H}_S$, and $\hat{H}$ is the effective Hamiltonian of the system $\mathcal{S}$. Typically, this Hamiltonian can be identified as the free Hamiltonian of the system plus correction terms resulting from the coupling to the reservoir. The first term on the rhs of Eq.(2.17) generates a unitary evolution, whereas the second term referred to as the dissipator, and thus responsible for the manifestation of decoherence and dissipation processes. It is worth noting that the generator $\mathcal{L}$ does not uniquely determine a microscopic physical model of the joint system $\mathcal{S} \vee \mathcal{R}$. The generator is invariant under the certain transformations for the operators $\hat{H}$ and $\hat{V}_j$ [Breuer 2002]. The necessity in a microscopic derivation of a Markovian master equation (MME) is discussed in section 2.1.4 and chapter 3.

The Heisenberg representation:

As was discussed in section 2.1.1 one can introduce the dual map Λ^*, and the adjoint master equation (the Heisenberg representation) takes the form,

$$\frac{d}{dt}\hat{A} = \mathcal{L}^\dagger\hat{\rho}_S \stackrel{\text{def}}{=} i[\hat{H}, \hat{A}] + \sum_j \hat{V}_j^\dagger\hat{A}\hat{V}_j + \frac{1}{2}\left\{\hat{V}_j^\dagger\hat{V}_j, \hat{A}\right\}, \tag{2.18}$$

[8] This form is known as the diagonal form introduced by Lindblad.
[9] Except for few cases there is no general characterization for unbounded operators.

with $\hat{A} \in \mathcal{B}(\mathcal{H}_S)$. Solving the master equation in the Heisenberg representation has advantages over solving the full density operator evolution. In many cases we will be interested only in the expectation values of some measured quantities. This fact can reduce significantly the dimensions of the problem. For example, in the standard thermalizing master equation with a non degenerate Hamiltonian the population and the coherences are decoupled, and the population of a certain level is given by solving a small set of differential equations. The full state of the system can be reconstructed by calculating all the expectation values of the Lie algebra of the system. Generally, a full reconstruction of the state will scale as the solution of Eq.(2.17). Nevertheless, in many cases we can use symmetries to reduce the dimensions of the problem. For example, if the initial state of harmonic oscillator is a Gaussian state, then it will remain Gaussian along the dynamics and only the first two moments are necessary to retrieve the full state. Given a set of operators $\{\hat{A}_k\}_{k=1}^{M}$ that forms a closed set under the operation $\mathcal{L}^\dagger$, i.e.

$$\mathcal{L}^\dagger \hat{A}_k = \sum_{j=1}^{M} l_{kj} \hat{A}_j \quad \text{with} \quad l_{kj} \in \mathbb{C}, \tag{2.19}$$

we can write a closed linear system of coupled differential equations for the expectation values $\left\langle \hat{A}_k \right\rangle$.

2.1.4 MME: Microscopic Derivations

The derivation of the MME Eq.(2.17) introduced by LGKS is axiomatic and lacks the microscopic physical motivation. Chapter 3 indicates the importance of a microscopic derivation. It is shown that applying arbitrary dissipative LGKS terms to some Hamiltonian may result in violation of the second law of thermodynamics. In the following we discuss three scenarios for which the Markov limit offers a good approximation for physical models. All these models will be of use in the next chapters. In section 2.2.2 we will review how MME of LGKS type can be deduced from stochastic master equations (SME). In this section we concentrate on the physical validity of the approximations rather than on the mathematical details, and properties of thermal reservoirs will be discussed. The rigorous derivations can be found in many text books [Alicki 1987, Breuer 2002, Weiss 1998, Louisell 1990] and also in the appendix of chapter 5.

Weak coupling limit:

We begin with the Hamiltonian description of the joint system $\mathcal{S} \vee \mathcal{R}$ (see Eq.(2.9)). The system Hamiltonian is of the form, $\hat{H}_S = \sum_k \epsilon_k |k\rangle \langle k|$. The interaction Hamil-

tonian $\hat{H}_{SR}$ is considered weak and can be expressed as[10],

$$\hat{H}_{SR} = \lambda \left(\hat{V} \otimes \hat{R} \right) \quad \text{with} \quad \hat{V} \in \mathcal{B}(\mathcal{H}_S),\ \hat{R} \in \mathcal{B}(\mathcal{H}_R). \tag{2.20}$$

Here λ is the small parameter, and the evolution is approximated up to second order in λ. The weak coupling between the system and the reservoir also implies that the state of the reservoir is only negligibly affected by its interaction with the system. The state of the system on the other hand can change significantly as a result of the interaction. Unlike the reservoir the system is considered small and consequently the interaction becomes meaningful. The state of the joint system can now be characterized by a tensor product at all times,

$$\hat{\rho}(t) \approx \hat{\rho}_S(t) \otimes \hat{\rho}_R. \tag{2.21}$$

This approximation is known as the Born approximation. In fact, this assumption can be weakened, it is sufficient to require that the reservoir correlation functions are negligibly effected from the interaction [Gardiner 2004]. Another assumption that is made is $\mathrm{Tr}_R(\hat{H}_{SR}\hat{\rho}(0)) = 0$. This implies that the interaction has no diagonal elements in the diagonal basis of $\hat{H}_R$. This assumption can always be satisfied by redefining the system Hamiltonian accordingly.

Next, the Markov approximation is performed. This approximation implies that the integro-differential equation for $\hat{\rho}_S$ is now simplified to a standard first order differential equation. The dynamics now becomes similar to classical Markov processes, the knowledge of the state $\hat{\rho}_S$ at a single point in time t_0 will determine the state for all times $t > t_0$. Physically, the Markov approximation is valid for evolution times t such that $t \gg \tau_R$. Here, τ_R is the typical time scale where the correlation functions of the reservoir decay. This assumptions also implies that the reservoir should be considered as infinitely large with a continuous spectrum. Then the Poincare recurrence time becomes infinite and any information about the system is lost. Obtaining the LGKS structure require additional assumptions on the intrinsic time scale of the system. This assumption is known as the rotating wave approximation, where terms oscillating fast on the evolution time scale are neglected. That is $t \gg |\omega - \omega'|^{-1}$, where ω are the Bohr frequencies of the system $\mathcal{S}$. We remark that the averaging procedure above over time t should always be much smaller than the decay time of

[10] The interaction can be easily generalized to $\hat{H}_{SR} = \lambda \sum_k \hat{V}_k \otimes \hat{R}_k$. Here we consider the simple case of a single coupling.

the system $\mathcal{S}$. In the Schrödinger representation the MME can be written as,

$$\frac{d}{dt}\hat{\rho}_S = -i\left[\hat{H}_S + \hat{H}', \hat{\rho}_S\right] + \sum_{\omega\in\mathbb{R}^{\pm}} \gamma(\omega)\left(\hat{V}(\omega)\hat{\rho}_S\hat{V}^{\dagger}(\omega) - \frac{1}{2}\left\{\hat{V}^{\dagger}(\omega)\hat{V}(\omega), \hat{\rho}_S\right\}\right). \tag{2.22}$$

Here the $\hat{V}(\omega)$ are the eigenoperators of the system satisfying $[\hat{H}_S, \hat{V}^{\dagger}(\omega)] = \omega\hat{V}^{\dagger}(\omega)$ and $\hat{V}(-\omega) = \hat{V}^{\dagger}(\omega)$. In this case the operator $\hat{V}$ in Eq.(2.20) is given by the sum,

$$\hat{V} = \sum_{\omega\in\mathbb{R}^{\pm}} \hat{V}(\omega). \tag{2.23}$$

The addition to the unitary part, $\hat{H}'$, is a shift to the energy levels of the system caused by the interaction with the reservoir,

$$\hat{H}' = \sum_{\omega} S(\omega)\hat{V}^{\dagger}(\omega)\hat{V}(\omega), \tag{2.24}$$

with,

$$S = \frac{1}{2i}\left[\left(\int_0^{\infty} ds e^{i\omega s}\left\langle \hat{R}^{\dagger}(s)\hat{R}(0)\right\rangle\right) - h.c.\right], \tag{2.25}$$

where *h.c.* stand for the hermitian conjugate. This Lamb type shift is proportional to λ^2 and typically can be neglected compared to the system Hamiltonian $\hat{H}_S$. The positive rate $\gamma(\omega)$ is given by the Fourier transform of the correlation function of the reservoir,

$$\gamma(\omega) = \int_{-\infty}^{\infty} ds e^{i\omega s}\left\langle \hat{R}^{\dagger}(s)\hat{R}(0)\right\rangle \tag{2.26}$$

The weak coupling limit can be used as a good approximation for describing the dynamics of atoms and molecules interacting with electromagnetic fields or for spins coupled to phonons. The first rigorous derivation of the MME in the weak coupling limit was introduced by Davies [Davies 1974], and a very nice summary of that derivation can be found in [Alicki 2006]. The weak coupling limit MME can also be obtained from the Nakajima-Zwanzig projection operators method [Nakajima 1958, Zwanzig 1960].

Low density limit:

The quantum master equation for an N-level system interacting with free Bose/Fermi gas was derived rigorously by Dümcke [Dumcke 1985]. Physically, this limit describe the dissipation and excitation of the internal degrees of freedom of a low density gas (the system $\mathcal{S}$) due to collisions between the gas particles. In this scenario the reservoir $\mathcal{R}$ is considered as the translational degrees of freedom of the gas particles.

The system Hamiltonian has a discrete spectrum,

$$\hat{H}_S = \sum_k \epsilon_k \left|k\right\rangle \left\langle k\right| , \tag{2.27}$$

and the reservoir Hamiltonian takes the form,

$$\hat{H}_R = \int d^3p E(p) \left|p\right\rangle \left\langle p\right| . \tag{2.28}$$

Here $|p\rangle$ is the momentum eigenstate and $E(p)$ is the kinetic energy of the free particle. The density matrix of the reservoir normalized to one particle in the volume V is expressed as,

$$\hat{\rho}_R = \frac{1}{V} \int d^3p G(p) \left|p\right\rangle \left\langle p\right| , \tag{2.29}$$

with $G(p)$ the momentum probability distribution of the gas particles. At low density and at thermal equilibrium $G(p)$ is simply given by the Maxwell distribution. The interaction between $\mathcal{S}$ and $\mathcal{R}$ is given by a scattering process. After collision the momentum of the particle change from p to p' and the internal levels changes from $|l\rangle$ to $|k\rangle$. Within the scattering theory [Landau 1958], the scattering amplitude can be written as,

$$\left\langle k, p'\right| S \left|l, p\right\rangle = \delta(p' - p)\delta_{kl} - 2\pi i \delta \left(\epsilon_k + E(p') - \epsilon_l - E(p)\right) T(k, p'|l, p), \tag{2.30}$$

where S and T are the familiar scattering matrix. In order to derive a MME an averaging procedure is carried out (similar to the rotating wave approximation in the weak coupling limit). The assumption of low gas density implies that the time between collisions is long compared to the collision time. Since we are interested in the long time behavior, which is the typical time between collisions, then averaging on this time scales will eliminate terms involving the collision time and a MME of the form of Eq.(2.22) can be deduced. In this scenario the eigen-operators $\hat{V}_\omega$ correspond to the transitions operators $|k\rangle \langle l| \in \mathcal{B}(\mathcal{H}_S)$, where $\omega \in \{\epsilon_k - \epsilon_l\}$. The relaxation rate can be expressed as[11],

$$\gamma(\omega) = 2\pi n \int dp \int dp' G(p) \delta \left(\epsilon_k + E(p') - \epsilon_l - E(p)\right) \left|T(k, p'|l, p)\right|^2. \tag{2.31}$$

Here, n is the density of the gas and the delta function reflects energy conservation. Below a critical temperature the density n should be replaced by the density of the exited states. This changes the scaling of $\gamma(\omega)$ with the temperature (see chapter

[11] Here we also assume that the system Hamiltonian has a non degenerate spectrum.

5).

Singular coupling limit:

In this scenario the interaction Hamiltonian takes the form Eq.(2.20), but now we are not restricted to small λ, and the interaction can become strong (singular). By rescaling the Hamiltonian $\hat{H}_R \to \epsilon^{-2}\hat{H}_R$ and $\hat{H}_{SR} \to \epsilon^{-1}\hat{H}_{SR}$ in the limit $\epsilon \to 0$, the decay of the correlations in the reservoir are accelerated and the interaction becomes singular [Gorini 1976b]. This limit implies that the reservoir correlations are approximated to a delta function, i.e. $\left\langle \hat{R}(s)\hat{R}(0) \right\rangle \propto \delta(s)$. Physically, this is reasonable only if the spectral density of the reservoir is flat in a wide enough range of frequencies that contain the Bohr frequencies of the system $\mathcal{S}$. Since the rotating wave approximation is not essential in order to obtain the LGKS form, the MME can be represented as,

$$\frac{d}{dt}\hat{\rho}_S = -i[\hat{H}_s + \hat{H}', \hat{\rho}_S] + \gamma\left(\hat{V}\hat{\rho}_S\hat{V}^\dagger + \frac{1}{2}\left\{\hat{V}^\dagger\hat{V}, \hat{\rho}_S\right\}\right), \tag{2.32}$$

with the constant rate,

$$\gamma = \int_{-\infty}^{\infty} ds \left\langle \hat{R}(s)\hat{R}(0) \right\rangle, \tag{2.33}$$

and S in Eq.(2.24) becomes

$$S = \frac{1}{2i}\left[\left(\int_0^\infty ds e^{i\omega s}\left\langle \hat{R}(s)\hat{R}(0) \right\rangle\right) - h.c.\right], \tag{2.34}$$

The structure of Eq.(2.32) can also be derived when the reservoir is considered as a classical stochastic surroundings [Luczka 1991]. In this case, the interaction Hamiltonian is modeled as $H_{SR} = \xi(t)\hat{V}$, where $\xi(t)$ is a real random variable satisfying $\langle\xi(t)\rangle = 0$ and $\langle\xi(t)\xi(t')\rangle \propto \delta(t-t')$. This is known as the white-noise idealization. One should also note that if $[\hat{H}_S, \hat{V}] = 0$, then energy dissipation is absent in the dynamics and only decoherence processes accrue. This follows immediately from the double commutator structure in the MME, and is often referred to as pure dephasing. In chapter 6 we will see that the structure of Eq.(2.32) is also related to continuous measurements and can be derived from a stochastic differential equations approach.

Thermal reservoirs:

An important class of reservoirs are the thermal reservoirs, which are usually termed heat baths or thermal baths. These types of reservoirs are of spacial interest in the study of quantum thermal devices where the heat bath becomes an integral part of the device. In the microscopic derivations above we assumed that the state of the

reservoir $\mathcal{R}$ is a stationery fixed state along the dynamics. Now, we additionally assume that the reservoir is in a Gibbs state (thermal state). The density operator of a thermal state has eigenvectors that coincide with those of the Hamiltonian and its eigenvalues are related to the energy levels. A thermal state can be expressed as,

$$\hat{\rho}_{th} = \frac{\exp(-\beta \hat{H})}{Z}, \tag{2.35}$$

where Z is the normalization factor (or the partition function from statistical mechanics), $Z = \mathrm{Tr}(\exp(-\beta \hat{H}))$, and $\beta \stackrel{\mathrm{def}}{=} 1/k_B T$ is the inverse temperature (in the remainder of the thesis we set the Boltzmann factor $k_B = 1$).

If we assume that $\mathcal{R}$ is a thermal bath with the Gibbs state, then in the weak coupling limit the Kubo-Martin-Schwinger (KMS) condition holds [Kubo 1957, Martin 1959] (see Appendix for details),

$$\left\langle \hat{R}^\dagger(t)\hat{R}(0) \right\rangle = \left\langle R(0)R^\dagger(t + i\beta) \right\rangle . \tag{2.36}$$

Applying this relation to Eq.(2.26), we obtain that the Fourier transform of the correlation function satisfy,

$$\gamma(-\omega) = e^{-\beta\omega}\gamma(\omega), \tag{2.37}$$

and the system $\mathcal{S}$ has a unique stationary state which is the thermal state $\hat{\rho}_S^\infty = \exp(-\beta \hat{H}_S)/Z$ with the bath temperature β. The dissipation part of Eq.(2.22) can be expressed as,

$$\begin{aligned} \mathcal{L}_D \hat{\rho}_S &= \sum_{\omega \in \mathbb{R}^+} \gamma(\omega) \left(\hat{V}(\omega)\hat{\rho}_S \hat{V}^\dagger(\omega) - 1/2\{\hat{V}^\dagger(\omega)\hat{V}(\omega), \hat{\rho}_S\} \right) \\ &+ e^{-\beta\omega}\gamma(\omega) \left(\hat{V}(\omega)^\dagger \hat{\rho}_S \hat{V}(\omega) - 1/2\{\hat{V}(\omega)\hat{V}^\dagger(\omega), \hat{\rho}_S\} \right) . \end{aligned} \tag{2.38}$$

If we further assume that $\hat{H}_S$ has a non degenerate spectrum then the off diagonal terms are decoupled from the diagonal ones. The detailed balance condition is satisfied and the rate γ can be deduced from Fermi's golden rule.

To prove that the thermal state is the stationary state in the low density limit we have to assume that besides a non degenerate Hamiltonian the micro-reversibility condition is satisfied [Dumcke 1985], that is $T(k, p'|l, p) = T(l, -p|k, -p')$. The structure of the generator in the singular coupling limit can also be restored by the thermelaizing generator in the high temperature limit. When $\beta\omega \to 0$ Eq.(2.38) reduces to Eq.(2.32). In the appendix of chapter 5 we present comprehensive thermodynamic relations satisfied by thermal baths.

2.1.5 Driven open quantum system

In the previous sections we assumed that the system Hamiltonian $\hat{H}_S$ is time independent. In this section we discuss few scenarios that MME in the weak coupling limit holds for driven open quantum systems. This is highly relevant for the study of quantum devices where control fields are typically applied to the system. In this case the system Hamiltonian can be expressed as,

$$\hat{H}_S(t) = \hat{H}_0 + \hat{H}_D(t), \tag{2.39}$$

where $\hat{H}_0$ is the free system Hamiltonian, and $\hat{H}_D(t)$ represents the time dependent driving Hamiltonian. The interaction with the reservoir is assumed weak and is similar to Eq.(2.20) (with the small parameter λ). The reduced dynamics of $\mathcal{S}$ is formally given by,

$$\hat{\rho}_S(t) = \Lambda(t)\hat{\rho}_S(0). \tag{2.40}$$

The cumalant expansion of $\Lambda(t)$ reads,

$$\Lambda(t) = \exp\left(\sum_n \lambda^n K_n(t)\right). \tag{2.41}$$

In the Born approximation the expansion is terminated at $n = 2$. The first cumalant vanishes, $K_1 = 0$, and we have $\Lambda(t) \simeq \exp\left(\lambda^2 K_2(t)\right)$. The Markov approximation implies that[12],

$$K_2(t) \simeq \int_0^t ds\mathcal{L}(s), \tag{2.42}$$

where $\mathcal{L}(s)$ is the time dependent generator in the LGKS form. Generally, when $\hat{H}_S(t)$ is time dependent, the Markov approximation is not justified, and non-Markovian[13] processes will dominate the dynamics. Next, we review shortly several scenarios where the Markov limit holds also for time dependent Hamiltonians.

Adiabatic driven systems:

The adiabatic theorem for closed quantum systems state that if the Hamiltonian changes slowly enough then the system remains in the instantaneous eigenstate of that Hamiltonian. We can define the adiabatic time scale,

$$\tau_A^{-1} \stackrel{\text{def}}{=} \max_{m\neq n} \left| \langle \epsilon_b(t)| \, \partial_t \, |\epsilon_a(t)\rangle \right|, \quad \text{for} \quad t \in [0, t_f], \tag{2.43}$$

[12]For short times $K_2(t) \sim t^2$, the Markov approximation implies that $K_2(t)$ is linear in time.

[13]Non-Markovianity has been studied extensively in the past decade. Nevertheless, the structure of the generator which leads to a CP dynamics is still an open problem. For a nice review on the subject see [Rivas 2014].

where $|\epsilon_a(t)\rangle$ is the instantaneous eigenstate of $\hat{H}_S$ with the eigenenergy $\epsilon_a(t)$. τ_A represents the temporal change in the instantaneous eigenstates. If this time is much longer than a certain timescale τ, then $\hat{H}_S$ is said to be adiabatic with respect to τ. For example, the adiabatic theorem holds if $\tau_A \gg \tau_{int}$, with,

$$\tau_{int}^{-1}(t) \stackrel{\text{def}}{=} \min_{m \neq n} |\epsilon_a(t) - \epsilon_b(t)|. \tag{2.44}$$

τ_{int} is the longest time scale of the intrinsic evolution (or just the inverse of the minimal instantaneous Bohr frequency). In this limit, transitions between eigenstates are suppressed at time t and the state follows the instantaneous eigenstates of $\hat{H}_S$.

The first rigorous derivation of the MME in the weak coupling limit for adiabatic time dependent Hamiltonian was introduced by Davies and Spohn [Davies 1978]. Since then, a wide variety of derivations with different limitations were suggested, for details see the recent comprehensive study [Albash 2012] and references therein. To derive a MME in this limit the reservoir must "experience" the instantaneous system. Similar to the time independent case the Markov approximation holds for long enough times for which the correlation function of the reservoir decay, i.e. $t \gg \tau_R$. In addition, we now require that the change in the instantaneous eigenbasis is small compared to the reservoir time scale, $\tau_A(t) \gg \tau_R$. In order to perform the rotating wave approximation and to obtain the LGKS form we assume that $\tau_A(t) \gg \tau_S(t)$. where we defined,

$$\tau_S^{-1}(t) = \min_{\omega(t) \neq \omega'(t)} |\omega(t) - \omega'(t)|, \tag{2.45}$$

with $\omega(t)$ the instantaneous Bohr frequencies. Thus, for the averaging procedure, the Hamiltonian must be constant over many inverse Bohr frequencies. In the Schrödinger representation the MME now takes the form,

$$\frac{d}{dt}\hat{\rho}_S = -i\left[\hat{H}_S(t) + \hat{H}'(t), \hat{\rho}_S\right] + \sum_{\omega(t)} \gamma(\omega(t)) \left(\hat{V}_\omega(t)\hat{\rho}_S\hat{V}_\omega^\dagger(t) - \frac{1}{2}\left\{\hat{V}_\omega^\dagger(t)\hat{V}_\omega(t), \hat{\rho}_S\right\}\right), \tag{2.46}$$

where now the rates γ are time dependent and the $\hat{V}_\omega(t)$ are the instantaneous eigenoperators of $\hat{H}_S(t)$. Some examples in the context of quantum thermal devices can be found in [Geva 1994, Alicki 2015, Alicki 2016].

Periodically driven systems:

In this scenario we treat two limiting cases, the strong driving limit and the weak driving limit. In the strong driving limit we make use of the Floquet theory [Hänggi 1998, Tannor 2007] to obtain the effective Bohr frequencies and to de-

compose the system-reservoir interaction Hamiltonian to its Fourier components [Alicki 2006]. The strong driving "dresses" the system $\mathcal{S}$ and the reservoir "experience" this effective system. The periodic Hamiltonian reads,

$$\hat{H}_S(t+\tau) = \hat{H}(t), \quad \tau = 2\pi/\nu, \tag{2.47}$$

with the period time τ. The Floquet unitary operator is defined as,

$$F(s) \stackrel{\text{def}}{=} U(s+\tau, s). \tag{2.48}$$

The Floquet eigenvectors $|\phi_j\rangle$ satisfy,

$$F(0)\,|\phi_j\rangle = e^{-i\epsilon_j\tau}\,|\phi_j\rangle\,, \tag{2.49}$$

and

$$U(t)\,|\phi_j\rangle = e^{-i\epsilon_j\tau}\sum_{n\in\mathbb{Z}} e^{-itn\nu}\,|\phi_j(n)\rangle\,, \tag{2.50}$$

where $\{|\phi_j(n)\rangle\}$ from a complete basis and ϵ_j are the Floquet quasi-energies. Assuming the interaction Eq.(2.20), the operator $\hat{V}$ is decomposed in the Floquet basis,

$$\hat{V}_n(\omega) = \sum_{m\in\mathbb{Z}}\sum_{\omega=\epsilon_j-\epsilon_i} \langle\phi_j(m+n)|\,\hat{V}\,|\phi_i(m)\rangle\,|\phi_j\rangle\,\langle\phi_i|\,, \tag{2.51}$$

with ω the effective Bohr frequencies. To perform the rotating wave approximation we average over time t such that $t \gg \max|\omega-\omega'+m\nu|^{-1}$ with $m\in\mathbb{Z}$. This implies that $t \gg \tau$, which means that the averaging should be done over many cycles of the driving field. If the dipole approximation is carried out, the Rabi frequency Ω becomes a relevant time scale in the problem. The difference of two Bohr frequencies is now proportional to the Rabi frequency, $\Omega \sim \omega - \omega'$ (an example can be found in chapter 5). This imposes an additional restriction. As was discussed above, the decay time scale of the system γ^{-1} should be greater than the coarse-grained time, that is $\gamma^{-1} \gg t$. Since $t \gg \Omega^{-1}$ we have $\gamma^{-1} \gg \Omega^{-1}$. Physically, this means that the Rabi frequency should be larger than the width of the spectral line γ. This is achieved in the strong driving limit. "The reservoir has enough time to experience the dressed system with the new spectrum shifted by the Rabi frequency". The MME can be expressed as,

$$\frac{d}{dt}\hat{\rho}_S = -i\left[\hat{H}_S+\hat{H}',\hat{\rho}_S\right] + \sum_{n\in\mathbb{Z}}\sum_{\omega\in\mathbb{R}^{\pm}} \gamma(\omega+n\nu)\left(\hat{V}_n(\omega)\hat{\rho}_S\hat{V}_n^{\dagger}(\omega) - \frac{1}{2}\left\{\hat{V}_n^{\dagger}(\omega)\hat{V}_n(\omega),\hat{\rho}_S\right\}\right). \tag{2.52}$$

The dissipative term[14] in Eq.(2.52) is a sum of LGKS generators that correspond to the effective Bohr frequencies ω. If the reservoir is a thermal bath then any such generator and any sum of them possess a unique stationary state. A rigorous derivation of the MME can be found in [Alicki 2006] and in chapter 5. Some explicit examples are found in [Levy 2012b, Szczygielski 2013].

The other limit we treat is the weak driving limit where we assume the dipole approximation. In this case, if the spectral line width is much bigger than the splitting of the energy levels due to driving, i.e. $\gamma \gg \Omega$, then the reservoir "experiences" the spectrum of the free Hamiltonian. We can then approximate the dynamics using Eq.(2.22) by changing only the unitary part, which now also consists of the driving Hamiltonian. A study of this approximation can be found in [Rivas 2010].

2.2 Quantum measurements and feedback control

In this section we introduce the necessary theoretical background for chapter 6. We give a very brief introduction to the field of continuous quantum measurement (monitoring) and feedback control. Progress in quantum technologies and devices hinges on the understanding and the ability to control quantum phenomena. The aim of quantum control theories is to develop protocols to prepare entangled states, coherent states, or any other state possessing novel properties for specific applications. Quantum control theory strategies can be divided into two categories, the closed-loop control and the opened-loop control. In opened-loop methods the control is determined in advance according to some control law. Finding the control law is usually accomplished by one of two ways, optimal control approach [Glaser 2015] or shortcuts to adiabaticity control approach [Torrontegui 2013]. In the closed-loop strategies, the controllers are determined according to information gained about the state of the system by measuring it [Rabitz 2000, Wiseman 2010]. The two common methods in this category are the learning control method and the quantum feedback control method. In this thesis we concentrate on the latter, where an active monitoring of the system determines in real time the feedback Hamiltonian applied to the system.

Many devices are regulated by monitoring and a feedback loop. The purpose is to control its timing, adjust its frequency, amplitude, and other physical properties to match the different parts of the device. The main idea is the following: By monitoring the system we gain some information about its state and according to this information we can adjust the controls to change the state of the system as desired. Moreover, feedback can speed up processes, tune the state of the system in

[14] The Hamiltonian $\hat{H}'$ can be expressed as in Eq.(2.24) with a Floquet decomposition in mind.

real time, reduce fluctuations in a robust way, and from a thermodynamic standpoint it allows us to optimally use our available resources.

Quantum monitoring and feedback control is quite similar to the classical theory, but with one important exception. In the classical theory the measurement usually does not affect the state of the system (e.g., one can measure the speed or the position of a car without affecting it). In the quantum world this is no longer true. Measurement requires interacting with the system which inevitably influences the state of the quantum system (E.g., if we perform a projective measurement our state will collapse to the measured eigenstate). Consequently, quantum properties such as coherence, entanglement, and superposition will be demolished. Weak quantum measurements are employed to overcome this problem. This means that we gain very little information about the system on the average, but we also only slightly disturb it. Then, by applying a feedback loop we can retrieve the quantum features. There is extensive literature on the subject, and some nice introduction and advance material can be found in [Wiseman 2010, Barchielli 2009, Clerk 2010, Zhang 2014], and references therein.

2.2.1 Stochastic differential equations

We next introduce some basic concepts from the field of stochastic differential equations that will be relevant to the quantum treatment of monitoring and feedback control. More details can be found in the appendix and for a comprehensive study we recommend the book by Gardiner [Gardiner 1985].

Chapman-Kolmogorov equations:

The Chapman-Kolmogorov equation (CKE) is an equation for the conditional probability of a Markovian stochastic process $X(t)$. The joint probability $p(x, y)$ for two random variables x and y can be expressed in terms of the conditional probability, $p(x|y)$ and $p(y|x)$, and the probability distributions $p(y)$ and $p(x)$,

$$p(x, y) = p(x|y)p(y) = p(y|x)p(x). \tag{2.53}$$

Assuming a Markov process $X(t)$, the CKE can be expressed as,

$$p(x_1, t_1|x_3, t_3) = \int dx_2\, p(x_1, t_1|x_2, t_2)p(x_2, t_2|x_2, t_2) \quad \text{for} \quad t_1 \geq t_2 \geq t_3. \tag{2.54}$$

Here, $p(x_1, t_1|x_3, t_3)$ is the conditional probability that event x_1 will occur at time t_1 given the event x_3 have occurred at time t_3. The differential Chapman-Kolmogorov equation (DCKE) reveals the physical aspects of the process described. The equation

reads,

$$\begin{aligned}\partial_t p(z,t|y,t') &= \int dx\,[\Gamma(z|x,t)p(x,t|y,t') - \Gamma(x|z,t)p(z,t|y,t')] \\ &- \sum_i \frac{\partial}{\partial z_i}\,[A_i(z,t)p(z,t|y,t')] + \sum_{i,j}\frac{\partial^2}{2\partial z_i \partial z_j}\,[B_{ij}(z,t|y,t')p(z,t|y,t')]\,.\end{aligned} \tag{2.55}$$

The equation describes three processes known as jumps, drift and diffusion. For the case $A_i = B_{i,j} = 0$ we obtain a Master equation which describes the jump process. $\Gamma(z|x,t)$ is the rate of change in the conditional probability due to jump from a state x to z. This equation reminds us of the MME Eq.(2.17) in the quantum treatment. Nevertheless, in the quantum treatment we have also information about the coherence which is absent in the classical case[15]. Assuming $\Gamma(z|x,t) = 0$ the DCKE reduces to the Fokker-Planck equation (FPE). The vector $A(z,t)$ is recognized as the drift vector and the matrix $B(z,t)$ as the diffusion matrix[16]. For the case where $A(z,t)$ and $B(z,t)$ are time independent (or weakly dependent) the solution $p(z,t+\Delta t|y,t)$ is given by the Gaussian distribution with a variance matrix $B(z,t)$ and mean $y + A(z,t)\Delta t$.

Wiener Processes (Brownian motion):

Setting the drift vector to zero and the diffusion coefficient to one in the FPE and considering the initial condition $p(w,t_0|w_0,t_0) = \delta(w-w_0)$, the process $X(t)$ becomes the well known Wiener process $W(t)$. The solution of the equation,

$$\partial_t\, p(w,t|w_0,t_0) = \frac{\partial^2}{2\partial w^2} p(w,t|w_0,t_0), \tag{2.56}$$

is given by

$$p(w,t|w_0,t_0) = \frac{1}{\sqrt{2\pi(t-t_0)}} \exp\left(-\frac{(w-w_0)^2}{2(t-t_0)}\right). \tag{2.57}$$

The mean value and the variance of the Wiener process are $\langle W(t)\rangle = w_0$ and $\langle (W(t)-w_0)^2\rangle = t - t_0$. Although the mean value of $W(t)$ is constant the mean square diverges as $t \to \infty$, thus the sample path may differ extremely from one to another. While the Wiener process is continuous it is not differentiable, which means that the speed is almost certainly infinite. We can define a Wiener increment,

$$dW(t) \stackrel{\text{def}}{=} W(t+dt) - W(t) \quad \text{for} \quad dt \geq 0, \tag{2.58}$$

[15] As discussed above, in the weak coupling limit when the spectrum of $\hat{H}_S$ is discrete the coherence and the population are decoupled and a similar equation is obtained for the population.

[16] It is a positive semidefinit symmetric matrix.

which satisfies the relations,

$$\langle dW(t)\rangle = 0, \tag{2.59}$$

$$\left\langle dW(t)^2\right\rangle = dt. \tag{2.60}$$

This will be of further use.

Itô stochastic differential calculus:

The simplest stochastic differential equation (SDE) also known as the Langevin equation takes the form

$$\frac{dx}{dt} = a(x,t) + b(x,t)\xi(t) \tag{2.61}$$

where $a(x,t)$ and $b(x,t)$ are known functions and $\xi(t)$ is a rapidly fluctuating random term, that is $\langle \xi(t)\xi(t')\rangle = \delta(t-t')$, and we also require that $\langle \xi(t)\rangle = 0$ (this can always be absorbed into $a(x,t)$). Note that idealization of delta correlated noise results in an infinite variance. Examples of a more realistic noise process are the Ornstien-Uhlenbeck process and the random telegraph signal for which the correlation time is finite, $\frac{\gamma}{2}\exp(-\gamma\,|t-t'|)$. In the limit $\gamma \to \infty$ this function becomes a delta function, which is one possible approach to model $\xi(t)$.

Another approach is to consider the integral form of the Langevin equation and to identify the integral of $\xi(t)$ as the Wiener process,

$$W(t) = \int_0^t ds\xi(s). \tag{2.62}$$

Notice the paradox that the integral of $\xi(t)$ is $W(t)$, but we stated before that $W(t)$ is not differentiable, which means that the Langevin equation (2.61) does not exist. Nevertheless, the integral equation,

$$x(t) - x(0) = \int_0^t a(x(s),s)ds + \int_0^t b(x(s),s)\xi(s)ds, \tag{2.63}$$

is consistent, and we can interpret $\xi(t)dt = dW(t)$ as the Wiener increment. The stochastic Itô integral is mathematically and technically more convenient to use and prove theorems but not always gives the best physical interpretation. The Stratonovich integral (see appendix) is the preferable candidate for physical interpretation since it assumes that $\xi(t)$ is real noise with a finite correlation time. After calculating measurable quantities this time can be assumed to be infinitesimally small. In Addition, the Stratonovich integral allows us to use ordinary calculus. In chapter 6 we will see that this becomes significant when we wish to define thermodynamic work.

The Itô SDE obeying Eq.(2.63) is expressed as,

$$dx(t) = a\left(x(t), t\right) dt + b\left(x(t), t\right) dW(t). \tag{2.64}$$

The SDE for arbitrary function $f\left(x(t)\right)$ is given by expanding df up to second order in dW which results in the Itô formula,

$$df\left(x(t)\right) = \left(f'\left(x(t)\right) a\left(x(t), t\right) + \frac{1}{2} f''\left(x(t)\right) b\left(x(t), t\right)^2 \right) dt + f'\left(x(t)\right) b\left(x(t), t\right) dW(t). \tag{2.65}$$

More details about the Itô and Stratonovich calculus are detailed in the appendix.

2.2.2 Quantum measurements

Quantum measurement lies at the heart of quantum mechanics theory. It provides the last link in the chain connecting the "quantum world" with the "classical" one. In this section we present a short introduction to the theory of quantum measurement.

Classical measurements:

We start with some basic concepts in the classical measurement theory, also known as Bayesian statistical inference. The classical measurement theory is based on the Bayes theorem. Using Eq.(2.53) and knowledge of the current prior system state $p(x)$, we can express the posterior state conditioned on the outcome value y,

$$p'(x|y) = \frac{p(y|x)p(x)}{p(y)}. \tag{2.66}$$

Here, the prime emphasizes that this is the posterior state and $p(y) = \sum_x p(y|x)p(x)$ in the denominator guarantees that the state is normalized. We can also define the unconditional posterior state by averaging over all possible measurement results,

$$p'(x) = \sum_y p'(x|y)p(y). \tag{2.67}$$

The terms conditional and unconditional are sometimes replaced by the terms selective and non-selective, respectively[17].

Bayes law can be generalized to treat the scenario that the state is changing due to measurement (back action on the system). Say, the system state is $p(x)$ and for simplicity we take X to be a discrete random variable and Y the result of the measurement. Then the state changing operation is described by $n \times n$ matrix B_y whose elements $B_y(x|x')$ are the probability that the measurement will enforce the

[17] In the case of non-disturbing measurement the unconditional posterior state is the same as the prior state, $p'(x) = p(x)$.

system to make a transition from a state $X = x'$ to a state $X = x$, given that $Y = y$ was obtained. Thus for all x' and all y

$$B_y(x|x') \geq 0, \quad \sum_x B_y(x|x') = 1. \tag{2.68}$$

Then the posterior system state is given by,

$$p'(x|y) = \frac{\sum_{x'} \mathcal{O}_y(x|x')p(x')}{p(y)}, \tag{2.69}$$

where we have defined the new matrix,

$$\mathcal{O}_y(x|x') \stackrel{\text{def}}{=} B_y(x|x')p(y|x'), \tag{2.70}$$

and used the relation, $P(y) = \sum_{x,x'} \mathcal{O}_y(x|x')p(x')$ to normalize the state. We also note that this map is a positive map.

Quantum projective measurements:

Traditional descriptions of measurements in quantum mechanics are often referred to as projective measurements, and were formulated by von Neumann [von Neumann 1955]. It is postulated that the measurement process instantaneously collapses the state of the quantum system into one of the eigenstates of the measured observable. That is, if we have an observable $\hat{A}$, then according to the spectral theorem it can be diagonalized,

$$\hat{A} = \sum_\lambda \lambda \hat{\Pi}_\lambda, \tag{2.71}$$

where $\{\lambda\}$ are real eigenvalues of $\hat{A}$ and $\hat{\Pi}_\lambda$ is the projection operator into the subspace of eigenstates of $\hat{A}$ with an eigenvalue λ. If the spectrum $\{\lambda\}$ is non-degenerate[18] then the projector is rank-1 projector $\Pi_\lambda = |\lambda\rangle \langle\lambda|$. The probability to obtain a particular value λ in the measurement is $p_\lambda = \mathrm{Tr}\left(\hat{\rho}\hat{\Pi}_\lambda\right)$. Then the conditional (posterior) state of the system after measuring the value λ is,

$$\tilde{\rho}_\lambda = \frac{\hat{\Pi}_\lambda \hat{\rho} \hat{\Pi}_\lambda}{p_\lambda}, \tag{2.72}$$

where the tilde on top of ρ_λ indicates a state resulting from measurement[19]. If we wish to describe the unconditional state of the system, that is if we make the

[18] In the general case, we have rank-N_λ projector $\hat{\Pi}_\lambda = \sum_{j=1}^{N_\lambda} |\lambda, j\rangle \langle\lambda, j|$.

[19] To avoid cumbersome notations we omitted the hat on top of ρ.

measurement but ignore the result, then the state is given by,

$$\tilde{\rho} = \sum_{\lambda} p_{\lambda} \tilde{\rho}_{\lambda} = \sum_{\lambda} \hat{\Pi}_{\lambda} \hat{\rho} \hat{\Pi}_{\lambda}. \tag{2.73}$$

If the state of the system before measurement was pure, and we make a measurement but ignore the result then in general after measurement the state will be mixed. That is, a projective measurement unlike unitary operation is usually an entropy increasing operation, unless one keeps track of the measurement results. We can further say that a projective measurement decreases the purity of the unconditional state unless the prior state $\hat{\rho}$ can be diagonalized in the same basis as can $\hat{A}$.

Indirect quantum measurements:

Although the projective measurements is the simplest description of quantum measurement it is not the most adequate. Typically, in real experiments the measurement is not performed directly on the quantum system of interest $\mathcal{S}$ but rather on a probe system $\mathcal{P}$ that interacts with $\mathcal{S}$. By measuring the change in the system $\mathcal{P}$ and because the systems $\mathcal{S}$ and $\mathcal{P}$ are correlated due to the interaction, it is possible to gain knowledge on the system of interest $\mathcal{S}$. We assume that the initial state of the joint systems is a product state, $\hat{\sigma}(0) = \hat{\rho}_P \otimes \hat{\rho}_S$, where $\hat{\rho}_S \in \mathcal{T}(\mathcal{H}_S)$ and $\hat{\rho}_P \in \mathcal{T}(\mathcal{H}_P)$. In addition, we take the initial state $\hat{\rho}_P = |\chi\rangle \langle\chi|$ to be a pure state[20]. The state of $\mathcal{S} \vee \mathcal{P}$ follows a unitary dynamics $\hat{U}$ for a duration time τ, and then a projective measurement[21] is performed on the probe system $\mathcal{P}$. The unnormalized final joint state after measurement is then given by,

$$\tilde{\sigma}(t) = \left(\hat{\Pi}_r \otimes \hat{I}\right) \hat{U}(\tau) \left(\hat{\rho}_P \otimes \hat{\rho}_S\right) \hat{U}^{\dagger}(\tau) \left(\hat{\Pi}_r \otimes \hat{I}\right). \tag{2.74}$$

$\hat{\Pi}_r$ is the projection operator that operates on Hilbert space $\mathcal{H}_P$. Tracing out the probe system $\mathcal{P}$ and normalizing it, we obtain the state of $\mathcal{S}$ conditioned on the measurement output r for the probe,

$$\tilde{\rho}_S^r(\tau) = \frac{\hat{M}_r \hat{\rho}_S \hat{M}_r^{\dagger}}{\mathrm{Tr}\left(\hat{M}_r^{\dagger} \hat{M}_r \hat{\rho}_S\right)}, \tag{2.75}$$

where $\hat{M}_r$ are measurement operators acting on $\mathcal{H}_S$ and are given by,

$$\hat{M}_r = \langle r| \hat{U}(\tau) |\chi\rangle. \tag{2.76}$$

[20]This procedure can be extended to mixed states and is known as insufficient measurement.
[21]The measurement is assumed to be much shorter than the evolution time τ.

These operators satisfy the relation, $\sum_r \hat{M}_r^\dagger \hat{M}_r = \hat{I}$ and are of the form of a Kraus operator (see section 2.1.2), which implies that Eq.(2.75) defines a completely positive map. The probability of measuring the value r is given by,

$$p_r = \mathrm{Tr}\Big(\hat{M}_r^\dagger \hat{M}_r \hat{\rho}_S\Big), \tag{2.77}$$

and the operator $\hat{E}_r = \hat{M}_r^\dagger \hat{M}_r$ is then identified as the probability operator (or effect), and the unconditioned state can be expressed as $\sum_r \hat{M}_r \hat{\rho}_S \hat{M}_r^\dagger$.

The structure of Eq.(2.75) defines a general measurement on a quantum system which is referred to as the posetive-operator-value-measure (POVM). The idea is that instead of having a probability distribution over all the space we have probability positive operators that are associated with the subsets belonging to the set of outcomes of the measurement. If we label the outcomes by r and chose a subset $\mathcal{M}$ of the outcomes then the probability of obtaining an outcome from this subset is,

$$\mathrm{Prob}\,(r \in \mathcal{M}) = \sum_{r\in\mathcal{M}} p_r = \sum_{r\in\mathcal{M}} \mathrm{Tr}\Big(\hat{M}_r^\dagger \hat{M}_r \hat{\rho}_S\Big) = \mathrm{Tr}\left(\sum_{r\in\mathcal{M}} \left(\hat{M}_r^\dagger \hat{M}_r\right) \hat{\rho}_S\right). \tag{2.78}$$

Apart from providing a more adequate and general description of quantum measurement, indirect measurements can describe simultaneously the measurement of two non-commutative observables as long as accuracy does not violate the Heisenberg uncertainty principle.

Continuous quantum measurement:

Continuous quantum measurement (Monitoring) is yet another important class of quantum measurements. There are few approaches to describe the continuum limit of measurements [Wiseman 2010]. These are known as quantum filtering where a stochastic differential equation for the operators (Heisenberg picture) is derived, or quantum trajectories where a stochastic Schrödinger equation or a stochastic master equation (SME) in the Schrödinger picture is used to describe the dynamics. Here, we will focus on the latter.

The description begins with a quantum system $\mathcal{S}$ that is weakly coupled to the environment. By measuring the state of the environment we can obtain some knowledge about the quantum system $\mathcal{S}$ as discussed above. Since in many "real" scenarios the measurement can be weak it is required to monitor the reservoir for some time in order for the effect to accumulate. The time scale of monitoring should be large compared to the reservoir correlation functions decay time but short compared to the decay time of the system $\mathcal{S}$. Now, if the reservoir is being monitored and the results are being ignored, then the conditioned state of $\mathcal{S}$ evolves according

to the standard MME in LGKS form. If the results of monitoring are registered then, because of the system-reservoir interaction, the state of the system is now conditioned on the outcome of the measurement. This approach is referred to as quantum trajectories. In this scenario we expect an additional noise term to the MME that will vanish once it is averaged over many realizations. Such stochastic equations are called unraveling since they unravel the MME. Obviously there are infinite unraveling SME which will produce the same averaged dynamics (the same MME). The typical procedure to derive the SME is to identify the measurement operators $\{M_r\}$ of the POVM as infinitesimal jump operators which have deterministic and stochastic parts. Then expending Eq.(2.75) up to order dt will result in a SME. Examples of this procedure for photodetection, homodyne and heterodyne detection can be found in [Wiseman 2010].

In chapter 6 we extended the result of [Diósi 1988] for monitoring both quadratures of the harmonic oscillator. We briefly present the main steps of [Diósi 1988] in deriving the SME. In order to monitor the position $\hat{x}$ of a free particle we assume that the instantaneous measured position is selected at random from a Gaussian probability distribution,

$$p_{\bar{x}} = \mathrm{Tr}\Big(\hat{\rho}\sqrt{\alpha/\pi}\exp\left[-\alpha\left(\hat{x}-\bar{x}\right)^2\right]\Big), \tag{2.79}$$

with the random variable $\bar{x}$ and variance α which represents the accuracy parameter. The conditioned state after the measurement is then given by,

$$\tilde{\rho}_{\bar{x}} = \frac{M_{\bar{x}}\hat{\rho}M_{\bar{x}}^{\dagger}}{p_{\bar{x}}}, \tag{2.80}$$

with,

$$M_{\bar{x}} = \sqrt[4]{\alpha/\pi}\exp\left[-\frac{1}{2}\alpha\left(\hat{x}-\bar{x}\right)^2\right]. \tag{2.81}$$

To attain the continuum limit the process is repeated at small time intervals Δt and satisfying the limit,

$$\alpha,\ \Delta t\ \to 0 \quad \text{and} \quad \frac{\alpha}{\Delta t} = \gamma = \text{const.} \tag{2.82}$$

This means that we gain very little knowledge from measurement in the small interval Δt but the ratio is fixed. The random variable $\bar{x}$ is defined only for instants of measurement processes. This implies that in the continuum limit this variable should be replaced by $\bar{x} \to \bar{x}(t)$, where $\bar{x}(t)$ is continuous but its differential should not exist. The differential of $\bar{x}(t)$ should be understood as an Itô differential that

satisfies,

$$\bar{x}dt = \langle \hat{x} \rangle_\sigma + \frac{dW}{\sqrt{\gamma}}, \tag{2.83}$$

with dW the Wiener increment that obeys the relations (2.58) and the average $\langle \cdot \rangle_\sigma$ is taken with respect to the conditioned stochastic state $\hat{\sigma}$. Applying the Itô calculus and keeping the terms of the order dt the SME in Itô form for the conditioned state reads,

$$d\hat{\sigma} = -i\left[\hat{H}, \hat{\sigma}\right] dt - \frac{\gamma}{4}\left[\hat{x}, [\hat{x}, \hat{\sigma}]\right] dt + \sqrt{\gamma}\{\hat{x} - \langle \hat{x} \rangle_\sigma, \hat{\sigma}\} dW \tag{2.84}$$

Taking the stochastic mean $\mathbf{M}$, the unconditional state is obtained from the conditional stochastic one, i.e. $\mathbf{M}\hat{\sigma} = \hat{\rho}$, and the SME (2.84) reduces to the familiar MME,

$$\frac{d}{dt}\hat{\rho} = -i\left[\hat{H}, \hat{\sigma}\right] - \frac{\gamma}{4}\left[\hat{x}, [\hat{x}, \hat{\sigma}]\right] \tag{2.85}$$

In chapter 6 we consider monitoring both quadratures $\hat{x}$ and $\hat{p}$ in the context of stabilizing and optimizing the performance of the quantum flywheel.

2.2.3 Feedback control

Feedback control is a process that uses information gained from measuring the state of the system in order to control it at later times. When applied to monitored quantum systems, feedback control can be performed in real-time before the quantum state collapses to a classical state. In this manner, quantum effects can be protected, noise can be reduced and controlling the state of the system becomes robust. In chapter 6 we will see that the feedback control plays an important role in optimizing the thermodynamic performance of the quantum flywheel. Feedback control based on monitoring requires to detect a continuous signal and applying a feedback Hamiltonian which depends on that signal. Generally, there is a delay between the signal being measured and the time it is fed back to the system according to the engineered Hamiltonian. Solving such a problem is typically complicated, resulting in nonlinear and non-Markovian dynamics. Simplification can be achieved if we assume that the delay time goes to zero [Wiseman 2010]. Then, the feedback Hamiltonian is proportional to the signal at that time and by averaging over all the trajectories a MME can be derived.

The heuristic description is the following: after deriving the SME for the monitoring process we can now apply the infentisimal change in the evolution due to the feedback Hamiltonian,

$$\hat{\sigma} + d\hat{\sigma} \to e^{-i\hat{H}_f(t)dt}\left(\hat{\sigma} + d\hat{\sigma}\right) e^{i\hat{H}_f(t)dt}. \tag{2.86}$$

Here, $\hat{\sigma}$ is the stochastic state conditioned on the signal output, and $\hat{H}_f$ is the feed-

back Hamiltonian which now possess a stochastic part since it is proportional to the stochastic signal output. Using the Itô calculus and expanding the terms up to order dt we obtain the SME which now accounts also for the feedback control operation. Taking the stochastic mean we end up with MME describing the dynamics of monitoring and feedback.

2.3 Thermodynamics in the quantum regime

The field of thermodynamics in the quantum regime is concerned with the delicate relation between standard and non-equilibrium thermodynamics with quantum mechanics treating small systems well below the thermodynamic limit. Among the main topics investigated are: thermalization of closed and open quantum systems, thermodynamic resource theories, information and thermodynamics, single shot thermodynamics, quantum fluctuation relations, and quantum thermal machines. For more information on these topics see recent reviews [Campisi 2011, Kosloff 2013, Kosloff, R. and Levy, A. 2014, Vinjanampathy 2015, Goold 2016] and references therein. In the present thesis we are concerned with the study of quantum thermal devices and the methodology employed is the theory of open quantum systems as discussed above.

2.3.1 Basic concepts and definitions

Entropy and relative entropy:

The notion of entropy was introduced by Clausius in the mid-19th Century. It was defined as an extensive thermodynamic variable which is useful to characterize quasi-thermodynamic processes. The change in entropy for a reversible process is given by,

$$dS = \frac{\delta Q}{T}, \tag{2.87}$$

where δQ is heat obtained or given by the system and T is the temperature in which the process occurs. This definition is referred to as the thermodynamic entropy. several decades later, statistical mechanics supplied the relation between thermodynamic entropy and the microscopic properties of the system. According to the Gibbs formula the entropy of the system is expressed as,

$$S = -\sum_j p_j \ln p_j, \tag{2.88}$$

with p_j being the probability of occupying a microstate that corresponds to the energy E_i. In the microcanonical ensemble the infinitesimal change in the Gibbs

entropy reduces to Eq.(2.87).

In quantum mechanics the entropy of a system which is described by a density operator $\hat{\rho}$, is defined by the von Neumann entropy,

$$S(\hat{\rho}) \stackrel{\text{def}}{=} -\text{Tr}(\hat{\rho} \ln \hat{\rho}) \tag{2.89}$$

In the diagonal basis of $\hat{\rho} = \sum_j p_j |\phi_j\rangle \langle\phi_j|$ the von Neumann entropy takes the form of the Gibbs entropy[22].

$$S(p_j) = -\sum_j p_j \ln p_j, \quad \text{where} \quad p_j \geq 0 \quad \text{and} \quad \sum_j p_j = 1. \tag{2.90}$$

The von Neumann entropy is a measure of the uncertainty in the details of the system and is invariant under a change of basis. The entropy is non-negative and equal to zero if and only if the state is a pure state (then we have maximal knowledge of the system). The entropy is maximized if the state is fully mixed (in equilibrium), which implies that all $\{p_i\}$ are equal. For the Gibbs state Eq.(2.35) the entropy satisfies the known relation,

$$S = \beta (U - F), \tag{2.91}$$

where β is the inverse temperature, and we have identified the internal energy $U = \text{Tr}(\hat{\rho}\hat{H})$ and the free energy $F = \beta^{-1} \ln Z$. The von Neumann entropy is a concave function which defines many mathematical properties and relations. These can be found in the appendix.

The relative entropy of two density operators $\hat{\rho}$ and $\hat{\sigma}$ is defined as,

$$S(\hat{\rho}|\hat{\sigma}) \stackrel{\text{def}}{=} \text{Tr}(\hat{\rho} \ln \hat{\rho}) - \text{Tr}(\hat{\rho} \ln \hat{\sigma}) \tag{2.92}$$

This quantity measures the distance between two states. For example, if we consider a composite system described by the state $\hat{\rho}$, then the relative entropy with respect to the uncorrelated state $\hat{\sigma} = \hat{\rho}_1 \otimes \hat{\rho}_2$ measure information loss (change in entropy) that results from tracing over the subsystems,

$$S(\hat{\rho}|\hat{\rho}_1 \otimes \hat{\rho}_2) = S(\hat{\rho}_1) + S(\hat{\rho}_2) - S(\hat{\rho}). \tag{2.93}$$

Here $\hat{\rho}_{1(2)} = \text{Tr}_{2(1)}\hat{\rho}$. The relative entropy is non-negative and equals zero if and only if $\hat{\rho} = \hat{\sigma}$. It is also invariant under a unitary transformation, i.e. $S(\hat{U}\hat{\rho}\hat{U}^\dagger|\hat{U}\hat{\sigma}\hat{U}^\dagger) = S(\hat{\rho}|\hat{\sigma})$. If $\hat{\sigma}$ is a Gibbs state, Eq.(2.35), then the relative entropy measures the

[22] This is also the form of the Shannon entropy from information theory, only p_j is now understood as the probability of an event j. In quantum mechanics it is sometimes more convenient to interpret the von Neumann entropy in this context.

distance between the free energy,

$$S(\hat{\rho}|\hat{\sigma}) = \beta\left(F(\hat{\rho}) - F(\hat{\sigma})\right). \tag{2.94}$$

Many of the relative entropy properties are based on the fact that it is jointly convex In the appendix we present some of these important relations in detail.

Ergotropy and passive states:

An important concept in quantum thermodynamics is the amount of maximal work that can be extracted from a system using a unitary cyclic operation only. This implies that the von Neumann entropy does not change during the process and the spectrum of the system is the same at the initial and final times. In the literature this amount of work is termed ergotropy [Allahverdyan 2004]. The unitary operation can be expressed as,

$$\hat{U}(\tau,0) = \mathtt{T}\exp\left[-i\int_0^\tau \hat{H} + \hat{V}(s)ds\right], \quad \text{with} \quad \hat{V}(\tau) = \hat{V}(0) = 0. \tag{2.95}$$

Here, we assume that the cyclic process initiated at time 0 and terminated at time τ, and $\hat{V}(s)$ is a time dependent control Hamiltonian. The maximal available work is then defined as,

$$W_{max} \stackrel{\text{def}}{=} \mathrm{Tr}\left(\hat{\rho}\hat{H}\right) - \min_{\hat{U}} \mathrm{Tr}\left(\hat{U}(\tau,0)\hat{\rho}\hat{U}^\dagger(\tau,0)\hat{H}\right), \tag{2.96}$$

where $\hat{H}$ is the system Hamiltonian at the beginning and at the end of the process and $\hat{\rho}$ is the initial state of the system. The minimum is taken over all the unitary transformations acting on the Hilbert space of the system. This definition is related to the notion of passive states.

A passive state $\hat{\rho}_{pass}$ is a state that no work can be extracted from it by a unitary operation, implying that for all unitaries $\hat{U}$ the inequality $\mathrm{Tr}\left(\hat{\rho}_{pass}\hat{H}\right) \leq \mathrm{Tr}\left(\hat{U}\hat{\rho}_{pass}\hat{U}^\dagger\hat{H}\right)$ holds. It was shown by Pusz and Woronowicz [Pusz 1978] that for the Hamiltonian,

$$\hat{H} = \sum_k \epsilon_k |k\rangle\langle k| \quad \text{with} \quad \epsilon_k + 1 \geq \epsilon_k, \tag{2.97}$$

the state $\hat{\rho}_{pass}$ is passive if and only if,

$$\hat{\rho}_{pass} = \sum_k \lambda_k |k\rangle\langle k| \quad \text{with} \quad \lambda_{k+1} \leq \lambda_k. \tag{2.98}$$

We conclude that a system is passive if and only if its state is diagonal in the energy eigenbasis, and its eigenvalues are non-increasing with energy. Then, in order to

extract maximal work from a state we have to find the unitary operation that will transform the state into a passive one.

We note that any Gibbs state is a passive state but conversely this is not necessarily true. A unitary operation that transforms an arbitrary state into a Gibbs state does not necessarily exist. In case the passive state of the system is a Gibbs state then the maximal work available reduces to the maximal thermodynamic work given by the difference in the free energy of the initial and final states, both evaluated by the final temperature. In the context of passive states, the Gibbs state is referred to as a complete passive state. If we consider n copies of the state $\hat{\rho}$ and look at the composite system $\hat{\rho}\otimes\hat{\rho}\otimes\cdots$, then $\hat{\rho}$ is completely passive if for all integer n the composite system is also a passive state. It can be shown [Lenard 1978] that this condition is satisfied only by the Gibbs state and the ground state. In addition, a thermal state is the passive state of any Gaussian state (including coherent and squeezed states). The notion of passivity and ergotropy come in hand in the study of quantum storage devices [Levy 2016, Alicki 2013, Binder 2015] and the availability of work from correlations [Perarnau-Llobet 2015].

2.3.2 The laws of thermodynamics

The laws of thermodynamics introduces the basic concepts of the thermodynamic quantities, energy, heat, work, entropy, temperature and the relation between them. These relations characterize systems at thermal equilibrium. In the following we introduce the laws of thermodynamics in the context of quantum mechanics. Since we are interested in quantum thermal devices that operate far from equilibrium we present the laws in their dynamical form adapting concepts from non-equalibrium thermodynamics.

The first law:

The first law of thermodynamics is a conservation law of energy which determines that the energy of an isolated system is constant and can be divided into two types; heat- which is an uncontrolled and wasteful form of energy, and work - which is controlled and useful. The increment in the internal energy is then given by,

$$dU = \delta Q + \delta W. \tag{2.99}$$

Here δQ and δW are the infinitesimal change in heat and work respectively. δ indicates that these quantities are not full differentials, and depend on the thermodynamic path, i.e. they are not a state functions, thus they don't correspond to observables. For a given quantum system described by the density operator $\hat{\rho}$ and

the Hamiltonian $\hat{H}$, the internal energy is defined according to,

$$U \stackrel{\text{def}}{=} \text{Tr}\Big(\hat{\rho}\hat{H}\Big). \tag{2.100}$$

Taking the time derivative of Eq.(2.100) we obtain the dynamical form of the first law in terms of energy flow,

$$\frac{d}{dt}U = \text{Tr}\Big(\dot{\hat{\rho}}\hat{H}\Big) + \text{Tr}\Big(\hat{\rho}\dot{H}\Big). \tag{2.101}$$

If the system is a closed quantum system, which implies that the dynamics is generated by $\hat{H}$, then $\text{Tr}\Big(\dot{\hat{\rho}}\hat{H}\Big) = 0$. In this scenario the energy flow in the system is caused only by the second term on the rhs of Eq.(2.101). Since the system is isolated and follow a unitary dynamics the entropy generation in the process is zero and we can identify the power with the change in the time dependent control Hamiltonian,

$$P = \text{Tr}\Big(\hat{\rho}\dot{H}\Big). \tag{2.102}$$

The work[23] is then given by integrating the power over the process time,

$$W \stackrel{\text{def}}{=} \int_0^t P ds. \tag{2.103}$$

If the Hamiltonian is time independent (no external field is applied to the system) and it is weakly coupled to a thermal bath, then all the energy flow results from the exchange of heat with the bath[24]. In this scenario the second term on the rhs of Eq.(2.101) vanishes and we can identify the heat current,

$$J \stackrel{\text{def}}{=} \text{Tr}\Big(\dot{\hat{\rho}}\hat{H}\Big). \tag{2.104}$$

Integrating J over time we obtain the heat[24] supplied to the system,

$$Q = \int_0^t J ds. \tag{2.105}$$

Equation (2.101) can then be expressed as,

$$dU = Jdt + Pdt. \tag{2.106}$$

When the system is simultaneously driven by an external field and weakly cou-

[23]Here the term work and heat refer to the average work and heat over an ensemble.

[24]The assumption of a thermal bath is important for defining heat current properly. Some authors mistakenly reported quantum engines that exceeds the Carnot efficiency. They misapplied the Carnot bound because they identified the energy flow out of a squeezed bath as the heat current.

ple to a thermal bath, these definitions of heat and work become less clear and extra care should be taken [Levy 2012b]. In the following we discuses this issue in detail. We further notice that the Hamiltonian in Eq.(2.104) is the bare system $\mathcal{S}$ Hamiltonian. This makes sense only if the the system-bath interaction is weak and the energy from interaction can be neglected. For strong coupling it is not clear how to account for the interaction energy. To overcome this problem different approaches where suggested, some of them are based on the Green's function approach [Esposito 2015], the polaron transformation [Gelbwaser-Klimovsky 2015], and the idea of heat exchangers [Uzdin 2016, Katz 2008]. Instead of gaining information about the dynamics of the process (calculating heat flows), it is possible to perform a two point measurement and obtain the heat exchanged during the process. In this approach we first measure the initial internal energy of the system $\mathcal{S}$, then we let it interact with the thermal bath (the interaction can be strong in this case), and at the end of the process we again measure the internal energy. The difference between the initial and final energy can be identified as heat. The main drawback from this procedure is that the first measurement destroy all the quantum features of the system.

The Hamiltonian and the state of the system are typically stochastic in the theory of monitoring and feedback control. Since stochastic fluctuations are microscopic, the thermodynamic definition of the internal energy is given by the stochastic mean of the microscopic energy,

$$U = \mathbf{M}\left[\mathrm{Tr}\left(\hat{\rho}\hat{H}\right)\right]. \tag{2.107}$$

This leads to the generalization of Eq.(2.106) [Levy 2016],

$$dU = \mathbf{M}\left[\mathrm{Tr}\left(d\hat{\sigma}\hat{H}\right)\right] + \mathbf{M}\left[\mathrm{Tr}\left(\hat{\sigma}d\hat{H}\right)\right] \equiv Jdt + Pdt., \tag{2.108}$$

where both $\hat{\sigma}$ and $\hat{H}$ are stochastic and conditioned on the measurement signal. The differentials in Eq.(2.108) must be Stratonovich ones instead of those of Ito. For the Ito differentials the rhs should contain the so-called Ito correction $\mathbf{M}\left[\mathrm{Tr}\left(d\hat{\sigma}d\hat{H}\right)\right]$ which would jeopardize the split of dU between heat flow and power. This implies that any systematic calculation of heat flow and power requires to transform the final SME from Ito into Stratonovich form (see appendix). In case that only the state is stochastic Eq.(2.108) reduces back to Eq.(2.106).

Heat flow and power for the LGKS master equation- As mentioned earlier the definition for the heat flow (2.104) is valid for constant Hamiltonian in the weak system-bath coupling limit. The description given by the thermal LGKS master equation, Eq.(2.22), is then consistent with this definition. The heat flow reduces

to the form,

$$J(t) = \mathrm{Tr}\Big((\mathcal{L}\hat{\rho}(t))\hat{H}\Big), \tag{2.109}$$

where $\mathcal{L}$ is the dissipative term of the master equation (2.38). The relation can also be expressed as,

$$J(t) = \beta^{-1}\mathrm{Tr}((\mathcal{L}\hat{\rho}(t))\ln\hat{\rho}_{th}) \tag{2.110}$$

where β^{-1} is the bath temperature and $\hat{\rho}_{th}$ is the Gibbs state of the system $\mathcal{S}$ with the same temperature. When the system is fully equalibriated then $\mathcal{L}\hat{\rho}_{th} = 0$ and the heat current vanishes. This definition can be extended for a system coupled to a number of thermal bath[25]. The heat flow from the i bath is then,

$$J^i(t) = -\beta_i^{-1}\mathrm{Tr}\big((\mathcal{L}\hat{\rho}(t))\ln\hat{\rho}^i_{th}\big). \tag{2.111}$$

In section 2.1.5 we introduced few scenarios for which a MME of the LGKS form can be deduced for a driven open quantum system. For adiabatic driven systems the definitions for the power and heat flow introduced in equation (2.102) and (2.104) holds true, where now the Hamiltonian includes the interaction with the external field. Some examples can be found in [Geva 1994, Alicki 2015, Alicki 2016]. For strong periodic driving these definitions are modified. This is one of the results of [Levy 2012b] (see chapter 5), and we next summaries the main results. For a thermal bath the LGKS generator Eq.(2.52) in the interaction picture can be written as the sum of generators that correspond to the quasi Bohr frequencies (see section 2.1.5),

$$\mathcal{L} = \sum_{n\in\mathbb{Z}}\sum_{\omega}\mathcal{L}_{n\omega}, \tag{2.112}$$

with,

$$\begin{aligned}\mathcal{L}_{n\omega}\hat{\rho}_S &= \gamma(\omega+n\nu)\left(\hat{V}_n(\omega)\hat{\rho}_S\hat{V}_n^\dagger(\omega) - \frac{1}{2}\left\{\hat{V}_n^\dagger(\omega)\hat{V}_n(\omega),\hat{\rho}_S\right\}\right) \\ &+ \gamma(\omega+n\nu)e^{-\beta(\omega+n\nu)}\left(\hat{V}_n^\dagger(\omega)\hat{\rho}_S\hat{V}_n(\omega) - \frac{1}{2}\left\{\hat{V}_n(\omega)\hat{V}_n^\dagger(\omega),\hat{\rho}_S\right\}\right).\end{aligned} \tag{2.113}$$

Each $\mathcal{L}_{n\omega}$ generator in itself has the LGKS structure and posses a Gibbs-like stationary state of the form,

$$\hat{\rho}^\infty_{n\omega} = Z^{-1}\exp\left(\frac{\omega+n\nu}{\omega}\beta\hat{H}\right). \tag{2.114}$$

Using the decomposition (2.112) the local heat current which corresponds to energy

[25] Here we assume that the baths are not correlated which implies that the dynamics is given by the sum of the LGKS generators.

exchange $\omega - n\nu$ can be identified as,

$$J_{n\omega}(t) = \beta^{-1}\mathrm{Tr}((\mathcal{L}_{n\omega}\hat{\rho}(t))\ln\hat{\rho}^{\infty}_{n\omega}). \tag{2.115}$$

Thus, heat is flowing in channels corresponding to the quasi energies obtained from the Floquet analysis. The power can be calculated from the first law of thermodynamics, i.e. $P(t) = \dot{U}(t) - J(t)$ with, $J(t) = \sum_{n\omega} J_{n\omega}(t)$. For weak periodic driving in the dipole approximation the standard definitions (2.102) and (2.104) holds with a local generator and the Hamiltonian now contains also the interaction with the external field.

The second law

The second law of thermodynamics is one of the most fundamental laws in physics. It concerns with irreversibility of thermodynamic process and imposes a direction to the arrow of time. The second law can be expressed in several ways and there is a huge number of different formulations. The first step towards establishing the law was introduced by Carnot who set a limitation on the efficiency of all heat engines working between two thermal baths. The efficiency is bounded because of wasted energy in the form of heat that can not be converted into work. The Clausius formulation of the second law and maybe the most intuitive one states that heat cannot spontaneously flow from a cold body to a hot body without external work being performed on the system. The second law can also be expressed in terms of entropy. This formulation determines that the entropy of a closed system will always tend to stay the same or increase with time, i.e. $\Delta S \geq 0$.

In quantum mechanics it is possible to show that the change in the entropy of the total closed system $\mathcal{S} \vee \mathcal{R}$ (the universe) is always non-negative if initially the systems $\mathcal{S}$ and $\mathcal{R}$ are not correlated [Peres 2006]. Making this assumption we write the initial joint state as a tensor product $\hat{\rho}^i = \hat{\rho}^i_S \otimes \hat{\rho}^i_R$. The final joint state is then given by $\hat{\rho}^f = \hat{U}\hat{\rho}^i\hat{U}^\dagger$ where, $\hat{U}$ is the global unitary evolution of the total system. The change in the entropy of both subsystems is then,

$$\begin{aligned} \Delta S_S + \Delta S_R &\equiv (S(\hat{\rho}^f_S) - S(\hat{\rho}^i_S)) + (S(\hat{\rho}^f_R) - S(\hat{\rho}^i_R)) \\ &= S(\hat{\rho}^f_S) + S(\hat{\rho}^f_R) - S(\hat{\rho}^i) \\ &= S(\hat{\rho}^f_S) + S(\hat{\rho}^f_R) - S(\hat{\rho}^f) \\ &\equiv S(\hat{\rho}^f|\hat{\rho}^f_S \otimes \hat{\rho}^f_R) \geq 0. \end{aligned} \tag{2.116}$$

The second equality is the consequence of the assumption of no initial correlations, the third equality stems from the fact that the von Neumann entropy is invariant under a unitary transformations, and the last inequality results from the fact the

the relative entropy is a non-negative quantity.

The description above is somewhat static and presents a global viewpoint of the second law. The entropy balance of the subsystems composing a closed system is non-decreasing. In thermodynamics of quantum devices we are often interested in the description of the local open system alone. Based on concepts from non-equilibrium thermodynamics the local form of the balance equation for the entropy reads,

$$\frac{dS}{dt} = \sigma + \zeta. \tag{2.117}$$

Here S is the local entropy of the open system, ζ is the entropy flux, that is the entropy per unite time exchanged between the open system and its environment, and σ is the entropy production. If the environment is composed of thermal baths and the system-baths entropy exchange is only due to heat, then $\zeta = \sum_i J_i/T_i$, where J_i and T_i are the heat and temperature of the bath i respectively[26]. The dynamical standpoint of the second law applied to open systems states that the entropy production σ is non-negative.

Sphon introduced the proof that a quantum dynamical semigroup will always result with $\sigma \geq 0$ [Spohn 1978]. The proof is based on the identification of the entropy production as the time derivative of the relative entropy with respect to a stationary state $\hat{\rho}_o$ of the the dynamical semigroup map $\Lambda(t)$.

$$\sigma(\hat{\rho}(t)) \stackrel{\text{def}}{=} -\frac{d}{dt}\mathrm{Tr}(\hat{\rho}(t)|\hat{\rho}_o), \quad \text{with} \quad \hat{\rho}(t) = \Lambda(t)\hat{\rho}(0), \quad \text{and} \quad \Lambda(t)\hat{\rho}_o = \hat{\rho}_o. \tag{2.118}$$

Here $\hat{\rho}$ is understood as the open system state $\hat{\rho} \equiv \hat{\rho}_S$. Taking the explicit derivative one obtains,

$$\sigma(\hat{\rho}(t)) = -\mathrm{Tr}((\mathcal{L}\hat{\rho}(t)) \ln \hat{\rho}(t)) + \mathrm{Tr}((\mathcal{L}\hat{\rho}(t))\hat{\rho}_o). \tag{2.119}$$

The first term on the rhs of the equation is just derivative of the von Neumann entropy (the local entropy). If we consider a thermal bath then the stationary state is a thermal state, $\hat{\rho}_o = \hat{\rho}_{th}$, and according to (2.110) the second term on the rhs is just the heat flow divided by the temperature, $-J/T$. Equation (2.117) is then satisfied for a thermal environment. This result motivates the definition (2.118) for the entropy production. The proof by Spohn for $\sigma(\hat{\rho}(t)) \geq 0$ is general and holds for any dynamical semigroup with a stationary state $\hat{\rho}_o$. The proof is based on the fact that the map $\hat{\rho} \mapsto \sigma(\hat{\rho})$ is a convex functional, which in itself is a result of Lieb's theorem and the LGKS structure. We remark here that in the microscopic regime one can define a family of second laws which generalize the standard second law. Details and implications can be found in [Brandão 2015, Lostaglio 2015].

[26] Generally ζ also accounts for entropy flux due to matter exchange between the system and the environment. In this thesis we concentrate on heat exchange only.

The third law

The third law of thermodynamics has two different formulations, both can originally be traced back to the work by Nernst. These are known as the Nernst heat theorem and the unattainability principle [Fowler 1939]. The first formulation is a static (equilibrium) one and states that the the entropy of any pure substance in thermodynamic equilibrium approaches zero as the temperature approaches zero. If the substance has defects and the ground state is degenerate then the entropy approaches to a constant number that is related to the level of degeneracy. This implies that the entropy change of a system undergoing a reversible isothermal process approaches zero as the temperature approaches the absolute zero temperature, i.e. $\Delta S_{T\to 0} = 0$. The second formulation states that it is impossible by any procedure, no matter how idealized, to reduce any assembly to absolute zero temperature in a finite number of operations. Chapter 5 is dedicated to the study of the third law of thermodynamics from a dynamical quantum mechanics standpoint[Levy 2012b, Levy 2012a]. This approach allows to quantify the third law in terms of characteristic exponents of the cooling process.

2.3.3 Quantum thermal machines

Up to this point we reviewed some basic concepts and the mathematical tools employed in the study of thermodynamics of quantum devices. We now proceed and introduce the main ingredients to establish quantum thermal machines with the intention of exploring thermodynamics in the quantum regime. The study of quantum thermal machines which operate far from thermal equilibrium typically requires a well-defined quantum system coupled to two or more thermal reservoirs or some external drive. These components can then serve as building blocks for constructing different quantum thermal machines such as quantum heat engines, quantum refrigerators and quantum energy storage devices. To some extent for the thermal device to operate in a nontrivial manner three or more reservoirs should be involved in the process. Otherwise energy will flow in a trivial way from the cold to the hot bath.

The study of quantum thermal device can be traced back to the pioneered work of Scovil and DuBois from 1959 [Scovil 1959]. In their work they considered the three level maser as a heat engine and showed that its efficiency is bounded by the Carnot efficiency (see figure 2.1). The proof is very simple, levels 1 and 3 are connected to a hot bath at temperature T_h using a filter that matches the transition frequency ω_h. The same is done to level 2 and 3 with the cold bath at temperature T_c, which matches the transition frequency ω_c. Here we take $\omega_h > \omega_c$ and $T_h > T_c$.

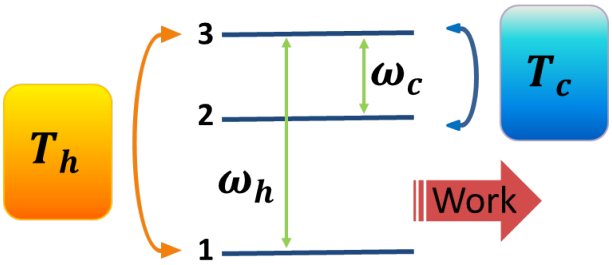

Figure 2.1: Illustration of the three level heat engine. The working medium is a three level system operating between two thermal baths with temperatures T_h and T_c.

Using the Boltzmann factor we obtain the ratios of the populations,

$$\frac{p_2}{p_3} = \exp\left(\frac{\omega_c}{T_c}\right), \quad \text{and} \quad \frac{p_3}{p_1} = \exp\left(-\frac{\omega_h}{T_h}\right). \tag{2.120}$$

Work can be extracted out of the engine if there is a population inversion between level 1 and 2. This is achieved when $p_2/p_1 > 1$. We can express this ratio in terms of the efficiency η and the Carnot efficiency η_C, which are defined as

$$\eta \overset{\text{def}}{=} \frac{\text{Benefit}}{Cost} = \frac{\omega_h - \omega_c}{\omega_h}, \quad \text{and} \quad \eta_C = 1 - \frac{T_c}{T_h}. \tag{2.121}$$

Then the ratio p_2/p_1 takes the form,

$$\frac{p_2}{p_1} = \exp\left(\frac{\omega_h - \omega_c}{T_c}\left(\eta^{-1}\eta_C - 1\right)\right), \tag{2.122}$$

and work can be extracted out if $\eta < \eta_C$, which completes the proposition. This model is static and a simplifying model, the only quantum feature it displays is the discrete spectrum of the quantum system. About twenty years later Alicki [Alicki 1979] and Kosloff [Kosloff 1984] employed the theory of open quantum system in order to study quantum heat engines. Doing so they introduced dynamics to field of quantum thermal machines. This also made quantum properties such as coherence, entanglement and superposition visible and significant to the study of quantum thermodynamics.

Quantum thermal machines can be classified into two main categories: reciprocating stroke machines and continuous ones. The first category includes the four stroke and two stroke engines which typically utilize the Otto or the Carnot cycle. Here the working segments (the adiabats[27]) are isolated from the heat transfer segments which are the isotherms in the Carnot cycle [Geva 1992, Lloyd 1997,

[27]Here we refer to thermodynamic adiabats, this should not be confused with quantum adiabatic process.

Bender 2002, Quan 2007, Esposito 2010], and the isochores in the Otto cycle [Feldmann 1996, Feldmann 2000, Rezek 2006, Henrich 2007, Allahverdyan 2008]. The adiabats are modeled by a time-dependent external control Hamiltonian. Since now the Hamiltonian typically does not commute with itself in different times friction effects are present. Reduction in the efficiency can then be traced to the inability of the system to stay in the instantaneous energy basis during the segment [Feldmann 2003]. Coherence terms that are created during the external driving process are then eliminated during the heat transfer segments, which leads to losses. If the driving is performed in quantum adiabatic manner these losses can be prevented, nevertheless, the power out put tends to zero. This is the manifestation of finite time thermodynamics and the trade off between power and efficiency. The heat transfer segments are typically modeled by the LGKS MME. We note that in order to operate the machines as engines or refrigerators the system does not have to fully equalibrate on the heat transfer segments. Then the dynamical description of the LGKS MME comes in hand, yet, one should make sure that the interaction time with the baths are sufficiently long in order to apply the Markov approximation.

The second category consist of continuous quantum machines [Kosloff 1984, Geva 1996, Linden 2010, Levy 2012c, Levy 2012b, Correa 2014b], see also review on the subject [Kosloff, R. and Levy, A. 2014] and references therein. In theses types of machines the quantum system (working medium) is connected simultaneously to all the components of the device. To construct a continuous engine or refrigerator a non linear interaction involving minimum of three energy currents is essential [Martinez 2013]. The description of such devices is typically more involved then the one described above for the stroke machines. The quantum system is now driven externally while it is coupled to two or more heat baths and a microscopic derivation of the master equation is essential. As was discussed in section 2.1.5 the LGKS master equation can be derived microscopically for adiabatically or periodically driven systems under some limiting assumptions. While in the stroke engines we are interested in the limiting cycle of the devices for the continuous machines we are focusing on the steady state (yet out of equilibrium) operation of the devices. Optimizing the power results in reduction of the efficiency similar to the expected behavior from finite time thermodynamics.

Chapter 3

The local approach to quantum transport may violate the second law of thermodynamics

The local approach to quantum trans- port may violate the second law of thermodynamics

Amikam Levy and Ronnie Kosloff

Published in: EPL (Europhysics Letters), vol. 107, no. 2, page 20004, 2014

epl A Letters Journal Exploring the Frontiers of Physics

July 2014

EPL, **107** (2014) 20004 www.epljournal.org
doi: 10.1209/0295-5075/107/20004

The local approach to quantum transport may violate the second law of thermodynamics

Amikam Levy and Ronnie Kosloff

Institute of Chemistry, The Hebrew University of Jerusalem - Jerusalem 91904, Israel

received 4 May 2014; accepted in final form 23 June 2014
published online 10 July 2014

PACS 03.65.Yz – Decoherence; open systems; quantum statistical methods
PACS 05.60.Gg – Quantum transport

Abstract – Clausius statement of the second law of thermodynamics reads: Heat will flow spontaneously from a hot to cold reservoir. This statement should hold for transport of energy through a quantum network composed of small subsystems each coupled to a heat reservoir. When the coupling between nodes is small, it seems reasonable to construct a local master equation for each node in contact with the local reservoir. The energy transport through the network is evaluated by calculating the energy flux after the individual nodes are coupled. We show by analyzing the most simple network composed of two quantum nodes coupled to a hot and cold reservoir, that the local description can result in heat flowing from cold to hot reservoirs, even in the limit of vanishing coupling between the nodes. A global derivation of the master equation which prediagonalizes the total network Hamiltonian and within this framework derives the master equation, is always consistent with the second law of thermodynamics.

Introduction. – Transport of energy in and out of a quantum device is a key issue in emerging technologies. Examples include molecular electronics, photovoltaic devices, quantum refrigerators and quantum heat engines [1–3]. A quantum network composed of quantum nodes each coupled to local reservoir and to other nodes constitutes the network. The framework for describing such devices is the theory of open quantum systems. The dynamics is postulated employing completely positive quantum master equations [4,5]. Solving the dynamics allows to calculate the steady-state transport of energy through the network.

It is desirable to have the framework consistent with thermodynamics. The first law of thermodynamics is a conservation law of energy; the energy of an isolated system is constant and can be divided into heat and work [6]. The dynamical version of the second law of thermodynamics states that for an isolated system the rate of entropy production is non-negative [7]. For a typical quantum device the second law can be expressed as

$$\frac{\mathrm{d}}{\mathrm{d}t}\Delta\mathcal{S}^u = \frac{\mathrm{d}\mathcal{S}_{int}}{\mathrm{d}t} + \frac{\mathrm{d}\mathcal{S}_m}{\mathrm{d}t} - \sum_i \frac{\mathcal{J}_i}{T_i} \geq 0, \tag{1}$$

where $\frac{\mathrm{d}\mathcal{S}_{int}}{\mathrm{d}t}$ is the rate of entropy production due to internal processes, expressed by the von Neumann entropy. $\frac{\mathrm{d}\mathcal{S}_m}{\mathrm{d}t}$ is the entropy flow associated with matter entering the system, and the last term is the contribution of heat flux, $\mathcal{J}_i$, from the reservoir i.

Microscopic derivation of a global Markovian master equation (MME) of Linblad-Gorini-Kossakowski-Sudarshan (LGKS) form [4,5], for the network is usually intricate. The local approach simplifies this task [8–14]. It is commonly considered that if the different parts of the network are weakly coupled to each other, a local master equation is sufficient to describe all the properties of the network. We will show that the local approach is only valid for local observables such as the population of each node, and is not valid for non-local observables describing energy fluxes.

The network model. – The simplest network model composed of two nodes shown in fig. 1 and is sufficient to demonstrate the distinction between the local and global approach. Heat is transported between two subsystems A and B, where each is coupled to a single heat bath with temperature T_h and T_c. The two subsystems are weakly coupled to each other. The global Hamiltonian is of the form

$$\hat{\mathbf{H}} = \hat{\mathbf{H}}_A + \hat{\mathbf{H}}_B + \hat{\mathbf{H}}_{AB} + \hat{\mathbf{H}}_h + \hat{\mathbf{H}}_c + \hat{\mathbf{H}}_{Ah} + \hat{\mathbf{H}}_{Bc}. \tag{2}$$

The bare network Hamiltonian, is $\hat{\mathbf{H}}_0 = \hat{\mathbf{H}}_A + \hat{\mathbf{H}}_B$ where the node Hamiltonians are $\hat{\mathbf{H}}_A = \omega_h \hat{\mathbf{a}}^\dagger \hat{\mathbf{a}}$ and $\hat{\mathbf{H}}_B = \omega_c \hat{\mathbf{b}}^\dagger \hat{\mathbf{b}}$,

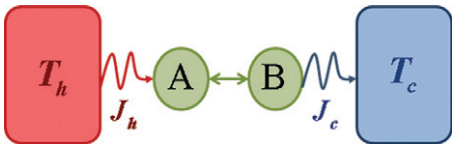

Fig. 1: (Colour on-line) The heat transfer network model; heat is transferred from a hot bath at temperature T_h to the a colder bath at temperature T_c. The heat current is mediated by two coupled subsystems A and B, where subsystem A is connected to the hot bath and subsystem B is connected to the cold bath.

which are composed of either two harmonic oscillators (HO) or of two two-level systems (TLS), depending on the commutation relation.

$$\begin{aligned} \hat{\mathbf{a}}\hat{\mathbf{a}}^\dagger + \delta\hat{\mathbf{a}}^\dagger\hat{\mathbf{a}} &= 1, \quad \hat{\mathbf{a}}\hat{\mathbf{a}} + \delta\hat{\mathbf{a}}\hat{\mathbf{a}} = 0, \\ \hat{\mathbf{b}}\hat{\mathbf{b}}^\dagger + \delta\hat{\mathbf{b}}^\dagger\hat{\mathbf{b}} &= 1, \quad \hat{\mathbf{b}}\hat{\mathbf{b}} + \delta\hat{\mathbf{b}}\hat{\mathbf{b}} = 0 \end{aligned} \tag{3}$$

with $\delta = 1$ for the TLS and $\delta = -1$ for oscillators. The interaction between the system A and B is described by the swap Hamiltonian, $\hat{\mathbf{H}}_{AB} = \epsilon(\hat{\mathbf{a}}^\dagger\hat{\mathbf{b}} + \hat{\mathbf{a}}\hat{\mathbf{b}}^\dagger)$, with $\epsilon > 0$. The hot (cold) baths Hamiltonians are denoted $\hat{\mathbf{H}}_{h(c)}$, where $T_h > T_c$. The system-bath interaction is given by, $\hat{\mathbf{H}}_{Ah} = g_h(\hat{\mathbf{a}} + \hat{\mathbf{a}}^\dagger) \otimes \hat{\mathbf{R}}_h$ and $\hat{\mathbf{H}}_{Bc} = g_c(\hat{\mathbf{b}} + \hat{\mathbf{b}}^\dagger) \otimes \hat{\mathbf{R}}_c$, with $\hat{\mathbf{R}}_{h(c)}$ operators belonging the hot (cold) bath Hilbert space, and $g_{h(c)}$ are the system-baths coupling parameters.

The dynamics of the reduced system $A + B$ is governed by the Master equation,

$$\frac{\mathrm{d}}{\mathrm{d}t}\hat{\boldsymbol{\rho}}_s = -i[\hat{\mathbf{H}}_0 + \hat{\mathbf{H}}_{AB}, \hat{\boldsymbol{\rho}}_s] + \mathcal{L}_h\hat{\boldsymbol{\rho}}_s + \mathcal{L}_c\hat{\boldsymbol{\rho}}_s. \tag{4}$$

With the LGKS dissipative terms, $\mathcal{L}_{h(c)}$, which differ for the local and global approaches. At steady state the heat flow from the hot (cold) bath is given by

$$\mathcal{J}_{h(c)} = \mathrm{Tr}[(\mathcal{L}_{h(c)}\hat{\boldsymbol{\rho}}_s)(\hat{\mathbf{H}}_0 + \hat{\mathbf{H}}_{AB})], \tag{5}$$

where $\hat{\boldsymbol{\rho}}_s$ is the steady-state density operator.

Local approach. – In the local approach it is assumed that the inter-system coupling does not affect the system bath coupling. Therefore in the derivation of the MME the Hamiltonian $\hat{\mathbf{H}}_{AB}$ is ignored and the dissipative terms takes the form,

$$\begin{aligned} \mathcal{L}_h\hat{\boldsymbol{\rho}}_s = \gamma_h \Big(& \hat{\mathbf{a}}\hat{\boldsymbol{\rho}}_s\hat{\mathbf{a}}^\dagger - \frac{1}{2}\{\hat{\mathbf{a}}^\dagger\hat{\mathbf{a}}, \hat{\boldsymbol{\rho}}_s\} \\ & + e^{-\beta_h\omega_h}\left(\hat{\mathbf{a}}^\dagger\hat{\boldsymbol{\rho}}_s\hat{\mathbf{a}} - \frac{1}{2}\{\hat{\mathbf{a}}\hat{\mathbf{a}}^\dagger, \hat{\boldsymbol{\rho}}_s\}\right)\Big), \end{aligned} \tag{6}$$

and

$$\begin{aligned} \mathcal{L}_c\hat{\boldsymbol{\rho}}_s = \gamma_c \Big(& \hat{\mathbf{b}}\hat{\boldsymbol{\rho}}_s\hat{\mathbf{b}}^\dagger - \frac{1}{2}\{\hat{\mathbf{b}}^\dagger\hat{\mathbf{b}}, \rho_s\} \\ & + e^{-\beta_c\omega_c}\left(\hat{\mathbf{b}}^\dagger\hat{\boldsymbol{\rho}}_s\hat{\mathbf{b}} - \frac{1}{2}\{\hat{\mathbf{b}}\hat{\mathbf{b}}^\dagger, \hat{\boldsymbol{\rho}}_s\}\right)\Big). \end{aligned} \tag{7}$$

when the node-to-node coupling is zero, $\hat{\mathbf{H}}_{AB} = 0$, each of the local master equations, eq. (6) and eq. (7), drives the local node to thermal equilibrium. The dynamics of the network is completely characterized by the expectation values of four operators: Two local observables $\langle\hat{\mathbf{a}}^\dagger\hat{\mathbf{a}}\rangle, \langle\hat{\mathbf{b}}^\dagger\hat{\mathbf{b}}\rangle$, and two AB correlations $\langle\hat{\mathbf{X}}\rangle \equiv \langle\hat{\mathbf{a}}^\dagger\hat{\mathbf{b}} + \hat{\mathbf{a}}\hat{\mathbf{b}}^\dagger\rangle$ and $\langle\hat{\mathbf{Y}}\rangle \equiv i\langle\hat{\mathbf{a}}^\dagger\hat{\mathbf{b}} - \hat{\mathbf{a}}\hat{\mathbf{b}}^\dagger\rangle$ with $\langle\ \cdot\ \rangle \equiv \mathrm{Tr}\{\hat{\boldsymbol{\rho}}_s\cdot\}$. For the dynamics we obtain

$$\begin{aligned} \frac{\mathrm{d}}{\mathrm{d}t}\langle\hat{\mathbf{a}}^\dagger\hat{\mathbf{a}}\rangle &= -\gamma_h(1 + \delta e^{-\beta_h\omega_h})\langle\hat{\mathbf{a}}^\dagger\hat{\mathbf{a}}\rangle + \gamma_h e^{-\beta_h\omega_h} - \epsilon\langle\hat{\mathbf{Y}}\rangle, \\ \frac{\mathrm{d}}{\mathrm{d}t}\langle\hat{\mathbf{b}}^\dagger\hat{\mathbf{b}}\rangle &= -\gamma_c(1 + \delta e^{-\beta_c\omega_c})\langle\hat{\mathbf{b}}^\dagger\hat{\mathbf{b}}\rangle + \gamma_c e^{-\beta_c\omega_c} + \epsilon\langle\hat{\mathbf{Y}}\rangle, \\ \frac{\mathrm{d}}{\mathrm{d}t}\langle\hat{\mathbf{X}}\rangle &= -\frac{1}{2}\left(\gamma_h(1 + \delta e^{-\beta_h\omega_h}) + \gamma_c(1 + \delta e^{-\beta_c\omega_c})\right)\langle\hat{\mathbf{X}}\rangle \\ &\quad + (\omega_h - \omega_c)\langle\hat{\mathbf{Y}}\rangle, \\ \frac{\mathrm{d}}{\mathrm{d}t}\langle\hat{\mathbf{Y}}\rangle &= -\frac{1}{2}\left(\gamma_h(1 + \delta e^{-\beta_h\omega_h}) + \gamma_c(1 + \delta e^{-\beta_c\omega_c})\right)\langle\hat{\mathbf{Y}}\rangle \\ &\quad - (\omega_h - \omega_c)\langle\hat{\mathbf{X}}\rangle + 2\epsilon(\langle\hat{\mathbf{a}}^\dagger\hat{\mathbf{a}}\rangle - \langle\hat{\mathbf{b}}^\dagger\hat{\mathbf{b}}\rangle). \end{aligned} \tag{8}$$

The rates $\gamma_{h(c)} > 0$ depend on the specific properties of the bath and its interaction with the system. Equations (8) fulfill the dynamical version of the first law of thermodynamics: The sum of all energy (heat) currents at steady state is zero, $\mathcal{J}_h + \mathcal{J}_c = 0$. The heat flow from the hot heat bath can be cast in the form (see [15] for details)

$$\mathcal{J}_h = (e^{\beta_c\omega_c} - e^{\beta_h\omega_h})\mathcal{F}, \tag{9}$$

where $\mathcal{F}$ is a function of all the parameters of the system, which is always positive, and is different for the HO and TLS medium. The Clausius statement for the second law of thermodynamics implies that heat can not flow from a cold body to a hot body without external work being performed on the system. It is apparent from eq. (9), that the direction of heat flow depends on the choice of parameters. For $\frac{\omega_c}{T_c} < \frac{\omega_h}{T_h}$ heat will flow from the cold bath to the hot bath, thus the second law is violated even at vanishing small AB coupling, cf. fig. 2. The breakdown of the second law has been examined in several models, see [16] and references therein. In [16] a Fermionic transport model between two heat baths at the same temperature was studied in the weak system-bath coupling limit MME and was compared to a solution within the formalism of nonequilibrium Green functions. At steady state, the current between the baths according to the weak coupling MME is nonzero, which implies a violation of the second law in the sense that heat flows constantly between two heat baths at the same temperature. This sort of violation can also be observed in eq. (9) when taking $T_h = T_c$. It was claimed in [16] that the violation of the second law is a consequence of neglecting higher-order coherent processes between the system and the baths due to the weak coupling limit. In fact, the treatment introduced in [16] corresponds to the local approach described above. Next, we introduce a proper weak coupling MME, which always obeys the second law of thermodynamics.

Global approach. – The global approach is based on the holistic perception where the MME is derived in the

$$\mathcal{J}_h = \frac{\left(e^{\beta_c\omega_-} - e^{\beta_h\omega_-}\right)\gamma_c^-\gamma_h^-\omega_-}{\sin^{-2}(\theta)e^{\beta_h\omega_-}\left(-1+e^{\beta_c\omega_-}\right)\gamma_c^- + e^{\beta_c\omega_+}\left(-1+e^{\beta_h\omega_-}\right)\cos^{-2}(\theta)\gamma_h^-} + \frac{\left(e^{\beta_c\omega_+} - e^{\beta_h\omega_+}\right)\gamma_c^+\gamma_h^+\omega_+}{e^{\beta_h\omega_+}\left(-1+e^{\beta_c\omega_+}\right)\cos^{-2}(\theta)\gamma_c^+ + \sin^{-2}(\theta)e^{\beta_c\omega_+}\left(-1+e^{\beta_h\omega_+}\right)\gamma_h^+}, \tag{13}$$

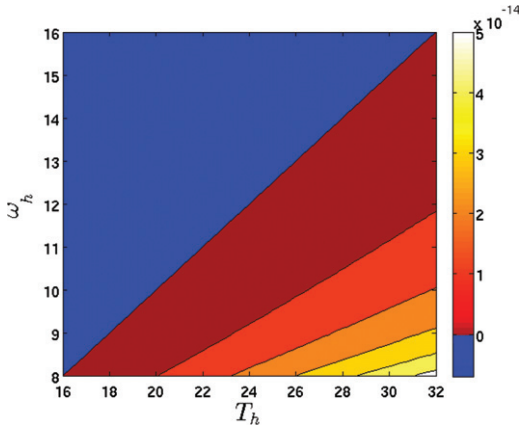

Fig. 2: (Colour on-line) The rate of entropy production $\Delta\mathcal{S}^u$ in the local description, as function of ω_h and T_h. The blue area corresponds to negative entropy production rate, a clear violation of the second law. The borderline between the blue and the red zones corresponds to $\omega_h/T_h = \omega_c/T_c$. Here $T_c = 10$, $\omega_c = 5$, $\epsilon = 10^{-4}$ and $\kappa = 10^{-7}$.

eigen-space representation of the combined system $A+B$. The reduced system, $A+B$, is first diagonalized, then the new basis set is used to expand the system-bath interactions. Finally, the standard weak system-bath coupling procedure is introduced to derive the MME [17,18]. This approach accounts for a shift in the spectrum of the subsystems A and B due to the coupling parameter ϵ. But more importantly, it creates an effective coupling of the system A with the cold bath and of the system B with the hot bath. This indirect coupling absent in the local approach is crucial, and essentially saves the second law of thermodynamics. The global MME, by construction, obeys Spohn's inequality and therefore is consistent with the second law of thermodynamics [19].

In it's diagonal form the Hamiltonian $\hat{\mathbf{H}}_0+\hat{\mathbf{H}}_{AB}$ is given by

$$\hat{\mathbf{H}}_S = \omega_+\hat{\mathbf{d}}_+^\dagger\hat{\mathbf{d}}_+ + \omega_-\hat{\mathbf{d}}_-^\dagger\hat{\mathbf{d}}_-. \tag{10}$$

Where we have defined the operators $\hat{\mathbf{d}}_+ = \hat{\mathbf{a}}\cos(\theta) + \hat{\mathbf{b}}\sin(\theta)$ and $\hat{\mathbf{d}}_- = \hat{\mathbf{b}}\cos(\theta) - \hat{\mathbf{a}}\sin(\theta)$, with $\cos^2(\theta) = \frac{\omega_h-\omega_-}{\omega_+-\omega_-}$ and $\omega_\pm = \frac{\omega_h\pm\omega_c}{2} \pm \sqrt{(\frac{\omega_h-\omega_c}{2})^2+\epsilon^2}$. For Bosons, the commutation relations of the operators are preserved, *i.e.* $[\hat{\mathbf{d}}_\pm, \hat{\mathbf{d}}_\pm^\dagger] = 1$, where all other combinations are zero. For TLS nodes the expressions are more intricate and therefore we restrict the analysis to the harmonic nodes. Following the standard weak coupling limit, in the regime where $\omega_- > 0$ the dissipative terms of the MME reads,

$$\begin{aligned}\mathcal{L}_h\hat{\boldsymbol{\rho}}_s =\ & \gamma_h^+\cos^2(\theta)\left(\hat{\mathbf{d}}_+\hat{\boldsymbol{\rho}}_s\hat{\mathbf{d}}_+^\dagger - \frac{1}{2}\{\hat{\mathbf{d}}_+^\dagger\hat{\mathbf{d}}_+, \hat{\boldsymbol{\rho}}_s\}\right.\\ &\left. + e^{-\beta_h\omega_+}\left(\hat{\mathbf{d}}_+^\dagger\hat{\boldsymbol{\rho}}_s\hat{\mathbf{d}}_+ - \frac{1}{2}\{\hat{\mathbf{d}}_+\hat{\mathbf{d}}_+^\dagger, \hat{\boldsymbol{\rho}}_s\}\right)\right)\\ &+ \gamma_h^-\sin^2(\theta)\left(\hat{\mathbf{d}}_-\hat{\boldsymbol{\rho}}_s\hat{\mathbf{d}}_-^\dagger - \frac{1}{2}\{\hat{\mathbf{d}}_-^\dagger\hat{\mathbf{d}}_-, \hat{\boldsymbol{\rho}}_s\}\right.\\ &\left. + e^{-\beta_h\omega_-}\left(\hat{\mathbf{d}}_-^\dagger\hat{\boldsymbol{\rho}}_s\hat{\mathbf{d}}_- - \frac{1}{2}\{\hat{\mathbf{d}}_-\hat{\mathbf{d}}_-^\dagger, \hat{\boldsymbol{\rho}}_s\}\right)\right)\end{aligned} \tag{11}$$

and

$$\begin{aligned}\mathcal{L}_c\hat{\boldsymbol{\rho}}_s =\ & \gamma_c^+\sin^2(\theta)\left(\hat{\mathbf{d}}_+\hat{\boldsymbol{\rho}}_s\hat{\mathbf{d}}_+^\dagger - \frac{1}{2}\{\hat{\mathbf{d}}_+^\dagger\hat{\mathbf{d}}_+, \hat{\boldsymbol{\rho}}_s\}\right.\\ &\left. + e^{-\beta_c\omega_+}\left(\hat{\mathbf{d}}_+^\dagger\hat{\boldsymbol{\rho}}_s\hat{\mathbf{d}}_+ - \frac{1}{2}\{\hat{\mathbf{d}}_+\hat{\mathbf{d}}_+^\dagger, \hat{\boldsymbol{\rho}}_s\}\right)\right)\\ &+ \gamma_c^-\cos^2(\theta)\left(\hat{\mathbf{d}}_-\hat{\boldsymbol{\rho}}_s\hat{\mathbf{d}}_-^\dagger - \frac{1}{2}\{\hat{\mathbf{d}}_-^\dagger\hat{\mathbf{d}}_-, \hat{\boldsymbol{\rho}}_s\}\right.\\ &\left. + e^{-\beta_c\omega_-}\left(\hat{\mathbf{d}}_-^\dagger\hat{\boldsymbol{\rho}}_s\hat{\mathbf{d}}_- - \frac{1}{2}\{\hat{\mathbf{d}}_-\hat{\mathbf{d}}_-^\dagger, \hat{\boldsymbol{\rho}}_s\}\right)\right)\end{aligned} \tag{12}$$

with $\gamma_{h(c)}^\pm = \gamma_{h(c)}(\omega_\pm)$. The calculated steady-state heat flow from the hot bath is given by

see eq. (13) *above*

which is positive for all physical choice of parameters. Rewriting eq. (11) and eq. (12) in the local basis, the effective coupling of subsystem A with the cold bath and of subsystem B with the hot bath is immediately apparent (see [15] for details). These equations converge to eq. (6) and eq. (7) for $\epsilon = 0$.

To further study the dynamics of A and B, the explicit form of heat baths is specified, characterizing the rates γ [20]:

$$\gamma_l \equiv \gamma_l(\Omega) = \pi\sum_k |g_l(k)|^2\delta(\omega(k)-\Omega)[1-e^{-\beta_l\omega(k)}]^{-1}, \tag{14}$$

where $\omega(k)$ are the frequencies of the baths modes. For the case of a 3-dimensional phonon bath with a linear dispersion relation the relaxation rate can be expressed as

$$\gamma_l(\Omega) = \kappa\Omega^3[1-e^{-\beta_l\Omega}]^{-1}, \tag{15}$$

where $\kappa > 0$ embodies all the constants and is proportional to the square of the system-bath coupling.

The steady-state observables of the local and global approached are compared in fig. 3 as a function of the node-to-node coupling strength ϵ. For local observables

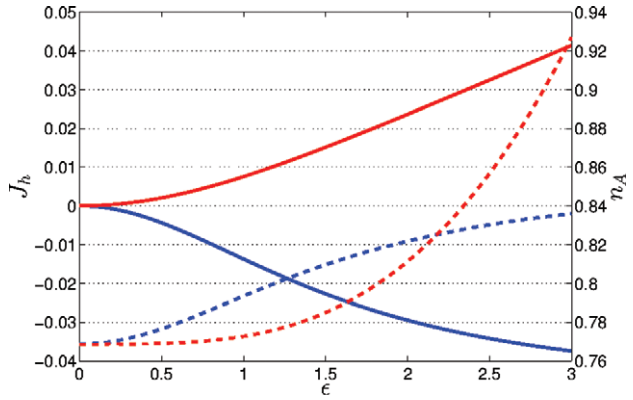

Fig. 3: (Colour on-line) The heat current $\mathcal{J}_h$ and the population as a function of the coupling parameter ϵ evaluated in the local (blue line) and the global (red line) approaches. The population of subsystem A (dashed line), and the heat flow from the hot bath $\mathcal{J}_h$ (solid line). Here $T_h = 12$, $T_c = 10$, $\omega_h = 10$, $\omega_c = 5$ and $\kappa = 10^{-4}$.

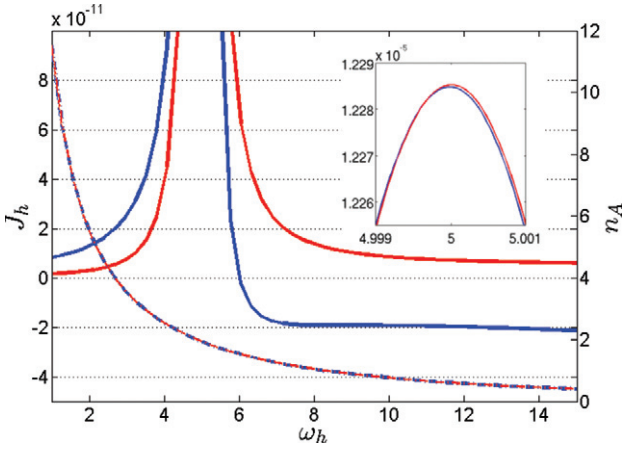

Fig. 4: (Colour on-line) Comparison between the local (blue line) and the global (red line) approaches. The population of subsystem A (dashed line), and the heat flow from the hot bath $\mathcal{J}_h$ (solid line), as a function of ω_h. The inset describes the domain of near resonance $\omega_h \approx \omega_c$. Here $T_h = 12$, $T_c = 10$, $\omega_c = 5$, $\epsilon = 10^{-3}$ and $\kappa = 10^{-7}$.

such as the local population $\hat{\mathbf{n}}_A \equiv \langle \hat{\mathbf{a}}^\dagger \hat{\mathbf{a}} \rangle$ the two approaches converge to the thermal population when $\epsilon \ll \{\omega_h, \omega_c, \sqrt{|\omega_h - \omega_c|}\}$. However, the non-local observables such as the current $\mathcal{J}_h$ deviate qualitatively. In the local approach when $\frac{\omega_c}{T_c} < \frac{\omega_h}{T_h}$ the second law is violated: the heat flow becomes negative for all values of the coupling ϵ while for the global approach $\mathcal{J}_h$ is always positive, cf. fig. 3.

The local approach is also not reliable even for parameters where the second law is obeyed: $\frac{\omega_c}{T_c} > \frac{\omega_h}{T_h}$. Deviations from the exact global approach appear in the favorable domain of small ϵ, as seen in fig. 4 displaying $\mathcal{J}_h$ for a wide range of ω_h. It is noteworthy that the behavior of the heat flows observed in fig. 4 will be the same for all ϵ, also when $\epsilon \ll \kappa$. The only domain where the global approach breaks down is on resonance, when $\omega_h = \omega_c$ and $\epsilon < \kappa$. At this point, the secular approximation is not justified since the two Bohr frequencies $\omega_\pm$ are not well separated, and on the time scale $1/\kappa\omega^3$, one can not neglect rotating terms such as $e^{i2\epsilon}$ [21].

Additional insight is obtained when examining the covariance matrix for the two-mode Gaussian state (see [15] for details). The correlations between subsystems A and B is fully determined by the set of correlation functions $\{\mathrm{cor}(x_A, x_B), \mathrm{cor}(x_A, p_B), \mathrm{cor}(p_A, x_B), \mathrm{cor}(p_A, p_B)\}$. Here $\{x, p\}$ are the position and momentum coordinates of the subsystems. In both approaches $\mathrm{cor}(x_A, x_B)$ and $\mathrm{cor}(p_A, p_B)$ are equal for small ϵ. The two additional correlations, $\mathrm{cor}(x_A, p_B)$ and $\mathrm{cor}(p_A, x_B)$, vanish at steady state in the global approach, where in the local approach they remain finite. Thus, in the local approach the nodes are over correlated compared to the global approach. It should be noted that in steady state none of the approaches generate entanglement. The two-mode Gaussian state is a separable state according to the separability criterion for continuous variable systems [22,23].

To summarize: As expected, the local dynamical approach is incorrect for strong coupling between the subsystems. In the weak coupling limit, local observables converge to their correct value. The non-local observables such as heat currents are qualitatively and quantitatively erroneous in the local MME. A strong indication is the violation of the second law of thermodynamics. The completely positive LGKS generator is a desired form for the master equation. However, for consistency with the physical world, a microscopic global derivation of the master equation is required. Such approaches are consistent with thermodynamics [24–28].

* * *

We want to thank Robert Alicki, Lajos Diosi and Angel Rivas for fruitful discussions and helpful comments. This work was supported by the Israel Science Foundation and by the COST action MP1209 "Thermodynamics in the quantum regime".

REFERENCES

[1] van der Wiel W. G., De Franceschi S., Elzerman J. M., Fujisawa T., Tarucha S. and Kouwenhoven L. P., *Rev. Mod. Phys.*, **75** (2002) 1.
[2] Kohler S., Lehmann J. and Hänggi P., *Phys. Rep.*, **406** (2005) 379.
[3] Kosloff R. and Levy A., *Annu. Rev. Phys. Chem.*, **65** (2014) 365.
[4] Lindblad G., *J. Phys. A: Math. Gen.*, **48** (1976) 119.
[5] Gorini V., Kossakowski A. and Sudarshan E. C. G., *J. Math. Phys.*, **17** (1976) 821.
[6] Alicki R., *J. Phys. A: Math. Gen.*, **12** (1979) L103.
[7] Kosloff R., *Entropy*, **15** (2013) 2100.

[8] Mari A. and Eisert J., *Phys. Rev. Lett.*, **108** (2012) 120602.
[9] Linden N., Popescu S. and Skrzypczyk P., *Phys. Rev. Lett.*, **105** (2010) 130401.
[10] Restrepo J., Ciuti C. and Favero I., *Phys. Rev. Lett.*, **112** (2014) 013601.
[11] Atalaya J. and Gorelik L. Y., *Phys. Rev. B*, **85** (2012) 245309.
[12] Wilson-Rae I., Zoller P. and Imamoglu A., *Phys. Rev. Lett.*, **92** (2004) 075507.
[13] Wichterich H., Henrich M. J., Breuer H.-P., Gemmer J. and Michel M., *Phys. Rev. E*, **76** (2007) 031115.
[14] Brunner N., Huber M., Linden N., Popescu S., Silva R. and Skrzypczyk P., *Phys. Rev. E*, **89** (2014) 032115.
[15] See supplemental material at: `http://www.fh.huji.ac.il/~ronnie/Papers/Supplument-the-local-approach.pdf`.
[16] Novotný T., *Europhys. Lett.*, **59** (2002) 648.
[17] Davies E., *Commun. Math. Phys.*, **39** (1974) 91.
[18] Breuer H.-P. and Petruccione F., *Open Quantum Systems* (Oxford University Press) 2002.
[19] Spohn H., *J. Math. Phys.*, **19** (1978) 1227.
[20] Levy A., Alicki R. and Kosloff R., *Phys. Rev. E*, **85** (2012) 061126.
[21] Rivas A., Plato A. D. K., Huelga S. F. and Plenio M. B., *New J. Phys.*, **12** (2010) 11303.
[22] Simon R., *Phys. Rev. Lett.*, **84** (2000) 2726.
[23] Duan L.-M., Giedke G., Cirac J. I. and Zoller P., *Phys. Rev. Lett.*, **84** (2000) 2722.
[24] Correa L. A., Palao J. P., Adesso G. and Alonso D., *Phys. Rev. E*, **87** (2013) 042131.
[25] Martinez E. A. and Paz J. P., *Phys. Rev. Lett.*, **110** (2013) 130406.
[26] Geva E., Kosloff R. and Skinner J., *J. Chem. Phys.*, **102** (1995) 8541.
[27] Gelbwaser-Klimovsky D., Alicki R. and Kurizki G., *EPL*, **103** (2013) 60005.
[28] Kolář M., Gelbwaser-Klimovsky D., Alicki R. and Kurizki G., *Phys. Rev. Lett.*, **109** (2012) 090601.

Supplemental Material: The Local Approach to Quantum Transport May Violate the Second Law of Thermodynamics

Amikam Levy and Ronnie Kosloff

Institute of Chemistry The Hebrew University,

Jerusalem 91904, Israel

I. LOCAL APPROACH HEAT FLOW

The heat flow from the hot bath calculated in the local approach is given by:

$$\mathcal{J}_h = \omega_h \gamma_h \left(e^{-\beta_h \omega_h} - \langle a^\dagger a \rangle \left(\delta e^{-\beta_h \omega_h} + 1 \right) \right) - \frac{\epsilon \gamma_h}{2} \langle X \rangle \left(\delta e^{-\beta_h \omega_h} + 1 \right)$$

placing the steady state solution of Eq.(8) for $\langle a^\dagger a \rangle$ and $\langle X \rangle$, we obtain:

$$\mathcal{J}_h = \left(e^{\beta_c \omega_c} - e^{\beta_h \omega_h} \right) \frac{4\epsilon^2 \gamma_c \gamma_h e^{\beta_c \omega_c + \beta_h \omega_h} \left(\omega_c \gamma_h e^{\beta_c \omega_c} \left(e^{\beta_h \omega_h} + \delta \right) + \gamma_c \omega_h e^{\beta_h \omega_h} \left(e^{\beta_c \omega_c} + \delta \right) \right)}{\gamma_c^3 \gamma_h e^{2\beta_h \omega_h} \left(e^{\beta_c \omega_c} + \delta \right)^3 \left(e^{\beta_h \omega_h} + \delta \right) + 2\gamma_c^2 \left(e^{\beta_c \omega_c} + \delta \right)^2 e^{\beta_c \omega_c + \beta_h \omega_h}} \cdot \cdot \cdot$$

$$\frac{}{\times \left(\gamma_h^2 \left(e^{\beta_h \omega_h} + \delta \right)^2 + 2\epsilon^2 e^{2\beta_h \omega_h} \right) + \gamma_c \gamma_h e^{2\beta_c \omega_c} \left(e^{\beta_c \omega_c} + \delta \right) \left(e^{\beta_h \omega_h} + \delta \right)} \cdot \cdot \cdot$$

$$\frac{}{\times \left(4e^{2\beta_h \omega_h} ((\omega_c - \omega_h)^2 + 2\epsilon^2) + \gamma_h^2 \left(e^{\beta_h \omega_h} + \delta \right)^2 \right) + 4\epsilon^2 \gamma_h^2 e^{3\beta_c \omega_c + \beta_h \omega_h} \left(e^{\beta_h \omega_h} + \delta \right)^2}$$

II. THE GLOBAL GENERATOR IN THE LOCAL REPRESENTATION

The global approach creates an indirect coupling of the subsystems with the baths. This indirect coupling is evident once we write the the global generator in the local representation, for example, Eq. (11) takes the form:

$$\begin{aligned}
\mathcal{L}_h \rho_s = & \gamma_h^+ c^4 \left(\hat{\mathbf{a}} \hat{\boldsymbol{\rho}}_s \hat{\mathbf{a}}^\dagger - \tfrac{1}{2} \{ \hat{\mathbf{a}}^\dagger \hat{\mathbf{a}}, \hat{\boldsymbol{\rho}}_s \} + e^{-\beta_h \omega_+} (\hat{\mathbf{a}}^\dagger \hat{\boldsymbol{\rho}}_s \hat{\mathbf{a}} - \tfrac{1}{2} \{ \hat{\mathbf{a}} \hat{\mathbf{a}}^\dagger, \hat{\boldsymbol{\rho}}_s \}) \right) \\
& + \gamma_h^- s^4 \left(\hat{\mathbf{a}} \hat{\boldsymbol{\rho}}_s \hat{\mathbf{a}}^\dagger - \tfrac{1}{2} \{ \hat{\mathbf{a}}^\dagger \hat{\mathbf{a}}, \hat{\boldsymbol{\rho}}_s \} + e^{-\beta_h \omega_-} (\hat{\mathbf{a}}^\dagger \hat{\boldsymbol{\rho}}_s \hat{\mathbf{a}} - \tfrac{1}{2} \{ \hat{\mathbf{a}} \hat{\mathbf{a}}^\dagger, \hat{\boldsymbol{\rho}}_s \}) \right) \\
& + \gamma_h^+ c^2 s^2 \left(\hat{\mathbf{b}} \hat{\boldsymbol{\rho}}_s \hat{\mathbf{b}}^\dagger - \tfrac{1}{2} \{ \hat{\mathbf{b}}^\dagger \hat{\mathbf{b}}, \rho_s \} + e^{-\beta_h \omega_+} (\hat{\mathbf{b}}^\dagger \hat{\boldsymbol{\rho}}_s \hat{\mathbf{b}} - \tfrac{1}{2} \{ \hat{\mathbf{b}} \hat{\mathbf{b}}^\dagger, \hat{\boldsymbol{\rho}}_s \}) \right) \\
& + \gamma_h^- c^2 s^2 \left(\hat{\mathbf{b}} \hat{\boldsymbol{\rho}}_s \hat{\mathbf{b}}^\dagger - \tfrac{1}{2} \{ \hat{\mathbf{b}}^\dagger \hat{\mathbf{b}}, \rho_s \} + e^{-\beta_h \omega_-} (\hat{\mathbf{b}}^\dagger \hat{\boldsymbol{\rho}}_s \hat{\mathbf{b}} - \tfrac{1}{2} \{ \hat{\mathbf{b}} \hat{\mathbf{b}}^\dagger, \hat{\boldsymbol{\rho}}_s \}) \right) \\
& + \gamma_h^+ c^3 s \left(\hat{\mathbf{a}} \hat{\boldsymbol{\rho}}_s \hat{\mathbf{b}}^\dagger + \hat{\mathbf{b}} \hat{\boldsymbol{\rho}}_s \hat{\mathbf{a}}^\dagger - \tfrac{1}{2} \{ \hat{\mathbf{a}}^\dagger \hat{\mathbf{b}} + \hat{\mathbf{b}}^\dagger \hat{\mathbf{a}}, \rho_s \} + e^{-\beta_h \omega_+} (\hat{\mathbf{a}}^\dagger \hat{\boldsymbol{\rho}}_s \hat{\mathbf{b}} + \hat{\mathbf{b}}^\dagger \hat{\boldsymbol{\rho}}_s \hat{\mathbf{a}} - \tfrac{1}{2} \{ \hat{\mathbf{a}}^\dagger \hat{\mathbf{b}} + \hat{\mathbf{b}}^\dagger \hat{\mathbf{a}}, \rho_s \}) \right) \\
& - \gamma_h^- c s^3 \left(\hat{\mathbf{a}} \hat{\boldsymbol{\rho}}_s \hat{\mathbf{b}}^\dagger + \hat{\mathbf{b}} \hat{\boldsymbol{\rho}}_s \hat{\mathbf{a}}^\dagger - \tfrac{1}{2} \{ \hat{\mathbf{a}}^\dagger \hat{\mathbf{b}} + \hat{\mathbf{b}}^\dagger \hat{\mathbf{a}}, \rho_s \} + e^{-\beta_h \omega_-} (\hat{\mathbf{a}}^\dagger \hat{\boldsymbol{\rho}}_s \hat{\mathbf{b}} + \hat{\mathbf{b}}^\dagger \hat{\boldsymbol{\rho}}_s \hat{\mathbf{a}} - \tfrac{1}{2} \{ \hat{\mathbf{a}}^\dagger \hat{\mathbf{b}} + \hat{\mathbf{b}}^\dagger \hat{\mathbf{a}}, \rho_s \}) \right)
\end{aligned}$$

where we have defined $s \equiv \sin(\theta)$ and $c \equiv \cos(\theta)$.

III. THE COVARIANCE MATRIX AND THE CORRELATION FUNCTIONS

We define a vector of the position and momentum operators $\xi = (x_A \ p_A \ x_B \ p_B)$. The covariance matrix is defined through $V_{ij} = \langle \{ \Delta\xi_i, \Delta\xi_j \} \rangle$, using the definitions $\{ \Delta\xi_i, \Delta\xi_j \} = \frac{1}{2} (\Delta\xi_i \Delta\xi_j + \Delta\xi_j \Delta\xi_i)$ and $\Delta\xi_i = \xi_i - \langle \xi_i \rangle$. The steady state coveraiance matrix is given by

$$V^{local} = \begin{pmatrix} \langle a^\dagger a\rangle + \frac{1}{2} & 0 & \frac{1}{2}\langle X\rangle & -\frac{1}{2}\langle Y\rangle \\ 0 & \langle a^\dagger a\rangle + \frac{1}{2} & \frac{1}{2}\langle Y\rangle & \frac{1}{2}\langle X\rangle \\ \frac{1}{2}\langle X\rangle & \frac{1}{2}\langle Y\rangle & \langle b^\dagger b\rangle + \frac{1}{2} & 0 \\ -\frac{1}{2}\langle Y\rangle & \frac{1}{2}\langle X\rangle & 0 & \langle b^\dagger b\rangle + \frac{1}{2} \end{pmatrix}$$

$$V^{global} = \begin{pmatrix} \langle d_+^\dagger d_+\rangle c^2 + \langle d_-^\dagger d_-\rangle s^2 + \frac{1}{2} & 0 & (\langle d_+^\dagger d_+\rangle - \langle d_-^\dagger d_-\rangle)cs & 0 \\ 0 & \langle d_+^\dagger d_+\rangle c^2 + \langle d_-^\dagger d_-\rangle s^2 + \frac{1}{2} & 0 & (\langle d_+^\dagger d_+\rangle - \langle d_-^\dagger d_-\rangle)cs \\ (\langle d_+^\dagger d_+\rangle - \langle d_-^\dagger d_-\rangle)cs & 0 & \langle d_+^\dagger d_+\rangle s^2 + \langle d_-^\dagger d_-\rangle c^2 + \frac{1}{2} & 0 \\ 0 & (\langle d_+^\dagger d_+\rangle - \langle d_-^\dagger d_-\rangle)cs & 0 & \langle d_+^\dagger d_+\rangle s^2 + \langle d_-^\dagger d_-\rangle c^2 + \frac{1}{2} \end{pmatrix}$$

with $s \equiv \sin(\theta)$ and $c \equiv \cos(\theta)$. The structure of the covariance matrix in both approaches immediately imply that the two subsystems are separable [1].

The correlation functions are defined by:

$$cor(\xi_i, \xi_j) = \frac{\langle \Delta\xi_i \Delta\xi_j\rangle}{\sqrt{\langle \Delta\xi_i^2\rangle \langle \Delta\xi_j^2\rangle}}$$

---

[1] R. Simon, Phys. Rev. Lett. **84**, 2726 (2000).

Chapter 4

Quantum Absorption Refrigerator

Quantum Absorption Refrigerator
Amikam Levy and Ronnie Kosloff
Published in: Phys. Rev. Lett., vol. 108, page 070604, 2012

Quantum Absorption Refrigerator

Amikam Levy and Ronnie Kosloff
Institute of Chemistry, The Hebrew University, Jerusalem 91904, Israel
(Received 30 August 2011; published 17 February 2012)

A quantum absorption refrigerator driven by noise is studied with the purpose of determining the limitations of cooling to absolute zero. The model consists of a working medium coupled simultaneously to hot, cold, and noise baths. Explicit expressions for the cooling power are obtained for Gaussian and Poisson white noise. The quantum model is consistent with the first and second laws of thermodynamics. The third law is quantified; the cooling power $\mathcal{J}_c$ vanishes as $\mathcal{J}_c \propto T_c^{\alpha}$, when $T_c \to 0$, where $\alpha = d + 1$ for dissipation by emission and absorption of quanta described by a linear coupling to a thermal bosonic field, where d is the dimension of the bath.

DOI: 10.1103/PhysRevLett.108.070604 PACS numbers: 05.70.Ln, 03.65.Yz, 05.30.−d, 07.20.Pe

The absorption chiller is a refrigerator which employs a heat source to replace mechanical work for driving a heat pump [1]. The first device was developed in 1850 by the Carré brothers which became the first useful refrigerator. In 1926, Einstein and Szilárd invented an absorption refrigerator with no moving parts [2]. This idea has been incorporated recently to an autonomous quantum absorption refrigerator with no external intervention [3,4]. The present study is devoted to a quantum absorption refrigerator driven by noise; for an experimental realization, cf. [5]. The objective is to study the scaling of the optimal cooling power when the absolute zero temperature is approached.

This study is embedded in the field of quantum thermodynamics, the study of thermodynamical processes within the context of quantum dynamics. Historically, consistence with thermodynamics led to Planck's law, the basics of quantum theory. Following the ideas of Planck on black body radiation, Einstein five years later (1905) quantized the electromagnetic field [6]. Quantum thermodynamics is devoted to unraveling the intimate connection between the laws of thermodynamics and their quantum origin [3,4,7–22]. In this tradition, the present study is aimed toward the quantum study of the third law of thermodynamics [23,24], in particular, quantifying the unattainability principle [25]: What is the scaling of the cooling power $\mathcal{J}_c$ of a refrigerator when the cold bath temperature approaches the absolute zero $\mathcal{J}_c \propto T_c^{\alpha}$ when $T_c \to 0$?

The quantum trickle.—The minimum requirement for a quantum thermodynamical device is a system connected simultaneously to three reservoirs [26]. These baths are termed hot, cold, and work reservoir as described in Fig. 1. A quantum description requires a representation of the dynamics working medium and the three heat reservoirs. A reduced description is employed in which the dynamics of the working medium is described by the Heisenberg equation for the operator $\hat{\mathbf{O}}$ for open systems [27,28]:

$$\frac{d}{dt}\hat{\mathbf{O}} = \frac{i}{\hbar}[\hat{\mathbf{H}}_s, \hat{\mathbf{O}}] + \frac{\partial \hat{\mathbf{O}}}{\partial t} + \mathcal{L}_h(\hat{\mathbf{O}}) + \mathcal{L}_c(\hat{\mathbf{O}}) + \mathcal{L}_w(\hat{\mathbf{O}}), \tag{1}$$

where $\hat{\mathbf{H}}_s$ is the system Hamiltonian and $\mathcal{L}_g$ are the dissipative completely positive superoperators for each bath ($g = h, c, w$). A minimal Hamiltonian describing the essence of the quantum refrigerator is composed of three interacting oscillators:

$$\begin{aligned} \hat{\mathbf{H}}_s &= \hat{\mathbf{H}}_0 + \hat{\mathbf{H}}_{\text{int}}, \\ \hat{\mathbf{H}}_0 &= \hbar\omega_h \hat{\mathbf{a}}^\dagger \hat{\mathbf{a}} + \hbar\omega_c \hat{\mathbf{b}}^\dagger \hat{\mathbf{b}} + \hbar\omega_w \hat{\mathbf{c}}^\dagger \hat{\mathbf{c}}, \\ \hat{\mathbf{H}}_{\text{int}} &= \hbar\omega_{\text{int}}(\hat{\mathbf{a}}^\dagger \hat{\mathbf{b}}\,\hat{\mathbf{c}} + \hat{\mathbf{a}}\hat{\mathbf{b}}^\dagger \hat{\mathbf{c}}^\dagger). \end{aligned} \tag{2}$$

$\hat{\mathbf{H}}_{\text{int}}$ represents an annihilation of excitations on the work and cold bath simultaneous with creating an

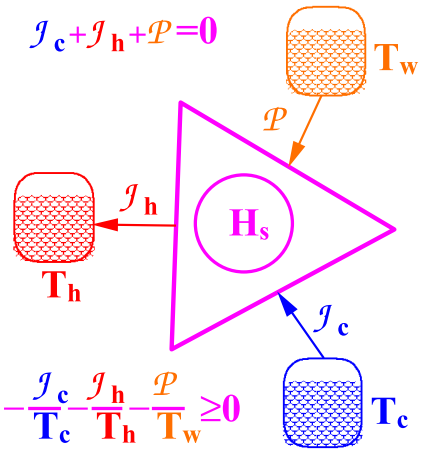

FIG. 1 (color online). The quantum trickle: A quantum heat pump designated by the Hamiltonian $\hat{\mathbf{H}}_s$ is coupled to a work reservoir with temperature T_w, a hot reservoir with temperature T_h, and a cold reservoir with temperature T_c. The heat and work currents are indicated. In the steady state, $\mathcal{J}_h + \mathcal{J}_c + \mathcal{P} = 0$.

excitation in the hot bath. In an open quantum system, the superoperators $\mathcal{L}_g$ represent a thermodynamic isothermal partition allowing heat flow from the bath to the system. Such a partition is equivalent to the weak coupling limit between the system and bath [11]. The superoperators $\mathcal{L}_g$ are derived from the Hamiltonian:

$$\hat{\mathbf{H}} = \hat{\mathbf{H}}_s + \hat{\mathbf{H}}_h + \hat{\mathbf{H}}_c + \hat{\mathbf{H}}_w + \hat{\mathbf{H}}_{sh} + \hat{\mathbf{H}}_{sc} + \hat{\mathbf{H}}_{sw}, \quad (3)$$

where $\hat{\mathbf{H}}_g$ are bath Hamiltonians and $\hat{\mathbf{H}}_{sg}$ represent system bath coupling. Each of the oscillators is linearly coupled to a heat reservoir, for example, for the hot bath: $\hat{\mathbf{H}}_{sh} = \lambda_{sh}(\hat{\mathbf{a}}\hat{\mathbf{A}}_h^\dagger + \hat{\mathbf{a}}^\dagger\hat{\mathbf{A}}_h)$. Each reservoir individually should equilibrate the working medium to thermal equilibrium with the reservoir temperature. In general, the derivation of a thermodynamically consistent master equation is technically very difficult [29]. Typical problems are approximations that violate the laws of thermodynamics. We therefore require that the master equations fulfill the thermodynamical laws. Under steady state conditions of operation, they become:

$$\mathcal{J}_h + \mathcal{J}_c + \mathcal{P} = 0, \qquad -\frac{\mathcal{J}_h}{T_h} - \frac{\mathcal{J}_c}{T_c} - \frac{\mathcal{P}}{T_w} \geq 0, \quad (4)$$

where $\mathcal{J}_k = \langle \mathcal{L}_k(\hat{\mathbf{H}})\rangle$. The first equality represents conservation of energy (first law) [8,9], and the second inequality represents positive entropy production in the universe $\Sigma_u \geq 0$ (second law). For refrigeration, $T_w \geq T_h \geq T_c$. From the second law, the scaling exponent $\alpha \geq 1$ [12].

Gaussian-noise-driven refrigerator.—In the absorption refrigerator, the noise source replaces the work bath and its contact $\hbar\omega_w\hat{\mathbf{c}}^\dagger\hat{\mathbf{c}}$, leading to

$$\hat{\mathbf{H}}_{\text{int}} = f(t)(\hat{\mathbf{a}}^\dagger\hat{\mathbf{b}} + \hat{\mathbf{a}}\hat{\mathbf{b}}^\dagger) = f(t)\hat{\mathbf{X}}, \quad (5)$$

where $f(t)$ is the noise field. $\hat{\mathbf{X}} = (\hat{\mathbf{a}}^\dagger\hat{\mathbf{b}} + \hat{\mathbf{a}}\hat{\mathbf{b}}^\dagger)$ is the generator of a swap operation between the two oscillators and is part of a set of $SU(2)$ operators, $\hat{\mathbf{Y}} = i(\hat{\mathbf{a}}^\dagger\hat{\mathbf{b}} - \hat{\mathbf{a}}\hat{\mathbf{b}}^\dagger)$, $\hat{\mathbf{Z}} = (\hat{\mathbf{a}}^\dagger\hat{\mathbf{a}} - \hat{\mathbf{b}}^\dagger\hat{\mathbf{b}})$ and the Casimir operator $\hat{\mathbf{N}} = (\hat{\mathbf{a}}^\dagger\hat{\mathbf{a}} + \hat{\mathbf{b}}^\dagger\hat{\mathbf{b}})$.

We first study a Gaussian source of white noise characterized by zero mean $\langle f(t)\rangle = 0$ and delta time correlation $\langle f(t)f(t')\rangle = 2\eta\delta(t - t')$. The Heisenberg equation for a time-independent operator $\hat{\mathbf{O}}$ reduced to

$$\frac{d}{dt}\hat{\mathbf{O}} = i[\hat{\mathbf{H}}_s, \hat{\mathbf{O}}] + \mathcal{L}_n(\hat{\mathbf{O}}) + \mathcal{L}_h(\hat{\mathbf{O}}) + \mathcal{L}_c(\hat{\mathbf{O}}), \quad (6)$$

where $\hat{\mathbf{H}}_s = \hbar\omega_h\hat{\mathbf{a}}^\dagger\hat{\mathbf{a}} + \hbar\omega_c\hat{\mathbf{b}}^\dagger\hat{\mathbf{b}}$. The noise dissipator for Gaussian noise is $\mathcal{L}_n(\hat{\mathbf{O}}) = -\eta[\hat{\mathbf{X}}, [\hat{\mathbf{X}}, \hat{\mathbf{O}}]]$ [30]. The same master equation is obtained for a system subject to a weak quantum measurement of the operator $\hat{\mathbf{X}}$ [28]. The next step is to derive the quantum master equation of each reservoir. We assume that the reservoirs are uncorrelated and also uncorrelated with the driving noise. These conditions simplify the derivation of $\mathcal{L}_h$, which become the standard energy relaxation terms driving oscillator $\omega_h\hat{\mathbf{a}}^\dagger\hat{\mathbf{a}}$ to thermal equilibrium with temperature T_h, and $\mathcal{L}_c$ drives oscillator $\hbar\omega_b\hat{\mathbf{b}}^\dagger\hat{\mathbf{b}}$ to equilibrium T_c [28]:

$$\begin{aligned}\mathcal{L}_h(\hat{\mathbf{O}}) &= \Gamma_h(N_h + 1)(\hat{\mathbf{a}}^\dagger\hat{\mathbf{O}}\,\hat{\mathbf{a}} - \tfrac{1}{2}\{\hat{\mathbf{a}}^\dagger\hat{\mathbf{a}}, \hat{\mathbf{O}}\}) \\ &\quad + \Gamma_h N_h(\hat{\mathbf{a}}\,\hat{\mathbf{O}}\,\hat{\mathbf{a}}^\dagger - \tfrac{1}{2}\{\hat{\mathbf{a}}\hat{\mathbf{a}}^\dagger, \hat{\mathbf{O}}\}), \\ \mathcal{L}_c(\hat{\mathbf{O}}) &= \Gamma_c(N_c + 1)(\hat{\mathbf{b}}^\dagger\hat{\mathbf{O}}\,\hat{\mathbf{b}} - \tfrac{1}{2}\{\hat{\mathbf{b}}^\dagger\hat{\mathbf{b}}, \hat{\mathbf{O}}\}) \\ &\quad + \Gamma_c N_c(\hat{\mathbf{b}}\,\hat{\mathbf{O}}\,\hat{\mathbf{b}}^\dagger - \tfrac{1}{2}\{\hat{\mathbf{b}}\hat{\mathbf{b}}^\dagger, \hat{\mathbf{O}}\}).\end{aligned} \quad (7)$$

In the absence of the stochastic driving field, these equations drive oscillators a and b separately to thermal equilibrium provided that $N_h = [\exp(\frac{\hbar\omega_h}{kT_h}) - 1]^{-1}$ and $N_c = [\exp(\frac{\hbar\omega_c}{kT_c}) - 1]^{-1}$. The kinetic coefficients $\Gamma_{h/c}$ are determined from the bath density functions [11].

The equations of motion are closed to the $SU(2)$ set of operators. To derive the cooling current $\mathcal{J}_c = \langle \mathcal{L}_c(\hbar\omega_c\hat{\mathbf{b}}^\dagger\hat{\mathbf{b}})\rangle$, we solve for stationary solutions of $\hat{\mathbf{N}}$ and $\hat{\mathbf{Z}}$, obtaining

$$\mathcal{J}_c = \hbar\omega_c\frac{(N_c - N_h)}{(2\eta)^{-1} + \Gamma_h^{-1} + \Gamma_c^{-1}}. \quad (8)$$

Cooling occurs for $N_c > N_h \Rightarrow \frac{\omega_h}{T_h} > \frac{\omega_c}{T_c}$. The coefficient of performance (COP) for the absorption chiller is defined by the relation $\text{COP} = \frac{\mathcal{J}_c}{\mathcal{J}_n}$; with the help of Eq. (8), we obtain the Otto cycle COP [31]:

$$\text{COP} = \frac{\omega_c}{\omega_h - \omega_c} \leq \frac{T_c}{T_h - T_c}. \quad (9)$$

A different viewpoint starts from the high temperature limit of the work bath T_w based on the weak coupling limit in Eqs. (2) and (3); then

$$\begin{aligned}\mathcal{L}_w(\hat{\mathbf{O}}) &= \Gamma_w(N_w + 1)(\hat{\mathbf{a}}^\dagger\hat{\mathbf{b}}\,\hat{\mathbf{O}}\,\hat{\mathbf{b}}^\dagger\hat{\mathbf{a}} - \tfrac{1}{2}\{\hat{\mathbf{a}}^\dagger\hat{\mathbf{a}}\,\hat{\mathbf{b}}\,\hat{\mathbf{b}}^\dagger, \hat{\mathbf{O}}\}) \\ &\quad + \Gamma_w N_w(\hat{\mathbf{a}}\hat{\mathbf{b}}^\dagger\hat{\mathbf{O}}\hat{\mathbf{a}}^\dagger\hat{\mathbf{b}} - \tfrac{1}{2}\{\hat{\mathbf{a}}\hat{\mathbf{a}}^\dagger\hat{\mathbf{b}}^\dagger\hat{\mathbf{b}}, \hat{\mathbf{O}}\}),\end{aligned} \quad (10)$$

where $N_w = [\exp(\frac{\hbar\omega_w}{kT_h}) - 1]^{-1}$. At a finite temperature, $\mathcal{L}_w(\hat{\mathbf{O}})$ does not lead to a closed set of equations. But in the limit of $T_w \to \infty$ it becomes equivalent to the Gaussian noise generator: $\mathcal{L}_w(\hat{\mathbf{O}}) = -\eta/2([\hat{\mathbf{X}}, [\hat{\mathbf{X}}, \hat{\mathbf{O}}]] + [\hat{\mathbf{Y}}, [\hat{\mathbf{Y}}, \hat{\mathbf{O}}]])$, where $\eta = \Gamma_w N_w$. This noise generator leads to the same current $\mathcal{J}_c$ and COP as Eqs. (8) and (9). We conclude that Gaussian noise represents the singular bath limit equivalent to $T_w \to \infty$. As a result, the entropy generated by the noise is zero.

The solutions are consistent with the first and second laws of thermodynamics. The COP is restricted by the Carnot COP. For low temperatures, the optimal cooling current can be approximated by $\mathcal{J}_c \simeq \omega_c\Gamma_c N_c$. Coupling to a thermal bosonic field such as an electromagnetic or acoustic phonon field implies $\Gamma_c \propto \omega_c^d$, where d is the heat bath dimension. Optimizing the cooling current with respect to ω_c, one obtains that the exponent α quantifying the third law $\mathcal{J}_c \propto T_c^\alpha$ is given by $\alpha = d + 1$.

Poisson-noise-driven refrigerator.—Poisson white noise can be referred to as a sequence of independent random pulses with exponential interarrival times. These impulses drive the coupling between the oscillators in contact with the hot and cold bath leading to [32]

$$\frac{d\hat{\mathbf{O}}}{dt} = (i/\hbar)[\tilde{\mathbf{H}}, \hat{\mathbf{O}}] - (i/\hbar)\lambda\langle\xi\rangle[\hat{\mathbf{X}}, \hat{\mathbf{O}}] + \lambda\left(\int_{-\infty}^{\infty} d\xi P(\xi) e^{(i/\hbar)\xi\hat{\mathbf{X}}}\hat{\mathbf{O}}e^{(-i/\hbar)\xi\hat{\mathbf{X}}} - \hat{\mathbf{O}}\right), \quad (11)$$

where $\tilde{\mathbf{H}}$ is the total Hamiltonian including the baths. λ is the rate of events, and ξ is the impulse strength averaged over a distribution $P(\xi)$. Using the Hadamard lemma and the fact that the operators form a closed $SU(2)$ algebra, we can separate the noise contribution to its unitary and dissipation parts, leading to the master equation

$$\frac{d\hat{\mathbf{O}}}{dt} = (i/\hbar)[\tilde{\mathbf{H}}, \hat{\mathbf{O}}] + (i/\hbar)[\hat{\mathbf{H}}', \hat{\mathbf{O}}] + \mathcal{L}_n(\hat{\mathbf{O}}). \quad (12)$$

The unitary part is generated with the addition of the Hamiltonian $\hat{\mathbf{H}}' = \hbar\epsilon\hat{\mathbf{X}}$ with the interaction

$$\epsilon = -\frac{\lambda}{2}\int d\xi P(\xi)[2\xi/\hbar - \sin(2\xi/\hbar)].$$

This term can cause a direct heat leak from the hot to cold bath. The noise generator $\mathcal{L}_n(\hat{\boldsymbol{\rho}})$ can be reduced to the form $\mathcal{L}_n(\hat{\mathbf{O}}) = -\eta[\hat{\mathbf{X}}, [\hat{\mathbf{X}}, \hat{\mathbf{O}}]]$, with a modified noise parameter:

$$\eta = \frac{\lambda}{4}\left(1 - \int d\xi P(\xi)\cos(2\xi/\hbar)\right).$$

The Poisson noise generates an effective Hamiltonian which is composed of $\tilde{\mathbf{H}}$ and $\hat{\mathbf{H}}'$, modifying the energy levels of the working medium. This new Hamiltonian structure has to be incorporated in the derivation of the master equation; otherwise, the second law will be violated. The first step is to rewrite the system Hamiltonian in its dressed form. A new set of bosonic operators is defined:

$$\begin{aligned}\hat{\mathbf{A}}_1 &= \hat{\mathbf{a}}\cos(\theta) + \hat{\mathbf{b}}\sin(\theta),\\ \hat{\mathbf{A}}_2 &= \hat{\mathbf{b}}\cos(\theta) - \hat{\mathbf{a}}\sin(\theta).\end{aligned} \quad (13)$$

The dressed Hamiltonian is given by

$$\hat{\mathbf{H}}_s = \hbar\Omega_+\hat{\mathbf{A}}_1^\dagger\hat{\mathbf{A}}_1 + \hbar\Omega_-\hat{\mathbf{A}}_2^\dagger\hat{\mathbf{A}}_2, \quad (14)$$

where $\Omega_\pm = \frac{\omega_h+\omega_c}{2} \pm \sqrt{[(\omega_h-\omega_c)/2]^2+\epsilon^2}$ and $\cos^2(\theta) = \frac{\omega_h-\Omega_-}{\Omega_+-\Omega_-}$ Eq. (14) impose the restriction $\Omega_\pm > 0$, which can be translated to $\omega_h\omega_c > \epsilon^2$. The master equation in the Heisenberg representation becomes

$$\frac{d\hat{\mathbf{O}}}{dt} = (i/\hbar)[\hat{\mathbf{H}}_s, \hat{\mathbf{O}}] + \mathcal{L}_h(\hat{\mathbf{O}}) + \mathcal{L}_c(\hat{\mathbf{O}}) + \mathcal{L}_n(\hat{\mathbf{O}}), \quad (15)$$

where

$$\begin{aligned}\mathcal{L}_h(\hat{\mathbf{O}}) &= \gamma_1^h\mathbf{c}^2(\hat{\mathbf{A}}_1\hat{\mathbf{O}}\hat{\mathbf{A}}_1^\dagger - \tfrac{1}{2}\{\hat{\mathbf{A}}_1\hat{\mathbf{A}}_1^\dagger, \hat{\mathbf{O}}\}) + \gamma_2^h\mathbf{c}^2(\hat{\mathbf{A}}_1^\dagger\hat{\mathbf{O}}\hat{\mathbf{A}}_1 - \tfrac{1}{2}\{\hat{\mathbf{A}}_1^\dagger\hat{\mathbf{A}}_1, \hat{\mathbf{O}}\}) + \gamma_3^h\mathbf{s}^2(\hat{\mathbf{A}}_2\hat{\mathbf{O}}\hat{\mathbf{A}}_2^\dagger - \tfrac{1}{2}\{\hat{\mathbf{A}}_2\hat{\mathbf{A}}_2^\dagger, \hat{\mathbf{O}}\}) + \gamma_4^h\mathbf{s}^2(\hat{\mathbf{A}}_2^\dagger\hat{\mathbf{O}}\hat{\mathbf{A}}_2 - \tfrac{1}{2}\{\hat{\mathbf{A}}_2^\dagger\hat{\mathbf{A}}_2, \hat{\mathbf{O}}\}),\\ \mathcal{L}_c(\hat{\mathbf{O}}) &= \gamma_1^c\mathbf{s}^2(\hat{\mathbf{A}}_1\hat{\mathbf{O}}\hat{\mathbf{A}}_1^\dagger - \tfrac{1}{2}\{\hat{\mathbf{A}}_1\hat{\mathbf{A}}_1^\dagger, \hat{\mathbf{O}}\}) + \gamma_2^c\mathbf{s}^2(\hat{\mathbf{A}}_1^\dagger\hat{\mathbf{O}}\hat{\mathbf{A}}_1 - \tfrac{1}{2}\{\hat{\mathbf{A}}_1^\dagger\hat{\mathbf{A}}_1, \hat{\mathbf{O}}\}) + \gamma_3^c\mathbf{c}^2(\hat{\mathbf{A}}_2\hat{\mathbf{O}}\hat{\mathbf{A}}_2^\dagger - \tfrac{1}{2}\{\hat{\mathbf{A}}_2\hat{\mathbf{A}}_2^\dagger, \hat{\mathbf{O}}\}) + \gamma_4^c\mathbf{c}^2(\hat{\mathbf{A}}_2^\dagger\hat{\mathbf{O}}\hat{\mathbf{A}}_2 - \tfrac{1}{2}\{\hat{\mathbf{A}}_2^\dagger\hat{\mathbf{A}}_2, \hat{\mathbf{O}}\}),\end{aligned} \quad (16)$$

where $\mathbf{s} = \sin(\theta)$ and $\mathbf{c} = \cos(\theta)$, and the noise generator

$$\mathcal{L}_n(\hat{\mathbf{O}}) = -\eta[\hat{\mathbf{W}}, [\hat{\mathbf{W}}, \hat{\mathbf{O}}]], \quad (17)$$

where $\hat{\mathbf{W}} = \sin(2\theta)\hat{\mathbf{Z}} + \cos(2\theta)\hat{\mathbf{X}}$ and a new set of operators which form an $SU(2)$ algebra is defined: $\hat{\mathbf{X}} = (\hat{\mathbf{A}}_1^\dagger\hat{\mathbf{A}}_2 + \hat{\mathbf{A}}_2^\dagger\hat{\mathbf{A}}_1)$, $\hat{\mathbf{Y}} = i(\hat{\mathbf{A}}_1^\dagger\hat{\mathbf{A}}_2 - \hat{\mathbf{A}}_2^\dagger\hat{\mathbf{A}}_1)$, and $\hat{\mathbf{Z}} = (\hat{\mathbf{A}}_1^\dagger\hat{\mathbf{A}}_1 - \hat{\mathbf{A}}_2^\dagger\hat{\mathbf{A}}_2)$. The total number of excitations is accounted for by the operator $\hat{\mathbf{N}} = (\hat{\mathbf{A}}_1^\dagger\hat{\mathbf{A}}_1 + \hat{\mathbf{A}}_2^\dagger\hat{\mathbf{A}}_2)$. The generalized heat transport coefficients become $\zeta_+^k = \gamma_2^k - \gamma_1^k$ and $\zeta_-^k = \gamma_4^k - \gamma_3^k$ for $k = h, c$. Applying the Kubo relation [33,34] $\gamma_1^k = e^{-\hbar\Omega_+\beta_k}\gamma_2^k$ and $\gamma_3^k = e^{-\hbar\Omega_-\beta_k}\gamma_4^k$ leads to the detailed balance relation

$$\frac{\gamma_1^k}{\zeta_+^k} = \frac{1}{e^{\hbar\Omega_+\beta_k}-1} \equiv N_+^k, \qquad \frac{\gamma_3^k}{\zeta_-^k} = \frac{1}{e^{\hbar\Omega_-\beta_k}-1} \equiv N_-^k.$$

In general, $\zeta_\pm^k$ is temperature-independent and can be calculated specifically for different choices of spectral density of the baths. For an electromagnetic or acoustic phonon field, $\zeta_\pm^k \propto \Omega_\pm^d$. The heat currents $\mathcal{J}_h$, $\mathcal{J}_c$, and $\mathcal{J}_n$ are calculated by solving the equation of motion for the operators at steady state and at the regime of low temperature, where $\cos^2(\theta) \approx 1$ and $\sin^2(\theta) \approx 0$:

$$\begin{aligned}\frac{d\hat{\mathbf{N}}}{dt} &= -\frac{1}{2}(\zeta_+^h + \zeta_-^c)\hat{\mathbf{N}} - \frac{1}{2}(\zeta_+^h - \zeta_-^c)\hat{\mathbf{Z}} + (\zeta_+^h N_+^h + \zeta_-^c N_-^c),\\ \frac{d\hat{\mathbf{Z}}}{dt} &= -\frac{1}{2}(\zeta_+^h + \zeta_-^c)\hat{\mathbf{Z}} - \frac{1}{2}(\zeta_+^h - \zeta_-^c)\hat{\mathbf{N}} + (\zeta_+^h N_+^h - \zeta_-^c N_-^c) - 4\eta\hat{\mathbf{Z}}.\end{aligned} \quad (18)$$

Once the set of linear equations is solved, the exact expression for the heat currents is extracted: $\mathcal{J}_h = \langle\mathcal{L}_h(\hat{\mathbf{H}}_s)\rangle$, $\mathcal{J}_c = \langle\mathcal{L}_c(\hat{\mathbf{H}}_s)\rangle$, and $\mathcal{J}_n = \langle\mathcal{L}_n(\hat{\mathbf{H}}_s)\rangle$. For simplicity, the distribution of impulses in Eq. (11) is chosen as $P(\xi) = \delta(\xi - \xi_0)$. Then the effective noise parameter becomes

$$\eta = \frac{\lambda}{4}[1 - \cos(2\xi_0/\hbar)]. \quad (19)$$

The energy shift is controlled by

$$\epsilon = -\frac{\lambda}{2}[2\xi_0/\hbar - \sin(2\xi_0/\hbar)]. \quad (20)$$

Figure 2 shows a periodic structure of the heat current $\mathcal{J}_c$ and the entropy production $\Sigma_c = -\mathcal{J}_c/T_c$ with the impulse ξ_0. The second law of thermodynamics is obtained by the balance of the large entropy generation on the hot bath compensating for the negative entropy generation of cooling the cold bath. The COP for the Poisson-driven refrigerator is restricted by the Otto and Carnot COP:

$$\mathrm{COP} = \frac{\Omega_-}{\Omega_+ - \Omega_-} \leq \frac{\omega_c}{\omega_h - \omega_c} \leq \frac{T_c}{T_h - T_c}. \quad (21)$$

The heat current $\mathcal{J}_c$ is given by

$$\mathcal{J}_c \approx \hbar\Omega_- \frac{N_-^c - N_+^h}{(2\eta)^{-1} + (\zeta_+^h)^{-1} + (\zeta_-^c)^{-1}}. \quad (22)$$

The scaling of the optimal cooling rate is now accounted for. The heat flow is maximized with respect to the impulse ξ_0 by maximizing η [Eq. (19)], which occurs for $\xi_0 = n\frac{\pi}{2}$ $(n = 1, 2, \ldots)$. On the other hand, the energy shift ϵ^2 [Eq. (20)] should be minimized. The optimum is obtained when $\xi_0 = \frac{\pi}{2}$. The cooling power of the Poisson noise case [Eq. (22)] is similar to the Gaussian one [Eq. (8)]. In the Poisson case, also the noise driving parameter η is restricted by ω_c. This is because ϵ is restricted by $\Omega_- \geq 0$, and therefore λ is restricted to scale with ω_c. In total, when $T_c \to 0$, $\mathcal{J}_c \propto T_c^{d+1}$.

The optimal scaling relation $\mathcal{J}_c \propto T_c^{\alpha}$ of the autonomous absorption refrigerators should be compared to the scaling of the discrete four-stroke Otto refrigerators [35]. In the driven discrete case, the scaling depends on the external control scheduling function on the expansion stroke. For a scheduling function determined by a constant frictionless nonadiabatic parameter, the optimal cooling rate scaled with $\alpha = 2$. Faster frictionless scheduling procedures were found based on a bang-bang type of optimal control solutions. These solutions led to a scaling of $\alpha = 3/2$ when positive frequencies were employed and $\mathcal{J}_c \propto -T_c/\log T_c$ when negative imaginary frequencies were allowed [36,37]. $\mathcal{J}_c \propto T_c$ was obtained in the limit of large energy levels for a swap-based Otto cycle [38]. The drawback of the externally driven refrigerators is that their analysis is complex. The optimal scaling assumes that the heat conductivity $\Gamma \gg \omega_c$ and that noise in the controls does not influence the scaling. For this reason, an analysis based on the autonomous refrigerators is superior.

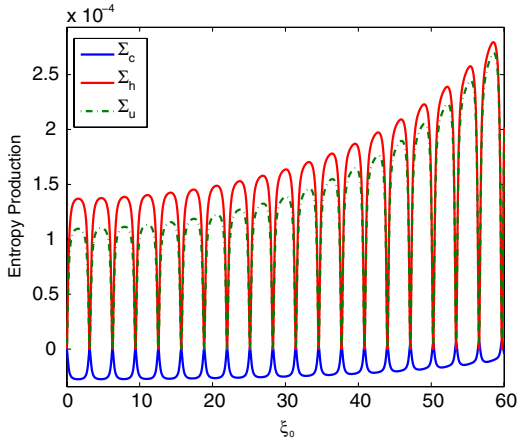

FIG. 2 (color online). Entropy production $\Sigma_k = -\mathcal{J}_k/T_k$ as a function of impulse ξ_0 for the cold Σ_c, hot Σ_h, and the total entropy production $\Sigma_u = \Sigma_h + \Sigma_c$. $T_c = 10^{-3}$, $T_h = 2$, $\omega_c = T_c$, $\omega_h = 10$, $\lambda = \omega_c$, and $\zeta_{\pm}^k = \omega_c/10$ $(\hbar = k = 1)$.

We thank Robert Alicki for his remarks and suggestions. The work was supported by the Israel Science Foundation.

[1] J. M. Gordon and K. C. Ng, *Cool Thermodynamics* (Cambridge International Science Publishing, Cambridge, England, 2000).
[2] A. Einstein and L. Szilárd, U.S. Patent No. 1 781 541 (1930).
[3] José P. Palao, Ronnie Kosloff, and Jeffrey M. Gordon, Phys. Rev. E **64**, 056130 (2001).
[4] N. Linden, S. Popescu, and P. Skrzypczyk, Phys. Rev. Lett. **105**, 130401 (2010).
[5] M. Kumakura, Y. Shirahata, Y. Takasu, Y. Takahashi, and T. Yabuzaki, Phys. Rev. A **68**, 021401 (2003).
[6] A. Einstein, Ann. Phys. (Berlin) **322**, 132 (1905).
[7] J. Geusic, E. S. du Bois, R. D. Grasse, and H. Scovil, Phys. Rev. **156**, 343 (1967).
[8] H. Spohn and J. Lebowitz, Adv. Chem. Phys. **109**, 38 (1978).
[9] R. Alicki, J. Phys. A **12**, L103 (1979).
[10] R. Kosloff, J. Chem. Phys. **80**, 1625 (1984).
[11] Eitan Geva and Ronnie Kosloff, J. Chem. Phys. **104**, 7681 (1996).
[12] Ronnie Kosloff, Eitan Geva and Jeffrey M. Gordon, J. Appl. Phys. **87**, 8093 (2000).
[13] S. Lloyd, Phys. Rev. A **56**, 3374 (1997).
[14] T. D. Kieu, Phys. Rev. Lett. **93**, 140403 (2004).
[15] D. Segal and A. Nitzan, Phys. Rev. E **73**, 026109 (2006).
[16] P. Bushev, D. Rotter, A. Wilson, F. Dubin, C. Becher, J. Eschner, R. Blatt, V. Steixner, P. Rabl, and P. Zoller, Phys. Rev. Lett. **96**, 043003 (2006).
[17] E. Boukobza and D. J. Tannor, Phys. Rev. A **78**, 013825 (2008).
[18] J. Birjukov, T. Jahnke, and G. Mahler, Eur. Phys. J. B **64**, 105 (2008).
[19] A. E. Allahverdyan, R. S. Johal, and G. Mahler, Phys. Rev. E **77**, 041118 (2008).
[20] D. Segal, J. Chem. Phys. **130**, 134510 (2009).
[21] H. Wang, S. Q. Liu, and J. Z. He, Phys. Rev. E **79**, 041113 (2009).
[22] J. Gemmer, M. Michel, and G. Mahler, *Quantum Thermodynamics* (Springer, New York, 2009).
[23] W. Nernst, Nachr. Kgl. Ges. Wiss. Gott. **1**, 40 (1906).
[24] P. T. Landsberg, Rev. Mod. Phys. **28**, 363 (1956).
[25] F. Belgiorno, J. Phys. A **36**, 8165 (2003).
[26] Bjarne Andresen, Peter Salamon, and R. Stephen Berry, Phys. Today **37**, No. 9, 62 (1984).
[27] G. Lindblad, Commun. Math. Phys. **48**, 119 (1976).

[28] H.-P. Breuer and F. Petruccione, *Open Quantum Systems* (Oxford University, New York, 2002).
[29] R. Alicki, D. A. Lidar, and P. Zanardi, Phys. Rev. A **73**, 052311 (2006).
[30] V. Gorini and A. Kossakowski, J. Math. Phys. (N.Y.) **17**, 1298 (1976).
[31] T. Jahnke, J. Birjukov, and G. Mahler, Ann. Phys. (Paris) **17**, 88 (2008).
[32] J. Łuczka and M. Niemeic, J. Phys. A **24**, L1021 (1991).
[33] R. Kubo, J. Phys. Soc. Jpn. **12**, 550 (1957).
[34] A. Kossakowski, A. Frigerio, V. Gorini, and M. Verri, Commun. Math. Phys. **57**, 97 (1977).
[35] Yair Rezek, Peter Salamon, Karl Heinz Hoffmann, and Ronnie Kosloff, Europhys. Lett. **85**, 30 008 (2009).
[36] Xi Chen, A. Ruschhaupt, S. Schmidt, A. del Campo, D. Guery-Odelin, and J. G. Muga, Phys. Rev. Lett. **104**, 063002 (2010).
[37] K. Heinz, Y. Rezek, P. Salamon, and R. Kosloff, Europhys. Lett. **96**, 60 015 (2011).
[38] A. E. Allahverdyan, K. Hovhannisyan, and G. Mahler, Phys. Rev. E **81**, 051129 (2010).

Chapter 5

Quantum refrigerators and the third law of thermodynamics

Quantum refrigerators and the third law of thermodynamics
Amikam Levy, Robert Alicki and Ronnie Kosloff
Published in: Phys. Rev. E, vol. 85, page 061126, 2012.

PHYSICAL REVIEW E **85**, 061126 (2012)

Quantum refrigerators and the third law of thermodynamics

Amikam Levy,[1] Robert Alicki,[2,3] and Ronnie Kosloff[1]
[1]*Institute of Chemistry, The Hebrew University, Jerusalem 91904, Israel*
[2]*Institute of Theoretical Physics and Astrophysics, University of Gdańsk, Poland*
[3]*Weston Visiting Professor, Weizmann Institute of Science, Rehovot, Israel*
(Received 30 April 2012; published 26 June 2012)

The rate of temperature decrease of a cooled quantum bath is studied as its temperature is reduced to absolute zero. The third law of thermodynamics is then quantified dynamically by evaluating the characteristic exponent ζ of the cooling process $\frac{dT(t)}{dt} \sim -T^{\zeta}$ when approaching absolute zero, $T \to 0$. A continuous model of a quantum refrigerator is employed consisting of a working medium composed either by two coupled harmonic oscillators or two coupled two-level systems. The refrigerator is a nonlinear device merging three currents from three heat baths: a cold bath to be cooled, a hot bath as an entropy sink, and a driving bath which is the source of cooling power. A heat-driven refrigerator (absorption refrigerator) is compared to a power-driven refrigerator. When optimized, both cases lead to the same exponent ζ, showing a lack of dependence on the form of the working medium and the characteristics of the drivers. The characteristic exponent is therefore determined by the properties of the cold reservoir and its interaction with the system. Two generic heat bath models are considered: a bath composed of harmonic oscillators and a bath composed of ideal Bose/Fermi gas. The restrictions on the interaction Hamiltonian imposed by the third law are discussed. In the Appendices, the theory of periodically driven open systems and its implication for thermodynamics are outlined.

DOI: 10.1103/PhysRevE.85.061126 PACS number(s): 05.30.−d, 03.65.Yz, 05.70.Ln, 07.20.Pe

I. INTRODUCTION

Thermodynamics was initially formed as a phenomenological theory, with the fundamental rules assumed as postulates based on experimental evidence. The well-established part of the theory concerns quasistatic macroscopic processes near thermal equilibrium. Quantum theory, on the other hand, treats the dynamical perspective of systems at atomic and smaller length scales. The two disciplines rely upon different sets of axioms. However, one of the first developments, namely Planck's law, which led to the basics of quantum theory, was achieved thanks to consistency with thermodynamics. Einstein, following the ideas of Planck on blackbody radiation, quantized the electromagnetic field [1].

With the establishment of quantum theory, quantum thermodynamics emerged in the quest to reveal the intimate connection between the laws of thermodynamics and their quantum origin [2–19]. In this tradition, the present study is aimed toward the quantum study of the third law of thermodynamics [20–24], in particular quantifying the unattainability principle. Apart from the fundamental interest in the emergence of the third law of thermodynamics from a quantum dynamical system, cooling mechanical systems reveal their quantum character. As the temperature decreases, degrees of freedom freeze out, leaving a simplified dilute effective Hilbert space. Ultracold quantum systems contributed significantly to our understanding of basic quantum concepts. In addition, such systems form the basis for emerging quantum technologies. The necessity to reach ultralow temperatures requires a focus on the cooling process itself, namely quantum refrigeration.

The minimum requirement for constructing a continuous refrigerator is a system connected simultaneously to three reservoirs [25]. These baths are termed hot, cold, and work reservoir, as described in Fig. 1. This framework has to be translated to a quantum description of its components, which includes the Hamiltonian of the system H_s and the implicit description of the reservoirs. We present a careful study on the influence of different components and cooling mechanisms on the cooling process itself. Namely, we consider a working medium composed of two harmonic oscillators or two two-level systems (TLSs). Two generic models of the cold heat bath are considered: a phonon and an ideal Bose/Fermi gas heat bath. Another classification of the refrigerator is due to the character of the work reservoir. The first studied example is a heat-driven refrigerator, an absorption refrigerator model proposed in Ref. [24], where $T_w \gg T_h \geqslant T_c$.[1] In a power-driven refrigerator, the work reservoir represents zero entropy mechanical work, which is modeled as a periodic time-dependent interaction Hamiltonian.

The models studied contain universal quantum features of such devices. The third law of thermodynamics is quantified by the characteristic exponent ζ of the change in temperature of the cold bath $\frac{dT_c(t)}{dt} \sim -T_c^{\zeta}$ when its temperature approaches absolute zero, $T_c \to 0$. The exponent ζ is determined by a balance between the heat capacity of the cold bath and the heat current $\mathcal{J}_c$ into the cooling device. When the performance of the refrigerator is optimized, the final third-law characteristics are found to be independent of the refrigerator type.

The analysis is based on a steady-state operational mode of the refrigerator. Then the first and second laws of thermodynamics have the form

$$\tilde{\mathcal{J}}_h + \tilde{\mathcal{J}}_c + \mathcal{P} = 0, \quad -\frac{\tilde{\mathcal{J}}_h}{T_h} - \frac{\tilde{\mathcal{J}}_c}{T_c} - \frac{\mathcal{P}}{T_w} \geqslant 0, \tag{1}$$

where $\tilde{\mathcal{J}}_k$ are the stationary heat currents from each reservoir. The first equality represents conservation of energy (first law) [3,4], and the second inequality represents non-negative entropy production in the Universe, $\Sigma_u \geqslant 0$ (second law). The

[1]A similar idea was also proposed in Phys. Rev. Lett. **108**, 120603 (2012) by Cleuren *et al*. However, one can show that this model violates the third law. The reason for this will be discussed elsewhere.

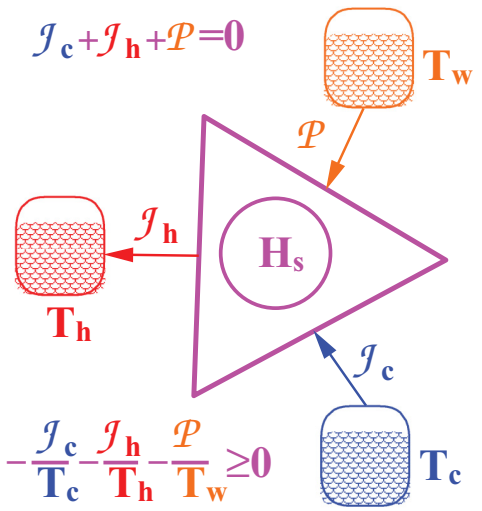

FIG. 1. (Color online) A quantum heat pump designated by the Hamiltonian H_s coupled to a work reservoir with temperature T_w, a hot reservoir with temperature T_h, and a cold reservoir with temperature T_c. The heat and work currents are indicated. In steady state, $\mathcal{J}_h + \mathcal{J}_c + \mathcal{P} = 0$.

fulfillment of the thermodynamic laws is employed to check the consistency of the quantum description. Inconsistencies can emerge either from wrong definitions of the currents $\mathcal{J}_k$ or from erroneous derivations of the quantum master equation. In Appendix A, we present a short and heuristic derivation of such a consistent Markovian master equation based on the rigorous weak coupling [26] or low density [27] limits for a constant system's Hamiltonian. Its generalization to periodic driving proposed in Ref. [28] and based on the Floquet theory is briefly discussed in Appendix B. In Appendix C the definition of heat currents is proposed which satisfies the second law of thermodynamics, not only for the stationary state but also during the evolution from an arbitrary initial state of the system. It allows us also to compute an averaged power in the stationary state. Finally, in Appendix D we discuss the condition on the interaction with a bosonic bath, to assure the existence of the ground state.

II. QUANTUM ABSORPTION REFRIGERATORS

We develop and discuss in detail the model of a quantum absorption refrigerator proposed in Ref. [24]. We extend the results of Ref. [24] treating in the same way the original model with two harmonic oscillators and its two two-level systems counterpart to stress the universality of the proposed cooling mechanism. The advantage of the absorption refrigerator is its underlying microscopic model with a time-independent Hamiltonian.

A. Absorption refrigerator model

The model consists of two harmonic oscillators or two TLSs (A and B) which are described by two pairs of annihilation and creation operators satisfying the commutation or anticommutation relations

$$\begin{aligned} aa^\dagger + \epsilon a^\dagger a = 1, \quad aa + \epsilon aa = 0, \\ bb^\dagger + \epsilon b^\dagger b = 1, \quad bb + \epsilon bb = 0 \end{aligned} \tag{2}$$

with $\epsilon = 1$ for the TLS and $\epsilon = -1$ for oscillators. Each subsystem A (B) is coupled to a hot (cold) bath at the temperature T_h (T_c). A collective coupling of the system $A + B$ to the third "work bath" at the temperature $T_w \gg T_h > T_c$ generates heat transport. The nonlinear coupling to the "work bath" is essential. A linearly coupled working medium cannot operate as a refrigerator.[2] The Hamiltonian of the working medium $A + B$ is given by

$$H = \omega_h a^+ a + \omega_c b^+ b, \quad \omega_h > \omega_c, \tag{3}$$

and the interaction with the three baths (hot, cold, and work) is assumed to be of the following form:

$$\begin{aligned} H_{\rm int} = (a + a^+) \otimes R_h + (b + b^+) \otimes R_c \\ + (ab^+ + a^+ b) \otimes R_w, \end{aligned} \tag{4}$$

with $R_{(\cdot)}$ being the corresponding bath operator. The third term in Eq. (4) contains the generator of a swap operation between A and B subsystems [29].

Applying now the derivation of the Markovian dynamics based on the weak-coupling limit (see Appendix A), one obtains the following Markovian master equation involving three thermal generators:

$$\frac{d\rho}{dt} = -\frac{i}{\hbar}[H,\rho] + \mathcal{L}_h\rho + \mathcal{L}_c\rho + \mathcal{L}_w\rho, \tag{5}$$

where

$$\mathcal{L}_h\rho = \tfrac{1}{2}\gamma_h([a,\rho a^\dagger] + e^{-\beta_h\omega_h}[a^\dagger,\rho a] + \text{H.c.}), \tag{6}$$

$$\mathcal{L}_c\rho = \tfrac{1}{2}\gamma_c([b,\rho b^\dagger] + e^{-\beta_c\omega_c}[b^\dagger,\rho b] + \text{H.c.}), \tag{7}$$

$$\mathcal{L}_w\rho = \tfrac{1}{2}\gamma_w([ab^\dagger,\rho a^\dagger b] + e^{-\beta_w(\omega_h-\omega_c)}[a^\dagger b,\rho ab^\dagger] + \text{H.c.}), \tag{8}$$

and $\beta_c > \beta_h \gg \beta_w$ are inverse temperatures for the cold, hot, and work bath, respectively.

The values of relaxation rates $\gamma_h,\gamma_c,\gamma_w > 0$ depend on the particular models of heat baths, and their explicit form is discussed in Appendix A. Notice that one can add also the generators describing pure decoherence (dephasing) in the form

$$\begin{aligned} \mathcal{D}_h\rho = -\tfrac{1}{2}\delta_h[a^\dagger a,[a^\dagger a,\rho]], \\ \mathcal{D}_c\rho = -\tfrac{1}{2}\delta_c[b^\dagger b,[b^\dagger b,\rho]], \quad \delta_h,\delta_c > 0, \end{aligned} \tag{9}$$

which, however, do not change the evolution of diagonal matrix elements and therefore have no influence on the cooling mechanism at the stationary state. The generator $\mathcal{L}_w$ is not ergodic in the sense that it does not drive the system $A + B$ to a Gibbs state because it preserves a total number of excitations $a^\dagger a + b^\dagger b$. This fault can be easily repaired by adding to $\mathcal{L}_w$ a term of the form (6) or/and (7) but with the temperature T_w. However, we assume that the processes described by Eqs. (6)–(8) dominate and additional contributions can be neglected.

B. The cooling mechanism

The stationary "cold current" describing heat flux from the cold bath to the working medium can be computed using the

[2]E. Martinez and J. P. Paz (unpublished).

definitions presented in Appendix C. The cooling of the cold bath takes place if this current is positive,

$$\tilde{\mathcal{J}}_c = \omega_c \mathrm{Tr}[(\mathcal{L}_c\tilde{\rho})b^\dagger b] > 0. \tag{10}$$

To compute $\tilde{\mathcal{J}}_c$, we need the following equations for the mean values of the relevant observables $\bar{n}_h = \mathrm{Tr}(\rho a^\dagger a)$ and $\bar{n}_c = \mathrm{Tr}(\rho b^+ b)$, which can be derived using the explicit form of the generators (6)–(8):

$$\frac{d}{dt}\bar{n}_h = -\gamma_h(1+\epsilon e^{-\beta_h\omega_h})\bar{n}_h + \gamma_h e^{-\beta_h\omega_h} + \gamma_w(\bar{n}_c - \bar{n}_h) - R, \tag{11}$$

$$\frac{d}{dt}\bar{n}_c = -\gamma_c(1+\epsilon e^{-\beta_c\omega_c})\bar{n}_c + \gamma_c e^{-\beta_c\omega_c} + \gamma_w(\bar{n}_h - \bar{n}_c) + R, \tag{12}$$

where R is the nonlinear rate

$$R = \gamma_w(1 - e^{-\beta_w(\omega_h-\omega_c)})\mathrm{Tr}[\rho(b^+b)(aa^+)]. \tag{13}$$

Equations (11)–(13) can be solved analytically in the high-temperature limit for the work bath $\beta_w \to 0$, which implies $R \to 0$. Under this condition, the stationary cold current reads

$$\tilde{\mathcal{J}}_c = \omega_c\gamma_w \times \frac{(e^{\beta_c\omega_c}+\epsilon)^{-1} - (e^{\beta_h\omega_h}+\epsilon)^{-1}}{1+\gamma_w[\gamma_h^{-1}(1+\epsilon e^{-\beta_h\omega_h})^{-1} + \gamma_c^{-1}(1+\epsilon e^{-\beta_c\omega_c})^{-1}]}. \tag{14}$$

The cooling condition $\tilde{\mathcal{J}}_c > 0$ is equivalent to a very simple one,

$$\frac{\omega_c}{\omega_h} < \frac{T_c}{T_h}. \tag{15}$$

One can similarly compute the other heat currents to obtain the coefficient of performance (COP),

$$\mathrm{COP} = \frac{\mathcal{J}_c}{\mathcal{J}_w} = \frac{\omega_c}{\omega_h - \omega_c}, \tag{16}$$

which becomes the Otto cycle COP [14,30].

We are interested in the final stage of the cooling process when the temperature T_c is close to absolute zero and hence we can assume that $\gamma_c(T_c) \ll \gamma_h(T_h)$. Optimizing the cooling current means keeping essentially constant the value of ω_c/T_c [31]. This leads to the following simplification of the formula (14):

$$\tilde{\mathcal{J}}_c \simeq \omega_c\gamma_c e^{-\omega_c/k_BT_c}. \tag{17}$$

III. PERIODICALLY DRIVEN REFRIGERATOR

An alternative to driving the refrigerator by a "very hot" heat bath is to apply a time-dependent perturbation to the system of the two harmonic oscillators. One can repeat the derivation for two TLSs, but the final expressions for the currents are more intricate and therefore we restrict ourselves to the oscillator working medium. The time-dependent Hamiltonian reads

$$H(t) = \omega_h a^\dagger a + \omega_c b^\dagger b + \lambda(e^{-i\Omega t}a^\dagger b + e^{i\Omega t}ab^\dagger), \tag{18}$$

where Ω denotes the driving frequency which is chosen to be in resonance $\Omega = \omega_h - \omega_c$ and $\lambda > 0$ measures the strength of the coupling to the external field. Interaction with the baths is given by

$$H_{\mathrm{int}} = (a + a^\dagger) \otimes R_h + (b + b^\dagger) \otimes R_c. \tag{19}$$

The general derivation of the weak-coupling limit Markovian master equation with periodic driving is discussed in Appendix B and is essential for consistency with the second law of thermodynamics [6]. The master equation has the form

$$\frac{d}{dt}\rho(t) = -i[H(t),\rho(t)] + \mathcal{L}_h(t)\rho(t) + \mathcal{L}_c(t)\rho(t) \tag{20}$$

with $\mathcal{L}_{h(c)}(t) = U(t,0)\mathcal{L}_{h(c)}U(t,0)^\dagger$, which under resonance conditions can be derived directly without applying the full Floquet formalism.

The main ingredients of the derivation are as follows:

(i) Transformation to interaction picture. The bath operators transform according to the free baths Hamiltonian, and the system operators transform according to the unitary propagator (under resonance conditions),

$$U(t,0) = \mathcal{T}\exp\left\{-i\int_0^t H(s)ds\right\} = e^{-iH_0t}e^{-iVt}, \tag{21}$$

where

$$H_0 = \omega_h a^\dagger a + \omega_c b^\dagger b, \quad V = \lambda(a^\dagger b + ab^\dagger). \tag{22}$$

(ii) Fourier decomposition of the interaction part,

$$a(t) = U(t,0)^\dagger a U(t,0) = e^{iVt}[e^{iH_0t}ae^{-iH_0}]e^{-iVt} = \cos(\lambda t)e^{-i\omega_h t}a - i\sin(\lambda t)e^{-i\omega_h t}b, \tag{23}$$

which gives the Fourier decomposition [compare with Eq. (B3)]

$$a(t) = \frac{1}{\sqrt{2}}(e^{-i(\omega_h^+)t}d_+ + e^{-i(\omega_h^-)t}d_-) \tag{24}$$

and

$$b(t) = \frac{1}{\sqrt{2}}(e^{-i(\omega_c^+)t}d_+ - e^{-i(\omega_c^-)t}d_-), \tag{25}$$

where $d_+ = \frac{a+b}{\sqrt{2}}$, $d_- = \frac{a-b}{\sqrt{2}}$, and $\omega^\pm_{h(c)} = (\omega_{h(c)} \pm \lambda)$. Similarly, we can calculate $a^\dagger(t), b^\dagger(t)$.

(iii) Performing the weak-coupling approximation, the total time-independent (interaction picture) generator has the form

$$\mathcal{L} = \mathcal{L}_h^{(+)} + \mathcal{L}_h^{(-)} + \mathcal{L}_c^{(+)} + \mathcal{L}_c^{(-)}, \tag{26}$$

where

$$\mathcal{L}^{(+)}_{h(c)}\rho = \tfrac{1}{4}\gamma^{(+)}_{h(c)}([d_+,\rho d_+^\dagger] + e^{-\beta_{h(c)}\omega^+_{h(c)}}[d_+^\dagger,\rho d_+] + \mathrm{H.c.}) \tag{27}$$

and

$$\mathcal{L}^{(-)}_{h(c)}\rho = \tfrac{1}{4}\gamma^{(-)}_{h(c)}([d_-,\rho d_-^\dagger] + e^{-\beta_{h(c)}\omega^-_{h(c)}}[d_-^\dagger,\rho d_-] + \mathrm{H.c.}) \tag{28}$$

with the relaxation rates $\gamma^{(\pm)}_{h(c)} = \gamma_{h(c)}(\omega_{h(c)} \pm \lambda)$ discussed explicitly in Appendices A and B. Any such generator and any sum of them possess a unique stationary state (under condition $\omega_{h(c)} \pm \lambda > 0$),

$$\tilde{\rho}^{(+)}_{h(c)} = Z^{-1}\exp[-\beta_{h(c)}\omega^+_{h(c)}d_+^\dagger d_+] \tag{29}$$

and

$$\tilde{\rho}_{h(c)}^{(-)} = Z^{-1}\exp[-\beta_{h(c)}\omega_{h(c)}^{-}d_{-}^{\dagger}d_{-}]. \tag{30}$$

The steady (time-independent) heat currents can be computed using the definitions of Appendix C. For example, the heat current from the cold bath is given by the sum of entropy flows, which are related to the quasienergies $\omega_c \pm \lambda$, times the bath temperature,

$$\tilde{\mathcal{J}}_c = -k_B T_c\{\mathrm{Tr}[(\mathcal{L}_c^{(+)}\tilde{\rho})\ln\tilde{\rho}_c^{(+)}] + \mathrm{Tr}[(\mathcal{L}_c^{(-)}\tilde{\rho})\ln\tilde{\rho}_c^{(-)}]\}. \tag{31}$$

This current can be calculated analytically. The result is the following:

$$\tilde{\mathcal{J}}_c = \frac{1}{2}\left[\omega_c^{-}\frac{(e^{\beta_c\omega_c^{-}}-1)^{-1}-(e^{\beta_h\omega_h^{-}}-1)^{-1}}{[\gamma_h^{(-)}(1-e^{-\beta_h\omega_h^{-}})]^{-1}+[\gamma_c^{(-)}(1-e^{-\beta_c\omega_c^{-}})]^{-1}}\right.$$
$$\left.+\,\omega_c^{+}\frac{(e^{\beta_c\omega_c^{+}}-1)^{-1}-(e^{\beta_h\omega_h^{+}}-1)^{-1}}{[\gamma_h^{(+)}(1-e^{-\beta_h\omega_h^{+}})]^{-1}+[\gamma_c^{(+)}(1-e^{-\beta_c\omega_c^{+}})]^{-1}}\right]. \tag{32}$$

Similarly to Sec. II B when the temperature T_c is close to absolute zero, we can assume $\gamma_c^{(-)} \ll \gamma_h^{(-)}$ and $\gamma_c^{(+)} \ll \gamma_h^{(+)}$ while keeping $\lambda/T_c < \omega_c/T_c$ as constants. This simplifies formula (32),

$$\tilde{\mathcal{J}}_c \simeq \tfrac{1}{2}[\omega_c^{+}\gamma_c^{(+)}e^{-\omega_c^{+}/k_BT_c} + \omega_c^{-}\gamma_c^{(-)}e^{-\omega_c^{-}/k_BT_c}]. \tag{33}$$

Notice that the cold current does not vanish when λ tends to zero, which obviously should be the case. This is due to the fact that the derivation of master equations in the weak-coupling regime involves time-averaging procedures eliminating certain oscillating terms. This procedure makes sense only if the corresponding Bohr frequencies are well-separated. In our case, it means that ω_c^{-} should be well separated from ω_c^{+}, which implies that $\lambda \sim \omega_c$. Indeed, if both ω_c and λ vanish, the cold current vanishes as well. This problem of time scales in the weak-coupling Markovian dynamics has been discussed, for constant Hamiltonians, in Ref. [32] (see also [33] for the related "dynamical symmetry breaking" phenomenon).

IV. THE DYNAMICAL THIRD LAW OF THERMODYNAMICS

There exist two seemingly independent formulations of the third law of thermodynamics, both originally stated by Nernst [20,22]. The first is a purely static (equilibrium) one, also known as the Nernst heat theorem, and can simply be phrased as follows:

(a) The entropy of any pure substance in thermodynamic equilibrium approaches zero as the temperature approaches zero.

The second is a dynamical one, known as the unattainability principle:

(b) It is impossible by any procedure, no matter how idealized, to reduce any assembly to absolute zero temperature in a finite number of operations [34].

Different studies investigating the relation between the two formulations have led to different answers regarding which of these formulations implies the other, or if neither does. Although interesting, this question is beyond the scope of this paper. For further considerations regarding the third law, we refer the reader to Refs. [23,34–38]. In particular, in Refs. [37,38] the validity of the static formulation (a) has been confirmed for a large class of open quantum systems. We shall use a more concrete version of the dynamical third law, which can be expressed as follows:

(b′) No refrigerator can cool a system to absolute zero temperature at finite time.

This formulation enables us to quantify the third law, i.e., evaluating the characteristic exponent ζ of the cooling process $\frac{dT(t)}{dt} \sim -T^{\zeta}$ for $T \to 0$. Namely, for $\zeta < 1$ the system is cooled to zero temperature at finite time. As a model of the refrigerator, we use the above-discussed continuous refrigerators with a cold bath modeled either by a system of harmonic oscillators (bosonic bath) or the ideal gas at low density, including the possible Bose-Einstein condensation effect. To check under what conditions the third law is valid, we consider a finite cold bath with the heat capacity $c_V(T_c)$ cooled down by the refrigerator with the optimized time-dependent parameter $\omega_c(t)$ and the additional parameter $\lambda(t)$ for the case of a periodically driven refrigerator. The equation which describes the cooling process reads

$$c_V[T_c(t)]\frac{dT_c(t)}{dt} = -\mathcal{J}_c[\omega_c(t),T_c(t)], \quad t \geqslant 0. \tag{34}$$

The third law would be violated if the solution $T_c(t)$ reached zero at finite time t_0. Now we can consider two generic models of the cold heat bath.

A. Harmonic oscillator cold heat bath

This is a generic type of quantum bath including, for example, an electromagnetic field in a large cavity or a finite but macroscopic piece of solid described in the thermodynamic limit. We assume the linear coupling to the bath and the standard form of the bath's Hamiltonian,

$$H_{\mathrm{int}} = (b+b^{\dagger})\left(\sum_k [g(k)a(k) + \bar{g}(k)a^{\dagger}(k)]\right),$$
$$H_B = \sum_k \omega(k)a^{\dagger}(k)a(k), \tag{35}$$

where $a(k)$,$a^{\dagger}(k)$ are annihilation and creation operators for mode k. For this model, the weak-coupling limit procedure leads to the generator (7) with the cold bath relaxation rate

$$\gamma_c \equiv \gamma_c(\omega_c) = \pi\sum_k |g(k)|^2\delta(\omega(k)-\omega_c)[1-e^{-\omega(k)/k_BT_c}]^{-1}. \tag{36}$$

For the bosonic field in d-dimensional space, where k is a wave vector, and with the linear low-frequency dispersion law $[\omega(k) \sim |k|]$, we obtain the following scaling properties at low frequencies (compare Appendix D):

$$\gamma_c \sim \omega_c^{\kappa}\omega_c^{d-1}[1-e^{-\omega_c/k_BT_c}]^{-1}, \tag{37}$$

where ω_c^{κ} represents scaling of the coupling strength $|g(\omega)|^2$, and ω_c^{d-1} is the density of modes scaling. This implies the

following scaling of the cold current:

$$\mathcal{J}_c \sim T_c^{d+\kappa}\left[\frac{\omega_c}{T_c}\right]^{d+\kappa}\frac{1}{e^{\omega_c/T_c}-1}. \tag{38}$$

Optimization of Eq. (38) with respect to ω_c leads to the frequency tuning $\omega_c \sim T_c$ and the final current scaling,

$$\mathcal{J}_c^{\mathrm{opt}} \sim T_c^{d+\kappa}. \tag{39}$$

Consider that for low temperatures the heat capacity of the bosonic systems scales like

$$c_V(T_c) \sim T_c^d, \tag{40}$$

which finally produces the following scaling of the dynamical equation (34):

$$\frac{dT_c(t)}{dt} \sim -(T_c)^\kappa. \tag{41}$$

Notice that in a similar way the same scaling (41) is achieved for the periodically driven refrigerator (33), with the optimization tuning $\omega_c,\lambda \sim T_c$. As a consequence, the third law implies a rather unexpected constraint on the form of interaction with a bosonic bath,

$$\kappa \geqslant 1. \tag{42}$$

For standard systems such as electromagnetic fields or acoustic phonons with the linear dispersion law $\omega(k) = v|k|$ and the form factor $g(k) \sim |k|/\sqrt{\omega(k)}$, the parameter $\kappa = 1$, as for low ω, $|g(\omega)|^2 \sim |k|$. However, the condition (42) excludes exotic dispersion laws $\omega(k) \sim |k|^\alpha$ with $\alpha < 1$, which nevertheless produce the infinite group velocity forbidden by the relativity theory. Moreover, the popular choice of Ohmic coupling is excluded for systems in dimension $d > 1$. The condition (42) can also be compared with the condition

$$\kappa > 2 - d, \tag{43}$$

which is necessary to assure the existence of the ground state for the bosonic field interacting by means of the Hamiltonian (35) (see Appendix D).

B. Ideal Bose/Fermi gas cold heat bath

We consider now a model of a cooling process where part B of the working medium is an (infinitely) heavy particle with the internal structure approximated (at least at low temperatures) by a TLS immersed in a low density gas at temperature T_c. The Markovian dynamics of such a system was rigorously derived by Dumcke [27] in the low density limit and N-level internal structure. The form of the corresponding LGKS generator is presented in Appendix A. For our case of TLS, we have only one Bohr frequency ω_c, because elastic scattering corresponding to $\omega = 0$ does not influence the cooling process. Cooling occurs due to the nonelastic scattering, giving the relaxation rate (Appendix A)

$$\gamma_c = 2\pi n \int d^3\vec{p} \int d^3\vec{p}\,'\delta(E(\vec{p}\,') - E(\vec{p}) - \hbar\omega_c) \times f_{T_c}(\vec{p}_g)|T(\vec{p}\,',\vec{p})|^2 \tag{44}$$

with n the particle density, $f_{T_c}(\vec{p}_g)$ the probability distribution of the gas momentum strictly given by the Maxwell distribution, and $\vec{p}$ and $\vec{p}\,'$ the incoming and outgoing gas particle momentum, respectively. $E(\vec{p}) = p^2/2m$ denotes the kinetic energy of gas particle.

At low energies (low temperature), scattering of neutral gas in three dimensions can be characterized by the s-wave scattering length a_s, having a constant transition matrix, $|T|^2 = (\frac{4\pi a_s}{m})^2$. For our model, the integral (44) is calculated as

$$\gamma_c = (4\pi)^4\left(\frac{\beta_c}{2\pi m}\right)^{\frac{1}{2}} a_s^2 n\omega_c \mathcal{K}_1\left(\frac{\beta_c\omega_c}{2}\right)e^{\frac{\beta_c\omega_c}{2}}, \tag{45}$$

where $\mathcal{K}_p(x)$ is the modified Bessel function of the second kind. Note that formula (45) is also valid for a harmonic oscillator instead of TLS, assuming only linear terms in the interaction and using the Born approximation for the scattering matrix.

Optimizing formula (17) with respect to ω_c leads to $\omega_c \sim T_c$ and to scaling of the heat current,

$$\mathcal{J}_c^{\mathrm{opt}} \sim n(T_c)^{\frac{3}{2}}. \tag{46}$$

When the Bose gas is above the critical temperature for the Bose-Einstein condensation, the heat capacity c_V and the density n are constants. Below the critical temperature, the density n in formula (44) should be replaced by the density n_{ex} of the exited states, having both $c_V, n_{\mathrm{ex}} \sim (T_c)^{\frac{3}{2}}$, which finally implies

$$\frac{dT_c(t)}{dt} \sim -(T_c)^{\frac{3}{2}}. \tag{47}$$

In the case of Fermi gas at low temperatures, only the small fraction $n \sim T_c$ of fermions participates in the scattering process and contributes to the heat capacity; the rest is "frozen" in the "Dirac sea" below the Fermi surface. Again, this effect modifies in the same way both sides of Eq. (34), and therefore (47) is still valid. Similarly, a possible formation of Cooper pairs below the critical temperature does not influence the scaling (47).

V. CONCLUSIONS

We have introduced and analyzed two types of continuous quantum refrigerators, namely an absorption refrigerator and a periodically driven refrigerator. The latter required us to present new definitions for heat flow for periodically driven open systems. These definitions are in line with the second law and are applicable for a time-independent Hamiltonian as well. Unlike the first and second laws, the third law of thermodynamics does not define a new state function. In its first formulation (cf. Sec. IV), the third law provides a reference point for scaling the entropy and becomes intuitive when thinking in terms of quantum states or levels. The second formulation, (b′) in Sec. IV, which states that no refrigerator can cool a system to absolute zero temperature at finite time, provides information on the characteristic exponent ζ, the speed of cooling, and gives an insight and restriction on the properties of realistic systems.

Universal behavior of the final scaling near absolute zero is obtained. The third law does not depend on the bath dimension. The type of refrigerator, either absorption or a periodically driven refrigerator, does not influence the characteristic exponent, nor does a different medium, i.e., a

harmonic oscillator and a TLS produce the same scaling. The characteristic exponent is governed only by the feature of the heat bath and its interaction with the system. For a harmonic oscillator heat bath, the third law imposes a restriction on the form of the interaction between the system and the bath, $\kappa \geqslant 1$, allowing only physical coupling and dispersion relations, thus for phonons with a linear dispersion relation $\zeta = \kappa = 1$. For an ideal Bose/Fermi gas heat bath, $\zeta = 3/2$, which implies faster cooling of the phonon bath than the gas bath. This distinction between the two baths may occur due to particle conservation for the gas, indicating a more efficient extraction of heat by eliminating particles from the system. The key component of a realistic refrigerator is the heat transport mechanism between the heat bath and the working medium. This mechanism determines the third-law scaling. The working medium is a nonlinear device combining three currents. If it is optimized properly by adjusting its internal structure, it does not pose a limit on cooling.

ACKNOWLEDGMENTS

We want to thank Tova Feldmann, Yair Rezek, Juan Paz, and Gershon Kurizki for crucial discussions. This work is supported by the Israel Science Foundation and the Polish Ministry of Science and Higher Education, Grant No. NN202208238.

APPENDIX A: THERMAL GENERATORS FOR A CONSTANT HAMILTONIAN

Consider a system and a reservoir (bath), with a "bare" system Hamiltonian H^0 and the bath Hamiltonian H_R, interacting via the Hamiltonian $\lambda H_{\rm int} = \lambda S \otimes R$. Here, S (R) is a Hermitian system (reservoir) operator and λ is the coupling strength (a generalization to more complicated $H_{\rm int}$ is straightforward). We assume also that

$$[\rho_R, H_R] = 0, \quad \mathrm{Tr}(\rho_R\, R) = 0. \tag{A1}$$

The reduced, system-only dynamics in the interaction picture is defined as a partial trace,

$$\rho(t) = \Lambda(t,0)\rho \equiv \mathrm{Tr}_R[U_\lambda(t,0)\rho \otimes \rho_R U_\lambda(t,0)^\dagger], \tag{A2}$$

where the unitary propagator in the interaction picture is given by the ordered exponential,

$$U_\lambda(t,0) = \mathcal{T} \exp\left\{\frac{-i\lambda}{\hbar}\int_0^t S(s)\otimes R(s)\,ds\right\}, \tag{A3}$$

where

$$S(t) = e^{(i/\hbar)Ht} S e^{-(i/\hbar)Ht}, \quad R(t) = e^{(i/\hbar)H_R t} R e^{-(i/\hbar)H_R t}. \tag{A4}$$

Notice that $S(t)$ is defined with respect to the renormalized, *physical*, H and not H^0, which can be expressed as

$$H = H^0 + \lambda^2 H_1^{\rm corr} + \cdots. \tag{A5}$$

The renormalizing terms containing powers of λ are *Lamb-shift* corrections due to the interaction with the bath, which cancel afterward the uncompensated term $H - H^0$, which, in principle, should also be present in Eq. (A3). The lowest-order (Born) approximation with respect to the coupling constant λ yields $H_1^{\rm corr}$, while the higher-order terms $(\cdots)$ require going beyond the Born approximation.

A convenient, albeit not used in the rigorous derivations, tool is a cumulant expansion for the reduced dynamics,

$$\Lambda(t,0) = \exp\sum_{n=1}^{\infty}[\lambda^n K^{(n)}(t)]. \tag{A6}$$

One finds that $K^{(1)} = 0$ and the Born approximation (weak coupling) consists of terminating the cumulant expansion at $n = 2$, hence we denote $K^{(2)} \equiv K$:

$$\Lambda(t,0) = \exp[\lambda^2 K(t) + O(\lambda^3)]. \tag{A7}$$

One obtains

$$K(t)\rho = \frac{1}{\hbar^2}\int_0^t ds \int_0^t du F(s-u) S(s)\rho S(u)^\dagger + (\text{similar terms}), \tag{A8}$$

where $F(s) = \mathrm{Tr}[\rho_R R(s) R]$. The *similar terms* in Eq. (A8) are of the form $\rho S(s)S(u)^\dagger$ and $S(s)S(u)^\dagger\rho$.

The Markov approximation (in the interaction picture) means in all our cases that for long enough time, one can use the following approximation:

$$K(t) \simeq t\mathcal{L}, \tag{A9}$$

where $\mathcal{L}$ is a Linblad-Gorini-Kossakowski-Sudarshan (LGKS) generator. To find its form, we first decompose $S(t)$ into its Fourier components,

$$S(t) = \sum_{\{\omega\}} e^{i\omega t} S_\omega, S_{-\omega} = S_\omega^\dagger, \tag{A10}$$

where the set $\{\omega\}$ contains *Bohr frequencies* of the Hamiltonian

$$H = \sum_k \epsilon_k |k\rangle\langle k|, \quad \omega = \epsilon_k - \epsilon_l. \tag{A11}$$

Then we can rewrite the expression (A8) as

$$K(t)\rho = \frac{1}{\hbar^2}\sum_{\omega,\omega'} S_\omega \rho S_{\omega'}^\dagger \int_0^t e^{i(\omega-\omega')u} du \int_{-u}^{t-u} F(\tau) e^{i\omega\tau} d\tau + (\text{similar terms}) \tag{A12}$$

and use two crucial approximations:

$$\int_0^t e^{i(\omega-\omega')u} du \approx t\delta_{\omega\omega'},$$
$$\int_{-u}^{t-u} F(\tau) e^{i\omega\tau} d\tau \approx G(\omega) = \int_{-\infty}^{\infty} F(\tau) e^{i\omega\tau} d\tau \geqslant 0. \tag{A13}$$

This makes sense for $t \gg \max\{1/(\omega-\omega')\}$. Applying these two approximations, we obtain $K(t)\rho_S = (t/\hbar^2)\sum_\omega S_\omega \rho_S S_\omega^\dagger G(\omega) + (\text{similar terms})$, and hence it follows from Eq. (A9) that $\mathcal{L}$ is a special case of the LGKS generator derived for the first time by Davies [26]. Returning to the Schrödinger picture, one obtains the following Markovian master equation:

$$\frac{d\rho}{dt} = -\frac{i}{\hbar}[H,\rho] + \mathcal{L}\rho,$$
$$\mathcal{L}\rho \equiv \frac{\lambda^2}{2\hbar^2}\sum_{\{\omega\}} G(\omega)([S_\omega, \rho S_\omega^\dagger] + [S_\omega \rho, S_\omega^\dagger]). \tag{A14}$$

Several remarks are in order:

(i) The absence of off-diagonal terms in Eq. (A14), compared to Eq. (A12), is the crucial property of the Davies generator which can be interpreted as a coarse-graining in time of fast oscillating terms. It implies also the commutation of $\mathcal{L}$ with the Hamiltonian part $[H,\cdot]$.

(ii) The positivity $G(\omega) \geqslant 0$ follows from Bochner's theorem and is a necessary condition for the complete positivity of the Markovian master equation.

(iii) The presented derivation showed implicitly that the notion of *bath's correlation time*, often used in the literature, is not well-defined—Markovian behavior involves a rather complicated cooperation between system and bath dynamics. In other words, contrary to what is often done in phenomenological treatments, *one cannot combine arbitrary H's with a given LGKS generator*. This is particularly important in the context of thermodynamics of controlled quantum open system, where it is common to assume Markovian dynamics and apply arbitrary control Hamiltonians. Erroneous derivations of the quantum master equation can easily lead to violation of the laws of thermodynamics.

If the reservoir is a quantum system at a thermal equilibrium state, the additional Kubo-Martin-Schwinger (KMS) condition holds,

$$G(-\omega) = \exp\left(-\frac{\hbar\omega}{k_B T}\right) G(\omega), \tag{A15}$$

where T is the bath's temperature. As a consequence of Eq. (A15), the Gibbs state

$$\rho_\beta = Z^{-1} e^{-\beta H}, \quad \beta = \frac{1}{k_B T} \tag{A16}$$

is a stationary solution of Eq. (A14). Under mild conditions (e.g., "the only system operators commuting with H and S are scalars"), the Gibbs state is a unique stationary state and any initial state relaxes toward equilibrium ("zeroth law of thermodynamics"). A convenient parametrization of the corresponding *thermal generator* reads

$$\mathcal{L}\rho = \frac{1}{2}\sum_{\{\omega \geqslant 0\}} \gamma(\omega)\{([S_\omega, \rho S_\omega^\dagger] + [S_\omega \rho, S_\omega^\dagger]) + e^{-\hbar\beta\omega}([S_\omega^\dagger, \rho S_\omega] + [S_\omega^\dagger \rho, S_\omega])\}, \tag{A17}$$

where finally

$$\gamma(\omega) = \frac{\lambda^2}{\hbar^2}\int_{-\infty}^{+\infty} \mathrm{Tr}(\rho_R\, e^{iH_R t/\hbar}\, R\, e^{-iH_R t/\hbar} R)\, dt. \tag{A18}$$

A closer look at the expressions (A17) and (A18) shows that the transition ratio from the state $|k\rangle$ to the state $|l\rangle$ is exactly the same as that computed from the Fermi Golden Rule,

$$W(|\mathrm{in}\rangle \to |\mathrm{fin}\rangle) = \frac{2\pi}{\hbar}|\langle \mathrm{in}|V|\mathrm{fin}\rangle|^2 \delta(E_{\mathrm{fin}} - E_{\mathrm{in}}). \tag{A19}$$

Namely, one should take as a perturbation $V = \lambda S \otimes R$, an initial state $|\mathrm{in}\rangle = |k\rangle \otimes |E\rangle$, a final state $|\mathrm{fin}\rangle = |l\rangle \otimes |E'\rangle$ ($|E\rangle$ denotes the reservoir's energy eigenstate), and integrate over the initial reservoir's states with the equilibrium distribution and over all the final reservoir's states.

The above interpretation allows us to justify the extension of the construction of a thermal generator to the case of a heat bath consisting of noninteracting particles at low density n and thermal equilibrium (see [27] for a rigorous derivation). In this case, a fundamental relaxation process is a scattering of a single bath particle with the system described by the scattering matrix T. The scattering matrix can be decomposed as $T = \sum_{\{\omega\}} S_\omega \otimes R_\omega$, where now R_ω are single-particle operators. Then the structure of the corresponding master equation is again given by Eq. (A17) with

$$\gamma(\omega) = 2\pi n \int d^3\vec{p} \int d^3\vec{p}\,' \delta(E(\vec{p}\,') - E(\vec{p}) - \hbar\omega) M(\vec{p})| \times T_\omega(\vec{p}\,', \vec{p})|^2 \tag{A20}$$

resembling a properly averaged expression (A19). Here the initial (final) state has a structure $|k\rangle \otimes |\vec{p}\rangle$ ($|l\rangle \otimes |\vec{p}\,'\rangle$), $M(\vec{p})$ is the equilibrium (Maxwell) initial distribution of particle momenta, with $|\vec{p}\rangle$ being the particle momentum eigenvector, and $E(\vec{p})$ is the kinetic energy of a particle. The perturbation V in Eq. (A19) is replaced by the scattering matrix T (equal to V for the Born approximation) and finally

$$T_\omega(\vec{p}\,', \vec{p}) = \langle \vec{p}\,'|R_\omega|\vec{p}\rangle. \tag{A21}$$

APPENDIX B: THERMAL GENERATORS FOR PERIODIC DRIVING

In order to construct models of quantum heat engines or powered refrigerators, we have to extend the presented derivations of the Markovian master equation to the case of periodically driven systems. Fortunately, we can essentially repeat the previous derivation with the following amendments:

(i) The system (physical, renormalized) Hamiltonian is now periodic,

$$H(t) = H(t+\tau), \quad U(t,0) \equiv \mathcal{T}\exp\left\{-\frac{i}{\hbar}\int_0^t H(s)\, ds\right\}, \tag{B1}$$

and the role of constant Hamiltonian is played by H defined as

$$H = \sum_k \epsilon_k |k\rangle\langle k|, \quad U(\tau,0) = e^{-iH\tau/\hbar}. \tag{B2}$$

(ii) The Fourier decomposition (A10) is replaced by the following one:

$$U(t,0)^\dagger\, S\, U(t,0) = \sum_{q\in\mathbf{Z}}\sum_{\{\omega\}} e^{i(\omega+q\Omega)t} S_{\omega q}, \tag{B3}$$

where $\Omega = 2\pi/\tau$ and $\{\omega\} = \{\epsilon_k - \epsilon_l\}$. The decomposition of the above follows from the Floquet theory, however for our model we can obtain it directly using the manifest expressions for the propagator $U(t,0)$.

(iii) The generator in the interaction picture has the form

$$\mathcal{L} = \sum_{q\in\mathbf{Z}}\sum_{\{\omega\}} = \mathcal{L}_{\omega q}, \tag{B4}$$

where

$$\mathcal{L}_{\omega q}\rho = \tfrac{1}{2}\gamma(\omega + q\Omega)\{([S_{\omega q}, \rho S_{\omega q}^\dagger] + [S_{\omega q}\rho, S_{\omega q}^\dagger]) + e^{-\hbar\beta(\omega+q\Omega)}([S_{\omega q}^\dagger, \rho S_{\omega q}] + [S_{\omega q}^\dagger \rho, S_{\omega q}])\}. \tag{B5}$$

Returning to the Schrödinger picture, we obtain the following master equation:

$$\frac{d\rho(t)}{dt} = -\frac{i}{\hbar}[H(t),\rho(t)] + \mathcal{L}(t)\rho(t), \quad t \geqslant 0, \tag{B6}$$

where

$$\begin{aligned} \mathcal{L}(t) &= \mathcal{L}(t+\tau) = \mathcal{U}(t,0)\mathcal{L}\mathcal{U}(t,0)^{\dagger}, \\ \mathcal{U}(t,0)\cdot &= U(t,0)\cdot U(t,0)^{\dagger}. \end{aligned} \tag{B7}$$

In particular, one can represent the solution of Eq. (B6) in the form

$$\rho(t) = \mathcal{U}(t,0)e^{\mathcal{L}t}\rho(0), \quad t \geqslant 0. \tag{B8}$$

Any state satisfying $\mathcal{L}\tilde{\rho} = 0$ defines a periodic steady state (limit cycle),

$$\tilde{\rho}(t) = \mathcal{U}(t,0)\tilde{\rho} = \tilde{\rho}(t+\tau), \quad t \geqslant 0. \tag{B9}$$

Finally, one should notice that in the case of multiple couplings and multiple heat baths, the generator $\mathcal{L}$ can always be represented as an appropriate sum of the terms like (A17).

APPENDIX C: HEAT FLOWS AND POWER FOR PERIODICALLY DRIVEN OPEN SYSTEMS

We consider a periodically driven system coupled to several heat baths with the additional index j labeling them. Then the generator in the interaction picture has the form

$$\mathcal{L} = \sum_{j=1}^{M}\sum_{q\in\mathbf{Z}}\sum_{\{\omega\geqslant 0\}}\mathcal{L}^{j}_{\omega q}, \tag{C1}$$

where any single $\mathcal{L}^{j}_{\omega q}$ has a structure of Eq. (B5) with the appropriate $\gamma_j(\omega)$. Notice that a single component $\mathcal{L}^{j}_{\omega q}$ is also a LGKS generator and possesses a Gibbs-like stationary state written in terms of the averaged Hamiltonian H,

$$\tilde{\rho}^{j}_{\omega q} = Z^{-1}\exp\left\{-\frac{\omega+q\Omega}{\omega}\frac{H}{k_B T_j}\right\}. \tag{C2}$$

The corresponding time-dependent objects satisfy

$$\begin{aligned} \mathcal{L}^{j}_{q\omega}(t)\tilde{\rho}^{j}_{q\omega}(t) = 0, \quad \mathcal{L}^{j}_{q\omega}(t) &= \mathcal{U}(t,0)\mathcal{L}^{j}_{q\omega}\mathcal{U}(t,0)^{\dagger}, \\ \tilde{\rho}^{j}_{q\omega}(t) = \mathcal{U}(t,0)\tilde{\rho}^{j}_{q\omega} &= \tilde{\rho}^{j}_{q\omega}(t+\tau). \end{aligned} \tag{C3}$$

Using the decomposition (C1), one can define a *local heat current* which corresponds to the exchange of energy $\omega + q\Omega$ with the jth heat bath for any initial state,

$$\mathcal{J}^{j}_{q\omega}(t) = \frac{\omega+q\Omega}{\omega}\mathrm{Tr}\left\{\left[\mathcal{L}^{j}_{q\omega}(t)\rho(t)\right]\tilde{H}(t)\right\}, \quad \tilde{H}(t) = \mathcal{U}(t,0)H, \tag{C4}$$

or in the equivalent form,

$$\mathcal{J}^{j}_{q\omega}(t) = -k_B T_j \mathrm{Tr}\left\{\left[\mathcal{L}^{j}_{q\omega}(t)\rho(t)\right]\ln\tilde{\rho}^{j}_{q\omega}(t)\right\}. \tag{C5}$$

The heat current associated with the jth bath is a sum of the corresponding local ones,

$$\mathcal{J}^{j}(t) = -k_B T_j \sum_{q\in\mathbf{Z}}\sum_{\{\omega\geqslant 0\}}\mathrm{Tr}\left\{\left[\mathcal{L}^{j}_{q\omega}(t)\rho(t)\right]\ln\tilde{\rho}^{j}_{q\omega}(t)\right\}. \tag{C6}$$

In order to prove the second law, we use Spohn's inequality [3],

$$\mathrm{Tr}([\mathcal{L}\rho][\ln\rho - \ln\tilde{\rho}]) \leqslant 0, \tag{C7}$$

which is valid for any LGKS generator $\mathcal{L}$ with a stationary state $\tilde{\rho}$.

Computing now the time derivative of the entropy $S(t) = -k_B\mathrm{Tr}\rho(t)\ln\rho(t)$ and applying (C7), one obtains the second law in the form

$$\frac{d}{dt}S(t) - \sum_{j=1}^{M}\frac{\mathcal{J}^{j}(t)}{T_j} \geqslant 0, \tag{C8}$$

where $S(t) = -k_B\mathrm{Tr}[\rho(t)\ln\rho(t)]$.

The heat currents in the steady state $\tilde{\rho}(t)$ are time-independent and given by

$$\tilde{\mathcal{J}}^{j} = -k_B T_j \sum_{q\in\mathbf{Z}}\sum_{\{\omega\geqslant 0\}}\mathrm{Tr}\left[\left(\mathcal{L}^{j}_{q\omega}\tilde{\rho}\right)\ln\tilde{\rho}^{j}_{q\omega}\right]. \tag{C9}$$

They satisfy the second law in the form

$$\sum_{j=1}^{M}\frac{\tilde{\mathcal{J}}^{j}}{T_j} \leqslant 0 \tag{C10}$$

while, according to the first law,

$$-\sum_{j=1}^{M}\tilde{\mathcal{J}}^{j} = -\tilde{\mathcal{J}} = \bar{\mathcal{P}} \tag{C11}$$

is the averaged power (negative when the system acts as a heat engine). Notice that in the case of a single heat bath, the heat current is always strictly positive except for the case of no driving, when it is equal to zero.

Notice that for the constant Hamiltonian, the above formulas are also applicable after removing the index q, which implies also that $\sum_{j=1}^{M}\tilde{\mathcal{J}}^{j} = 0$.

APPENDIX D: VAN HOVE PHENOMENON

A natural physical stability condition which should be satisfied by any model of an open quantum system is that its total Hamiltonian should be bounded from below and should possess a ground state. In the case of systems coupled linearly to bosonic heat baths, it implies the existence of the ground state for the following bosonic Hamiltonian [compare with Eq. (35)]:

$$H_{\mathrm{bos}} = \sum_{k}\{\omega(k)a^{\dagger}(k)a(k) + [g(k)a(k) + \bar{g}(k)a^{\dagger}(k)]\}. \tag{D1}$$

Introducing a formal transformation to a new set of bosonic operators,

$$a(k) \mapsto b(k) = a(k) + \frac{\bar{g}(k)}{\omega(k)}, \tag{D2}$$

we can write

$$H_{\mathrm{bos}} = \sum_{k}\omega(k)b^{\dagger}(k)b(k) - E_0, \quad E_0 = \sum_{k}\frac{|g(k)|^2}{\omega(k)} \tag{D3}$$

with the formal ground state $|0\rangle$ satisfying

$$b(k)|0\rangle = 0 \quad \text{for all} \quad k. \tag{D4}$$

For the interesting case of an infinite set of modes $\{k\}$, labeled by the d-dimensional wave vectors, two problems can appear:

(i) The ground state energy E_0 can be infinite, i.e., it does not satisfy

$$\sum_k \frac{|g(k)|^2}{\omega(k)} < \infty. \tag{D5}$$

(ii) The transformation (D2) can be implemented by a unitary one, i.e., $b(k) = Ua(k)U^\dagger$ if and only if

$$\sum_k \frac{|g(k)|^2}{\omega(k)^2} < \infty. \tag{D6}$$

Nonexistence of such a unitary implies nonexistence of the ground state (D4) (in the Fock space of the bosonic field), and this is called the *van Hove phenomenon* [39].

While the divergence of the sums (D5) and (D6) (or integrals for the infinite volume case) for large $|k|$ can be avoided by applying the *ultraviolet cutoff*, the stronger condition (D6) puts restrictions on the form of $g(k)$ at low frequencies. Assuming that $\omega(k) = v|k|$ and $g(k) \equiv g(\omega)$, the condition (D6) is satisfied for the following low-frequency scaling in the d-dimesional case:

$$|g(\omega)|^2 \sim \omega^\kappa, \quad \kappa > 2 - d. \tag{D7}$$

[1] A. Einstein, Ann. Phys. **17**, 132 (1905).
[2] J. Geusic, E. S. du Bois, R. D. Grasse, and H. Scovil, Phys. Rev. **156**, 343 (1967).
[3] H. Spohn, J. Math. Phys. **19**, 1227 (1978).
[4] R. Alicki, J. Phys. A **12**, L103 (1979).
[5] R. Kosloff, J. Chem. Phys. **80**, 1625 (1984).
[6] E. Geva and R. Kosloff, J. Chem. Phys. **104**, 7681 (1996).
[7] R. Kosloff, E. Geva, and J. M. Gordon, Appl. Phys. **87**, 8093 (2000).
[8] J. P. Palao, R. Kosloff, and J. M. Gordon, Phys. Rev. E **64**, 056130 (2001).
[9] S. Lloyd, Phys. Rev. A **56**, 3374 (1997).
[10] T. D. Kieu, Phys. Rev. Lett. **93**, 140403 (2004).
[11] D. Segal and A. Nitzan, Phys. Rev. E **73**, 026109 (2006).
[12] P. Bushev, D. Rotter, A. Wilson, F. Dubin, C. Becher, J. Eschner, R. Blatt, V. Steixner, P. Rabl, and P. Zoller, Phys. Rev. Lett. **96**, 043003 (2006).
[13] E. Boukobza and D. J. Tannor, Phys. Rev. A **78**, 013825 (2008).
[14] J. Birjukov, T. Jahnke, and G. Mahler, Eur. Phys. J. B **64**, 105 (2008).
[15] A. E. Allahverdyan, R. S. Johal, and G. Mahler, Phys. Rev. E **77**, 041118 (2008).
[16] D. Segal, J. Chem. Phys. **130**, 134510 (2009).
[17] H. Wang, S. Q. Liu, and J. Z. He, Phys. Rev. E **79**, 041113 (2009).
[18] J. Gemmer, M. Michel, and G. Mahler, *Quantum Thermodynamics* (Springer, Berlin, Heidelberg, 2009).
[19] N. Linden, S. Popescu, and P. Skrzypczyk, Phys. Rev. Lett. **105**, 130401 (2010).
[20] W. Nernst, Nachr. Kgl. Ges. Wiss. Gött. **1**, 1 (1906).
[21] W. Nernst, Er. Kgl. Pr. Akad. Wiss. **52**, 933 (1906).
[22] W. Nernst, Sitzber. preuss. Akad. Wiss. Physik-math. Kl.134 (1912).
[23] P. T. Landsberg, Rev. Mod. Phys. **28**, 363 (1956).
[24] A. Levy and R. Kosloff, Phys. Rev. Lett. **108**, 070604 (2012).
[25] B. Andresen, P. Salamon, and R. Stephen Berry, Phys. Today **37**(9), 62 (1984).
[26] E. Davies, Commun. Math. Phys. **39**, 91 (1974).
[27] R. Dumcke, Commun. Math. Phys. **97**, 331 (1985).
[28] R. Alicki, D. A. Lidar, and P. Zanardi, Phys. Rev. A **73**, 052311 (2006).
[29] N. Brunner, N. Linden, S. Popescu, and P. Skrzypczyk, Phys. Rev. E **85**, 051117 (2012).
[30] Y. Rezek and R. Kosloff, New J. Phys. **8**, 83 (2006).
[31] Y. Rezek, P. Salamon, K. H. Hoffmann, and R. Kosloff, Europhys. Lett. **85**, 30008 (2009).
[32] R. Alicki, Phys. Rev. A **40**, 4077 (1989).
[33] E. Davies, Ann. Inst. H. Poincare A **28**, 91 (1978).
[34] R. H. Fowler and E. A. Guggenheim, *Statistical Thermodynamics* (Cambridge University Press, Cambridge, 1939).
[35] F. Belgiorno, J. Phys. A **36**, 8165 (2003).
[36] F. Belgiorno, J. Phys. A **36**, 8195 (2003).
[37] R. O'Connell, J. Stat. Phys. **124**, 15 (2006).
[38] G. Ford and R. O'Connell, Physica E **29**, 82 (2005).
[39] G. G. Emch, *Algebraic Methods in Statistical Mechanics and Quantum Field Theory* (Wiley Interscience, New York, 1972).

Chapter 6

Quantum flywheel

Quantum flywheel
Amikam Levy, Lajos Diósi and Ronnie Kosloff
Published in: Phys. Rev. A, vol. 93, no. 5, page 052119, 2016.

PHYSICAL REVIEW A **93**, 052119 (2016)

Quantum flywheel

Amikam Levy,[1] Lajos Diósi,[2] and Ronnie Kosloff[1]
[1]*Fritz Haber Research Center for Molecular Dynamics, The Institute of Chemistry, The Hebrew University, Jerusalem 91904, Israel*
[2]*Wigner Research Center for Physics, H-1525 Budapest, P.O. Box 49, Hungary*
(Received 15 February 2016; published 27 May 2016)

In this work we present the concept of a quantum flywheel coupled to a quantum heat engine. The flywheel stores useful work in its energy levels, while additional power is extracted continuously from the device. Generally, the energy exchange between a quantum engine and a quantized work repository is accompanied by heat, which degrades the charging efficiency. Specifically when the quantum harmonic oscillator acts as a work repository, quantum and thermal fluctuations dominate the dynamics. Quantum monitoring and feedback control are applied to the flywheel in order to reach steady state and regulate its operation. To maximize the charging efficiency one needs a balance between the information gained by measuring the system and the information fed back to the system. The dynamics of the flywheel are described by a stochastic master equation that accounts for the engine, the external driving, the measurement, and the feedback operations.

DOI: 10.1103/PhysRevA.93.052119

I. INTRODUCTION

A *flywheel* is a device that stores kinetic energy in the rotational motion of the wheel and supplies it on demand. In many devices the flywheel is an essential component for extracting work from an engine. The main tasks of a flywheel are twofold: transducing discrete energy into continuous power and storing useful *work*. This energy reserve can be rapidly drained on demand, ultimately extracting more power than the charging engine can supply. Miniaturizing heat engines and refrigerators received much attention in the past decade. Experimental setups of such devices were constructed in the micrometers domain [1,2], and recently the operation of a single-atom heat engine was reported [3]. Many theoretical studies of these devices were extended to the quantum domain, concentrated on the study of efficiency, power extraction, and thermodynamic laws (see reviews [4–8] and references therein). Work extraction from quantum systems and their charging were also studied extensively [9–12].

Any realistic engine is regulated by monitoring and a feedback loop. The purpose is to control its timing, adjust its frequency and amplitude to match the other parts of the device, and to compensate for unpredictable disturbances. Recent theoretical studies demonstrated that quantum properties such as coherence and correlations enhance the work extracted from the system [13–17]. Future quantum technologies aiming to exploit these quantum features will encounter the issue of regulating the device. Standard ideal quantum measurements will demolish these features. Therefore, to overcome this problem a conceivable approach to regulate the quantum device is by continuous weak measurements (*monitoring*) and *feedback control*. Another fundamental problem which is demonstrated in this study and that is resolved by monitoring and feedback control is the unlimited entropy increase of the work repository; i.e., proliferating fluctuations catastrophically heat up the flywheel.

In this paper we introduce the concept of a quantum flywheel as part of a quantum *heat engine*. The flywheel is composed of a quantum harmonic oscillator (HO) interacting with a two-qubit quantum heat engine. It is worth comparing this setup to two cases. The first is when the HO (the flywheel) is driven by a laser field in the semiclassical approximation instead of being driven by a quantum heat engine. In this case, energy is constantly flowing into the HO and in principle can be fully extracted back as useful work. The entropy of the HO will not change under the driving of the laser field. The second is when the flywheel (the HO) is replaced by an external classical field. In such case the engine would operate in steady state and power can continuously be extracted from the engine (see Appendix A). However, we will see that when all the parts of the device are quantized, i.e., the medium of the engine is a single qubit and the work repository is a quantum HO, the flywheel will be subject to a fatal growth of fluctuations and establishment of *steady state* is impossible. The HO is unstable even when an external *driving* field is utilized to extract power and stabilize it. Note that the instability we are facing is not the amplification of the energy in the flywheel. Such instability will accrue in any unbounded system that is constantly fed with energy. In this study we are interested in the quality of the energy stored in the flywheel and in overcoming the destructive fluctuations. By applying monitoring and feedback control we obtain a steady-state operation for the flywheel, continuously gaining power, and storing useful work in the flywheel that later can be extracted.

Monitored and controlled quantum heat engines are still to be realized experimentally; however, the individual components already exist. Quantum monitoring and feedback control experiments exists for various HO's such as electromagnetic cavity, nanomechanical oscillators, trapped particles, and superconducting circuits; see the review [18] and references therein. Single microscopic quantum heat engine realizations are still under development with only a few examples available [3,19].

II. HEAT ENGINE OPERATION

The basic concept of a quantum heat engine (similar to the classical one) consists of two thermal heat baths at different temperature, a working medium, and a work repository. In the quantum counterpart the working medium is quantized and the work repository can be an external classical field [4,20] or it can be quantized as well [21]. Here we consider

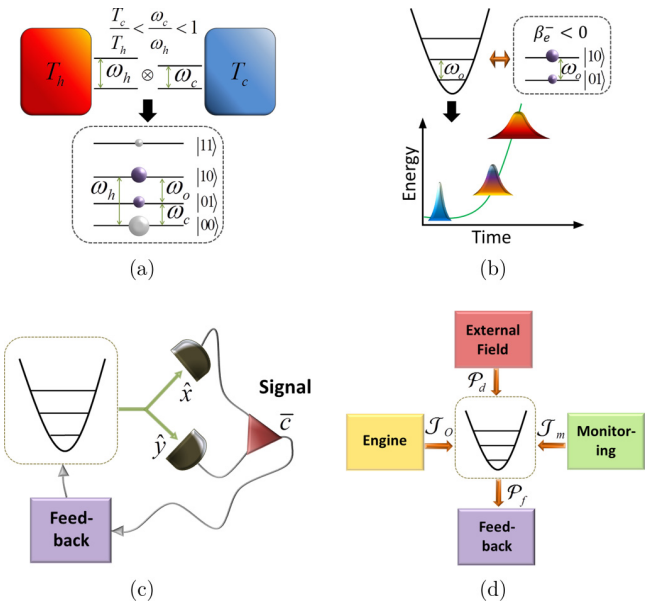

FIG. 1. General scheme of a heat engine with a flywheel. (a) The state of two qubits of the heat engine, coupled to heat baths at temperatures T_h and T_c, is represented as a two-qubit state with population inversion between the second and third energy levels. The size of the sphere represents the population in each level. (b) The population inversion in the engine corresponds to a heat bath with the inverse negative temperature β_e^-. This bath is coupled to the harmonic oscillator (flywheel), increasing exponentially its energy and the width of phase-space probability distribution. (c) Measurement of the quadratures of the harmonic oscillator, resulting in the signal $\bar{c}$. The signal is then fed back to the oscillator to ensure a steady state. (d) Energy flow chart of the different components in the steady state of the flywheel.

the operation of a continuous quantum engine for which the heat baths and the work repository are coupled simultaneously and continuously to the working medium [4]. The working medium is comprised of two qubits, with the Hamiltonians $\hat{H}_a = \omega_h \hat{a}^\dagger \hat{a}$ and $\hat{H}_b = \omega_c \hat{b}^\dagger \hat{b}$. Each qubit is weakly coupled to a different heat bath with the inverse temperature β_h and β_c, where the indexes h and c stand for *hot* and *cold*. The dynamics of the qubits follow the standard thermalizing master equation of Lindblad-Gorini-Kossakowski-Sudarshan (LGKS) [22–24]. The asymptotic two-qubit state $\hat{\rho}_h^\infty \otimes \hat{\rho}_c^\infty$ is the product of the thermal equilibrium Gibbs states of the two qubits, respectively, at hot and cold temperatures $1/\beta_h$ and $1/\beta_c$. Satisfying the heat engine conditions, $\beta_h/\beta_c < \omega_c/\omega_h < 1$, population inversion is obtained between the third level $|10\rangle$ and the second level $|01\rangle$ [see Fig. 1(a)]. The populations of these states are given by $p_{10} = n_h(1-n_c)$ and $p_{01} = n_c(1-n_h)$. Here, $n_{h(c)} = [\exp(\beta_{h(c)}\omega_{h(c)}) + 1]^{-1}$ are the thermal occupation numbers in $\hat{\rho}_{h(c)}^\infty$. The second and the third levels are treated as an effective two-level system (TLS) with the energy gap $\omega_o = \omega_h - \omega_c$ (we take $\hbar = k_B = 1$). The state of this TLS is a Gibbs state with a negative effective temperature

$$\frac{1}{\beta_e^-} = \frac{\omega_h - \omega_c}{\beta_h\omega_h - \beta_c\omega_c} < 0. \tag{1}$$

We exploit the TLS population inversion to "charge" a quantum harmonic oscillator (HO) with useful work. The Hamiltonian of the HO and the TLS-HO interaction Hamiltonian are given by $\hat{H}_o = \omega_o \hat{c}^\dagger \hat{c}$ and $\hat{K} = ig(\hat{a}^\dagger \hat{b} \hat{c} - \hat{a}\hat{b}^\dagger \hat{c}^\dagger)$, respectively. Given that the thermalization time of the qubits is much shorter then the internal time scale, $g\sqrt{\langle \hat{c}^\dagger \hat{c}\rangle + 1} \ll \Gamma_{h(c)}[1 + \exp(-\beta_{h(c)}\omega_{h(c)})]$, the TLS can be considered heuristically as a heat bath with negative temperature weakly coupled to the HO. We prove that indeed the state $\hat{\rho}$ of the HO satisfies the standard thermalizing master equation extended to negative temperature $1/\beta_e^-$, which in the interaction picture of $\hat{H}_o$ takes the form

$$\frac{d\hat{\rho}}{dt} = \mathcal{L}_e\hat{\rho} \equiv \Gamma_e(\hat{c}\hat{\rho}\hat{c}^\dagger - \mathcal{H}\hat{c}^\dagger\hat{c}\hat{\rho}) + \Gamma_e e^{-\beta_e^-\omega_o}(\hat{c}^\dagger\hat{\rho}\hat{c} - \mathcal{H}\hat{c}\hat{c}^\dagger\hat{\rho}). \tag{2}$$

The damping rate Γ_e is proportional to the squared coupling g^2, and depends on the parameters of the engine, such as the occupations $n_{h(c)}$ and the rates $\Gamma_{h(c)}$ (see Appendix B). The notation $\mathcal{H}$ stands for the Hermitian part of everything coming after it (different from the convention in Ref. [25]). A rigorous derivation of Eq. (2) can be found in Appendix B. The following results are not limited to the specific medium of the engine and will apply to any dynamics that will lead to the thermalizing master equation with negative temperature. For example the two qubits can be replaced by a three-level system or two HO's. As long as the three-body interaction $\hat{K}$ is kept, the structure of Eq. (2) with negative temperature is preserved. The only difference would be the specifics of the relaxation rate Γ_e.

Since $\beta_e^- < 0$ the master equation (2) has no steady-state solution, energy will constantly flow into the flywheel. The parameters containing the superscript $^-$ are negative. The standard equations remain valid for the mean amplitude $\langle \hat{c}\rangle_t$ and the occupation $\langle \hat{c}^\dagger \hat{c}\rangle_t$:

$$\frac{d\langle \hat{c}\rangle_t}{dt} = -(\kappa_e^- + i\omega_o)\langle \hat{c}\rangle_t, \tag{3}$$

$$\frac{d\langle \hat{c}^\dagger \hat{c}\rangle_t}{dt} = -2\kappa_e^-\langle \hat{c}^\dagger \hat{c}\rangle_t + \Gamma_e e^{-\beta_e^-\omega_o}, \tag{4}$$

where the amplitude damping rate

$$\kappa_e^- = \tfrac{1}{2}\Gamma_e(1 - e^{-\beta_e^-\omega_o}) \tag{5}$$

takes negative values since $\beta_e^- < 0$ (Appendix B). Therefore both $\langle \hat{c}\rangle_t$ and $\langle \hat{c}^\dagger \hat{c}\rangle_t$ (and all higher moments) diverge exponentially with time [see Fig. 1(b)] resulting in the instability of the dynamics against small perturbations. In particular, an initial Gibbs state maintains its form but with an exponentially growing temperature $1/\beta_t = \omega_o/\ln(1 + \langle \hat{c}^\dagger \hat{c}\rangle_t^{-1})$. Thus, $\hat{\rho}(t) \propto \exp(-\beta_t\omega_o\hat{c}^\dagger\hat{c})$ is an unstable solution of the master equation (2). Any small perturbation will divert it from the class of Gibbs states. A more general class of solutions, displaced Gibbs states $\hat{\rho}(t) \propto \exp[-\beta_t\omega_o(\hat{c} - \langle \hat{c}\rangle_t)^\dagger(\hat{c} - \langle \hat{c}\rangle_t)]$, with effective temperature $1/\beta_t = \omega_o/\ln[1 + (\langle \hat{c}^\dagger \hat{c}\rangle_t - |\langle \hat{c}\rangle_t|^2)^{-1}]$ will, in principle, be suitable for work extraction. But this option is misleading since the instability of the above solutions is not yet resolved.

A reasonable approach to stabilize the flywheel while extracting additional power is achieved by driving the HO via a resonant oscillating external field. The field is expressed by the time-dependent Hamiltonian, $\hat{H}_d(t) = -i\epsilon_d \hat{c}^\dagger e^{-i\omega_o t} +$ H.c. The master equation in the interaction picture (2) becomes modified by a static Hamiltonian term (see Appendix C):

$$\frac{d\hat{\rho}}{dt} = \mathcal{L}_e\hat{\rho} - \epsilon_d[\hat{c}^\dagger - \hat{c}, \hat{\rho}_o]. \tag{6}$$

Indeed, Eq. (6) leads to a stationary amplitude with a rotating phase: $\langle\hat{c}\rangle_t = -(\epsilon_d/\kappa_e^-)e^{-i\omega_o t}$. Nevertheless, the stationary state remains unstable, the occupation number and higher moments diverge invariably. Driving in itself cannot solve the instability issue. Unlimited growth of quantum and thermal fluctuations must be suppressed by active control of the flywheel.

III. MEASUREMENT AND FEEDBACK CONTROL

A. Monitoring

Continuous measurement, i.e., monitoring, is the first task towards implementing feedback control [25]. By applying monitoring and feedback control we can stabilize the flywheel and charge it with useful work. Consider a time-continuous measurement of both quadratures $\hat{x} = \frac{1}{\sqrt{2}}(\hat{c}^\dagger + \hat{c})$ and $\hat{y} = \frac{i}{\sqrt{2}}(\hat{c}^\dagger - \hat{c})$ of the HO. Generalizing the result of [26], we simultaneously monitor $\hat{x}$ and $\hat{y}$ [see Fig. 1(c)]. The dynamics is described by a stochastic master equation (SME) for the density operator $\hat{\sigma}$ conditioned on both measurement signals $\bar{x}, \bar{y}$ (see Appendix D). The stochastic mean $\mathbf{M}$ of the conditional state yields the unconditional state, i.e., $\mathbf{M}\hat{\sigma} = \hat{\rho}$ satisfying a corresponding master equation of the usual LGKS structure. It differs from the master equation of Eq. (6) by the additional monitoring term

$$\mathcal{L}_m\hat{\rho} = \frac{\gamma_m}{4}(\hat{c}\hat{\rho}\hat{c}^\dagger - \mathcal{H}\hat{c}^\dagger\hat{c}\hat{\rho} + \hat{c}^\dagger\hat{\rho}\hat{c} - \mathcal{H}\hat{c}\hat{c}^\dagger\hat{\rho}), \tag{7}$$

where γ_m is the measurement strength. This generator corresponds to an infinite-temperature heat bath. Hence, the act of monitoring additionally heats the flywheel and contributes to the undesirable proliferating fluctuations of the HO.

B. Feedback control

Stabilization is accomplished by a feedback loop conditioned on the measured signals $\bar{x}, \bar{y}$. As a result, the HO is kept in the vicinity of the constant rotating amplitude set by the external driving. The feedback Hamiltonian in the Schrödinger picture is given by $\hat{H}_f(t) = -i\kappa_f\bar{c}(t)\hat{c}^\dagger +$ H.c., where $\bar{c} = \frac{1}{\sqrt{2}}(\bar{x} + i\bar{y})$ is the complex representation of the two real signals $\bar{x}$ and $\bar{y}$, and κ_f is the feedback strength. By setting the value of κ_f the steady state of the flywheel is guaranteed. The feedback is applied on top of the monitored evolution [27], $\hat{\sigma} + d\hat{\sigma} \to e^{-i\hat{H}_f dt}(\hat{\sigma} + d\hat{\sigma})e^{i\hat{H}_f dt}$, yielding a SME for the conditional state, Appendix E. Averaging over many realizations, the master equation of the unconditional state reads

$$\frac{d\hat{\rho}}{dt} = (\mathcal{L}_e + \mathcal{L}_m + \mathcal{L}_f)\hat{\rho} - \epsilon_d[\hat{c}^\dagger - \hat{c}, \hat{\rho}]. \tag{8}$$

The dissipative contribution of the feedback is

$$\mathcal{L}_f\hat{\sigma} = \left(\frac{\kappa_f^2}{\gamma_m} + \kappa_f\right)(\hat{c}\hat{\sigma}\hat{c}^\dagger - \mathcal{H}\hat{c}^\dagger\hat{c}\hat{\sigma}) + \left(\frac{\kappa_f^2}{\gamma_m} - \kappa_f\right)(\hat{c}^\dagger\hat{\sigma}\hat{c} - \mathcal{H}\hat{c}\hat{c}^\dagger\hat{\sigma}). \tag{9}$$

For $\kappa_f > \gamma_m$ this corresponds to a thermal bath of positive temperature. Entering the regime $0 < \kappa_f < \gamma_m$, the cooling effect of $\mathcal{L}_f$ within the sum $\mathcal{L}_e + \mathcal{L}_m + \mathcal{L}_f$ becomes enhanced although $\mathcal{L}_f$ ceases to be a mathematically correct dissipator in itself. Equation (8) can be written in a compact form,

$$\frac{d\hat{\rho}}{dt} = \Gamma(\hat{c}\hat{\rho}\hat{c}^\dagger - \mathcal{H}\hat{c}^\dagger\hat{c}\hat{\rho}) + \Gamma e^{-\beta\omega_o}(\hat{c}^\dagger\hat{\rho}\hat{c} - \mathcal{H}\hat{c}\hat{c}^\dagger\hat{\rho}) - \epsilon_d[\hat{c}^\dagger - \hat{c}, \hat{\rho}], \tag{10}$$

where Γ and β are determined by

$$\Gamma = \Gamma_e + \frac{\gamma_m}{4} + \frac{\kappa_f^2}{\gamma_m} + \kappa_f, \tag{11}$$

$$e^{-\beta\omega_o}\Gamma = \Gamma_e e^{-\beta_e^-\omega_o} + \frac{\gamma_m}{4} + \frac{\kappa_f^2}{\gamma_m} - \kappa_f. \tag{12}$$

The effective temperature $1/\beta$ becomes positive by setting the feedback strength above the threshold: $\kappa_f > -\kappa_e^-$. To summarize, as a result of the feedback the negative-temperature heat bath and the negative amplitude damping rate κ_e^- for HO become an effective positive-temperature heat bath with the amplitude damping rate $\kappa_f + \kappa_e^- > 0$.

IV. STEADY STATE AND WORK EXTRACTION

For sufficiently strong feedback κ_f, satisfying $\kappa_f + \kappa_e^- > 0$, Eq. (10) is a standard thermalizing master equation with resonant external driving. It has a unique stationary state which in the Schrödinger picture is a thermal state with rotating displacement also known as a thermal coherent state (see Appendix E),

$$\hat{\rho}^\infty \propto \exp[-\beta\omega_o(\hat{c} - c_\infty e^{-i\omega_o t})^\dagger(\hat{c} - c_\infty e^{-i\omega_o t})]. \tag{13}$$

where $c_\infty = -\frac{\epsilon_d}{\kappa_f + \kappa_e} < 0$. Hence, the mean amplitude rotates, $\langle\hat{c}\rangle_\infty = c_\infty e^{-i\omega_o t}$, its phase is shifted by $-\pi/2$ with respect to the external driving. The average population is given by the sum of the Bose statistic n_o and the yield of displacement

$$\langle\hat{c}^\dagger\hat{c}\rangle_\infty = \frac{1}{e^{\beta\omega_o} - 1} + |c_\infty|^2 \equiv n_o + |c_\infty|^2. \tag{14}$$

We distinguish two opposing regimes of the steady-state operation of the flywheel. The first is the deep quantum regime, $n_o, |c_\infty|^2 \ll 1$, where the flywheel is operating in the vicinity of its ground state. The second is the classical regime in which both the thermal occupation and the displacement are large numbers, $n_o, |c_\infty|^2 \gg 1$. The two crossed regimes also present peculiar quantum features. Recall that weak coupling condition sets an asymptotic upper limit on the total occupation in Eq. (14). This implies asymptotic upper limits on the temperature $1/\beta$, excluding too high thermal occupations n_o, as well as on the driving strength ϵ_d, confining

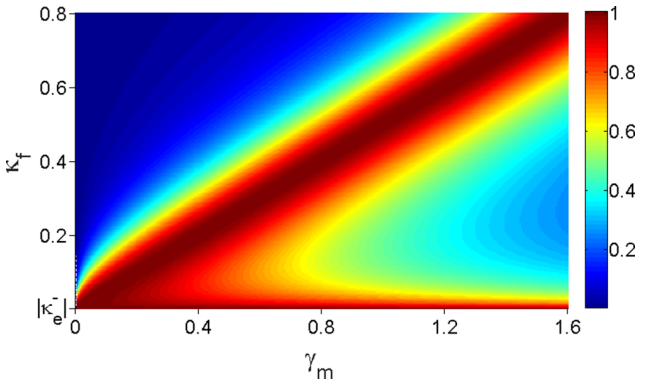

FIG. 2. Charging efficiency as function of measurement strength γ_m and feedback strength κ_f. The percentage of useful work out of the entire energy stored in the flywheel has a maximum for the ratio $\gamma_m/\kappa_f = 2$, and it is further maximized for κ_f approaching its threshold $|\kappa_e^-| = 5 \times 10^{-8}$. Here: $\omega_o = 1$, $\beta_e^- = -10^{-1}$, $\Gamma_e = 10^{-6}$, and $\epsilon_d = 9 \times 10^{-2}$.

the displacements $\langle \hat{c} \rangle_\infty$. Thus, accessibility to the classical regime depends on the physical properties of the two-qubit heat engine and its coupling g to the flywheel. The steady state (13) becomes a displaced Gibbs state and as such, it is suitable for work extraction. The internal energy of the steady state is given by $\mathcal{E} = \omega_o(n_o + |c_\infty|^2)$. Applying a unitary displacement transformation can bring the state in Eq. (13) into a Gibbs state (passive state) with the temperature $1/\beta$. Thus, the part of the internal energy that is due to c_∞ can all be extracted by the unitary operation as the maximum useful work

$$\mathcal{W} = \omega_o |c_\infty|^2 = \frac{\omega_o \epsilon_d^2}{(\kappa_f + \kappa_e^-)^2}, \tag{15}$$

which is independent of the strength γ_m of the monitoring. The *charging efficiency* of the flywheel can be defined as the ratio between useful work and the internal energy stored in the HO (see Fig. 2),

$$\eta = \frac{\mathcal{W}}{\mathcal{E}} = \frac{1}{1 + n_o/|c_\infty|^2}. \tag{16}$$

The efficiency is improved for small thermal occupation n_o and large displacement c_∞. The occupation n_o becomes small when the effective temperature $1/\beta$ is reduced. Interestingly, this singles out the optimum measurement strength γ_m which has so far remained unconstrained. From Eqs. (11) and (12) we find that $1/\beta$ takes its minimum value with the choice $\gamma_m = 2\kappa_f$ obtaining minimum for n_o and maximum for the charging efficiency:

$$\eta|_{\gamma_m = 2\kappa_f} = \frac{1}{1 + \frac{\Gamma_e}{2\epsilon_d^2} e^{-\beta_e^- \omega_o} (\kappa_f + \kappa_e^-)^2}. \tag{17}$$

The efficiency $\eta_{\gamma_m = 2\kappa_f}$ together with the extractable work $\mathcal{W}$ reach higher values if we increase the displacement $|c_\infty|$. In particular, the efficiency approaches its maximal value 1 when the feedback κ_f approaches its lower threshold, $\kappa_f \to -\kappa_e^-$. A different technique to maximize both the efficiency and the work is by increasing ϵ_d, i.e., applying a stronger driving field. Nevertheless, as was already mentioned, these two approaches are limited by the weak-coupling condition.

V. ENERGY FLOWS IN STEADY STATE

A macroscopic flywheel at rest requires an input work (initial push) to reach the vicinity of steady state. At this point the output power is larger than the input power. Regulating the flywheel also has energetic costs that should be accounted for. These energetic considerations, in principle, also apply to the quantum flywheel. However, the related calculations require a novel approach to heat flow and power in quantum systems under stochastic control.

The standard definition of thermodynamic heat flow $\mathcal{J}$ and power $\mathcal{P}$ in open quantum systems is given [28] by the time derivative of the internal energy $\mathcal{E} = \mathrm{tr}[\hat{\rho}\hat{H}]$ in the following manner:

$$d\mathcal{E} = \mathrm{tr}[d\hat{\rho}\hat{H}] + \mathrm{tr}[\hat{\rho} d\hat{H}] \equiv \mathcal{J}dt + \mathcal{P}dt. \tag{18}$$

The Hamiltonian and the state of the system are typically stochastic in the theory of monitoring and feedback control. Since stochastic fluctuations are microscopic, the thermodynamic definition of the internal energy is given by the stochastic mean of the microscopic energy, $\mathbf{M}\mathrm{tr}(\hat{\sigma}\hat{H})$. This leads to the following generalization of the standard thermodynamic relation:

$$d\mathcal{E} = \mathbf{M}\mathrm{tr}[d\hat{\sigma}\hat{H}] + \mathbf{M}\mathrm{tr}[\hat{\sigma} d\hat{H}] \equiv \mathcal{J}dt + \mathcal{P}dt. \tag{19}$$

The differentials in Eq. (19) must be Stratonovich ones instead of those of Ito. For the Ito differentials the right-hand side should contain the so-called Ito correction $\mathbf{M}\mathrm{tr}[d\hat{\sigma}\, d\hat{H}]$ which would jeopardize the split of $d\mathcal{E}$ between heat flow and power. In Appendix F we derive a lower bound on the extractable power, demonstrating that the power is gained from the device and not consumed by it.

We summarize the plausible structure of energy currents [see Fig. 1(d)]. The steady-state energy balance contains five different currents: $\dot{\mathcal{E}} = \mathcal{J}_e + \mathcal{J}_m + \mathcal{J}_f + \mathcal{P}_d + \mathcal{P}_f = 0$. The heat flowing into the flywheel has two contributions, the first is from the engine, $\mathcal{J}_e$, the second is from the monitoring device, $\mathcal{J}_m$. Power from the driving field, $\mathcal{P}_d$, is also consumed by the flywheel, and serves as an input power activating the flywheel. This power is overcompensated by the output power $\mathcal{P}_f$ realized by the feedback. In addition, the outflow $\mathcal{J}_f$ cools the flywheel, thereby stabilizing it and lowering the entropy produced in the flywheel as a result of the engine and the monitoring operations. In the case $\beta_e^- \to 0^-$ of no population inversion in the engine, the heat flow $\mathcal{J}_e$ and the consumable power must vanish. The work in Eq. (15) stored in the flywheel reaches its minimal, yet positive, value $\mathcal{W} = \omega_o \epsilon_d^2/\kappa_f^2$.

VI. SUMMARY

Population inversion, corresponding to negative temperature $1/\beta_e^-$ in a few-level quantum heat engine was established a long time ago [29] and has been considered in detail [30]. In this paper we have shown that the heat engine operation is equivalent to a negative-temperature heat bath in the standard dynamical sense. Thus, its influence on the work repository is

the typical thermalizing master equation extended to negative temperature $1/\beta_e^-$.

Work extraction is still an outstanding issue because of the spread of thermal and quantum noise over the work repository, which in our case is a quantum HO. If the HO is replaced by an idealized classical field, all the energy flowing out of the engine can in principle be extracted as power. If the HO is driven by a coherent laser field instead of the quantum heat engine then all energy stored in the flywheel can be extracted from it as work. However, when the work repository is quantized and the heat engine medium is a single qubit, the work exchange is accompanied with heat exchange, which degrades the charging efficiency. In this paper we introduced a generic approach that can be applied to resolve such problems. Specifically, we demonstrated the difficulties of storing useful work in a quantum harmonic oscillator. Overcoming the unlimited growth of fluctuations, regulating and stabilizing the flywheel is achieved by applying monitoring and feedback control to the system.

The steady state, the power, and the stored extractable energy of the flywheel are determined analytically. While the amount of work stored in the flywheel is independent of the accuracy of the monitoring, the charging efficiency is optimized for a particular ratio between the monitoring and the feedback strength. Thus, a maximum is achieved by balancing the information gained by monitoring the flywheel with the information fed back to the flywheel. The balance coincides with minimum temperature of the flywheel. Breaking this balance implies that the phase-space distribution is no longer optimal for work extraction from the flywheel. Note that to obtain steady-state operation one could cool the HO by coupling it to a cold thermal bath instead of applying monitoring and feedback control. A second cold bath would mean a new thermodynamic resource in addition to the heat engine with its two heat baths. We wished, however, to investigate how to exploit the thermodynamic resource given by the heat engine itself, using additional control mechanisms only. A more crucial point is that by monitoring and feedback we can optimize the charging efficiency and obtain a regime of operation that no thermal bath will allow. In this regime, where $\kappa_f < \gamma_m$, the cooling is enhanced and the dynamics cannot be described by a thermal bath.

This model is a prototype of an analytically tractable model of a quantum heat engine coupled to a single degree-of-freedom work repository, operating continuously in steady state under quantum control. Experiments which employ quantum monitoring and feedback strategies are becoming common [18,31–33]. Future advances in quantum technologies depend on our ability to control and manipulate quantum systems. A firm theoretical foundation relating systems that are subject to quantum monitoring and feedback control with basic concepts of thermodynamics is still missing.

ACKNOWLEDGMENTS

We thank Raam Uzdin, Saar Rahav, David Gelbwaser-Klimovsky, Peter Salamon, and Walter Singaram for fruitful discussions. This work was supported by the Israeli Science Foundation and the Hungarian Scientific Research Fund under Grant No. 103917. Part of this work was supported by the COST Action MP1209 "Thermodynamics in the quantum regime."

APPENDIX A: POWER EXTRACTION VIA CLASSICAL PERIODIC FIELD

Steady-state power extraction *without* storing work is possible by just by driving the engine directly without the flywheel. Power is gained by amplification of a classical rotating field in resonance with the two TLS's. The interaction Hamiltonian is given by $\hat{K}(t) = -i\epsilon(\hat{a}\hat{b}^\dagger e^{i\omega_o t} - \hat{a}^\dagger\hat{b}\, e^{-i\omega_o t})$. For weak driving, the master equation for the two TLS's, $\hat{\rho}_{hc}$, in the interaction picture of $\hat{H}_h$ and $\hat{H}_c$ is

$$\frac{d\hat{\rho}_{hc}}{dt} = -[\epsilon(\hat{a}\hat{b}^\dagger - \hat{a}^\dagger\hat{b}), \hat{\rho}_{hc}] + \mathcal{L}_h\hat{\rho}_{hc} + \mathcal{L}_c\hat{\rho}_{hc}, \tag{A1}$$

where $\mathcal{L}_{h(c)}$ are defined in Eq. (B1). The master equation (A1) possesses a unique stationary state. The stationary output power

$$-\mathcal{P}^\infty = \frac{4\epsilon^2\omega_o(n_h - n_c)}{4\epsilon^2\left[\Gamma_h^{-1}(1-n_h) + \Gamma_c^{-1}(1-n_c)\right] + \Gamma_h(1+e^{-\beta_h\omega_h}) + \Gamma_c(1+e^{-\beta_c\omega_c})} > 0 \tag{A2}$$

is positive. This implies that steady-state power extraction can be obtained from a periodically driven field. Note that for strong driving there is also a steady-state power extraction from the engine. Nevertheless, the master equation (A1) must be modified. Derivation of a master equation driven by a strong periodic field can be found in [20].

APPENDIX B: TRIPARTITE HEAT ENGINE

We use an interaction picture for its convenience especially for our master equations. The stochastic master equations of monitoring and feedback are presented in the Schrödinger picture for transparency. Heat flow and power are, as a rule, defined in the Schrödinger picture. We derive the master equation for the harmonic oscillator (HO) subject to the operation of the engine. The quantum heat engine is comprised of two two-level systems (TLS's), with the Hamiltonians $\hat{H}_h = \omega_h\hat{a}^\dagger\hat{a}$ and $\hat{H}_c = \omega_c\hat{b}^\dagger\hat{b}$. The two TLS's are coupled to a hot and a cold heat bath, respectively, at temperatures $T_h > T_c$. The dynamics follow the Lindblad-Gorini-Kossakowski-Sudarshan dynamics [22,23], and in the interaction picture of $\hat{H}_{h(c)}$ the corresponding master equations read

$$\begin{aligned}\frac{d\hat{\rho}_h}{dt} &= \Gamma_h[\hat{a}\hat{\rho}_h\hat{a}^\dagger - \mathcal{H}\hat{a}^\dagger\hat{a}\hat{\rho}_h + e^{-\beta_h\omega_h}(\hat{a}^\dagger\hat{\rho}_h\hat{a} - \mathcal{H}\hat{a}\hat{a}^\dagger\hat{\rho}_h)] \\ &\equiv \mathcal{L}_h\hat{\rho}_h,\end{aligned}$$

$$\frac{d\hat{\rho}_c}{dt} = \Gamma_c[\hat{b}\hat{\rho}_c\hat{b}^\dagger - \mathcal{H}\hat{b}^\dagger\hat{b}\hat{\rho}_c + e^{-\beta_c\omega_c}(\hat{b}^\dagger\hat{\rho}_c\hat{b} - \mathcal{H}\hat{b}\hat{b}^\dagger\hat{\rho}_c)] \equiv \mathcal{L}_c\hat{\rho}_c, \tag{B1}$$

where $\Gamma_{h(c)}$ are the damping rates. (In our convention, different from that of Ref. [25], $\mathcal{H}$ denotes the Hermitian part of all that stands after it.) The heat baths bring the TLS's to thermal equilibrium states $\hat{\rho}^\infty_{h(c)}$ with the occupation numbers $n_{h(c)} = 1/(e^{\beta_{h(c)}\omega_{h(c)}} + 1)$, and with the inverse temperatures $\beta_{h(c)} = 1/T_{h(c)}$, respectively.

The two TLS's are then weekly coupled to a quantum HO of the self-Hamiltonian $\hat{H}_o = \omega_o\hat{c}^\dagger\hat{c}$, via the tripartite Hamiltonian

$$\hat{K} = -ig\hat{a}\hat{b}^\dagger\hat{c}^\dagger + \text{H.c.} \tag{B2}$$

We work in resonance, $\omega_o = \omega_h - \omega_c$, and in the weak coupling regime for which a local master equation holds [34]. The master equation in the interaction picture for the tripartite state $\hat{\rho}_3$ of the TLS's coupled to the HO is written as

$$\frac{d\hat{\rho}_3}{dt} = (\mathcal{L} + \mathcal{K})\hat{\rho}_3, \tag{B3}$$

with $\mathcal{L} = \mathcal{L}_h + \mathcal{L}_c$ and

$$\mathcal{K}\hat{\rho}_3 = -i[\hat{K}, \hat{\rho}_3]. \tag{B4}$$

We will derive the effective master equation for the HO state $\hat{\rho}$ assuming that the TLS's are initially in their equilibrium states $\hat{\rho}^\infty_{hc} = \hat{\rho}^\infty_h \otimes \hat{\rho}^\infty_c$ and the initial state of the tripartite system is the product state $\hat{\rho}_3(0) = \hat{\rho}^\infty_{hc} \otimes \hat{\rho}(0)$. The solution of the master equation (B3) can be written in the implicit form

$$\hat{\rho}_3(t) = \hat{\rho}_3(0) + \int_0^t ds\, e^{\mathcal{L}(t-s)}\mathcal{K}\hat{\rho}_3(s), \tag{B5}$$

which we can confirm by taking the time derivative of both sides of the equation, and using the relation $\mathcal{L}\hat{\rho}_3(0) = 0$. Inserting the above solution into the right-hand side of Eq. (B3), we obtain

$$\frac{d\hat{\rho}_3(t)}{dt} = \mathcal{K}\hat{\rho}_3(0) + (\mathcal{L} + \mathcal{K})\int_0^t ds\, e^{\mathcal{L}(t-s)}\mathcal{K}\hat{\rho}_3(s). \tag{B6}$$

We assume that $\hat{\rho}_3(s) \approx \hat{\rho}^\infty_{hc} \otimes \hat{\rho}(s)$. This assumption is justified when the thermalization time of the TLS's is faster than the time scale in which the system is changed significantly due to coupling (B2). Taking the partial trace over the TLS's

$$\frac{d\hat{\rho}(t)}{dt} = \text{tr}_{hc}\left[\mathcal{K}\int_0^t ds\, e^{\mathcal{L}(t-s)}\mathcal{K}\hat{\rho}^\infty_{hc} \otimes \hat{\rho}(s)\right]. \tag{B7}$$

Here we have used the relations $\text{tr}_{hc}[\mathcal{K}\hat{\rho}^\infty_{hc}] = 0$ and $\text{tr}_{hc}[\mathcal{L}\int_0^t e^{\mathcal{L}(t-s)}\mathcal{K}\hat{\rho}^\infty_{hc}] = 0$. Performing the standard Markovian approximations [24] we obtain

$$\frac{d\hat{\rho}(t)}{dt} = \text{tr}_{hc}\left[\mathcal{K}\int_0^\infty ds\, e^{\mathcal{L}s}\mathcal{K}\hat{\rho}^\infty_{hc} \otimes \hat{\rho}(t)\right], \tag{B8}$$

which can be written explicitly as

$$\frac{d\hat{\rho}}{dt} = -\text{tr}_{hc}\left[\hat{K}, \int_0^\infty ds\, e^{\mathcal{L}s}\left[\hat{K}, \hat{\rho}^\infty_{hc} \otimes \hat{\rho}\right]\right] = -\text{tr}_{hc}\int_0^\infty ds[(e^{\mathcal{L}^\dagger s}\hat{K}), [\hat{K}, \hat{\rho}^\infty_{hc} \otimes \hat{\rho}]]. \tag{B9}$$

Making use of the relation

$$e^{\mathcal{L}^\dagger s}\hat{K} = \hat{K}\exp\left[-\frac{1}{2}\sum_{l=h,c}\Gamma_l(1 + e^{-\beta_l\omega_l})s\right], \tag{B10}$$

we have

$$\frac{d\hat{\rho}}{dt} = \frac{(2g)^2}{\sum_{l=h,c}\Gamma_l(1 + e^{-\beta_l\omega_l})}[\langle\hat{a}\hat{a}^\dagger\rangle_\infty\langle\hat{b}^\dagger\hat{b}\rangle_\infty(\hat{c}\hat{\rho}\hat{c}^\dagger - \mathcal{H}\hat{c}^\dagger\hat{c}\hat{\rho}) + \langle\hat{a}^\dagger\hat{a}\rangle_\infty\langle\hat{b}\hat{b}^\dagger\rangle_\infty(\hat{c}^\dagger\hat{\rho}\hat{c} - \mathcal{H}\hat{c}\hat{c}^\dagger\hat{\rho})], \tag{B11}$$

where $\langle\cdot\rangle_\infty$ stands for the expectation value with respect to the TLS's thermal equilibrium states $\hat{\rho}^\infty_{h(c)}$. Finally, the master equation for the HO subject to the engine operation takes the form

$$\frac{d\hat{\rho}}{dt} \equiv \mathcal{L}_e\hat{\rho} = \Gamma_e(\hat{c}\hat{\rho}\hat{c}^\dagger - \mathcal{H}\hat{c}^\dagger\hat{c}\hat{\rho}) + \Gamma_e e^{-\beta_e^-\omega_o}(\hat{c}^\dagger\hat{\rho}\hat{c} - \mathcal{H}\hat{c}\hat{c}^\dagger\hat{\rho}), \tag{B12}$$

where

$$\Gamma_e = (2g)^2\frac{(1 - n_h)^2(1 - n_c)n_c}{\Gamma_h(1 - n_c) + \Gamma_c(1 - n_h)}, \tag{B13}$$

and the output temperature of the heat engine is

$$\beta_e^- = \frac{\beta_h\omega_h - \beta_c\omega_c}{\omega_h - \omega_c}, \tag{B14}$$

which is a function of the TLS's excitation energies and temperatures only. We operate the system as a heat engine, i.e., $T_h/T_c > \omega_h/\omega_c > 1$, the effective temperature is negative, i.e., $1/\beta_e^- < 0$, and the HO will not reach a stable asymptotic state, as we show below. The master equation (B12) together with the Hamiltonian $\hat{H}_o$ yield closed evolution equations for the mean amplitude $\langle\hat{c}\rangle_t$ as well as for the occupation $\langle\hat{c}^\dagger\hat{c}\rangle_t$:

$$\frac{d\langle\hat{c}\rangle_t}{dt} = -(\kappa_e^- + i\omega_o)\langle\hat{c}\rangle_t, \tag{B15}$$

$$\frac{d\langle\hat{c}^\dagger\hat{c}\rangle_t}{dt} = -2\kappa_e^-\langle\hat{c}^\dagger\hat{c}\rangle_t + \Gamma_e e^{-\beta_e^-\omega_o}, \tag{B16}$$

where

$$\kappa_e^- = \tfrac{1}{2}\Gamma_e(1 - e^{-\beta_e^-\omega_o}) < 0 \tag{B17}$$

is the standard amplitude damping constant. This time it is negative since $\beta_e^- < 0$ therefore both $\langle\hat{c}\rangle_t$ and $\langle\hat{c}^\dagger\hat{c}\rangle_t$ diverge exponentially with time. In particular, a thermal state remains thermal, the temperature is increasing exponentially as can be shown by the simple solution of Eq. (B16) for the occupation. Note, however, that our model is only valid in the weak coupling regime where the thermalization time is shorter than the internal time scale. This implies that the occupation must be limited by

$$g\sqrt{\langle\hat{c}^\dagger\hat{c}\rangle + 1} \ll \Gamma_{h(c)}(1 + e^{-\beta_{h(c)}\omega_{h(c)}}). \tag{B18}$$

APPENDIX C: EXTERNAL DRIVING

Coupling the HO to a resonant oscillating external field. Via such *driving* one would expect to extract power. Consider

the time-dependent Hamiltonian in the Schrödinger picture,

$$\hat{H}_d(t) = -i\epsilon_d(\hat{c}^\dagger e^{-i\omega_o t} - \hat{c}\, e^{i\omega_o t}), \tag{C1}$$

where $\epsilon_d > 0$. In the interaction picture, the master equation (B12) is modified by an additional static Hamiltonian:

$$\frac{d\hat{\rho}}{dt} = \mathcal{L}_e\hat{\rho} - \epsilon_d[\hat{c}^\dagger - \hat{c},\hat{\rho}]. \tag{C2}$$

Now the right-hand side of Eq. (B15) of the mean amplitude acquires an additional term $-\epsilon_d e^{-i\omega_o t}$. This allows an exceptional stationary solution of constant amplitude with the rotating phase:

$$\langle\hat{c}\rangle_t = -\frac{\epsilon_d}{\kappa_e^-}e^{-i\omega_o t} = \text{const} \times e^{-i\omega_o t}. \tag{C3}$$

This solution is unstable since all neighboring solutions exponentially diverge with t. As to the occupation $\langle\hat{c}^\dagger\hat{c}\rangle_t$, the right-hand side of Eq. (B16) acquires the additional linear term $-\epsilon_d(\langle\hat{c}^\dagger\rangle_t - \langle\hat{c}\rangle_t)$, hence the occupation remains exponentially divergent; there is no steady-state solution under external driving. The stability issue of the HO is still not resolved.

APPENDIX D: MONITORING

Continuous measurement, i.e., *monitoring*, is the first task towards feedback control on the system [25]. Here we consider the time-continuous measurement of both quadratures $\hat{x} = \frac{1}{\sqrt{2}}(\hat{c}^\dagger + \hat{c})$ and $\hat{y} = \frac{i}{\sqrt{2}}(\hat{c}^\dagger - \hat{c})$ of the HO. Generalizing the result of [26] for monitoring simultaneously $\hat{x}$ and $\hat{y}$, we can write the following stochastic master equation (SME) in the Schrödinger picture for the density matrix $\hat{\sigma}$ conditioned on both measurement signals $\bar{x},\bar{y}$:

$$\begin{aligned} d\hat{\sigma} &= -i[\hat{H}_o,\hat{\sigma}]dt - \frac{\gamma_m}{8}[\hat{x},[\hat{x},\hat{\sigma}]]dt - \frac{\gamma_m}{8}[\hat{y},[\hat{y},\hat{\sigma}]]dt \\ &\quad + \mathcal{H}\sqrt{\gamma_m}(\hat{x} - \langle\hat{x}\rangle_\sigma)\hat{\sigma}\, d\xi_x + \mathcal{H}\sqrt{\gamma_m}(\hat{y} - \langle\hat{y}\rangle_\sigma)\hat{\sigma}\, d\xi_y. \end{aligned} \tag{D1}$$

All expectation values $\langle\cdot\rangle_\sigma$ are understood in the stochastic conditional state $\hat{\sigma}$. The measurement signals satisfy

$$\bar{x}dt = \langle\hat{x}\rangle_\sigma dt + \frac{d\xi_x}{\sqrt{\gamma_m}}, \quad \bar{y}dt = \langle\hat{y}\rangle_\sigma dt + \frac{d\xi_y}{\sqrt{\gamma_m}}. \tag{D2}$$

Here $d\xi_x, d\xi_y$ are Ito increments of independent standard Wiener processes, satisfying

$$(d\xi_x)^2 = (d\xi_y)^2 = dt, \quad d\xi_x d\xi_y = 0, \quad \mathbf{M}d\xi_x = \mathbf{M}d\xi_y = 0, \tag{D3}$$

with the symbol $\mathbf{M}$ for stochastic mean, and γ_m for the measurement strength. (Note that we changed γ_m in Ref. [26] for $\gamma_m/2$.) We can return to complex notation, i.e., we rewrite the above equations in terms of $\hat{c},\hat{c}^\dagger$ and the corresponding complex signal $\bar{c} = (\bar{x} + i\,\bar{y})/\sqrt{2}$. We define the complex Wiener increment as

$$d\xi = \frac{d\xi_x + i d\xi_y}{\sqrt{2}}, \tag{D4}$$

which satisfies

$$(d\xi)^2 = (d\xi^*)^2 = 0, \quad d\xi^* d\xi = dt, \quad \mathbf{M}d\xi = \mathbf{M}d\xi^* = 0. \tag{D5}$$

The SME (D1) of the conditional state becomes

$$\begin{aligned} d\hat{\sigma} &= -i[\hat{H}_o,\hat{\sigma}]dt + \frac{\gamma_m}{4}(\hat{c}\hat{\rho}\hat{c}^\dagger - \mathcal{H}\hat{c}^\dagger\hat{c}\hat{\sigma} + \hat{c}^\dagger\hat{\rho}\hat{c} - \mathcal{H}\hat{c}\hat{c}^\dagger\hat{\sigma}) \\ &\quad + \sqrt{\gamma_m}\mathcal{H}[(\hat{c} - \langle\hat{c}\rangle_\sigma)d\xi^* + \text{H.c.}]\hat{\sigma} \equiv -i[\hat{H}_o,\hat{\sigma}]dt \\ &\quad + \mathcal{L}_m\hat{\sigma}dt + \sqrt{\gamma_m}\mathcal{H}[(\hat{c} - \langle\hat{c}\rangle_\sigma)d\xi^* + \text{H.c.}]\hat{\sigma}. \end{aligned} \tag{D6}$$

Equations (D2) of the real signals take the following form for the complex signal:

$$\bar{c}\,dt = \langle\hat{c}\rangle_\sigma dt + \frac{d\xi}{\sqrt{\gamma_m}}. \tag{D7}$$

Applying this time-continuous measurement to the HO which is coupled to the heat engine and driven by the external field, cf. Eq. (C2), we get the following SME:

$$\begin{aligned} d\hat{\sigma} &= -i[\hat{H}_o,\hat{\sigma}]dt + (\mathcal{L}_e + \mathcal{L}_m)\hat{\sigma}dt - \epsilon_d[\hat{c}^\dagger e^{i\omega_o t} - \hat{c},\hat{\sigma}]dt \\ &\quad + \sqrt{\gamma_m}\mathcal{H}[(\hat{c} - \langle\hat{c}\rangle_\sigma)d\xi^* + \text{H.c.}]\hat{\sigma}. \end{aligned} \tag{D8}$$

The state $\hat{\sigma}$ of the HO is the conditioned state on the measured signal (D7), its stochastic mean is the unconditional density matrix: $\mathbf{M}\hat{\sigma} = \hat{\rho}$. Taking the stochastic mean $\mathbf{M}$ of both sides of the SME, we are left with the master equation of the unconditional state:

$$\frac{d\hat{\rho}}{dt} = (\mathcal{L}_e + \mathcal{L}_m)\hat{\rho} - \epsilon_d[\hat{c}^\dagger - \hat{c},\hat{\rho}]. \tag{D9}$$

As a result of the measurement, additional heat flows into the oscillator, the damping rate becomes $\Gamma_e + \gamma_m$, and the inverse "temperature" β_e^- is modified but remains negative. The exceptional steady amplitude (C3) exists with the modified parameters, but it is unstable like all other solutions.

APPENDIX E: FEEDBACK CONTROL

Using the measured signal in Eq. (D7), we control the state of the HO in the vicinity of the constant rotating amplitude set by the external driving in such a way that we get a true stable steady state. Consider the following *feedback* Hamiltonian in the Schrödinger picture:

$$\hat{H}_f(t) = -i\kappa_f\bar{c}(t)\hat{c}^\dagger + \text{H.c.} \tag{E1}$$

Here κ_f is the feedback strength. We apply the feedback [27] on top of the monitored evolution described by Eq. (D8):

$$\hat{\sigma} + d\hat{\sigma} \to e^{-i\hat{H}_f dt}(\hat{\sigma} + d\hat{\sigma})e^{i\hat{H}_f dt}. \tag{E2}$$

Expanding the right-hand side into a series, keeping first-order terms in dt, and keeping in mind that $|d\xi|^2 = dt$, the terms that are left for evaluation are $-i[H_f dt,\hat{\sigma}]$, $-i[H_f dt, g\hat{\sigma}]$, and $-\frac{1}{2}[H_f dt,[H_f dt,\hat{\sigma}]]$. The final SME including feedback reads

$$\begin{aligned} d\hat{\sigma} &= -i[\hat{H}_o,\hat{\sigma}]dt + (\mathcal{L}_e + \mathcal{L}_m + \mathcal{L}_f)\hat{\sigma}dt \\ &\quad - \epsilon_d[\hat{c}^\dagger e^{i\omega_o t} - \hat{c}\, e^{-i\omega_o t},\hat{\sigma}]dt - \frac{\kappa_f}{\sqrt{\gamma_m}}[\hat{c}^\dagger d\xi - \hat{c}d\xi^*,\hat{\sigma}] \\ &\quad + \sqrt{\gamma_m}\mathcal{H}[(\hat{c} - \langle\hat{c}\rangle_\sigma)d\xi^* + \text{H.c.}]\hat{\sigma}. \end{aligned} \tag{E3}$$

The dissipative contribution of the feedback reads

$$\mathcal{L}_f\hat{\sigma} = \left(\frac{\kappa_f^2}{\gamma_m} + \kappa_f\right)(\hat{c}\hat{\sigma}\hat{c}^\dagger - \mathcal{H}\hat{c}^\dagger\hat{c}\hat{\sigma}) + \left(\frac{\kappa_f^2}{\gamma_m} - \kappa_f\right)(\hat{c}^\dagger\hat{\sigma}\hat{c} - \mathcal{H}\hat{c}\hat{c}^\dagger\hat{\sigma}). \quad \text{(E4)}$$

For $\kappa_f > \gamma_m$ this corresponds to a thermal bath of positive temperature. Entering the regime $0 < \kappa_f < \gamma_m$, the cooling effect of $\mathcal{L}_f$ within the sum $\mathcal{L}_e + \mathcal{L}_m + \mathcal{L}_f$ becomes enhanced although $\mathcal{L}_f$ ceases to be a mathematically correct dissipator in itself. Taking the stochastic mean over Eq. (E3) we obtain the master equation of the unconditional state which in the interaction picture takes this form:

$$\frac{d\hat{\rho}}{dt} = (\mathcal{L}_e + \mathcal{L}_m + \mathcal{L}_f)\hat{\rho} - \epsilon_d[\hat{c}^\dagger - \hat{c}, \hat{\rho}]. \quad \text{(E5)}$$

What we have for the HO dynamics is the following: The HO is excited by the negative-temperature $(1/\beta_e^-)$ bath $\mathcal{L}_e$ due to population inversion, heated by the infinite-temperature bath $\mathcal{L}_m$ due to noise of monitoring, and cooled by the feedback $\mathcal{L}_f$. On top of this, the external driving shifts the Hamiltonian $\hat{H}_o$. We write the full master equation (E5) in a compact form:

$$\frac{d\hat{\rho}}{dt} = \Gamma(\hat{c}\hat{\rho}\hat{c}^\dagger - \mathcal{H}\hat{c}^\dagger\hat{c}\hat{\rho}) + \Gamma e^{-\beta\omega_o}(\hat{c}^\dagger\hat{\rho}\hat{c} - \mathcal{H}\hat{c}\hat{c}^\dagger\hat{\rho}) - \epsilon_d[\hat{c}^\dagger - \hat{c}, \hat{\rho}], \quad \text{(E6)}$$

where Γ and β are determined by

$$\Gamma = \Gamma_e + \frac{\gamma_m}{4} + \frac{\kappa_f^2}{\gamma_m} + \kappa_f, \quad \text{(E7)}$$

$$e^{-\beta\omega_o}\Gamma = \Gamma_e\, e^{-\beta_e^-\omega_o} + \frac{\gamma_m}{4} + \frac{\kappa_f^2}{\gamma_m} - \kappa_f. \quad \text{(E8)}$$

We turn the effective temperature β positive by choosing the feedback strength above the following threshold:

$$\kappa_f > -\kappa_e^- = \tfrac{1}{2}\Gamma_e(e^{-\beta_e^-\omega_o} - 1). \quad \text{(E9)}$$

Note that the driving on the right-hand side of the master equation (E6) can be absorbed into the standard thermal dissipator at (inverse) temperature β if we displace $\hat{c}, \hat{c}^\dagger$ by a suitable real number. Accordingly, the master equation (E6) must have a unique stationary state which is the following displaced thermal state of the HO:

$$\hat{\rho}^\infty = \mathcal{N}\exp[-\beta\omega_o(\hat{c} - c_\infty)^\dagger(\hat{c} - c_\infty)], \quad \text{(E10)}$$

with the static real displacement in interaction picture:

$$c_\infty = -\frac{\epsilon_d}{\kappa_f + \kappa_e^-} < 0. \quad \text{(E11)}$$

In the Schrödinger picture the stationary state is a thermal state with the rotating displacement:

$$\hat{\rho}^\infty \Rightarrow \mathcal{N}\exp[-\beta\omega_o(\hat{c} - c_\infty e^{-i\omega_o t})^\dagger(\hat{c} - c_\infty e^{-i\omega_o t})]. \quad \text{(E12)}$$

Hence the mean amplitude rotates, and its phase is shifted by $-\pi/2$ with respect to the external driving:

$$\langle\hat{c}\rangle_\infty = c_\infty\, e^{-i\omega_o t}. \quad \text{(E13)}$$

The average population is the Planckian thermal value plus the yield of displacement:

$$\langle\hat{c}^\dagger\hat{c}\rangle_\infty = \frac{1}{e^{\beta\omega_o} - 1} + |c_\infty|^2 \equiv n_o + |c_\infty|^2. \quad \text{(E14)}$$

We use the redundant expression $|c_\infty|^2$ for c_∞^2 to capture an occasionally different phase convention of driving. Both terms on the right-hand side diverge at the edge of the regime of operation $\kappa_f + \kappa_e^- \to +0$ where the model breaks down because it violates the weak coupling condition (B18).

APPENDIX F: ENERGY FLOWS IN STEADY STATE

Any systematic calculation of heat flow and power requires us to transform the final SME from Ito into Stratonovich form. We postpone this very novel task to future research. Rather, we focus on the minimal calculations and considerations confirming that our model represents a genuine heat engine.

Next, we show that there is a consumable output power in the steady-state operation of the flywheel. The total Hamiltonian has two time-dependent contributions $H_d(t)$ and $H_f(t)$. Accordingly, the power $\mathcal{P}$ consists of two contributions corresponding to the power invested by the driving and the power gained from the feedback. The first, in the steady state $\mathbf{M}\hat{\sigma} = \hat{\rho}^\infty$, reads

$$\mathcal{P}_d = \mathbf{M}\mathrm{tr}\left[\hat{\sigma}\frac{d\hat{H}_d}{dt}\right] = \mathrm{tr}\left[\hat{\rho}^\infty\frac{d}{dt}(-i\epsilon_d\hat{c}^\dagger e^{-i\omega_o t} + \mathrm{H.c.})\right] = -2\epsilon_d\omega_o c_\infty > 0, \quad \text{(F1)}$$

where the positivity indicates power going into (consumed by) the flywheel. We restrict our calculations for the deterministic part of feedback, i.e., we replace $\hat{H}_f(t)$ by its deterministic part $\hat{H}_{f,\mathrm{det}} = -i\kappa_f\langle\hat{c}\rangle_\sigma\hat{c}^\dagger + \mathrm{H.c.}$ As was mentioned before, considering the stochastic part $\hat{H}_{f,\mathrm{sto}} = -i\kappa_f/\sqrt{\gamma_m}\hat{c}^\dagger d\xi + \mathrm{H.c.}$ requires the Stratonovich calculus. The power reads

$$\mathcal{P}_{f,\mathrm{det}} = \mathbf{M}\mathrm{tr}\left[\hat{\sigma}\frac{d\hat{H}_{f,\mathrm{det}}}{dt}\right] = \mathbf{M}\mathrm{tr}\left[\hat{\sigma}\frac{d}{dt}(-\kappa_f\langle\hat{c}\rangle_\sigma\hat{c}^\dagger + \mathrm{H.c.})\right] = -i\kappa_f\mathbf{M}\mathrm{tr}\left[\frac{d\hat{\sigma}}{dt}\hat{c}\right]\langle\hat{c}^\dagger\rangle_\sigma + \mathrm{c.c.} \quad \text{(F2)}$$

The power in Eq. (F2) is proportional to the (weighted) mean of the phase drift of the amplitude $\langle\hat{c}\rangle_\sigma$. To calculate $d\hat{\sigma}$ we apply the final SME given in Appendix E. The only relevant yield is the unitary rotation $-i\omega_o\langle\hat{c}\rangle_\sigma dt$ since the dissipative part does not alter the phase of $\langle\hat{c}\rangle_\sigma$ and the Ito stochastic part will cancel out by the mean operation $\mathbf{M}$. Therefore we get

$$\mathcal{P}_{f,\mathrm{det}} = -2\kappa_f\omega_o\mathbf{M}|\langle\hat{c}\rangle_\sigma|^2 < 0. \quad \text{(F3)}$$

Negativity means that power is gained (supplied) by feedback. Although analytical solutions for similar SMEs such as ours exist [35], we restrict ourselves to a simple guess. Using the Cauchy-Schwartz relation $\mathbf{M}|\langle\hat{c}\rangle_\sigma|^2 \geqslant |\mathbf{M}\langle\hat{c}\rangle_\sigma|^2$, we obtain the lower bound $-\mathcal{P}_{f,\mathrm{det}} \geqslant 2\kappa_f\omega_o|c_\infty|^2$ for the stationary power gained by feedback in the steady-state. Hence the overall stationary power satisfies the inequality

$$-\mathcal{P}_{\mathrm{det}} = -\mathcal{P}_d - \mathcal{P}_{f,\mathrm{det}} \geqslant 2\omega_o\epsilon_d^2\frac{-\kappa_e^-}{(\kappa_f + \kappa_e^-)^2}. \quad \text{(F4)}$$

The sign is negative and thus the consumable power of the flywheel is positive and bounded from below. We conjecture that the contribution of the stochastic part $\hat{H}_{f,\mathrm{sto}}(t)$ of driving cannot invalidate the positivity of the consumable power.

[1] V. Blickle and C. Bechinger, Nat. Phys. **8**, 143 (2012).
[2] P. Steeneken, K. Le Phan, M. Goossens, G. Koops, G. Brom, C. Van der Avoort, and J. Van Beek, Nat. Phys. **7**, 354 (2011).
[3] J. Roßnagel, S. T. Dawkins, K. N. Tolazzi, O. Abah, E. Lutz, F. Schmidt-Kaler, and K. Singer, Science **352**, 325 (2016).
[4] R. Kosloff and A. Levy, Annu. Rev. Phys. Chem. **65**, 365 (2014).
[5] J. Goold, M. Huber, A. Riera, L. del Rio, and P. Skrzypczyk, J. Phys. A: Math. Theor. **49**, 143001 (2016).
[6] S. Vinjanampathy and J. Anders, arXiv:1508.06099.
[7] J. Millen and A. Xuereb, New J. Phys. **18**, 011002 (2016).
[8] D. Gelbwaser-Klimovsky, W. Niedenzu, and G. Kurizki, Adv. At. Mol. Opt. Phys. **64**, 329 (2015).
[9] A. E. Allahverdyan, R. Balian, and Th. M. Nieuwenhuizen, Eur. Phys. Lett. **67**, 565 (2004).
[10] R. Alicki and M. Fannes, Phys. Rev. E **87**, 042123 (2013).
[11] P. Skrzypczyk, A. J. Short, and S. Popescu, Nat. Commun. **5**, 4185 (2014).
[12] F. C. Binder, S. Vinjanampathy, K. Modi, and J. Goold, New J. Phys. **17**, 075015 (2015).
[13] R. Uzdin, A. Levy, and R. Kosloff, Phys. Rev. X **5**, 031044 (2015).
[14] M. Perarnau-Llobet, K. V. Hovhannisyan, M. Huber, P. Skrzypczyk, N. Brunner, and A. Acín, Phys. Rev. X **5**, 041011 (2015).
[15] K. Korzekwa, M. Lostaglio, J. Oppenheim, and D. Jennings, New J. Phys. **18**, 023045 (2016).
[16] J. Åberg, Phys. Rev. Lett. **113**, 150402 (2014).
[17] M. O. Scully, M. S. Zubairy, G. S. Agarwal, and H. Walther, Science **299**, 862 (2003).
[18] J. Zhang, Y.-x. Liu, R.-B. Wu, K. Jacobs, and F. Nori, arXiv:1407.8536.
[19] J. V. Koski, V. F. Maisi, J. P. Pekola, and D. V. Averin, Proc. Natl. Acad. Sci. USA **111**, 13786 (2014).
[20] A. Levy, R. Alicki, and R. Kosloff, Phys. Rev. E **85**, 061126 (2012).
[21] D. Gelbwaser-Klimovsky and G. Kurizki, Sci. Rep. **5** (2015).
[22] G. Lindblad, J. Phys. A: Math. Gen. **48**, 119 (1976).
[23] V. Gorini, A. Kossakowski, and E. C. G. Sudarshan, J. Math. Phys. **17**, 821 (1976).
[24] H.-P. Breuer F. Petruccione, *Open Quantum Systems* (Oxford University, Oxford, 2002).
[25] H. Wiseman and G. Milburn, *Quantum Measurement and Control* (Cambridge University, New York, 2010).
[26] L. Diósi, Phys. Lett. A **129**, 419 (1988).
[27] L. Diosi and N. Gisin, Phys. Rev. Lett. **72**, 4053 (1994).
[28] R. Alicki, J. Phys. A: Math. Gen. **12**, L103 (1979).
[29] N. F. Ramsey, Phys. Rev. **103**, 20 (1956).
[30] N. Brunner, N. Linden, S. Popescu, and P. Skrzypczyk, Phys. Rev. E **85**, 051117 (2012).
[31] A. Clerk, F. Marquardt, and K. Jacobs, New J. Phys. **10**, 095010 (2008).
[32] J. Geremia, J. K. Stockton, and H. Mabuchi, Science **304**, 270 (2004).
[33] R. Vijay, C. Macklin, D. Slichter, S. Weber, K. Murch, R. Naik, A. N. Korotkov, and I. Siddiqi, Nature **490**, 77 (2012).
[34] A. Levy and R. Kosloff, Europhys. Lett. **107**, 20004 (2014).
[35] D. Gatarek and N. Gisin, J. Math. Phys. **32**, 2152 (1991).

Chapter 7

Conclusions and outlook

Thermodynamic irreversibility is not inherent in quantum mechanics. It is manifested by assumptions made on the quantum system and its environment (see section 2.3.2). If initially the system and the environment (the rest of the universe) are correlated it is not unacceptable that in future the entropy will decrease, leading to a violation of the second law. Nevertheless, as far as our current observations go, the second law is valid. Thus, any approximated treatment of quantum mechanics should respect restrictions set by the thermodynamic laws. In chapter 3 we uncovered a common flaw in the literature using thermodynamic arguments. We then introduced a quantum thermodynamic consistent framework for analyzing energy flow thorough a quantum network using a global LGKS master equation. This framework reflects the global nature of quantum mechanics and should be applied when studying quantum devices operating out of equilibrium.

Based on this work, Trushechkin and Volovich [Trushechkin 2016] developed a perturbative treatment of inter-site couplings in the local description of open quantum networks. They suggested to add correction terms to the local LGKS generator. In practice, these terms can be obtained by expanding the global LGKS generator in orders of inter-site coupling strength. Although this treatment successfully solves the problem of violating the second law, it is not necessarily easier to apply than the accurate global approach. Later works attempted to approach the problem we introduced by applying different techniques: The repeated interaction scheme [Barra 2015]; the Redfield quantum master equation [Purkayastha 2016]; and the stochastic Liouville-von Neumann equation [Stockburger 2016].

In chapter 4 we coined the concept of quantum absorption refrigerator as an autonomous quantum device that exploits noise or heat to drive a cooling process. It was proposed that the minimal model of an autonomous refrigerator must involve three energy currents via a non-linear interaction. Later, it was shown in [Martinez 2013] that it is impossible to build a quantum absorption refrigerator using linear networks, therefore, such refrigerators require non-linearity as a crucial

ingredient.

The idea of a quantum absorption refrigerator aroused great interest and many studies followed. In [Correa 2014b] the efficiency at a maximum cooling power and the effect of squeezing the heat source that drives an absorption cooling cycle was considered. Entanglement in an absorption refrigerator composed of three qubits was shown to enhance the cooling process, implying that quantum refrigerators can outperform classical ones [Brunner 2014]. The transient regime of a quantum absorption refrigerator was also investigated [Mitchison 2015, Das 2016] suggesting protocols for single-shot cooling. A study [Correa 2014a] examining a parallel multistage quantum absorption refrigerator suggested that the construction introduced in chapters 4 and 5 is the optimal compromise between performance and complexity. This indicates that it should be considered for practical applications of absorption cooling to quantum technologies.

Suggestions for experimental realizations were soon to follow. Among these are: A quantum refrigerator system composed of three rf-SQUID qubits [Chen 2012]; an electronic quantum absorption refrigerator based on four quantum dots [Venturelli 2013]; quantum absorption refrigerators in an atom-cavity systems [Mitchison 2016]; and a quantum absorption refrigerator with a circuit QED architecture in Josephson junction [Hofer 2016]. The study of quantum absorption refrigerators is developing tremendously nowadays. Noise and heat are free resources and in many cases are unavoidable in experiments. The concept of quantum absorption cooling suggests exploiting these resources for our needs, making it significant for future nano-scale quantum devices. Additional studies of quantum absorption refrigerators can be found in [Gelbwaser-Klimovsky 2013, Silva 2015, Silva 2016].

The formulation of the third law of thermodynamics presented in chapter 5 sets the limitation on the optimal cooling speed, binding any refrigerator when approaching the absolute zero. This formulation unravels the relation between the two known formulations of the law, the unattainability principle and Nernst's heat theorem. For a cooling process, the unattainability principle is quantified by the scaling of the cooling speed with temperature, whereas Nernst's heat theorem is quantified by the scaling of heat extraction speed with temperature. This quantification resolves the dispute regarding the preeminence of the formulations. It is suggested that the unattainability principle is superior to Nernst's heat theorem, and sets stronger limitations on the cooling process. In [Levy 2012a] (appendix A) we comment on a refrigeration mechanism powered by photons introduced in [Cleuren 2012]. We show that the proposed model upholds Nernst's heat theorem but violates the unattainability principle. This is another example of how consistency with the laws of thermodynamics and their appropriate formulation can reveal flaws when applying approximations to study models of quantum devices.

An additional advantage of the formulation introduced in chapter 5 is its universality. The characteristic exponent does not depend on the type of the quantum refrigerator. The dimension of the substance being cooled also does not play a role. This behavior can be traced back to the scaling of the density of modes and the heat capacity with temperature which nullifies the dependence on dimension. The characteristic exponent depends only on the type of interaction between the working medium and the substance being cooled. The relation of this coupling with the dispersion relation of a Bosonic field excludes exotic dispersion laws that are forbidden by the relativity theory. This implies that the formulation of the third law predicts independently of relativity theory the finite group velocity property.

Kolář et al. [Kolář 2012] have challenged the unattainability principle by looking for systems with exotic dispersion laws such as magnons and materials that exhibit effects of fractal disorder. We note that these kinds of systems are typically integrable systems which implies that they will not thermalize, making them unsuitable for examining the third law. In [Masanes 2014] the authors attempted to derive the third law of thermodynamics by quantifying the resources needed to cool a system to any particular temperature. By obtaining a lower bound on the achievable temperature which depends on time they showed consistency with the formulation introduced in chapter 5. This formulation was also shown to hold for suggested realizations of nonlinear dc thermoelectric devices [Whitney 2013], and for a four-level refrigerator driven by photons [Wang 2015].

Another novel and important result of chapter 5 is the definitions for the heat currents when the quantum device is strongly driven by an external periodic field and simultaneously coupled to heat reservoirs. The external field "dresses" the quantum system and heat flows through channels corresponding to the quasi-Bohr frequencies obtained from the Floquet analysis. As a consequence of the strong driving, heat leaks are manifested in the quantum refrigerator, thus heat will flow from the hot to the cold reservoir, leading to a reduction in the efficiency of the cooling process. Once the mechanisms that causes heat leaks are understood we can attempt and overcome these by applying different control protocols.

In physics, the second quantum revolution, termed by Dowling and Milburn [Dowling 2003], is the perception that we humans are no longer passive observers of the quantum world, but can now actively manipulate it. Developing and improving quantum control techniques pave the road to this revolution. Quantum thermodynamics provides the complimentary information about the quantum properties that can be exploited as resources for future quantum technologies and set restrictions on its operations. The aim of quantum control theories is to develop protocols for preparing entangled states, coherent states, or any other state possessing novel properties for specific applications.

Relating quantum control theories with thermodynamics would be extremely beneficial. On the one hand, thermodynamics sets limitations on physical processes. Including such restrictions gained from the study of quantum thermodynamics to quantum control theories will introduce additional physical constraints on manipulating quantum systems and will set bounds on the achievable fidelity of the target state. On the other hand, by applying quantum control theories to thermodynamics in the quantum regime we can optimally exploit resources to drive thermodynamic processes. The first attempt to do so was introduced in chapter 6, where we applied quantum monitoring and feedback control to manage a charging process of a quantum energy storage device. It was shown that when the storage device is a quantum harmonic oscillator, fluctuations dominate the dynamics leading to divergence of the thermodynamic properties of the flywheel. Gaining information about the state of the system in real time by monitoring it, and then using this information to apply a feedback Hamiltonian, we attain a steady state operation of the device. A balance between information gained from monitoring the device and information fed back to the device is found to maximize the charging efficiency.

Although constructing quantum energy storage devices may seem like a futuristic technology, some of these concepts were recently demonstrated in the laboratory [Roßnagel 2016]. In this experiment, a single atom heat engine was constructed. The working medium is a single ion trapped in a linear Paul trap that interacts with a cold bath on one side of the trap and with a hot bath on the other side. The output is used to drive an harmonic oscillator (increasing the axial potential energy of the trapped ion). In order to stabilize the harmonic oscillator, an additional resource in the form of laser cooling is introduced, and more power is invested in cooling than actually can be stored in the harmonic oscillator. Applying the concept proposed in chapter 6 of quantum monitoring feedback control would make this process energetically profitable. In such an experimental setup feedback control can be achieved by monitoring the oscillations of the ion in the trap and change accordingly the trap potential. We conclude that by relating thermodynamics with quantum monitoring and feedback control we can optimally exploit the available quantum-thermodynamic resources. This will have significant implications in designing and managing energetic processes of future quantum devices.

Many of the quantum control methods are applicable to closed quantum systems. Since any realistic quantum system is coupled to the environment, full control over the dynamics requires manipulating the environment. Typically, the environment poses an enormous number of degrees of freedom that are not directly accessible to the experimentalists in the laboratory. Instead of attempting to isolate the system from its environment using different protocols, we propose to optimally control it under a set of thermodynamic constraints that would mimic the environment's in-

fluence. As an example, it might be possible to extend shortcuts to adiabaticity control methods [Torrontegui 2013] to open quantum systems.

Quantum thermodynamics is a growing field of research which nowadays receives recognition in many branches of quantum mechanics. There are different approaches studying thermodynamics in the quantum regime. These are: quantum thermodynamic resource theories, information and thermodynamics, single shot thermodynamics, quantum fluctuation relations, and the approach taken in this thesis, viz. the study of quantum thermal machines. The field of quantum thermodynamics will benefit from relating these different approaches in a common language.

The future of the filed, just like in any other field of science, crucially depends on experiments. As a theoretician, revealing novel quantum thermodynamic signatures are necessary for identifying and quantifying quantum effects in thermodynamics of quantum systems. Such ideas are presented in appendices B and C, where we introduced quantum thermodynamic signatures in the operation of quantum thermal machines. That is, for a given set of thermal resources and thermodynamic measurements (for example, power output) we can determine if the device exploits coherence in its operation. This theoretical result is now being tested in collaboration with an experimental group on superconducting circuits.

Another direction for future research is relating quantum thermodynamics with quantum sensing and metrology. This will provide insight on the energetic and entropic cost for attaining a certain accuracy in measurement. For given resources that depend on the experimental setup, thermodynamic considerations will set fundamental bounds on the ability to measure physical properties at optimal precision. It is applicable to a wide variety of systems, from magnetoreception in migrating species to quantum clocks.

"Excellently observed," answered Candide; "but let us cultivate our garden." – Voltair, Candide or Optimism, 1759

Bibliography

[Albash 2012] Tameem Albash, Sergio Boixo, Daniel A Lidar and Paolo Zanardi. *Quantum adiabatic markovian master equations.* New Journal of Physics, vol. 14, no. 12, page 123016, 2012. (Cited on page 21.)

[Alicki 1979] R. Alicki. *The quantum open system as a model of the heat engine.* J. Phys A: Math.Gen., vol. 12, page L103, 1979. (Cited on pages 2, 43.)

[Alicki 1987] R. Alicki and K. Lendi. Quantum Dynamical Semigroups and Applications . Springer-Verlag, Berlin, 1987. (Cited on pages 7, 14.)

[Alicki 2001] R. Alicki and M. Fannes. Quantum dynamical systems. Oxford University Press, 2001. (Cited on pages 10, 11.)

[Alicki 2006] Robert Alicki, Daniel A. Lidar and Paolo Zanardi. *Internal consistency of fault-tolerant quantum error correction in light of rigorous derivations of the quantum Markovian limit.* Phys. Rev. A, vol. 73, page 052311, May 2006. (Cited on pages 16, 22, 23.)

[Alicki 2013] Robert Alicki and Mark Fannes. *Entanglement boost for extractable work from ensembles of quantum batteries.* Physical Review E, vol. 87, no. 4, page 042123, 2013. (Cited on page 36.)

[Alicki 2015] Robert Alicki, David Gelbwaser-Klimovsky and Krzysztof Szczygielski. *Solar cell as a self-oscillating heat engine.* Journal of Physics A: Mathematical and Theoretical, vol. 49, no. 1, page 015002, 2015. (Cited on pages 21, 39.)

[Alicki 2016] Robert Alicki. *Thermoelectric generators as self-oscillating heat engines.* Journal of Physics A: Mathematical and Theoretical, vol. 49, no. 8, page 085001, 2016. (Cited on pages 21, 39.)

[Allahverdyan 2004] A. E. Allahverdyan, R. Balian and Th. M. Nieuwenhuizen. *"Maximal work extraction from finite quantum systems".* Eur. Phys. Lett., vol. 67, page 565, 2004. (Cited on page 35.)

[Allahverdyan 2008] A. E. Allahverdyan, R.S. Johal and G. Mahler. *Work extremum principle: Structure and function of quantum heat engines.* Phys. Rev. E, vol. 77, page 041118, 2008. (Cited on page 44.)

[Am-Shallem 2015] Morag Am-Shallem, Amikam Levy, Ido Schaefer and Ronnie Kosloff. *Three approaches for representing Lindblad dynamics by a matrix-vector notation.* arXiv preprint arXiv:1510.08634, 2015. (Cited on page 144.)

[Barchielli 2009] Alberto Barchielli and Matteo Gregoratti. Quantum trajectories and measurements in continuous time: the diffusive case, volume 782. Springer, 2009. (Cited on page 24.)

[Barra 2015] Felipe Barra. *The thermodynamic cost of driving quantum systems by their boundaries.* Scientific reports, vol. 5, 2015. (Cited on page 81.)

[Baugh 2005] Jonathan Baugh, Osama Moussa, Colm A Ryan, Ashwin Nayak and Raymond Laflamme. *Experimental implementation of heat-bath algorithmic cooling using solid-state nuclear magnetic resonance.* Nature, vol. 438, no. 7067, pages 470–473, 2005. (Cited on page 2.)

[Belgiorno 2003a] F. Belgiorno. *Notes on the third law of thermodynamics I.* J. Phys A: Math.Gen., vol. 36, page 8165, 2003. (Cited on page 4.)

[Belgiorno 2003b] F. Belgiorno. *Notes on the third law of thermodynamics II.* J. Phys A: Math.Gen., vol. 36, page 8195, 2003. (Cited on page 4.)

[Bender 2002] Carl M Bender, Dorje C Brody and Bernhard K Meister. *Entropy and temperature of a quantum Carnot engine.* In Proceedings of the Royal Society of London A: Mathematical, Physical and Engineering Sciences, volume 458, pages 1519–1526. The Royal Society, 2002. (Cited on page 44.)

[Binder 2015] Felix C Binder, Sai Vinjanampathy, Kavan Modi and John Goold. *Quantacell: powerful charging of quantum batteries.* New Journal of Physics, vol. 17, no. 7, page 075015, 2015. (Cited on page 36.)

[Brandão 2015] Fernando Brandão, Michał Horodecki, Nelly Ng, Jonathan Oppenheim and Stephanie Wehner. *The second laws of quantum thermodynamics.* Proceedings of the National Academy of Sciences, vol. 112, no. 11, pages 3275–3279, 2015. (Cited on page 41.)

[Breuer 2002] H.-P. Breuer and F. Petruccione. Open quantum systems. Oxford university press, 2002. (Cited on pages 7, 13, 14.)

[Brunner 2014] Nicolas Brunner, Marcus Huber, Noah Linden, Sandu Popescu, Ralph Silva and Paul Skrzypczyk. *Entanglement enhances cooling in microscopic quantum refrigerators.* Physical Review E, vol. 89, no. 3, page 032115, 2014. (Cited on page 82.)

[Campisi 2011] Michele Campisi, Peter Hänggi and Peter Talkner. *Colloquium: Quantum fluctuation relations: Foundations and applications.* Reviews of Modern Physics, vol. 83, no. 3, page 771, 2011. (Cited on page 33.)

[Chen 2012] Yi-Xin Chen and Sheng-Wen Li. *Quantum refrigerator driven by current noise.* EPL (Europhysics Letters), vol. 97, no. 4, page 40003, 2012. (Cited on page 82.)

[Clerk 2010] Aashish A Clerk, Michel H Devoret, Steven M Girvin, Florian Marquardt and Robert J Schoelkopf. *Introduction to quantum noise, measurement, and amplification.* Reviews of Modern Physics, vol. 82, no. 2, page 1155, 2010. (Cited on page 24.)

[Cleuren 2012] B. Cleuren, B. Rutten and C. Van den Broeck. *Cooling by Heating: Refrigeration Powered by Photons.* Phys. Rev. Lett., vol. 108, page 120603, Mar 2012. (Cited on page 82.)

[Correa 2014a] Luis A Correa. *Multistage quantum absorption heat pumps.* Physical Review E, vol. 89, no. 4, page 042128, 2014. (Cited on page 82.)

[Correa 2014b] Luis A Correa, José P Palao, Daniel Alonso and Gerardo Adesso. *Quantum-enhanced absorption refrigerators.* Scientific Reports, vol. 4, 2014. (Cited on pages 4, 44, 82.)

[Das 2016] Sreetama Das, Avijit Misra, Amit Kumar Pal, Aditi Sen De and Ujjwal Sen. *Necessarily transient quantum refrigerator.* arXiv preprint arXiv:1606.06985, 2016. (Cited on page 82.)

[Davies 1974] E.B. Davies. *Markovian Master Equations.* Comm. Math. Phys., vol. 39, page 91, 1974. (Cited on page 16.)

[Davies 1978] EB Davies and H Spohn. *Open quantum systems with time-dependent Hamiltonians and their linear response.* Journal of Statistical Physics, vol. 19, no. 5, pages 511–523, 1978. (Cited on page 21.)

[Diósi 1988] Lajos Diósi. *Continuous quantum measurement and It{ô} formalism.* Physics Letters A, vol. 129, no. 8, pages 419–423, 1988. (Cited on page 31.)

[Dowling 2003] Jonathan P Dowling and Gerard J Milburn. *Quantum technology: the second quantum revolution.* Philosophical Transactions of the Royal Society of London A: Mathematical, Physical and Engineering Sciences, vol. 361, no. 1809, pages 1655–1674, 2003. (Cited on page 83.)

[Dumcke 1985] R. Dumcke. *The low density limit for N-level system interacting with a free bose or fermi gas.* Comm. Math. Phys., vol. 97, pages 331–359, 1985. (Cited on pages 16, 19.)

[Elkana 1982] Yehuda Elkana and Gerald James Holton. Albert einstein, historical and cultural perspectives. Princeton University Press, 1982.

[Esposito 2010] Massimiliano Esposito, Ryoichi Kawai, Katja Lindenberg and Christian Van den Broeck. *Quantum-dot Carnot engine at maximum power.* Physical Review E, vol. 81, no. 4, page 041106, 2010. (Cited on page 44.)

[Esposito 2015] Massimiliano Esposito, Maicol A Ochoa and Michael Galperin. *Quantum thermodynamics: A nonequilibrium green's function approach.* Physical review letters, vol. 114, no. 8, page 080602, 2015. (Cited on page 38.)

[Feldmann 1996] Tova Feldmann, Eitan Geva, Ronnie Kosloff and Peter Salamon. *Heat Engines in Finite Time Governed by Master Equations.* Am. J. Phys., vol. 64, pages 485–492, 1996. (Cited on page 44.)

[Feldmann 2000] Tova Feldmann and Ronnie Kosloff. *Performance of discrete heat engines and heat pumps in finite time.* Physical Review E, vol. 61, no. 5, page 4774, 2000. (Cited on page 44.)

[Feldmann 2003] Tova Feldmann and Ronnie Kosloff. *Quantum four-stroke heat engine: Thermodynamic observables in a model with intrinsic friction*. Physical Review E, vol. 68, no. 1, page 016101, 2003. (Cited on page 44.)

[Fornieri 2015] Antonio Fornieri, Christophe Blanc, Riccardo Bosisio, Sophie D'Ambrosio and Francesco Giazotto. *Nanoscale phase engineering of thermal transport with a Josephson heat modulator*. Nature nanotechnology, 2015. (Cited on page 2.)

[Fowler 1939] R. H. Fowler and E. A. Guggenheim. Statistical thermodynamics. Cambridge university press, 1939. (Cited on page 42.)

[Gardiner 1985] C.W. Gardiner. Handbook of Stochastic Methods. Springer-Verlag, Berlin, 1985. (Cited on page 24.)

[Gardiner 2004] C. Gardiner and P. Zoller. Quantum noise: A handbook of markovian and non-markovian quantum stochastic methods with applications to quantum optics. Springer Series in Synergetics. Springer, 2004. (Cited on page 15.)

[Gelbwaser-Klimovsky 2013] D Gelbwaser-Klimovsky, R Alicki and G Kurizki. *Autonomous quantized refrigerator: performance beyond the classical bound*. arXiv preprint arXiv:1309.5716, 2013. (Cited on page 82.)

[Gelbwaser-Klimovsky 2015] David Gelbwaser-Klimovsky and Alán Aspuru-Guzik. *Strongly coupled quantum heat machines*. The journal of physical chemistry letters, vol. 6, no. 17, pages 3477–3482, 2015. (Cited on page 38.)

[Geva 1992] Eitan Geva and Ronnie Kosloff. *A Quantum Mechanical Heat Engine Operating in Finite Time. A Model Consisting of Spin $half$ Systems as The Working Fluid*. J. Chem. Phys., vol. 96, pages 3054–3067, 1992. (Cited on page 44.)

[Geva 1994] Eitan Geva and Ronnie Kosloff. *The Three-level Quantum Amplifier as a Heat Engine: A Study in Finite-time Thermodynamics*. Phys. Rev. E, vol. 49, pages 3903–3918, 1994. (Cited on pages 21, 39.)

[Geva 1996] Eitan Geva and Ronnie Kosloff. *The quantum heat engine and heat pump: An irreversible thermodynamic analysis of the three-level amplifier*. The Journal of chemical physics, vol. 104, no. 19, pages 7681–7699, 1996. (Cited on page 44.)

[Glaser 2015] Steffen J. Glaser, Ugo Boscain, Tommaso Calarco, Christiane P. Koch, Walter Köckenberger, Ronnie Kosloff, Ilya Kuprov, Burkhard Luy, Sophie

Schirmer, Thomas Schulte-Herbrüggen, Dominique Sugny and Frank K. Wilhelm. *Training Schrödinger's cat: quantum optimal control*. The European Physical Journal D, vol. 69, no. 12, 2015. (Cited on page 23.)

[Goold 2016] John Goold, Marcus Huber, Arnau Riera, Lídia del Rio and Paul Skrzypczyk. *The role of quantum information in thermodynamics—a topical review*. Journal of Physics A: Mathematical and Theoretical, vol. 49, no. 14, page 143001, 2016. (Cited on page 33.)

[Gorini 1976a] V Gorini, A Kossakowski and E.C.G. Sudarshan. *Completely positive dynamical semigroup of N-level system*. jmp, vol. 17, page 821, 1976. (Cited on page 13.)

[Gorini 1976b] Vittorio Gorini and Andrzej Kossakowski. *N-level system in contact with a singular reservoir*. J. Math. Phys., vol. 17, page 1298, 1976. (Cited on page 18.)

[Hänggi 1998] Peter Hänggi. *Driven quantum systems*. Quantum Transport and Dissipation (Wiley-VCH, Weinheim, 1998), pages 249–286, 1998. (Cited on page 21.)

[Henrich 2007] Markus J Henrich, Florian Rempp and Günter Mahler. *Quantum thermodynamic Otto machines: A spin-system approach*. The European Physical Journal Special Topics, vol. 151, no. 1, pages 157–165, 2007. (Cited on page 44.)

[Hofer 2016] Patrick P Hofer, Martí Perarnau-Llobet, Jonatan Bohr Brask, Ralph Silva, Marcus Huber and Nicolas Brunner. *Autonomous Quantum Refrigerator in a Circuit-QED Architecture Based on a Josephson Junction*. arXiv preprint arXiv:1607.05218, 2016. (Cited on page 82.)

[Horodecki 1996] Michał Horodecki, Paweł Horodecki and Ryszard Horodecki. *Separability of mixed states: necessary and sufficient conditions*. Physics Letters A, vol. 223, no. 1, pages 1–8, 1996. (Cited on page 12.)

[Katz 2008] Gil Katz, David Gelman, Mark A Ratner and Ronnie Kosloff. *Stochastic surrogate Hamiltonian*. The Journal of chemical physics, vol. 129, no. 3, page 034108, 2008. (Cited on page 38.)

[Kolář 2012] Michal Kolář, David Gelbwaser-Klimovsky, Robert Alicki and Gershon Kurizki. *Quantum bath refrigeration towards absolute zero: Challenging the unattainability principle*. Physical review letters, vol. 109, no. 9, page 090601, 2012. (Cited on page 83.)

[Kosloff, R. and Levy, A. 2014] Kosloff, R. and Levy, A. *Quantum Heat Engines and Refrigerators: Continuous Devices*. Annual Review of Physical Chemistry, vol. 65, pages 365–393, 2014. (Cited on pages 4, 6, 33, 44.)

[Kosloff 1984] Ronnie Kosloff. *A quantum mechanical open system as a model of a heat engine*. The Journal of chemical physics, vol. 80, no. 4, pages 1625–1631, 1984. (Cited on pages 2, 43, 44.)

[Kosloff 2000] Ronnie Kosloff, Eitan Geva and Jeffrey M Gordon. *The quantum refrigerator in quest of the absolute zero*. J. Appl. Phys., vol. 87, pages 8093–8097, 2000. (Cited on page 4.)

[Kosloff 2013] Ronnie Kosloff. *Quantum thermodynamics: a dynamical viewpoint*. Entropy, vol. 15, no. 6, pages 2100–2128, 2013. (Cited on page 33.)

[Kraus 1971] K. Kraus. *STATES EFFECTS OPERATORS*. Ann.Phys., vol. 64, page 311, 1971. (Cited on page 11.)

[Kubo 1957] R. Kubo. J. Phys. Soc. Jpn., vol. 12, page 550, 1957. (Cited on page 19.)

[Landau 1958] L.D. Landau and E.M. Lifshitz. Quantum Mechanics . Pergamon Press, Paris, 1958. (Cited on page 17.)

[Landsberg 1956] P. T. Landsberg. *Foundations of Thermodynamics*. Rev. Mod. Phys., vol. 28, page 363, 1956. (Cited on page 4.)

[Lenard 1978] A Lenard. *Thermodynamical proof of the Gibbs formula for elementary quantum systems*. Journal of Statistical Physics, vol. 19, no. 6, pages 575–586, 1978. (Cited on page 36.)

[Levy 2012a] Amikam Levy, Robert Alicki and Ronnie Kosloff. *Comment on "Cooling by Heating: Refrigeration Powered by Photons"*. Phys. Rev. Lett., vol. 109, page 248901, Dec 2012. (Cited on pages 2, 3, 5, 42, 82.)

[Levy 2012b] Amikam Levy, Robert Alicki and Ronnie Kosloff. *Quantum refrigerators and the third law of thermodynamics*. Phys. Rev. E, vol. 85, page 061126, Jun 2012. (Cited on pages 4, 5, 23, 38, 39, 42, 44.)

[Levy 2012c] Amikam Levy and Ronnie Kosloff. *Quantum Absorption Refrigerator*. Phys. Rev. Lett., vol. 108, page 070604, Feb 2012. (Cited on pages 3, 4, 44.)

[Levy 2014] Amikam Levy and Ronnie Kosloff. *The local approach to quantum transport may violate the second law of thermodynamics*. EPL (Europhysics Letters), vol. 107, no. 2, page 20004, 2014. (Cited on pages 2, 3.)

[Levy 2016] Amikam Levy, Lajos Diósi and Ronnie Kosloff. *Quantum flywheel.* Physical Review A, vol. 93, no. 5, page 052119, 2016. (Cited on pages 4, 36, 38.)

[Lindblad 1976] G. Lindblad. *On the generators of quantum dynamical semigroups.* J. Phys A: Math.Gen., vol. 48, page 119, 1976. (Cited on page 13.)

[Linden 2010] Noah Linden, Sandu Popescu and Paul Skrzypczyk. *How Small Can Thermal Machines Be? The Smallest Possible Refrigerator.* Phys. Rev. Lett., vol. 105, no. 13, page 130401, 2010. (Cited on page 44.)

[Lloyd 1997] S. Lloyd. Phys. Rev. A, vol. 56, page 3374, 1997. (Cited on page 44.)

[Lostaglio 2015] Matteo Lostaglio, Kamil Korzekwa, David Jennings and Terry Rudolph. *Quantum Coherence, Time-Translation Symmetry, and Thermodynamics.* Phys. Rev. X, vol. 5, page 021001, Apr 2015. (Cited on page 41.)

[Louisell 1990] W. H. Louisell. Quantum Statistical Properties of Radiation . Wiley, 1990. (Cited on page 14.)

[Luczka 1991] J. Luczka. *"Quantum open system in two-state stochastic reservoir ".* Czechoslovak Journal of Physics, vol. 41, page 289, 1991. (Cited on page 18.)

[Machnes 2014] Shai Machnes and Martin B. Penio. *Surprising Interactions of Markovian noise and Coherent Driving.* arXiv:1408.3056v1, 2014. (Cited on page 143.)

[Martin 1959] Paul C. Martin and Julian Schwinger. *Theory of Many-Particle Systems. I.* Phys. Rev., vol. 115, pages 1342–1373, Sep 1959. (Cited on page 19.)

[Martinez 2013] Esteban A Martinez and Juan Pablo Paz. *Dynamics and thermodynamics of linear quantum open systems.* Physical review letters, vol. 110, no. 13, page 130406, 2013. (Cited on pages 44, 81.)

[Masanes 2014] Lluis Masanes and Jonathan Oppenheim. *A derivation (and quantification) of the third law of thermodynamics.* arXiv preprint arXiv:1412.3828, 2014. (Cited on page 83.)

[Mitchison 2015] Mark T Mitchison, Mischa P Woods, Javier Prior and Marcus Huber. *Coherence-assisted single-shot cooling by quantum absorption refrigerators.* New Journal of Physics, vol. 17, no. 11, page 115013, 2015. (Cited on page 82.)

[Mitchison 2016] Mark T Mitchison, Marcus Huber, Javier Prior, Mischa P Woods and Martin B Plenio. *Realising a quantum absorption refrigerator with an atom-cavity system.* Quantum Science and Technology, vol. 1, no. 1, page 015001, 2016. (Cited on page 82.)

[Nakajima 1958] Sadao Nakajima. *On quantum theory of transport phenomena steady diffusion.* Progress of Theoretical Physics, vol. 20, no. 6, pages 948–959, 1958. (Cited on page 16.)

[Pekola 2007] J. P. Pekola and F. W. J. Hekking. *Normal-Metal-Superconductor Tunnel Junction as a Brownian Refrigerator.* Phys. Rev. Lett., vol. 98, page 210604, May 2007. (Cited on page 2.)

[Perarnau-Llobet 2015] Martí Perarnau-Llobet, Karen V. Hovhannisyan, Marcus Huber, Paul Skrzypczyk, Nicolas Brunner and Antonio Acín. *Extractable Work from Correlations.* Phys. Rev. X, vol. 5, page 041011, Oct 2015. (Cited on pages 5, 36.)

[Peres 1996] Asher Peres. *Separability Criterion for Density Matrices.* Phys. Rev. Lett., vol. 77, pages 1413–1415, Aug 1996. (Cited on page 12.)

[Peres 2006] Asher Peres. Quantum theory: concepts and methods, volume 57. Springer Science & Business Media, 2006. (Cited on page 40.)

[Purkayastha 2016] Archak Purkayastha, Abhishek Dhar and Manas Kulkarni. *Out-of-equilibrium open quantum systems: A comparison of approximate quantum master equation approaches with exact results.* Physical Review A, vol. 93, no. 6, page 062114, 2016. (Cited on page 81.)

[Pusz 1978] W. Pusz and S.L. Wornwicz. *Passive states and KMS states for general quantum systems.* Comm. Math. Phys., vol. 58, page 273, 1978. (Cited on page 35.)

[Quan 2007] HT Quan, Yu-xi Liu, CP Sun and Franco Nori. *Quantum thermodynamic cycles and quantum heat engines.* Physical Review E, vol. 76, no. 3, page 031105, 2007. (Cited on page 44.)

[Rabitz 2000] Herschel Rabitz, Regina de Vivie-Riedle, Marcus Motzkus and Karl Kompa. *Whither the future of controlling quantum phenomena?* Science, vol. 288, no. 5467, pages 824–828, 2000. (Cited on page 23.)

[Rezek 2006] Yair Rezek and Ronnie Kosloff. *Irreversible performance of a quantum harmonic heat engine.* New Journal of Physics, vol. 8, no. 5, page 83, 2006. (Cited on page 44.)

[Rezek 2008] Yair Rezek and Ronnie Kosloff. *Quantum refrigerator in the quest for the absolute zero temperature.* In Integrated Optoelectronic Devices 2008, pages 69070F–69070F. International Society for Optics and Photonics, 2008. (Cited on page 4.)

[Rezek 2009] Yair Rezek, Peter Salamon, Karl Heinz Hoffmann and Ronnie Kosloff. *The quantum refrigerator: The quest for absolute zero.* EPL (Europhysics Letters), vol. 85, no. 3, page 30008, 2009. (Cited on page 4.)

[Rivas 2010] Á. Rivas, A.D.K. Plato, S.F. Huelga and M.B. Plenio. *Markovian master equations: a critical study.* New Journal of Physic, vol. 12, page 11303, 2010. (Cited on page 23.)

[Rivas 2014] Ángel Rivas, Susana F Huelga and Martin B Plenio. *Quantum non-Markovianity: characterization, quantification and detection.* Reports on Progress in Physics, vol. 77, no. 9, page 094001, 2014. (Cited on page 20.)

[Roger 1994] Horn Roger and R Johnson Charles. Topics in matrix analysis. Cambridge University Press, 1994. (Cited on page 143.)

[Roßnagel 2016] Johannes Roßnagel, Samuel T Dawkins, Karl N Tolazzi, Obinna Abah, Eric Lutz, Ferdinand Schmidt-Kaler and Kilian Singer. *A single-atom heat engine.* Science, vol. 352, no. 6283, pages 325–329, 2016. (Cited on pages 2, 84.)

[Scovil 1959] HED Scovil and EO Schulz-DuBois. *Three-level masers as heat engines.* Physical Review Letters, vol. 2, no. 6, page 262, 1959. (Cited on pages 2, 42.)

[Silva 2015] Ralph Silva, Paul Skrzypczyk and Nicolas Brunner. *Small quantum absorption refrigerator with reversed couplings.* Physical Review E, vol. 92, no. 1, page 012136, 2015. (Cited on page 82.)

[Silva 2016] Ralph Silva, Gonzalo Manzano, Paul Skrzypczyk and Nicolas Brunner. *Performance of autonomous quantum thermal machines: Hilbert space dimension as a thermodynamical resource.* Phys. Rev. E, vol. 94, page 032120, Sep 2016. (Cited on page 82.)

[Spohn 1978] Herbert Spohn. *Entropy production for quantum dynamical semigroups.* Journal of Mathematical Physics, vol. 19, no. 5, pages 1227–1230, 1978. (Cited on page 41.)

[Stockburger 2016] Jürgen T Stockburger. *Exact propagation of open quantum systems in a system-reservoir context.* EPL (Europhysics Letters), vol. 115, no. 4, page 40010, 2016. (Cited on page 81.)

[Szczygielski 2013] Krzysztof Szczygielski, David Gelbwaser-Klimovsky and Robert Alicki. *Markovian master equation and thermodynamics of a two-level system in a strong laser field.* Phys. Rev. E, vol. 87, page 012120, Jan 2013. (Cited on page 23.)

[Tannor 2007] D.J. Tannor. Introduction to quantum mechanics: A time-dependent perspective. University Science Books, 2007. (Cited on page 21.)

[Thierschmann 2015] Holger Thierschmann, Rafael Sánchez, Björn Sothmann, Fabian Arnold, Christian Heyn, Wolfgang Hansen, Hartmut Buhmann and Laurens W Molenkamp. *Three-terminal energy harvester with coupled quantum dots.* Nature nanotechnology, vol. 10, no. 10, pages 854–858, 2015. (Cited on page 2.)

[Torrontegui 2013] Erik Torrontegui, Sara Ibáñez, Sofia Martínez-Garaot, Michele Modugno, Adolfo del Campo, David Guéry-Odelin, Andreas Ruschhaupt, Xi Chen and Juan Gonzalo Muga. *Shortcuts to adiabaticity.* Adv. At. Mol. Opt. Phys, vol. 62, pages 117–169, 2013. (Cited on pages 23, 85.)

[Trushechkin 2016] AS Trushechkin and IV Volovich. *Perturbative treatment of inter-site couplings in the local description of open quantum networks.* EPL (Europhysics Letters), vol. 113, no. 3, page 30005, 2016. (Cited on page 81.)

[Uzdin 2015] Raam Uzdin, Amikam Levy and Ronnie Kosloff. *Equivalence of Quantum Heat Machines, and Quantum-Thermodynamic Signatures.* Phys. Rev. X, vol. 5, page 031044, Sep 2015. (Cited on page 5.)

[Uzdin 2016] Raam Uzdin, Amikam Levy and Ronnie Kosloff. *Quantum heat machines equivalence, work extraction beyond markovianity, and strong coupling via heat exchangers.* Entropy, vol. 18, no. 4, page 124, 2016. (Cited on pages 6, 38.)

[Venturelli 2013] Davide Venturelli, Rosario Fazio and Vittorio Giovannetti. *Minimal self-contained quantum refrigeration machine based on four quantum dots.* Physical review letters, vol. 110, no. 25, page 256801, 2013. (Cited on page 82.)

[Vinjanampathy 2015] Sai Vinjanampathy and Janet Anders. *Quantum Thermodynamics.* arXiv preprint arXiv:1508.06099, 2015. (Cited on page 33.)

[von Neumann 1955] J. von Neumann. Mathematical Foundations of Quantum Mechanics . Princeton U. P., Princeton, 1955. (Cited on pages 9, 28.)

[Wang 2015] Jianhui Wang, Yiming Lai, Zhuolin Ye, Jizhou He, Yongli Ma and Qinghong Liao. *Four-level refrigerator driven by photons.* Physical Review E, vol. 91, no. 5, page 050102, 2015. (Cited on page 83.)

[Weiss 1998] Ulrich Weiss. Quantum dissipative systems, 2nd edition. World Scientific, 1998. (Cited on pages 7, 14.)

[Whitney 2013] Robert S Whitney. *Thermodynamic and quantum bounds on nonlinear dc thermoelectric transport.* Physical Review B, vol. 87, no. 11, page 115404, 2013. (Cited on page 83.)

[Wiseman 2010] H.M. Wiseman and G.J. Milburn. Quantum measurement and control. Cambridge University Press, 2010. (Cited on pages 23, 24, 30, 31, 32.)

[Zhang 2014] Jing Zhang, Yu-xi Liu, Re-Bing Wu, Kurt Jacobs and Franco Nori. *Quantum feedback: theory, experiments, and applications.* arXiv preprint arXiv:1407.8536, 2014. (Cited on page 24.)

[Zwanzig 1960] Robert Zwanzig. *Ensemble method in the theory of irreversibility.* The Journal of Chemical Physics, vol. 33, no. 5, pages 1338–1341, 1960. (Cited on page 16.)

Appendix A

Comment on "Cooling by Heating: Refrigeration Powered by Photons"

Comment on "Cooling by Heating: Refrigeration Powered by Photons"

In a recent Letter, Cleuren *et. al.* [1] proposed a model of a refrigerator composed of two metallic leads connected to two coupled quantum dots and powered by (solar) photons. In their analysis the refrigerator can cool one of the leads to arbitrarily low temperature, $T_r \to 0$, with the cooling flux $\dot{Q}_r \propto T_r$. We comment that this model strongly violates the dynamical version of the third law of thermodynamics. Furthermore, under more realistic assumptions concerning transitions between dot levels mediated by an electromagnetic field, we show that their model will not operate as a refrigerator.

There are seemingly two independent formulations of the third law. The first, known as the Nernst heat theorem, implies that the entropy flow from any substance at absolute zero is zero. Consider a system coupled simultaneously to a few heat baths with the aim to cool one of these baths to zero temperature. The entropy flow from this bath, given by $-\frac{\dot{Q}_k}{T_k}$, satisfies the Nerst theorem if the heat current $\dot{Q}_k$ flowing from the bath to the system scales like $\propto T_k^\alpha$ with $\alpha > 1$.

The second formulation of the third law is a dynamical one, known as the unattainability principle: No refrigerator can cool a system to absolute zero temperature at finite time. The dynamics of the cooling process is governed by the equation

$$\dot{Q}_k(T_k(t)) = -c_V(T_k(t))\frac{dT_k(t)}{dt}, \tag{1}$$

where c_V is heat capacity of the bath. Putting $\dot{Q}_k \propto T_k^\alpha$ and $c_V \propto T^\delta$, $\delta \geq 0$, we can quantify this formulation by evaluating the characteristic exponent ζ of the cooling process,

$$\frac{dT(t)}{dt} \propto -T^\zeta, \qquad T \to 0, \qquad \zeta = \alpha - \delta. \tag{2}$$

Namely, for $\zeta < 1$ the bath is cooled to zero temperature in a finite time. This formulation is more restrictive than the Nernst heat theorem and imposes limitations on the spectral density and the dispersion law of the heat bath [2].

The model of the refrigerator presented in Ref. [1] strongly violates the unattainability principle. For an electron reservoir at low temperatures, heat capacity is $c_V \propto T$. The heat current of the refrigerator of Ref. [1] is $\dot{Q}_r \propto T_r$, therefore, one obtains $\zeta = 0$, and zero temperature is reached at finite time.

Finding the flaw in the analysis of Ref. [1] is not a trivial task. A possible explanation emerges from the assumption made in Ref. [1] that transitions between lower and higher levels within the individual dots are negligible. However, photon- assisted tunneling between dots produces a rather weak tunneling current [3], while quenching transition rates in the individual dots are at least comparable and hence cannot be neglected.

A modified master equation that includes quenching transitions can be constructed for a five-level system: $\dot{\vec{p}} = M \cdot \vec{p}$, where $\vec{p} = (p_0, p_{ld}, p_{rd}, p_{lu}, p_{ru})^T$. Here, p_0 is the probability of finding no electron in the double dots and p_{ij} is the probability of finding one electron in the corresponding energy level, with l for left, r for right, d for down, and u for up. The 5×5 matrix M contains all transition rates, including quenching transition within the individual dots. Using this modified model, we can show analytically that, under the technical assumption that strictly positive quenching rates are equal for both dots, the condition for cooling ($\dot{Q}_r > 0$) and the condition of zero net electric current cannot be simultaneously satisfied at the stationary state. On the other hand, a crucial condition for this device to operate as a refrigerator [1] is that there is no net electric charging of the baths (leads). Otherwise, the electric current flowing through the device must be compensated by an external flow of electrons from the hot to the cold bath which would annihilate the cooling effect.

In conclusion, transitions in the individual dots, which are always present in real systems, cannot be neglected when treating electron transport in the double-dot systems. The dynamical form of the third law is a strong tool for testing designs of such nanodevices acting as refrigerators. Quantum models of refrigerators powered by heat (absorption refrigerators), which do not violate the third law, were studied in Refs. [2,4,5].

Amikam Levy,[1] Robert Alicki,[2,3] and Ronnie Kosloff[1]
[1]Institute of Chemistry
Hebrew University
Jerusalem 91904, Israel
[2]Institute of Theoretical Physics and Astrophysics
University of Gdańsk
Wita Stwosza 57, PL 80-952 Gdańsk, Poland
[3]Weston Visiting Professor
Weizmann Institute of Science
Rehovot 76100, Israel

Received 15 August 2012; published 11 December 2012
DOI: 10.1103/PhysRevLett.109.248901
PACS numbers: 05.70.Ln

[1] B. Cleuren, B. Rutten, and C. Van den Broeck, Phys. Rev. Lett. **108**, 120603 (2012).
[2] A. Levy and R. Kosloff, Phys. Rev. Lett. **108**, 070604 (2012).
[3] W. G. van der Wiel, S. De Franceschi, J. M. Elzerman, T. Fujisawa, S. Tarucha, and L. P. Kouwenhoven, Rev. Mod. Phys. **75**, 1 (2002).
[4] A. Levy, R. Alicki, and R. Kosloff, Phys. Rev. E **85**, 061126 (2012).
[5] J. P. Pekola and F. W. J. Hekking, Phys. Rev. Lett. **98**, 210604 (2007).

Appendix B

Equivalence of Quantum Heat Machines, and Quantum-Thermodynamic Signatures

Equivalence of Quantum Heat Machines, and Quantum-Thermodynamic Signatures

Raam Uzdin,* Amikam Levy, and Ronnie Kosloff
Fritz Haber Research Center for Molecular Dynamics, Hebrew University of Jerusalem, Jerusalem 91904, Israel
(Received 14 May 2015; published 29 September 2015)

Quantum heat engines (QHE) are thermal machines where the working substance is a quantum object. In the extreme case, the working medium can be a single particle or a few-level quantum system. The study of QHE has shown a remarkable similarity with macroscopic thermodynamical results, thus raising the issue of what is quantum in quantum thermodynamics. Our main result is the thermodynamical equivalence of all engine types in the quantum regime of small action with respect to Planck's constant. They have the same power, the same heat, and the same efficiency, and they even have the same relaxation rates and relaxation modes. Furthermore, it is shown that QHE have quantum-thermodynamic signature; i.e., thermodynamic measurements can confirm the presence of quantum effects in the device. We identify generic coherent and stochastic work extraction mechanisms and show that coherence enables power outputs that greatly exceed the power of stochastic (dephased) engines.

DOI: 10.1103/PhysRevX.5.031044 Subject Areas: Quantum Physics

I. INTRODUCTION

Thermodynamics emerged as a practical theory for evaluating the performance of steam engines. Since then, the theory proliferated and has been utilized in countless systems and applications. Eventually, thermodynamics became one of the pillars of theoretical physics. Amazingly, it survived great scientific revolutions such as quantum mechanics and general relativity. To a certain extent, thermodynamics even contributed to these theories (e.g., black hole entropy and temperature).

Despite its success, it is not expected that thermodynamics will hold all the way to the atomic scale, where the number of particles in the relevant substance is small or even equal to 1. Thus, it was anticipated that in the quantum regime new thermodynamic effects will surface. However, quantum-thermodynamic systems (even with a single particle) show a remarkable similarity to the macroscopic system described by classical thermodynamic. When the baths are thermal, the Carnot efficiency limit is equally applicable for a small quantum system [1,2]. Even classical fluctuation theorems hold without any alteration [3–5].

Since real engines have a finite cycle time, they cannot be in an exact equilibrium state and perform as a reversible machine. Consequently, the efficiency is always lower than the Carnot limit. Furthermore, the performance of a real engine is more severely limited by heat leaks, friction, and heat transport. This led to the study of efficiency at maximal power [6–9] and finite-time thermodynamics [10,11]. In analogy to the classical case, nonadiabatic couplings in finite-time quantum evolution give rise to a new quantum frictionlike mechanism [12,13]. However, this friction effect is not a generic feature of quantum heat machines. It can be avoided by applying different schemes. (See Ref. [14], or the multilevel embedding scheme in Sec. II E of this paper. See also the discussion in Ref. [15].)

Is there really nothing *generic*, new, and profound in the thermodynamics of small quantum system? Can classical thermodynamics and stochastic analysis predict and explain any observed thermodynamic effect in quantum heat machines? Do quantum effects always lead to friction and losses, or can they boost the heat machine performance? In this work, we present a generic thermodynamic behavior that is purely quantum in its essence and has no classical counterpart. Furthermore, it is shown that in the quantum regime, the generic coherent work extraction mechanism can significantly outperform the stochastic work extraction mechanism.

Quantum thermodynamics is the study of thermodynamic quantities such as temperature, heat, work, and entropy in microscopic quantum systems or even for a single particle. This study includes dynamical analysis of engines and refrigerators in the quantum regime [1,14,16–40], theoretical frameworks that take into account single-shot events [41,42], and the study of thermalization mechanisms [43–45]. Another topic of interest in quantum thermodynamics is algorithmic cooling [46–50]. For updated reviews on quantum thermodynamics, we recommend Refs. [51,52].

Several proposals for quantum-heat-engine realization and experimental setup have been studied [53–57].

*raam@mail.huji.ac.il

However, as will be explained later, only some of them are suited for exploring the quantum effects studied here. We hope our findings will motivate experimentalists to come up with more schemes that can probe the coherent work extraction regime.

Recently, some progress on the role of quantum coherence in quantum thermodynamics has been made [58–64]. In addition, quantum coherence has been shown to quantitatively affect the performance of heat machines [65–67]. In this work, we associate coherence with a specific thermodynamic effect and relate it to a thermodynamic work extraction mechanism.

Heat engines can be classified by their different scheduling of the interactions with the baths and the work repository. These types include the four-stroke, two-stroke, and the continuous engines (these engine types will be described in more detail later). The choice of engine type is usually guided by convenience of analysis or ease of implementation. Nevertheless, from a theoretical point of view, the fundamental differences or similarities between the various engine types are still uncharted. This is particularly true in the microscopic quantum regime. For brevity, we discuss engines, but all our results are equally applicable to other heat machines such as refrigerators and heaters.

Our first result (21)–(23) is that all three engine types are thermodynamically equivalent in the limit of small engine action (weak thermalization and a weak driving field). The equivalence holds also for transients and for states that are very far from thermal equilibrium. On top of providing a thermodynamic unification limit for the various engine types, this equivalence also establishes a connection to quantum mechanics, as it crucially depends on phase coherence and quantum interference. In particular, the validity regime of the equivalence is expressed in terms of $\hbar$.

Our second result (32) is the identification of a quantum-thermodynamic signatures. Let us define a quantum signature as a signal extracted from measurements that unambiguously indicates the presence of quantum effects (e.g., entanglement or interference). The Bell inequality for the EPR experiment is a good example. A quantum-thermodynamic signature is a quantum signature obtained from measuring thermodynamic quantities. We show that it is possible to set an upper bound on the work output of a stochastic, coherence-free engine. Any engine that surpasses this bound must have some level of coherence. Hence, work exceeding the stochastic bound constitutes a quantum-thermodynamic signature. Furthermore, we distinguish between a coherent work extraction mechanism and a stochastic work extraction mechanism. This explains why in the equivalence regime, coherent engines produce significantly more power compared to the corresponding stochastic engine. We estimate that our findings can be verified with present-day experimental capabilities. For a suggested realization in solid-state superconducting qubits, see Ref. [68].

The equivalence derivation is based on three ingredients. First, we introduce a multilevel embedding framework that enables the analysis of all three types of engines in the same physical setup. Next, a "norm action" smallness parameter, s, is defined for engines using Liouville space. The third ingredient is the symmetric rearrangement theorem that is used to show why all three engine types have the same thermodynamic properties despite the fact that they exhibit very different density matrix dynamics.

In Sec. II, we describe the main engine types and introduce the multilevel embedding framework. Next, in Sec. III, the multilevel embedding and the symmetric rearrangement theorem are used to show the various equivalence relation of different engine types. After discussing the two fundamental work extraction mechanisms, in Sec. IV, we present a quantum-thermodynamic signature that separates quantum engines from stochastic engines. In Sec. V, the over-thermalization effect in coherent quantum heat engines is studied. Finally, in Sec. VI, we conclude and discuss extensions and future prospects.

II. HEAT ENGINES TYPES AND THE MULTILEVEL EMBEDDING SCHEME

Heat engines are either discrete or continuous. Discrete engines include the two-stroke and four-stroke engines, whereas a turbine is a continuous engine [69]. These engine types appear in the macroscopic world as well as in the microscopic (quantum) realm. Here, we present a theoretical framework where all three types of engines can be embedded in a unified physical framework. This framework, termed "multilevel embedding," is an essential ingredient in our theory as it enables a meaningful comparison between different engine types.

A. Heat and work

A heat engine is a device that uses at least two thermal baths in different temperatures to extract work. Work is the transfer of energy from the engine to some external repository without changing the entropy of the repository. For example, increasing the excitation number of an oscillator, increasing the photon number in a specific optical mode (lasing), or increasing the kinetic energy in a single predefined direction. "Battery" or "flywheel" are terms often used in this context of work storage [70,71]. We shall use the more general term "work repository." Heat, on the other hand, is an energy exchange between the system and a thermal bath that involves entropy change in the bath. In the weak system-bath coupling limit, the heat is related to the temperature, via the well-known relation $dQ = TdS$, where dS is the entropy change in the bath.

In the elementary quantum heat engines, the working substance is comprised of single particle (or a few at the

most). Thus, the working substance cannot reach equilibrium on its own. Furthermore, excluding a few nongeneric cases, it is not possible to assign an equation of state that establishes a relation between thermodynamic quantities. Nevertheless, QHE's satisfy the second law and therefore are also bounded by the Carnot efficiency limit [1,72].

Work strokes are characterized by zero contact with the baths and an inherently time-dependent Hamiltonian. The unitary evolution generated by this Hamiltonian can change the energy of the system. On the other hand, the von Neumann entropy and the purity remain fixed (unitary evolution at this stage). Hence, the energy change of the system in this case constitutes pure work. The system's energy change is actually an energy exchange with the work repository.

When the system is coupled to a thermal bath and the Hamiltonian is fixed in time, the bath can change the populations of the energy levels. In a steady state, the system reaches a Gibbs state where the density matrix has no coherences in the energy basis and the population of the levels is given by $p_{n,b} = e^{-(E_n/T_b)} / \sum_{n=1}^{N} e^{-(E_n/T_b)}$, where N is the number of levels and "b" stands for "c" (cold) or "h" (hot). In physical models where the system thermalizes via collision with bath particles, a full thermalization can be achieved in finite time [15,73–76]. However, it is not necessary that the baths will bring the system close to a Gibbs state for the proper operation of the engine. In particular, maximal efficiency (e.g., in Otto engines) can be achieved without full thermalization. Maximal power (work per cycle time) is also associated with partial thermalization [6,8]. The definitive property of a thermal bath is its aspiration to bring the system to a predefined temperature regardless of the initial state of the system. The evolution in this stage does not conserve the eigenvalues of the density matrix of the system, and therefore, not only energy but entropy as well is exchanged with the bath. Therefore, the energy exchange in this stage is considered as heat.

In contrast to definitions of heat and work that are based on the derivative of the internal energy [1,77,78], our definitions are obtained by energy balance when coupling only one element (bath or external field) at a time. As we see later, in some engine types, several agents change the internal energy simultaneously. Even in this case, this point of view of heat and work will still be useful for obtaining consistent and physical definitions of heat and work.

B. Three types of engines

There are three core engine types that operate with two thermal baths: four-stroke engine, two-stroke engine, and a continuous engine. A stroke is a time segment where a certain operation takes place, for example, thermalization or work extraction. By definition, adjacent strokes in heat engines do not commute with each other. If they do commute (for example, see the "cold" and "hot" operations in the two-stroke engine later), they can be combined into a single stroke since the total effect of the two strokes can be generated by applying the two operations simultaneously.

Each stroke is a completely positive (CP) map [79], and therefore, the one-cycle evolution operator of the engine is also a CP map. For the extraction of work, it is imperative that some of the stroke propagators do not commute [80].

Otto engines and Carnot engines are examples of four-stroke engines. The simplest quantum four-stroke engine is the two-level Otto engine shown in Fig. 1(a). In the first stroke, only the cold bath is connected to the system. Thus, the internal energy changes are associated with heat exchange with the cold bath. The expansion and compression of the levels are fully described by a time-dependent Hamiltonian of the form $H(t) = f(t)\sigma_z$ (the baths are disconnected at this stage). In the second stroke, work is consumed in order to expand the levels, and in the fourth stroke, work is produced when levels revert to their original values. There is a net work extraction since the populations in stages II and IV are different. In different engines, much more general unitary transformation can be used to extract work. Nevertheless, this particular operation resembles the classical expansion and compression of classical engines. The work is the energy exchanged with the system during the unitary stages: $W = W_{II} + W_{IV} = (\langle E_3 \rangle - \langle E_2 \rangle) + (\langle E_5 \rangle - \langle E_4 \rangle)$. We consider only energy expectation values for two main reasons. First, investigations of work fluctuations revealed that quantum heat engines follow classical fluctuation laws [72], and we search for quantum signatures in heat engines. The second reason is that, in our view, the engine should not be measured during operation. The measurement protocol used in quantum fluctuation theorems [3,4,72] eliminates the density-matrix coherences. These coherences have a critical component in

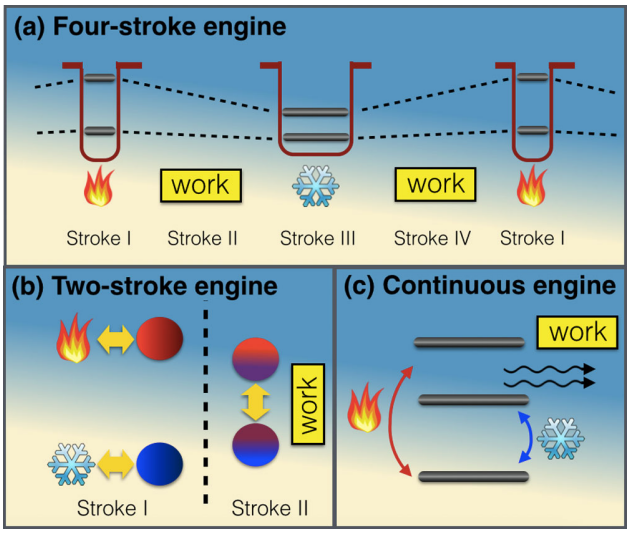

FIG. 1. (a) A two-level scheme of a four-stroke engine. (b) A two-particle scheme of a two-stroke engine. (c) A three-level scheme of a continuous engine.

the equivalence and quantum signature we study in this paper. As shown in Sec. IV, measurements or dephasing dramatically change the engine. Thus, although we frequently calculate work per cycle, the measured quantity is the cumulative work, and it is measured only at the end of the process. The averaged quantities are obtained by repeating the full experiment many times. Engines are designed to perform a task, and we assume that this completed task is the subject of measurement. The engine internal state is not measured.

The heat per cycle taken from the cold bath is $Q_c = \langle E_2\rangle - \langle E_1\rangle$, and the heat taken from the hot bath is $Q_h = \langle E_4\rangle - \langle E_3\rangle$. In a steady state, the average energy of the *system* returns to its initial value after one cycle [81] so that $\langle E_5\rangle = \langle E_1\rangle$. From this result, it follows immediately that $Q_c + Q_h + W = 0$; i.e., the first law of thermodynamics is obeyed. There is no instantaneous energy conservation of *internal* energy, as energy may be temporarily stored in the interaction field or in the work repository.

In the two-stroke engine shown in Fig 1(b), the engine consists of two parts (e.g., two qubits) [82]. One part may couple only to the hot bath, and the other may couple only to the cold bath. In the first stroke, both parts interact with their bath (but do not necessarily reach equilibrium). In the second unitary stroke, the two engine parts are disconnected from the baths and are coupled to each other. They undergo a mutual unitary evolution, and work is extracted in the process.

In the continuous engine shown in Fig. 1(c), the two baths and the external interaction field are connected continuously. For example, in the three-level laser system shown in Fig 1(c), the laser light represented by $\mathcal{H}_w(t)$ generates stimulated emission that extracts work from the system. This system was first studied in a thermodynamics context in Ref. [83], while a more comprehensive dynamical analysis of the system was given in Ref. [84]. It is imperative that the external field is time dependent. If it is time independent, the problem becomes a pure heat transport problem where $Q_h = -Q_c \neq 0$. In heat transport, the interaction field merely "dresses" the level so that the baths see a slightly modified system. The Lindblad generators are modified accordingly, and heat flows without extracting or consuming work [85]. Variations on these engine types may emerge because of realization constraints. For example, in the two-stroke engine, the baths may be continuously connected. This variation and others can still be analyzed using the tools presented in this paper.

C. Efficiency vs work and heat

Since the early days of Carnot, efficiency received considerable attention for two main reasons. First, this quantity is of great interest from both theoretical and practical points of view. Second, unlike other thermodynamics quantities, the efficiency satisfies a universal bound that is independent of the engine details. The Carnot efficiency bound is a manifestation of the second law of thermodynamics. Indeed, for Markovian bath dynamics, it was shown that quantum heat engines cannot exceed the Carnot efficiency [1]. Recently, a more general approach based on a fluctuation theorem for QHE showed that the Carnot bound still holds for quantum engines [72]. Studies in which higher-than-Carnot efficiency are reported [66] are interesting, but they use nonthermal baths and therefore, not surprisingly, deviate from results derived in the thermodynamic framework that deals with thermal baths. For example, an electric engine is not limited to Carnot efficiency since its power source is not thermal. Although the present work has an impact on efficiency as well, we focus on work and heat separately in order to unravel quantum effects. As will be exemplified later, in some elementary cases, these quantum effects do not influence the efficiency.

D. Bath description and Liouville space

The dynamics of the working fluid (system) interacting with the heat baths is described by the Lindblad-Gorini-Kossakowski-Sudarshan (LGKS) master equation for the density matrix [79,86,87]:

$$\hbar d_t\rho = L(\rho) = -i[H_s,\rho] + \sum_k A_k\rho A_k^\dagger - \frac{1}{2}A_k^\dagger A_k\rho - \frac{1}{2}\rho A_k^\dagger A_k, \tag{1}$$

where the A_k operators depend on the temperature, relaxation time of the bath, system bath coupling, and also on the system Hamiltonian H_s [79]. This form already encapsulates within the Markovian assumption of no bath memory. The justification for these equations arises from a "microscopic derivation" in the weak system-bath coupling limit [88]. In this derivation, a weak interaction field couples the system of interest to a large system (the bath) with temperature T. This interaction brings the system into a Gibbs state at temperature T. The Lindblad thermalization operators A_k used for the baths are described in the next section. The small Lamb shift is ignored.

Equation (1) is a linear equation, so it can always be rearranged into a vector equation. Given an index mapping $\rho_{N\times N} \to |\rho\rangle_{1\times N^2}$, the Lindblad equation now reads

$$i\hbar d_t|\rho\rangle = (\mathcal{H}_H + \mathcal{L})|\rho\rangle \doteq \mathcal{H}|\rho\rangle, \tag{2}$$

where $\mathcal{H}_H$ is a Hermitian $N^2\times N^2$ matrix that originates from H_s, and $\mathcal{L}$ is a non-Hermitian $N^2\times N^2$ matrix that originates from the Lindblad evolution generators A_k. This extended space is called Liouville space [89]. In this paper, we use calligraphic letters to describe operators in Liouville space and ordinary letters for operators in Hilbert space. For states, however, $|A\rangle$ will denote a vector in Liouville space formed from $A_{N\times N}$ by "vec-ing" A into a column in the same procedure ρ is converted into $|\rho\rangle$. A short review

of Liouville space and some of its properties is given in Appendix A.

In unitary dynamics, the largest energy gap of the Hamiltonian sets a speed limit on the rate of change of a state (e.g., rotation speed in the Bloch sphere). Since $\mathcal{H}$ is not Hermitian, the energy scalar that sets a speed limit on the evolution speed is the spectral norm (or operator norm) of $\mathcal{H}$, $\|\mathcal{H}\| = \max\sqrt{\mathrm{eig}(\mathcal{H}^\dagger\mathcal{H})}$ (The spectral norm is the largest singular value of $\mathcal{H}$ [90]). In particular, we show in Appendix B that the norm action, defined as

$$s = \int_0^\tau \|\mathcal{H}(t)\| dt, \tag{3}$$

sets a limit on how much a state can change during a time τ because of the operation of $\mathcal{H}$. For time-independent super-Hamiltonian $\mathcal{H}$, the evolution operator in Liouville space is

$$|\rho(t)\rangle = \mathcal{K}|\rho(t')\rangle = e^{-i\mathcal{H}(t-t')/\hbar}|\rho(t')\rangle. \tag{4}$$

Writing the evolution operator as an exponent of a matrix has a significant advantage since commutator exponentiation is avoided. Furthermore, the action has a natural definition in this formalism. In principal, it should be possible to reformulate the derivations using density matrixes and the Kraus operators. However, it seems that the Hilbert space formalism is far more cumbersome and complicated (for example, see Refs. [91,92]).

While the Lindblad description works very well for sufficiently long times, it fails for very short times where some of the approximation breaks down. In scales where the bath still has a memory of the system's past states, the semigroup property of the Lindblad equation no longer holds: $|\rho(t+t')\rangle \neq e^{-i(\mathcal{H}_s+\mathcal{L})(t-t')/\hbar}|\rho(t')\rangle$. This will set a cutoff limit for the validity of the engine-type equivalence in the Markovian approximation.

Next we introduce the multilevel embedding scheme that enables us to discuss various heat engines in the same physical setup.

E. Multilevel embedding

Let the working substance of the quantum engine be an N-level system. These levels are fixed in time [i.e., they do not change as in Fig. 1(a)]. For simplicity, the levels are assumed to be nondegenerate. We divide the energy levels into a cold manifold and a hot manifold. During the operation of the engine, the levels in the cold manifold interact only with the cold bath, and the levels in the hot manifold interact only with the hot bath. Each thermal coupling can be turned on and off as a function of time, but the aliasing of a level to a manifold does not change in time.

If the manifolds do not overlap, the hot and cold thermal operations commute and they can be applied at the same time or one after the other. The end result will be the same. Nevertheless, our scheme also includes the possibility that one level appears in both manifolds. This is the case for the three-level continuous engine shown in Fig. 1(c). For simplicity, we exclude the possibility of more than one mutual level. If there are two or more overlapping levels, there is an inevitable heat transport in the steady state from the hot bath to the cold bath even in the absence of an external field that extracts work. In the context of heat engines, this can be interpreted as heat leak. This "no field–no transport" condition holds for many engines studied in the literature. Nonetheless, this condition is not a necessary condition for the validity of our results.

This manifold division seems sensible for the continuous engine and even for the two-stroke engine in Fig. 1(b), but how can it be applied to the four-stroke engine shown in Fig. 1(a)? The two levels interact with both baths and also change their energy value in time, contrary to the assumption of fixed energy levels. Nevertheless, this engine is also incorporated into the multilevel embedding framework. Instead of two levels as in Fig. 1(a), consider the four-level system shown in the dashed green lines in Fig. 2.

Initially, only levels 2 and 3 are populated and coupled to the cold bath (2 and 3 are in the cold manifold). In the unitary stage, an interaction Hamiltonian H_{swap} generates a full swap of populations and coherence according to the rule $1 \leftrightarrow 2, 3 \leftrightarrow 4$. Now, levels 1 and 4 are populated and 2 and 3 are empty. Therefore, this system fully simulates the expanding-level engine shown in Fig. 1(a). At the same time, this system satisfies the separation into well-defined

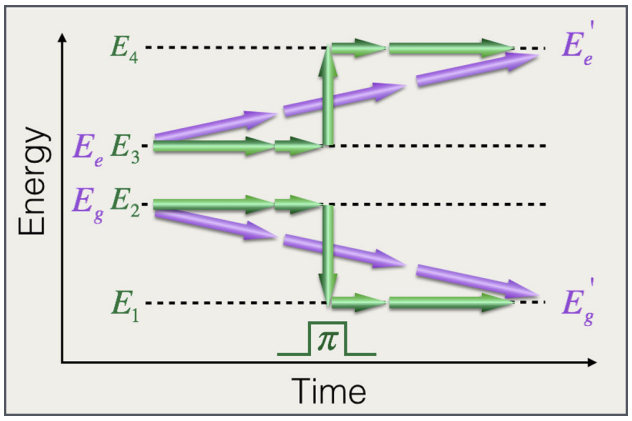

FIG. 2. In the standard two-level Otto engine, there are two-level $E_{g,e}$ (purple arrows) that change in time to $E'_{g,e}$. In the multilevel embedding framework, the levels (E_{1-4}) are fixed in time (black dashed lines), but a time-dependent field (π pulse, swap operation) transfers the population (green arrows) to the other levels. For a swap operation, the two schemes lead to the same final state and therefore are associate with the same work. Nonetheless, the multilevel scheme is more general since for weaker unitary transformation (instead of the π pulse), coherences are generated. We show that this type of coherence can significantly boost the power output of the engine.

time-independent manifolds, as defined in the multilevel embedding scheme.

The full swap used to embed the traditional four-stroke Otto engine is not mandatory, and other unitary operations can be applied. This extension of the four-stroke scheme is critical for our work since the equivalence of engines appears when the unitary operation is fairly close to the identity transformation. A full swap turns one diagonal state into another. Consequently, the steady state of an engine with full swap operation will not contain any coherences in the energy basis. As will be shown later, a partial swap or a different "weaker than full swap" unitary leads to steady-state coherences that dramatically enhance the power output. Note that these coherences between the hot and cold manifold imply a superposition of the cold and hot states. In other words, in contrast to the full swap case, the particle is not localized exclusively on either the hot or cold manifold.

Figures 3(a)–(c) show how the three types of engines are represented in the multilevel embedding scheme. The advantage of the multilevel scheme now becomes clear. All three engine types can be described in the same physical system with the same baths and the same coupling to external fields (work extraction). The engine types differ only in the order of the coupling to the baths and to the work repository. While the thermal operations commute if the manifolds do not overlap, the unitary operation never commutes with the thermal strokes.

In the present paper, we use a direct sum structure for the hot and cold manifolds. However, when there are two or more particles in the engine [82], it is more natural to apply a tensor product structure for the manifolds of the multilevel embedding scheme.

On the right of Fig. 3, we plotted a "brick" diagram for the evolution operator. Black stands for unitary transformation generated by some external field, while blue and red stand for hot and cold thermal coupling, respectively. When the bricks are on top of each other, it means that they operate simultaneously. Now we are in a position to derive the first main results of this paper: the thermodynamic equivalence of the different engine types in the quantum regime.

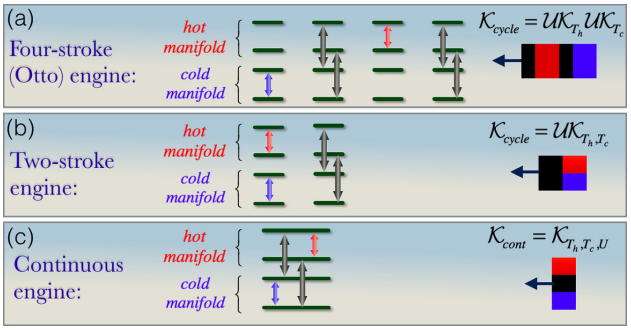

FIG. 3. Representation of the three types of engines (a)–(c) in the multilevel embedding framework. In this scheme, the different engine types differ only in the order of coupling to the baths and work repository. Since the interactions and energy levels are the same for all engine types, a meaningful comparison of performance becomes possible.

III. CONTINUOUS AND STROKE ENGINE EQUIVALENCE

We first discuss the equivalence of continuous and four-stroke engines. Nevertheless, all the arguments are valid for the two-stroke engines as well, as explained later. Although our results are not limited to a specific engine model, it will be useful to consider the simple engine shown in Fig. 4. We use this model to highlight a few points and also for numerical simulations. The Hamiltonian part of the system is

$$H_0 + \cos(\omega t) H_w, \tag{5}$$

where $H_0 = -(\Delta E_h/2)|1\rangle\langle 1| - (\Delta E_c/2)|2\rangle\langle 2| + (\Delta E_c/2)|3\rangle\langle 3| + (\Delta E_h/2)|4\rangle\langle 4|$, $H_w = \epsilon(t)|1\rangle\langle 2| + \epsilon(t)|3\rangle\langle 4| +$ H.c. and $\omega = (\Delta E_h - \Delta E_c)/2\hbar$.

The driving frequency that couples the system to the work repository is in resonance with the top and bottom energy gaps. The specific partitioning into hot and cold manifolds was chosen so that only one frequency (e.g., a single laser) is needed for implementing the system instead of two.

We assume that the Rabi frequency of the drive ϵ is smaller than the decay time scale of the baths, $\epsilon \ll \gamma_c, \gamma_h$. Under this assumption, the dressing effect of the driving field on the system-bath interaction can be ignored. It is justified, then, to use "local" Lindblad operators obtained in the absence of a driving field [85,93]. For plotting purposes (reasonable duty cycle), in the numerical examples, we often use $\epsilon = \gamma_c = \gamma_h$. While this poses no problem for stroke-engine realizations, for experimental demonstration of equivalence with continuous engines, one has to increase the duty cycle so that $\epsilon \ll \gamma_c, \gamma_h$. In other words, the unitary stage should be made longer but with a weaker driving field.

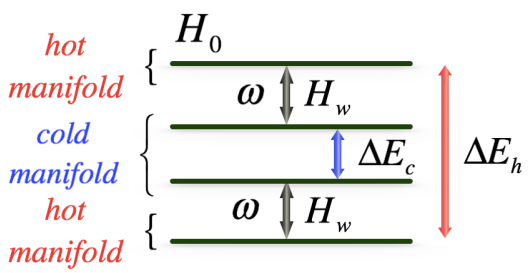

FIG. 4. Illustration of the engine used in the numerical simulation. By changing the time order of the coupling to H_w and to thermal baths, all three types of engines can be realized in the model.

The Lindblad equation is given by Eq. (1) with the Hamiltonian (5) and with the following Lindblad operators in Hilbert space:

$$A_1 = \sqrt{\gamma_h} e^{-(\Delta E_h/2T_h)} |4\rangle\langle 1|, \tag{6}$$

$$A_2 = \sqrt{\gamma_h} |1\rangle\langle 4|, \tag{7}$$

$$A_3 = \sqrt{\gamma_c} e^{-(\Delta E_c/2T_c)} |3\rangle\langle 2|, \tag{8}$$

$$A_4 = \sqrt{\gamma_c} |2\rangle\langle 3|. \tag{9}$$

In all the numerical simulations, we use $\Delta E_h = 4$, $\Delta E_c = 1$, $T_h = 5$, $T_c = 1$. The interaction with the baths or with work repository can be turned on and off at will.

Starting with the continuous engine, we choose a unit cell that contains exactly $6m$ (m is an integer) complete cycles of the drive ($\tau_d = 2\pi/\omega$) so that $\tau_{\rm cyc} = 6m\tau_d$. The difference between the engine cycle time and the cycles of the external drive will become clear in stroke engines (also, the factor of 6 will be clarified).

For the validity of the secular approximation used in the Lindblad microscopic derivation [79], the evolution time scale must satisfy $\tau \gg (2\pi\hbar)/\min(\Delta E_h, \Delta E_c)$. Therefore, m must satisfy $m \gg (\hbar\omega)/\min(\Delta E_h, \Delta E_c)$. Note that if the Lindblad description is obtained from a different physical mechanism (e.g., thermalizing collisions), then this condition is not required.

Next, we transform to the interaction picture (denoted by tilde) using the transformation $\mathcal{U} = e^{-i\mathcal{H}_0 t/\hbar}$, and perform the rotating wave approximation (RWA) by dropping terms oscillating at a frequency of 2ω. For the RWA to be valid, the amplitude of the field must satisfy $\epsilon \ll \omega$. The resulting Liouville space super-Hamiltonian is

$$\tilde{\mathcal{H}} = \mathcal{L}_c + \mathcal{L}_h + \frac{1}{2}\mathcal{H}_w. \tag{10}$$

Note that $\mathcal{L}_{h,c}$ were not modified by the transformation to the rotating system since $[\mathcal{L}_{h,c}, \mathcal{H}_0] = 0$ in the microscopic derivation [94]. The oscillatory time dependence has disappeared because of the RWA and the interaction picture. There is still an implicit time dependence that determines which of the terms $\mathcal{L}_c, \mathcal{L}_h, \mathcal{H}_w$ is coupled to the system at a given time. We point out that when the RWA is not valid, the dynamics becomes considerably more complicated. First, even the basic unitary evolution has no simple analytical solution. Second, the Lindblad description of the continuous engine becomes more complicated. Thus, our analysis is restricted to the validity regime of the RWA.

The Lindblad Markovian dynamics and the RWA set a validity regime for our theory. This regime is the default regime used in quantum open systems (see Refs. [77,79]). It is intriguing to study how the results presented here are modified by the breakdown of the RWA or by bath memory effects. However, this analysis is beyond the scope of the present paper.

Now that we have established a regime of validity and the super-Hamiltonian that governs the system, we can turn to the task of transforming from one engine type to other types and study what properties change in this transformation. The engine-type transformation is based on the Strang decomposition [95–97] for two noncommuting operators $\mathcal{A}$ and $\mathcal{B}$ (the operators may not be Hermitian):

$$e^{(\mathcal{A}+\mathcal{B})dt} = e^{\frac{1}{2}\mathcal{A}dt} e^{\mathcal{B}dt} e^{\frac{1}{2}\mathcal{A}dt} + O[(s/\hbar)^3] \cong e^{\frac{1}{2}\mathcal{A}dt} e^{\mathcal{B}dt} e^{\frac{1}{2}\mathcal{A}dt}, \tag{11}$$

where the norm action (3), $s = (\|\mathcal{A}\| + \|\mathcal{B}\|)dt$, must be small for the expansion to be valid. $\|\mathcal{A}\|$ is the spectral norm of $\mathcal{A}$. In Appendix C, we derive the condition $s \ll \frac{1}{2}\hbar$ for the validity of Eq. (11). We use the symbol $\cong$ to denote equality with correction $O[(s/\hbar)^3]$.

Let the evolution operator of the continuous engine over the chosen cycle time $\tau_{\rm cyc} = 6m\tau_d$ be

$$\tilde{\mathcal{K}}^{\rm cont} = e^{-i\tilde{\mathcal{H}}\tau_{\rm cyc}/\hbar}. \tag{12}$$

By first splitting $\mathcal{L}_c$ and then splitting $\mathcal{L}_h$, we get

$$\begin{aligned}\tilde{\mathcal{K}}^{\text{four stroke}} = {} & e^{-i(3\mathcal{L}_c)(\tau_{\rm cyc}/6\hbar)} e^{-i(\frac{3}{2}\mathcal{H}_w)(\tau_{\rm cyc}/6\hbar)} e^{-i(3\mathcal{L}_h)(\tau_{\rm cyc}/3\hbar)} \\ & \times e^{-i(\frac{3}{2}\mathcal{H}_w)(\tau_{\rm cyc}/6\hbar)} e^{-i(3\mathcal{L}_c)(\tau_{\rm cyc}/6\hbar)}.\end{aligned} \tag{13}$$

Note that the system is periodic so the first and last stages are two parts of the same thermal stroke. Consequently, Eq. (13) describes an evolution operator of a four-stroke engine, where the unit cell is symmetric. This splitting is illustrated in Figs. 5(a) and 5(b). There are two thermal strokes and two work strokes that together constitute an evolution operator that describes a four-stroke engine. The cumulative evolution time as written above is $(m+m+2m+m+m)\tau_d = 6m\tau_d = \tau_{\rm cyc}$. Yet, to maintain the same cycle time as chosen for the continuous engine, the coupling to the baths and field were multiplied by 3. In this four-stroke engine, each thermal or work stroke operates, in total, only a third of the cycle time compared to the continuous engine. Hence, the coupling must be 3 times larger in order to generate the same evolution.

By virtue of the Strang decomposition, $\tilde{\mathcal{K}}^{\text{four stroke}} \cong \tilde{\mathcal{K}}^{\rm cont}$ if $s \ll \hbar$. The action parameter s of the engine is defined as $s = \int_{-\tau_{\rm cyc}/2}^{\tau_{\rm cyc}/2} \|\tilde{\mathcal{H}}\| dt = (\frac{1}{2}\|\mathcal{H}_w\| + \|\mathcal{L}_h\| + \|\mathcal{L}_c\|)\tau_{\rm cyc}$. Note that the relation $\tilde{\mathcal{K}}^{\text{four stroke}} \cong \tilde{\mathcal{K}}^{\rm cont}$ holds only when the engine action is small compared to $\hbar$. This first appearance of a quantum scale will be discussed later.

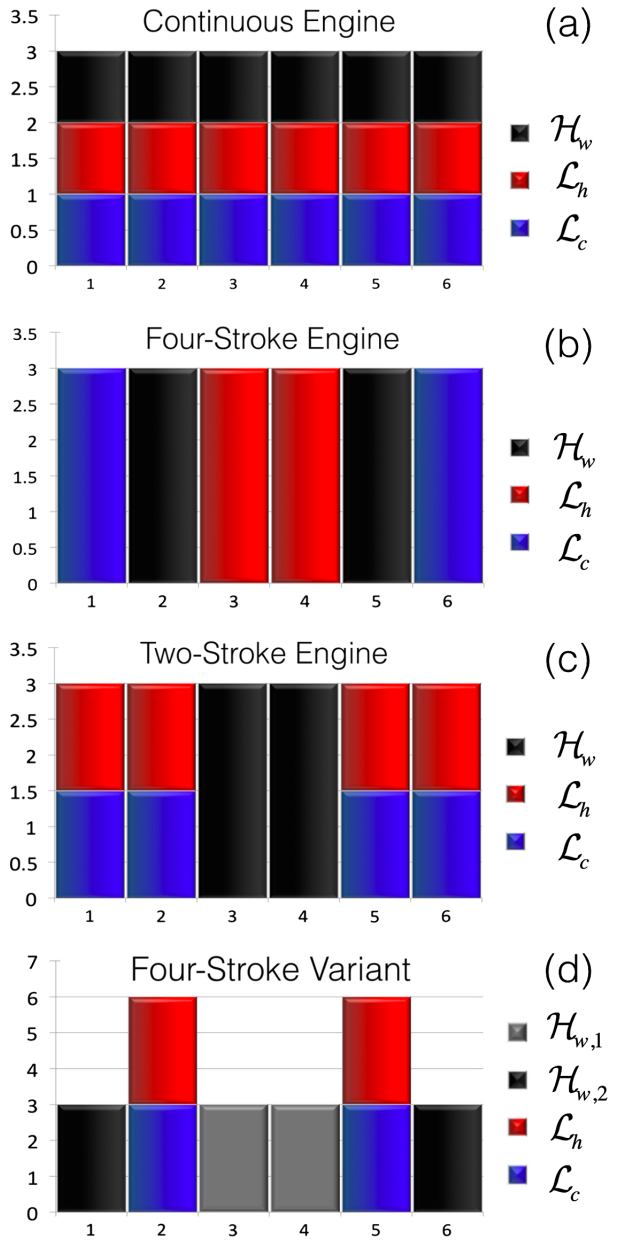

FIG. 5. Graphical illustrations of the super-Hamiltonians of various engines (a)–(d). The horizontal axis corresponds to time. The brick size corresponds to the strength of the coupling to the work repository or to the baths. The Hamiltonians are related to each other by applying the Strang decomposition to the evolution operators (12), (13), and (20). The symmetric rearrangement theorem ensures that in the limit of small action, any rearrangement that is symmetric with respect to the center and conserves the area of each color does not change the total power and heat over one cycle.

A. Dynamical aspect of the equivalence

The equivalence of the evolution operators $\tilde{\mathcal{K}}^{\text{four stroke}} \cong \tilde{\mathcal{K}}^{\text{cont}}$ has two immediate important consequences. First, both engines have the same steady-state solution over one cycle $|\tilde{\rho}_s\rangle$:

$$\tilde{\mathcal{K}}^{\text{four stroke}}(\tau_{\text{cyc}})|\tilde{\rho}_s\rangle \cong \tilde{\mathcal{K}}^{\text{cont}}(\tau_{\text{cyc}})|\tilde{\rho}_s\rangle = |\tilde{\rho}_s\rangle, \quad (14)$$

$$\left(\mathcal{L}_c + \mathcal{L}_h + \frac{1}{2}\mathcal{H}_w\right)|\tilde{\rho}_s\rangle = 0. \quad (15)$$

At time instances that are not integer multiples of τ_{cyc}, the states of the engines will differ significantly ($O[(s/\hbar)^1]$) since $\tilde{\mathcal{K}}^{\text{four stroke}}(t < \tau_{\text{cyc}}) \neq \tilde{\mathcal{K}}^{\text{cont}}(t < \tau_{\text{cyc}})$. In other words, the engines are still significantly different from each other. The second consequence is that the two engines have the same transient modes as well. When monitored at multiples of τ_{cyc}, both engines will have the same relaxation dynamics to the steady state if they started from the same initial condition. In the remainder of the paper, when the evolution operator is written without a time tag, this means that we are considering the evolution operator of a complete cycle.

We point out that there are higher-order decompositions where the correction terms are smaller than $O[(s/\hbar)^3]$. However, it turns out that these decompositions inherently involve negative coefficients [98]. A negative coefficient implies a thermal stroke of the form $e^{+i\mathcal{L}dt/\hbar}$ (instead of $e^{-i\mathcal{L}dt/\hbar}$). This type of evolution cannot be generated by a Markovian bath. Therefore, among the symmetric decompositions, the Strang decomposition seems to be the only one that can be used for decomposing Markovian thermal engine evolution operators.

B. Thermodynamic aspect of the equivalence

The equivalence of the one-cycle evolution operators of the two engines does not immediately imply that the engines are thermodynamically equivalent. Generally, in stroke engines, the heat and work depend on the dynamics of the state inside the cycle, which is very different ($O[(s/\hbar)^1]$) from the constant state of the continuous engine. However, in this section, we show that all thermodynamics properties are equivalent in both engines up to $O[(s/\hbar)^3]$ corrections, similarly to the evolution operator. We start by evaluating the work and heat in the continuous engine. By considering infinitesimal time elements where $\mathcal{L}_c$, $\mathcal{L}_h$, and $\mathcal{H}_w$ operate separately, one obtains that the heat and work currents are $j_{c(h)} = \langle H_0|(1/\hbar)\mathcal{L}_{c(h)}|\tilde{\rho}_s(t)\rangle$ and $j_w = \langle H_0|(1/2\hbar)\mathcal{H}_w|\tilde{\rho}_s(t)\rangle$, where $\langle H_0| = |H_0\rangle^\dagger$ is the vectorized form of the field-free Hamiltonian H_0 of the system [see Eq. (5)]. See Appendix A for the use of bracket notation to describe expectation values $\langle A\rangle = \text{tr}(A\rho) = \langle A|\rho\rangle$. In principle, to calculate $\langle A\rangle$ in the rotating frame using $|\tilde{\rho}_s(t)\rangle$, $\langle A|$ must be rotated as well. However, because of the property $\langle H_0|\mathcal{H}_0 = 0$ shown in Appendix A, $\langle H_0|$ is not affected by this rotation.

In the continuous engine, the steady state satisfies $|\tilde{\rho}_s(t)\rangle = |\tilde{\rho}_s\rangle$, so the total heat and work in the steady state in one cycle are

$$W^{\text{cont}} = \left\langle H_0 \left| \frac{1}{2\hbar}\mathcal{H}_w \right| \tilde{\rho}_s \right\rangle \tau_{\text{cyc}}, \tag{16}$$

$$Q^{\text{cont}}_{c(h)} = \left\langle H_0 \left| \frac{1}{\hbar}\mathcal{L}_{c(h)} \right| \tilde{\rho}_s \right\rangle \tau_{\text{cyc}}. \tag{17}$$

These quantities should be compared to the work and heat in the four-stroke engine. Instead of carrying out the explicit calculation for this specific four-stroke splitting, we use the symmetric rearrangement theorem (SRT) derived in Appendix D. Symmetric rearrangement of a Hamiltonian is a change in the order of couplings $\epsilon(t), \gamma_c(t), \gamma_h(t)$ that satisfies $\int \epsilon(t)dt = \text{const}$, $\int \gamma_c(t)dt = \text{const}$, $\int \gamma_h(t)dt = \text{const}$, and with the symmetry $\epsilon(t) = \epsilon(-t), \gamma_c(t) = \gamma_c(-t), \gamma_c(t) = \gamma_c(-t)$. Any super-Hamiltonian obtained using the Strang splitting of the continuous engine [for example, $\mathcal{H}^{\text{two stroke}}(t)$, $\mathcal{H}^{\text{four stroke}}(t)$] constitutes a symmetric rearrangement of the continuous engine. The SRT exploits the symmetry of the Hamiltonian to show that symmetric rearrangement changes heat and work only in $O[(s/\hbar)^3]$. In Appendix D, we show that

$$W^{\text{four stroke}} \cong W^{\text{cont}}, \tag{18}$$

$$Q^{\text{four stroke}}_{c(h)} \cong Q^{\text{cont}}_{c(h)}. \tag{19}$$

Thus, we conclude that up to $(s/\hbar)^3$ corrections, the engines are thermodynamically equivalent. When $s \ll 1$, work, power, heat, and efficiency converge to the same value for all engine types. Clearly, inside the cycle, the work and heat in the two engines are significantly different ($O[(s/\hbar)^1]$), but after a complete cycle, they become equivalent. The symmetry makes this equivalence more accurate as it holds up to $(s/\hbar)^3$ [rather than $(s/\hbar)^2$]. Interestingly, the work done in the first half of the cycle is $\frac{1}{2}W^{\text{cont}} + O[(s/\hbar)^2]$. However, when the contribution of the other half is added, the $O[(s/\hbar)^2]$ correction cancels out and Eq. (18) is obtained (see Appendix D).

We emphasize that the SRT and its implications (18) and (19) are valid for transients and for any initial state—not just for steady-state operation. In Fig. 6(a), we show the cumulative work as a function of time for a four-stroke engine and a continuous engine. The vertical lines indicate a complete cycle of the four-stroke engine. In addition to the parameter common to all examples specified before, we used $\epsilon = \gamma_c = \gamma_h = 10^{-4}$, and the equivalence of work at the vertical lines is apparent. In Fig. 6(b), the field and thermal coupling were increased to $\epsilon = \gamma_c = \gamma_h = 5 \times 10^{-3}$. Now the engines perform differently, even at the end of each cycle. This example is a somewhat extreme situation where the system changes quite rapidly (consequence of the initial state we chose). In other cases, such as steady-state operation, the equivalence can be observed for much larger action values.

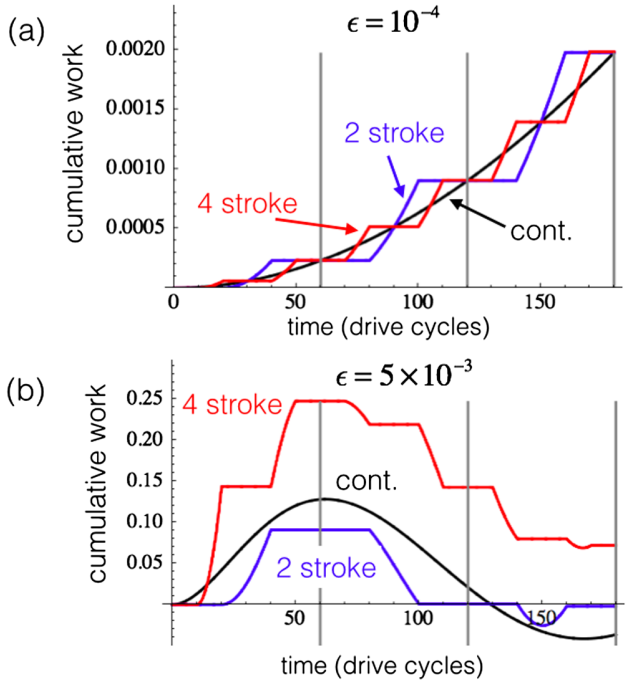

FIG. 6. (a) The equivalence of heat engine types in transient evolution when the engine action is small compared to $\hbar$. (a) The cumulative power transferred to the work repository is plotted as a function of time. All engines start in the excited state $|4\rangle$, which is very far from the steady state of the system. At complete engine cycles (vertical lines), the power in all engines is the same. (b) Once the action is increased (here, the field ϵ was increased), the equivalence no longer holds.

The splitting used in Eq. (13) was based on first splitting $\mathcal{L}_c$ and then $\mathcal{H}_w$. Other engines can be obtained by different splitting of $\tilde{\mathcal{K}}^{\text{cont}}$. For example, consider the two-stroke engine obtained by splitting $\mathcal{L}_c + \mathcal{L}_h$:

$$\tilde{\mathcal{K}}^{\text{two stroke}} = e^{-i\frac{3}{2}(\mathcal{L}_c+\mathcal{L}_h)(\tau_{\text{cyc}}/3)} e^{-i(\frac{3}{2}\mathcal{H}_w)(\tau_{\text{cyc}}/3)} \times e^{-i\frac{3}{2}(\mathcal{L}_c+\mathcal{L}_h)(\tau_{\text{cyc}}/3)}. \tag{20}$$

Note that in the two-stroke engine, the thermal coupling has to be $\frac{3}{2}$ stronger compared to the continuous case in order to provide the same action. Using the SRT, we obtain the complete equivalence relations of the three main engine types:

$$W^{\text{two stroke}} \cong W^{\text{four stroke}} \cong W^{\text{cont}}, \tag{21}$$

$$Q^{\text{two stroke}}_{c(h)} \cong Q^{\text{four stroke}}_{c(h)} \cong Q^{\text{cont}}_{c(h)}, \tag{22}$$

$$\tilde{\mathcal{K}}^{\text{two stroke}} \cong \tilde{\mathcal{K}}^{\text{four stroke}} \cong \tilde{\mathcal{K}}^{\text{cont}}. \tag{23}$$

Note that since $\mathcal{K} = e^{-i\mathcal{H}_0\tau_{\text{cyc}}}\tilde{\mathcal{K}}$, the equivalence of the evolution operators holds also in the original frame, not just in the interaction frame. Another type of engine exists when the interaction with the work repository is carried out by two physically distinct couplings. This happens

naturally if $E_4 - E_3 \neq E_2 - E_1$ so that two different driving lasers have to be used and the Hamiltonian is $H_0 + \cos[(E_2 - E_1)t]H_{w1} + \cos[(E_4 - E_3)t]H_{w2}$. In such cases, one can make the splitting shown in Fig. 5(d). In this numerical example, we used $H_{w1} = \epsilon(t)|1\rangle\langle 2| + \text{H.c.}$ and $H_{w2} = \epsilon(t)|3\rangle\langle 4| + \text{H.c.}$ Since there are two different work strokes in addition to the thermal stroke, this engine constitutes a four-stroke engine.

C. Power and energy flow balance

The average power and heat flow in the equivalence regime are independent of the cycle time:

$$P_W = \frac{W}{\tau_{\text{cyc}}} = \left\langle H_0 \middle| \frac{1}{2\hbar}\mathcal{H}_w \middle| \tilde{\rho}_s \right\rangle, \tag{24}$$

$$J_{c(h)} = \frac{Q_{c(h)}}{\tau_{\text{cyc}}} = \left\langle H_0 \middle| \frac{1}{\hbar}\mathcal{L}_{c(h)} \middle| \tilde{\rho}_s \right\rangle. \tag{25}$$

Using the steady-state definition (15), one obtains the steady-state energy balance equation:

$$P_w + J_c + J_h = 0. \tag{26}$$

Equation (26) does not necessarily hold if the system is not in a steady state, as energy may be temporarily stored in the baths or in the work repository.

Figure 7 shows the power in a steady state as a function of the action. The action is increased by increasing the time duration of each stroke (see top illustration in Fig. 7). The field and the thermal coupling are $\epsilon = \gamma_h = \gamma_c = 5 \times 10^{-4}$. The coupling strengths to the bath and work repository are not changed. When the engine action is large compared to $\hbar$, the engines behave very differently [Fig. 7(a)]. On the other hand, in the equivalence regime, where s is small with respect to $\hbar$, the power of all engines types converges to the same value. In the equivalence regime, the power rises quadratically with the action since the correction to the power is $s^3/\tau_{\text{cyc}} \propto \tau_{\text{cyc}}^2$. This power plateau in the equivalence regime is a manifestation of quantum interference effects (coherence in the density matrix), as will be further discussed in the next section.

The behavior of different engines for large action with respect to $\hbar$ is very rich and strongly depends on the ratio between the field and the bath coupling strength.

Finally, we comment that the same formalism and results can be extended for the case in which the drive is slightly detuned from the gap.

D. Lasing condition via the equivalence to a two-stroke engine

Laser medium can be thought of as a continuous engine where the power output is light amplification. It is well known that lasing requires population inversion. Scovil *et al.* [83] were the first to show the relation between the population inversion lasing condition and the Carnot efficiency.

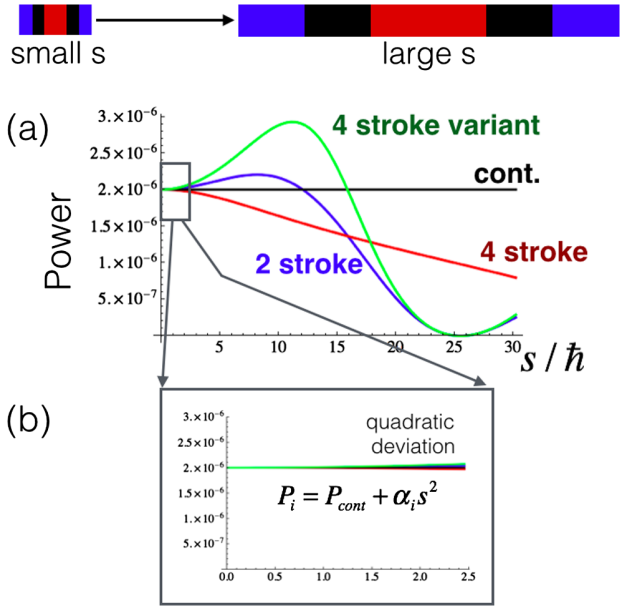

FIG. 7. Power as a function of action for various engine types in a steady state. The four-stroke variant (green line) is described in Fig. 5(d). The action is increased by increasing the stroke duration (top illustration). (a) For large action with respect to $\hbar$, the engines significantly differ in performance. In this example, all engines have the same efficiency, but they extract different amounts of heat from the hot bath. (b) In the equivalence regime where the action is small, all engine types exhibit the same power and also the same heat flows. The condition $s < \hbar/2$ that follows from the Strang decomposition agrees with the observed regime of equivalence. The time-symmetric structure of the engines causes the deviation from equivalence to be quadratic in the action.

Using the equivalence principle presented here, the most general form of the lasing condition can be obtained without any reference to light-matter interaction.

Let us start by decomposing the continuous engine into an equivalent two-stroke engine. For simplicity, it is assumed that the hot and cold manifolds have some overlap so that, in the absence of the driving field, this bath leads the system to a unique steady state ρ_0. If the driving field is tiny with respect to the thermalization rates, then the system will be very close to ρ_0 in the steady state.

To see when ρ_0 can be used for work extraction, we need to discuss passive states. A passive state is a state that is diagonal in the energy basis, and with populations that decrease monotonically with energy [99]. The energy of a passive state cannot be decreased (or work cannot be extracted from the system) by applying some unitary transformation (the Hamiltonian after the transformation is the same as it was before the transformation) [70,99]. Thus, if ρ_0 is passive, work cannot be extracted from the device, regardless of the details of the driving field (as long as it is weak and the equivalence holds).

A combination of thermal baths will lead to an energy diagonal ρ_0. Consequently, to enable work extraction,

passivity must be broken by population inversion. Therefore, we obtain the standard population inversion condition. Note that the derivation does not require an Einstein rate equation or any information on the processes of emission and absorption of photons.

Furthermore, it now becomes clear that if "coherent baths" are used [66] so that ρ_0 is no longer diagonal in the energy basis (and therefore no longer passive), it is possible to extract work even without population inversion.

In conclusion, using the equivalence principle, it is possible to import known results from work extraction in stroke schemes to continuous machines.

IV. QUANTUM-THERMODYNAMIC SIGNATURE

Can the measurements of thermodynamics quantities reveal quantum effects in heat engines? To answer this, we first need to define the corresponding classical engine.

The term "classical engine" is rather ambiguous. There are different protocols of modifying the system so that it behaves classically. To make a fair comparison to the fully quantum engine, we look for the minimal modification that satisfies the following conditions:

(1) The dynamics of the device should be fully described using population dynamics (no coherences, no entanglement).
(2) The modification should not alter the energy levels of the system, the couplings to the baths, and the coupling to the work repository.
(3) The modification should not introduce a new source of heat or work.

To satisfy the first requirement, we introduce a dephasing operator that eliminates the coherences [100] and leads to a stochastic description of the engine. Clearly, a dephasing operator satisfies the second requirement. To satisfy the third requirement, we require "pure dephasing," a dephasing in the energy basis. The populations in the energy basis are invariant to this dephasing operation. Such a natural source of energy-basis dephasing emerges if there is some scheduling noise [101]. In other words, if there is some error in the switching time of the strokes.

Let us define a "quantum-thermodynamic signature" as a signal that is impossible to produce by the corresponding classical engine as defined above.

Our goal is to derive a threshold for power output that a stochastic engine cannot exceed but a coherent quantum engine can.

Before analyzing the effect of decoherence, it is instructive to distinguish between two different work extraction mechanisms in stroke engines.

A. Coherent and stochastic work extraction mechanisms

Let us consider the work done in the work stroke of a two-stroke engine [as in Fig. 5(c)]:

$$W = \langle H_0 | e^{-i(1/2\hbar)\mathcal{H}_w\tau_w} | \tilde{\rho}\rangle - \langle H_0|\tilde{\rho}\rangle, \tag{27}$$

where τ_w is the duration of the work stroke. Writing the state as a sum of population and coherences $|\tilde{\rho}\rangle = |\tilde{\rho}_{\rm pop}\rangle + |\tilde{\rho}_{\rm coh}\rangle$, we get

$$W = \left\langle H_0 \left| \sum_{n=1} \frac{(-i\frac{1}{2\hbar}\mathcal{H}_w\tau_w)^{2n-1}}{(2n-1)!} \right| \tilde{\rho}_{\rm coh} \right\rangle + \left\langle H_0 \left| \sum_{n=1} \frac{(-i\frac{1}{2\hbar}\mathcal{H}_w\tau_w)^{2n}}{(2n)!} \right| \tilde{\rho}_{\rm pop} \right\rangle. \tag{28}$$

This result follows from the generic structure of Hamiltonians in Liouville space. Any $\mathcal{H}$ that originates from a Hermitian Hamiltonian in Hilbert space (in contrast to Lindblad operators as a source) has the structure shown in Fig. 8(b) (see Appendix A for Liouville space derivation of this property). In other words, it connects only populations to coherences and vice versa, but it cannot connect populations to populations directly [102]. In addition, since $\langle H_0|$ acts as a projection on population space, one gets that odd powers of $\mathcal{H}_w$ can only operate on coherences and even powers can only operate on populations. Thus, the power can be extracted using two different mechanisms: a coherent mechanism that operates on coherences and a stochastic mechanism that operates on populations.

The effects of the "stochastic" terms $\sum_{n=1}(-i\frac{1}{2\hbar}\mathcal{H}_w\tau_w)^{2n}/(2n)!$ on the populations are equivalently described by a single doubly stochastic operator. If there are no coherences (next section), this leads to a simple interpretation in terms of full swap events that take place with some probability.

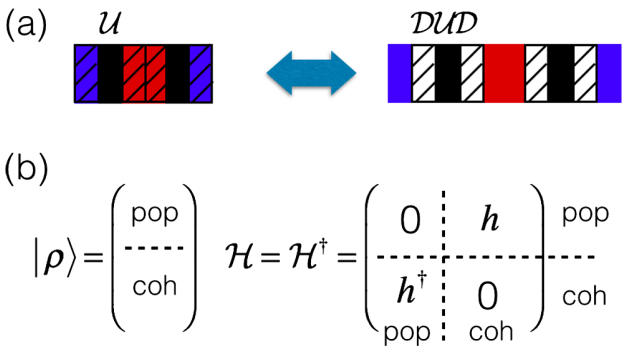

FIG. 8. Panel (a), left side: Dephasing operations (slanted line, operator $\mathcal{D}$) commute with thermal baths so the dephased engine in the left side of (a) is equivalent to the one on the right. In the new engine, the unitary evolution is replace by $\mathcal{DUD}$. If $\mathcal{D}$ eliminates all coherences, the effect of $\mathcal{DUD}$ on the populations can always be written as a doubly stochastic operator. (b) Any Hermitian Hamiltonian in Liouville space has the structure shown in (b). Thus, first-order changes in populations critically depend on the existence of coherence.

Continuous engines, on the other hand, have only a coherent work extraction mechanism. This can be seen from the expression for their work output,

$$P^{\text{cont}} = \left\langle H_0 \left| \frac{1}{2\hbar}\mathcal{H}_w \right| \tilde{\rho} \right\rangle = \left\langle H_0 \left| \frac{1}{2\hbar}\mathcal{H}_w \right| \tilde{\rho}_{\text{coh}} \right\rangle, \quad (29)$$

where again we used the population projection property of $\langle H_0|$ and the structure of $\mathcal{H}_w$ [Fig. 8(b)]. We conclude that in contrast to stroke engines, continuous engines have no stochastic work extraction mechanism. This difference stems from the fact that in continuous engines, the steady state is stationary. Consequently, there are no higher-order terms that can give rise to a population-population stochastic work extraction mechanism. This is a fundamental difference between stroke engines and continuous engines. This effect is pronounced outside the equivalence regime where the stochastic terms become important (see Sec. V).

B. Engines subjected to pure dephasing

Consider the engine shown in Fig. 8(a). The slanted lines on the baths indicate that there is an additional dephasing mechanism that takes place in parallel to the thermalization [103]. Let us denote the evolution operator of the pure dephasing by $\mathcal{D}$. In principle, to analyze the deviation from the coherent quantum engine, first the steady state has to be solved and then work and heat can be compared. Even for simple systems, this is a difficult task. Hence, we shall take a different approach and derive an upper bound for the power of stochastic engines. It is important that the bound contains only quantities that are unaffected by the level of coherence in the system. For example, the dipole expectation value, does contain information on the coherence. We construct a bound in terms of the parameters of the system (e.g., the energy levels, coupling strengths, etc.), which is independent of the state of the system. In the pure dephasing stage, the energy does not change. Hence, the total energy change in the $\mathcal{DUD}$ stage is associated with work.

Let $\mathcal{D}_{\text{comp}} = |\text{pop}\rangle\langle\text{pop}|$ be a projection operator on the population space. This operator generates a complete dephasing that eliminates all coherences. In such a case, the leading order in the work expression becomes

$$\begin{aligned} W &= \langle H_0|\mathcal{D}_{\text{comp}} e^{-i(1/2\hbar)\mathcal{H}_w\tau_w}\mathcal{D}_{\text{comp}}|\tilde{\rho}\rangle \\ &= \frac{\tau_w^2}{8\hbar^2}\langle H_0|\mathcal{H}_w^2|\tilde{\rho}_{\text{pop}}\rangle + O[(s/\hbar)^4], \end{aligned} \quad (30)$$

where we used $\langle H_0|\mathcal{D} = \langle H_0|$ and $\mathcal{D}_{\text{comp}}|\tilde{\rho}\rangle = |\tilde{\rho}_{\text{pop}}\rangle$. Since $\mathcal{D}_{\text{comp}}$ eliminates coherences, W does not contain a linear term in time. Next, by using the following relation, $\langle H_0|B|\rho\rangle \le \sqrt{\langle H_0|H_0\rangle\langle\rho|\rho\rangle}\|B\|$, $\sqrt{\langle H_0|H_0\rangle} = \sqrt{\text{tr}(H_0^2)}$, we find that for $s \ll \hbar$ the power of a stochastic engine satisfies

$$\begin{aligned} P_{\text{stoch}} &\le \frac{z}{8\hbar^2}\sqrt{tr(H_0^2) - tr(H_0)^2}\,\Delta_w^2 d^2 \tau_{\text{cyc}}, \\ z &= 1 \text{ two-stroke}, \\ z &= 1/2 \text{ four-stroke}, \end{aligned} \quad (31)$$

where Δ_w is the gap of the interaction Hamiltonian (maximal eigenvalue minus minimal eigenvalue of H_w), and d is the duty cycle—the fraction of time dedicated to work extraction ($d = \tau_w/\tau_{\text{cyc}}$, e.g., $d = 1/3$ in all the examples in this paper). We also used the fact that $\langle\rho_{\text{pop}}|\rho_{\text{pop}}\rangle$ is always smaller than the purity $\langle\rho|\rho\rangle$ and therefore smaller than 1. Note that, as we required, this bound is state independent, and the right-hand side of Eq. (31) contains no information on the coherences in the system. Thus, we conclude that for power measurements,

$$P > P_{\text{stoch}} \Rightarrow \text{quantum-thermodynamic signature}. \quad (32)$$

As shown earlier, in coherent quantum engines (in the equivalence regime), the work scales linearly with τ_{cyc} [see Eqs. (16) and (18)], and therefore, the power is constant as a function of τ_{cyc}. When there are no coherences, the power scales linearly with τ_{cyc}.

Numerical results of power as a function of cycle time are shown in Fig. 9. The power is not plotted as a function of action as before because, at the same cycle time, the coherent engine and the dephased engine have different actions. The coupling parameters are as in Fig. 7. The action of the dephased engine is

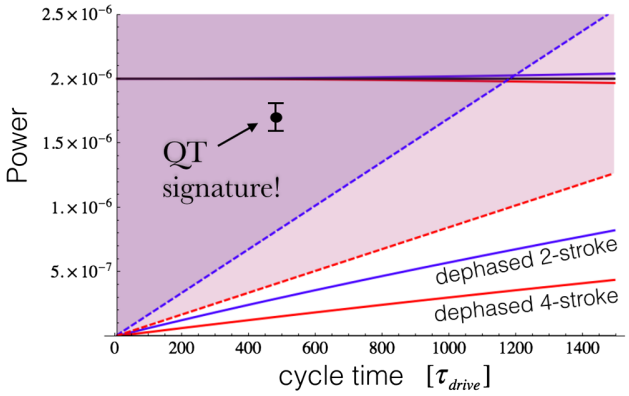

FIG. 9. The power output of the three types of engines (two-stroke blue, four-stroke red, continuous black) with and without dephasing [top horizontal solid lines are without dephasing—same as in Fig. 7(b)]. The power of the continuous dephased engine is zero. The dashed lines show the stochastic upper bounds on the power of two-stroke (dashed blue line) and four-stroke (dashed red line) engines. Any power measurement in the shaded area of each engine indicates the presence of quantum interference in the engine. This plot also demonstrates that for short cycle times (low action), coherent engines produce much more power compared to stochastic dephased engines.

$$s_{\mathrm{deph}} = \left(\|\mathcal{L}_c\| + \|\mathcal{L}_h\| + \left\| \frac{1}{2}\mathcal{H}_w \right\| + \|\mathcal{L}_{\mathrm{dephasing}}\| \right) \tau_{\mathrm{cyc}}. \tag{33}$$

If the dephasing is significant, the action is large and equivalence cannot be observed. In other words, a fully stochastic engine in a quantum system has a large action and cannot satisfy $s \ll \hbar$.

The stochastic power bounds for a two-stroke engine (dashed blue line) and for a four-stroke engine (dashed red line) define a power regime (shaded areas) that is inaccessible to fully stochastic engines. Thus, any power measurement in this regime unequivocally indicates the presence of quantum coherences in the engine.

In practice, the dephasing time may be very small but different from zero. When the cycle time is large compared to the dephasing time, the system behaves as if there is complete dephasing. If, however, the cycle time is small with respect to the decoherence time (close to the origin of Fig. 9), the power will form a plateau of finite power instead of reducing to zero.

Note that to measure power, the measurement is carried out on the work repository and not on the engine. Furthermore, the engine must operate for many cycles to reduce fluctuations in the accumulated work. To calculate the average power, the accumulated work is divided by the total operation time and compared to the stochastic power threshold (31).

Also, note that a complete dephasing would have resulted in zero power output for the continuous engine (29).

In summary, the quantum-thermodynamics signature in stroke engines can be observed in the weak action limit.

V. OVER-THERMALIZATION EFFECT IN COHERENT QUANTUM HEAT ENGINE

In all the numerical examples studied so far, the unitary action and the thermal action were roughly comparable for reasons that will soon become clear. In this section, we study some generic features that take place when the thermal action takes over.

Let us now consider the case where the unitary contribution to the action $\|\mathcal{H}_\omega\|\tau$ is small with respect to $\hbar$. All the time intervals are fixed, but we can control the thermalization rate γ (for simplicity, we assume it is the same value for both baths). Common sense suggests that increasing γ should increase the power output. At some stage, this increase will stop since the system will already reach thermal equilibrium with the bath (or baths in two-stroke engines). Yet, Fig. 10 shows that there is a very distinctive peak where an optimal coupling takes place. In other words, in some cases, less thermalization leads to more power. We call this effect over-thermalization. This effect is generic and not unique to the specific model used in the numerical simulations. The parameters used for the plot are $\epsilon = \gamma_c = \gamma_h = 2 \times 10^{-4}$, and the number of drives cycles per engine cycle is $m = 600$.

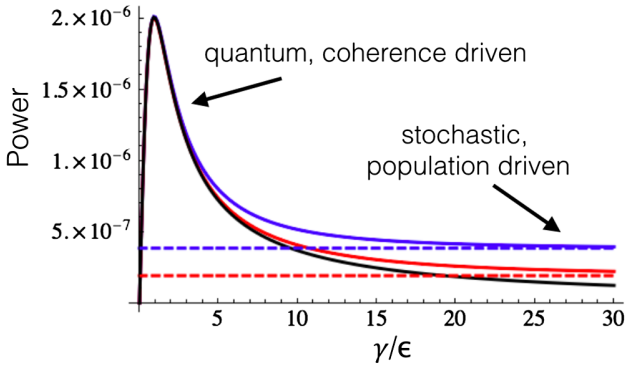

FIG. 10. The over-thermalization effect is the decrease of power when the thermalization rate is increased. Over-thermalization degrades the coherent work extraction mechanism without affecting the stochastic work extraction mechanism. When the coherent mechanism gets weak enough, the power is dominated by the stochastic power extraction mechanisms and power saturation is observed (dashed lines). The continuous engine has no stochastic work extraction mechanism, and therefore, it decays to zero without reaching saturation.

The peak and the saturation are a consequence of the interplay between the two different work extraction mechanisms (see Sec. IV A). For low γ, the coherences in the system are significant, and the leading term in the power is $\langle H_0|-i(1/2\hbar)\mathcal{H}_w|\tilde{\rho}_{\mathrm{coh}}\rangle d$ (where d is the duty cycle). In principle, all Lindblad thermalization processes are associated with some level of decoherence. This decoherence generates an exponential decay of $|\tilde{\rho}_{\mathrm{coh}}\rangle$ that explains the decay on the right-hand side of the peak. At a certain stage, the linear term becomes so small that the stochastic second-order term $-(1/8\hbar^2)\langle H_0|\mathcal{H}_w^2|\tilde{\rho}_{\mathrm{pop}}\rangle d^2\tau_{\mathrm{cyc}}$ dominates the power. $|\tilde{\rho}_{\mathrm{pop}}\rangle$ eventually saturates for large γ, and therefore, the stochastic second-order term leads to a power saturation. Interestingly, in the example shown in Fig. 10, we observe that the peak is obtained when γ and ϵ are roughly equal. Of course, what really matters is the thermal action with respect to unitary action and not just the values of the parameters γ and ϵ. We point out that this effect for a continuous engine can be seen in Fig. 3 of Ref. [20] and in Fig. 11 of Ref. [104]. In the present work, the mechanism that generates this general effect has been clarified.

If thermalization occurs faster, the thermal stroke can be shortened, and this increases the power. However, this effect is small with respect to the exponential decay of the coherences. We conclude that even without additional dephasing as in the previous section, excessive thermal coupling turns the engine into a stochastic machine. For small unitary action, this effect severely degrades the power output. The arguments presented here are valid for any small-action coherent quantum engine.

VI. CONCLUDING REMARKS

We identified coherent and stochastic work extraction mechanisms in quantum heat engines. While stroke engines have both mechanisms, continuous engines only have the coherent mechanism. We introduced the "norm action" of the engine using Liouville space and showed that when this action is small compared to $\hbar$, all three engine types are equivalent. This equivalence emerges because, for small actions, only the coherent mechanism is important. Despite the equivalence, before the engine cycle is completed, the state of the different engine type differs by $O[(s/\hbar)^1]$. This also holds true for work and heat. Remarkably, at the end of each engine cycle, a much more accurate $O[(s/\hbar)^3]$ equivalence emerges. Furthermore, the equivalence also holds for transient dynamics, even when the initial state is very far from the steady state of the engine. It was shown that, for small actions, the coherent work extraction is considerably stronger than the stochastic work extraction mechanism. This enabled us to derive a power bound for stochastic engines that constitutes a quantum-thermodynamics signature. Any power measurement that exceeds this bound indicates the presence of quantum coherence and the operation of the coherent work extraction mechanism.

Experimental schemes where the work is extracted by changing the energy levels (e.g., Refs. [53–55]) correspond to a full swap in the multilevel embedding framework. Consequently, such setups have an inherently large action, and they are not suited for demonstrating the effects presented here. In contrast, the scheme in Ref. [105] seems highly suitable. There, the unitary operation that makes a swap between superconducting qubits is generated by creating a magnetic flux through a superconducting ring. In the original paper, the authors use a flux that generates a full swap. However, by using weaker magnetic fields, the unitary operation will become a partial swap, and it should be possible to attain the small action regime where the equivalence can be observed. In addition, NV centers in diamonds also have the potential for exploring heat engine equivalence in the quantum regime.

The present derivation makes no assumption on the direction of heat flows and the sign of work. Thus, our results are equally applicable to refrigerators and heaters.

It is interesting to try and apply these concepts of equivalence and quantum-thermodynamic signatures to more general scenarios: non-Markovian baths, engines with a nonsymmetric unit cell, and engines with quantum correlation between different particles (entanglement and quantum discord). We conjecture that in multiple particle engines, entanglement will play a similar role to that of coherence in single-particle engines.

ACKNOWLEDGMENTS

This work was support by the Israeli Science Foundation. Part of this work was supported by the COST Action MP1209 "Thermodynamics in the quantum regime."

APPENDIX A: LIOUVILLE SPACE FORMULATION OF QUANTUM DYNAMICS

Quantum dynamics is traditionally described in Hilbert space. However, it is convenient, in particular, for open quantum systems, to introduce an extended space where density operators are vectors and time evolution is generated by a Schrödinger-like equation. This space is usually referred to as Liouville space [89]. We denote the "density vector" by $|\rho\rangle \in \mathbb{C}^{1\times N^2}$. It is obtained by reshaping the density matrix ρ into a larger single vector with index $\alpha \in \{1, 2, \ldots N^2\}$. The one-to-one mapping of the two matrix indices into a single vector index $\{i, j\} \to \alpha$ is arbitrary but has to be used consistently. The vector $|\rho\rangle$ is not normalized to unity, in general. Its norm is equal to the purity, $\mathcal{P} = tr(\rho^2) = \langle\rho|\rho\rangle$, where $\langle\rho| = |\rho\rangle^\dagger$ as usual. The equation of motion of the density vector in Liouville space follows from $d_t\rho_\alpha = \sum_\beta \rho_\beta \partial(d_t\rho_\alpha)/\partial\rho_\beta$. Using this equation, one can verify that the dynamics of the density vector $|r\rangle$ is governed by a Schrödinger-like equation in the new space,

$$i\partial_t|\rho\rangle = \mathcal{H}|\rho\rangle, \tag{A1}$$

where the super-Hamiltonian $\mathcal{H} \in \mathbb{C}^{N^2\times N^2}$ is given by

$$\mathcal{H}_{\alpha\beta} = i\frac{\partial(d_t\rho_\alpha)}{\partial\rho_\beta}. \tag{A2}$$

A particularly useful index mapping is described in Ref. [106] and in Ref. [90]. In this mapping, the Liouville index of $|\rho\rangle$ is related to the original row and column index of ρ via $\alpha = \mathrm{col} + N(\mathrm{row} - 1)$. For this form, $\mathcal{H}$ can be compactly written in term of the original H and A:

$$\mathcal{H} = -i(H \otimes I - I \otimes H^t) + i\sum_k \left[(A_k \otimes A_k^*) - \frac{1}{2} I \otimes (A_k^\dagger A_k)^t - \frac{1}{2} A_k^\dagger A_k \otimes I\right], \tag{A3}$$

where the superscript t stands for transposition and * for complex conjugation. $\mathcal{H} = \mathcal{H}^H + \mathcal{L}$ is non-Hermitian for open quantum systems. $\mathcal{H}^H$ originates from the Hilbert space Hamiltonian H, and $\mathcal{L}$ from the Lindblad terms. $\mathcal{H}^H$ is always Hermitian. The skew-Hermitian part $(\mathcal{L} - \mathcal{L}^\dagger)/2$ is responsible for purity changes. Yet, in Liouville space, the Lindblad operators A_k in Eq. (1) may also generate a Hermitian term $(\mathcal{L} + \mathcal{L}^\dagger)/2$. Though Hermitian in Liouville space, this term cannot be associated with a Hamiltonian in Hilbert space. If $\mathcal{L} = 0$, $\mathcal{K}$ is unitary. It is important to note that not all eigenvectors of $\mathcal{H}$ in Liouville

space can be populated exclusively. This is due to the fact that only positive ρ with unit trace are legitimate density matrices. The states that can be populated exclusively describe steady states, while others correspond to transient changes. We remind the reader that, in this paper, we use calligraphic letters to describe operators in Liouville space and ordinary letters for operators in Hilbert space. For states, however, $|A\rangle$ will denote a vector in Liouville space formed from $A_{N\times N}$ by "vec-ing" A into a column in the same procedure ρ is converted into $|\rho\rangle$.

1. Useful relations in Liouville space

In Liouville space, the standard inner product of two operators in Hilbert space $trA^\dagger B$ reads

$$trA^\dagger B = \langle A|B\rangle.$$

In particular, the purity $\mathcal{P} = \langle r|r\rangle$ is just the square of the distance from the origin in Liouville space.

A useful relation for $\mathcal{H}^H$ is

$$\mathcal{H}^H|H\rangle = \langle H|\mathcal{H}^H = 0. \tag{A4}$$

The proof is as follows:

$$\mathcal{H}^H_{ij,mn} = H_{im}\delta_{jn} - H_{nj}\delta_{im}. \tag{A5}$$

Therefore, using Eq. (A5) we get

$$\mathcal{H}^H|H\rangle = \sum_\beta \mathcal{H}^H_{\alpha\beta}H_\beta = \sum_{mn}\mathcal{H}^H_{ijmn}H_{mn} = [H,H] = 0. \tag{A6}$$

This property is highly useful. We stress that Eq. (A4) is a property of Hermitian operators in Hilbert space, where both H and $\mathcal{H}$ are well defined. A general Hermitian operator in Liouville space may not have a corresponding H in Hilbert space.

Another property that immediately follows from Eq. (A5) is

$$\mathcal{H}^H_{ii,kk} = 0. \tag{A7}$$

This corresponds to a well-known property of unitary operation. If the system starts from a diagonal density matrix, then for short times, the evolution generated by $\mathcal{H}^H$, $e^{-i\mathcal{H}^H dt} = I - i\mathcal{H}^H dt + O(dt^2)$ does not change the population in the leading order.

2. Expectation values and their time evolution in Liouville space

The expectation value of an operator in Hilbert space is $\langle A\rangle = tr(\rho A)$. Since ρ is Hermitian, the expectation value is equal to the inner product of A and ρ, and therefore,

$$\langle A\rangle = tr(\rho A) = \langle\rho|A\rangle.$$

The dynamics of $\langle A\rangle$ under the Lindblad evolution operator is

$$\frac{d}{dt}\langle A\rangle = -i\langle A|\mathcal{H}|\rho\rangle + \left\langle \rho\middle|\frac{d}{dt}A\right\rangle. \tag{A8}$$

Note that in Liouville space there is no commutator term since $\mathcal{H}$ operates on $|\rho\rangle$ just from the left. If the total Hamiltonian is Hermitian and time independent, the conservation of energy follows immediately from applying Eqs. (A8) and (A4) for $A = H$.

APPENDIX B: GEOMETRIC MEANING OF THE NORM ACTION

This appendix establishes the relation between the norm action and the path length in Liouville space. The action constitutes an upper bound on the length of the path over one cycle. The infinitesimal path dl between two states $|\rho(t+dt)\rangle$ and $|\rho(t)\rangle$ in Liouville space is given by

$$\begin{aligned} dl^2 &= \||\rho(t+dt)\rangle - |\rho(t)\rangle\|_2^2 \\ &= \langle\rho(t)|\mathcal{H}^\dagger\mathcal{H}|\rho(t)\rangle dt^2/\hbar^2 + O(dt^3), \end{aligned} \tag{B1}$$

where $\||\rho(t+dt)\rangle - |\rho(t)\rangle\|_2^2 = tr([\rho(t+dt)-\rho(t)]^2)$. Consequently, the path in Liouville space is given by

$$L = \int_0^{\tau_{\rm cyc}}\left(\frac{dl}{dt}\right)dt \le \frac{1}{\hbar}\int_0^{\tau_{\rm cyc}}\|\mathcal{H}\|\langle\rho|\rho\rangle dt, \tag{B2}$$

where we have used the property of the spectral norm $\langle\rho(t)|\mathcal{H}^\dagger\mathcal{H}|\rho(t)\rangle/\langle\rho|\rho\rangle \le \|\mathcal{H}\|_{\rm sp}^2$. Since the purity $\langle\rho|\rho\rangle$ is always smaller than 1,

$$L \le \frac{1}{\hbar}\int_0^{\tau_{\rm cyc}}\|\mathcal{H}\|dt \equiv s/\hbar. \tag{B3}$$

Thus, the path length per cycle in Liouville space is bounded by the action. For previous uses of the norm action to quantify quantum dynamics, see Refs. [107–110]. This is also true for times shorter than the cycle time $\tau_{\rm cyc}$,

$$L(\tau) = \int_0^{\tau}\left(\frac{dl}{dt}\right)dt \le s/\hbar. \tag{B4}$$

The triangle inequality implies $\||\rho(\tau)\rangle - |\rho(0)\rangle\|_2 \le L(\tau)$; therefore,

$$\max(\||\rho(\tau)\rangle - |\rho(0)\rangle\|_2) \le s/\hbar. \tag{B5}$$

Hence, the action limits the maximal state change during the cycle. For example, if the action is $10^{-3}\hbar$, the state will change by 10^{-3} at the most.

APPENDIX C: STRANG DECOMPOSITION VALIDITY

Let $\mathcal{K}$ be an operator generated by two noncommuting operators $\mathcal{A}$ and $\mathcal{B}$:

$$\mathcal{K} = e^{(\mathcal{A}+\mathcal{B})d\lambda}, \tag{C1}$$

where we use $d\lambda = dt/\hbar$ for brevity. The splitted operator is

$$\mathcal{K}_s = e^{\frac{1}{2}\mathcal{A}d\lambda} e^{\mathcal{B}d\lambda} e^{\frac{1}{2}\mathcal{A}d\lambda}. \tag{C2}$$

Our goal is to quantify the difference between $\mathcal{K}$ and $\mathcal{K}_s$, $\|\mathcal{K}_s - \mathcal{K}\|$, where $\|\cdot\|$ stands for the spectral norm. In principle, other submultiplicative matrix norms can be used (such as the Hilbert-Schmidt norm). However, the spectral norm more accurately captures aspects of quantum dynamics [108–111]. $\mathcal{K}$ can be expanded as

$$\mathcal{K} = \sum \frac{(\mathcal{A}+\mathcal{B})^n d\lambda^n}{n!}. \tag{C3}$$

$\mathcal{K}_s$, on the other hand, is

$$\begin{aligned}\mathcal{K}_s &= \sum_{k,l,m=0}^{\infty} \frac{(\mathcal{A}/2)^k d\lambda^k}{k!} \frac{\mathcal{B}^l d\lambda^l}{l!} \frac{(\mathcal{A}/2)^m d\lambda^m}{m!} \\ &= \sum_{n=0}^{\infty} \sum_{l=0}^{n} \sum_{k=0}^{n-l} \frac{(\mathcal{A}/2)^k}{k!} \frac{\mathcal{B}^l}{l!} \frac{(\mathcal{A}/2)^{n-l-k}}{(n-l-k)!} d\lambda^n. \end{aligned} \tag{C4}$$

Because of the symmetric splitting, the terms up to $n = 2$ (including $n = 2$) are identical for both operators. Therefore, the difference can be written as

$$\begin{aligned}\|\mathcal{K}_s - \mathcal{K}\| = \Bigg\| &\sum_{n=3}^{\infty} \sum_{l=0}^{n} \sum_{k=0}^{n-l} \frac{(\mathcal{A}/2)^k}{k!} \frac{\mathcal{B}^l}{l!} \frac{(\mathcal{A}/2)^{n-l-k}}{(n-l-k)!} d\lambda^n \\ &- \sum_{n=3} \frac{(\mathcal{A}+\mathcal{B})^n d\lambda^n}{n!} \Bigg\|. \end{aligned} \tag{C5}$$

Next, we apply the triangle inequality and the submultiplicativity property to get

$$\begin{aligned}\|\mathcal{K}_s - \mathcal{K}\| \le \Bigg\| &\sum_{n=3}^{\infty} \sum_{l=0}^{n} \sum_{k=0}^{n-l} \frac{\|\mathcal{A}/2\|^k}{k!} \frac{\|B\|^l}{l!} \frac{\|\mathcal{A}/2\|^{n-l-k}}{(n-l-k)!} d\lambda^n \\ &+ \sum_{n=3}^{\infty} \frac{(\|\mathcal{A}\| + \|\mathcal{B}\|)^n d\lambda^n}{n!} \Bigg\|. \end{aligned} \tag{C6}$$

Using the binomial formula two times, one finds

$$\begin{aligned}&\sum_{n=3}^{\infty} \sum_{l=0}^{n} \sum_{k=0}^{n-l} \frac{\|\mathcal{A}/2\|^k}{k!} \frac{\|\mathcal{B}\|^l}{l!} \frac{\|\mathcal{A}/2\|^{n-l-k}}{(n-l-k)!} d\lambda^n \\ &= \sum_{n=3}^{\infty} \frac{(\|\mathcal{A}\| + \|\mathcal{B}\|)^n d\lambda^n}{n!}, \end{aligned} \tag{C7}$$

and therefore,

$$\begin{aligned}\|\mathcal{K}_s - \mathcal{K}\| &\le 2 \sum_{n=3}^{\infty} \frac{(\|\mathcal{A}\| + \|\mathcal{B}\|)^n d\lambda^n}{n!} \\ &= 2R_2[(\|\mathcal{A}\| + \|\mathcal{B}\|)d\lambda]. \end{aligned} \tag{C8}$$

The right-hand side is the Taylor remainder of a power series of an exponential with $(\|\mathcal{A}\| + \|\mathcal{B}\|)d\lambda$ as an argument. The Taylor remainder formula for the exponent function is $R_k(x) = e^{\xi}(|x|^{k+1})/(k+1)!$, where $0 \le \xi \le 1$ (for now, we assume $x < 1$). Setting $k = 2$ and $\xi = 1$ (worst case), we finally obtain

$$\|\mathcal{K}_s - \mathcal{K}\| \le \frac{e}{3}[(\|A\| + \|\mathcal{B}\|)d\lambda]^3 \le \left(\frac{s}{\hbar}\right)^3, \tag{C9}$$

$$s = (\|A\| + \|\mathcal{B}\|)dt, \tag{C10}$$

where we call s the norm action of the evolution operator. To get an estimation where the leading non-neglected term of $\mathcal{K}$, $(\mathcal{A}+\mathcal{B})^2 d\lambda^2/2$, is larger than the remainder, we require that

$$(\|\mathcal{A}+\mathcal{B}\|)^2 d\lambda^2/2 \ge \left(\frac{s}{\hbar}\right)^3. \tag{C11}$$

Using the triangle inequality, we get the estimated condition for the Strang decomposition:

$$s \le \hbar/2. \tag{C12}$$

This condition explains why it was legitimate to limit the range of x to 1 in the remainder formula.

APPENDIX D: SYMMETRIC REARRANGEMENT THEOREM

The goal of this appendix is to explain why the equivalence of evolution operators leads to equivalence of work and equivalence of heat. In addition, we show why this is also valid for transients. For the equivalence of the evolution operator, we require that the super-Hamiltonian is symmetric and that the action is small:

$$\mathcal{H}(t) = \mathcal{H}(-t), \tag{D1}$$

$$s = \int_{-\tau/2}^{+\tau/2} \|\mathcal{H}\| dt \ll \hbar. \tag{D2}$$

Let the initial state at time $t = -\tau/2$ be

$$|\tilde{\rho}_i\rangle = |\tilde{\rho}(-\tau/2\rangle. \tag{D3}$$

This state leads to a final state at $\tau/2$,

$$|\tilde{\rho}_f\rangle = |\tilde{\rho}(\tau/2\rangle. \tag{D4}$$

Our goal is to evaluate a symmetric expectation value difference of the form

$$\begin{aligned} dA_{\text{tot}} &= [\langle A(t_2)\rangle - \langle A(t_1)\rangle] + [\langle A(-t_1)\rangle - \langle A(-t_2)\rangle] \\ &= [\langle A|\tilde{\rho}(t_2)\rangle - \langle A|\tilde{\rho}(t_1)\rangle] \\ &\quad + [\langle A|\tilde{\rho}(-t_1)\rangle - \langle A|\tilde{\rho}(-t_2)\rangle], \\ t_2, t_1 &\geq 0, \end{aligned} \tag{D5}$$

that is, the change in the expectation value of A in the segment $[t_1, t_2]$ and its symmetric counterpart in negative time [e.g., the green areas in Fig. 11(a)]. When A is equal to H_0, this difference will translate into work or heat. We start with the expansion

$$\begin{aligned} [\langle A(t_2)\rangle - \langle A(t_1)\rangle] &= \langle A|\mathcal{K}_{t_1\to t_2} - I|\tilde{\rho}(t_1)\rangle \\ &= \left\langle A\left|-i\mathcal{H}(t_1)\frac{\delta t}{\hbar} - \frac{1}{2}\mathcal{H}(t_1)^2\frac{\delta t^2}{\hbar^2}\right|\tilde{\rho}(t_1)\right\rangle \\ &\quad + O\left[\left(\frac{s}{\hbar}\right)^3\right]. \end{aligned} \tag{D6}$$

For the negative side, we get

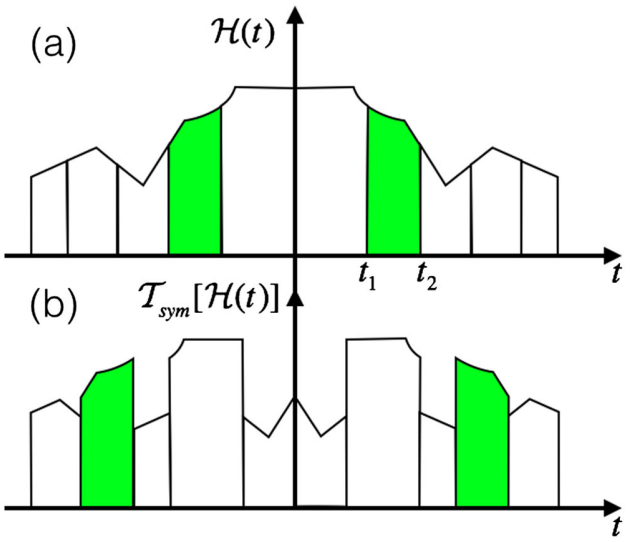

FIG. 11. The Hamiltonians in (a) and (b) are related by symmetric rearrangement of the time segments. Up to a small correction $O(s^3)$, the change in expectation values of an observable A that takes place during the green segments is the same in both cases. This effect explains why work and heat are the same in various types of engines when s is small compared to $\hbar$ (equivalence regime).

$$\begin{aligned} [\langle A(-t_1)\rangle - \langle A(-t_2)\rangle] &= \langle A|I - \mathcal{K}_{-t_1\to -t_2}|r(-t_1)\rangle \\ &= \left\langle A\left|-i\mathcal{H}(-t_1)\frac{\delta t}{\hbar} + \frac{1}{2}\mathcal{H}(-t_1)^2\frac{\delta t^2}{\hbar^2}\right|\tilde{\rho}(-t_1)\right\rangle \\ &\quad + O\left[\left(\frac{s}{\hbar}\right)^3\right]. \end{aligned} \tag{D7}$$

Next, we use the fact that

$$|\tilde{\rho}(t_1)\rangle = |\tilde{\rho}(0)\rangle - i\int_0^{t_1}\mathcal{H}(t)\frac{dt}{\hbar}|\tilde{\rho}(0)\rangle + O\left[\left(\frac{s}{\hbar}\right)^2\right], \tag{D8}$$

$$|\tilde{\rho}(-t_1)\rangle = |\tilde{\rho}(0)\rangle + i\int_0^{t_1}\mathcal{H}(t)\frac{dt}{\hbar}|\tilde{\rho}(0)\rangle + O\left[\left(\frac{s}{\hbar}\right)^2\right]. \tag{D9}$$

When adding the two segments, the second order terms cancel out and we get

$$\delta A_{\text{tot}} = -2i\langle A|\mathcal{H}(t_1)|\tilde{\rho}(0)\rangle\delta t + O\left[\left(\frac{s}{\hbar}\right)^3\right]. \tag{D10}$$

Note that the result is expressed using $|\tilde{\rho}(0)\rangle$, which is not given explicitly. To correctly relate it to $|\tilde{\rho}(-\tau/2)\rangle$, we have to use the symmetric rearrangement properties of the evolution operator.

1. Symmetric rearrangement

In Fig. 11(a), there is an illustration of some time-dependent Hamiltonian with reflection symmetry $\mathcal{H}(t) = \mathcal{H}(-t)$. We use $\mathcal{H}$ to denote a Liouville space operator which may be any unitary operation or Markovian Lindblad operation. Assume that in addition to the symmetric bins of interest (green bins), the remainder of the time is also divided into bins in a symmetric way so that there is still a reflection symmetry in the bin partitioning also. Now, we permute the bins in the positive side as desired and then make the opposite order in the negative side so that the reflection symmetry is kept. An example of such an operation is shown in Fig. 11(b). Because of the Strang decomposition, we know that the total evolution operator will stay the same under this rearrangement up to third order:

$$\mathcal{K}_{-\frac{\tau}{2}\to\frac{\tau}{2}} = \mathcal{T}_{\text{sym}}[\mathcal{K}]_{-\frac{\tau}{2}\to\frac{\tau}{2}} + O\left[\left(\frac{s}{\hbar}\right)^3\right], \tag{D11}$$

where $\mathcal{T}_{\text{sym}}[x]$ stands for evaluation of x after a symmetric reordering.

2. Symmetric rearrangement theorem

From Eq. (D11), we see that if the initial state is the same for a system described by $\mathcal{K}$, and for a system described by

$\mathcal{T}_{\rm sym}[\mathcal{K}]$, the final state at $t=\tau/2$ is the same for both systems up to a third-order correction:

$$\left|\tilde{\rho}\left(\frac{\tau}{2}\right)\right\rangle = \mathcal{T}_{\rm sym}\left[\left|\tilde{\rho}\left(\frac{\tau}{2}\right)\right\rangle\right] + O\left[\left(\frac{s}{\hbar}\right)^3\right]. \tag{D12}$$

Using Eqs. (D8) and (D9), we see that

$$|\tilde{\rho}(0)\rangle = \frac{|\tilde{\rho}(\frac{\tau}{2})\rangle + |\tilde{\rho}(-\frac{\tau}{2})\rangle}{2} + O\left[\left(\frac{s}{\hbar}\right)^2\right], \tag{D13}$$

and because of Eq. (D12), it also holds that

$$\begin{aligned}\mathcal{T}_{\rm sym}[|\tilde{\rho}(0)\rangle] &= |\tilde{\rho}(0)\rangle + O\left[\left(\frac{s}{\hbar}\right)^2\right] \\ &= \frac{|\tilde{\rho}(\frac{\tau}{2})\rangle + |\tilde{\rho}(-\frac{\tau}{2})\rangle}{2} + O\left[\left(\frac{s}{\hbar}\right)^2\right],\end{aligned} \tag{D14}$$

using this in Eq. (D10), we get

$$\delta A_{\rm tot} = -2i\langle A|\mathcal{H}(t_1)\frac{|\tilde{\rho}(\frac{\tau}{2})\rangle + |\tilde{\rho}(-\frac{\tau}{2})\rangle}{2}\delta t + O\left[\left(\frac{s}{\hbar}\right)^3\right]. \tag{D15}$$

Expression (D15) no longer depends on the position of the time segment but only on its duration and on the value of $\mathcal{H}$. Thus, the SRT states that the expression above also holds for any symmetric rearrangement,

$$dA_{\rm tot} = \mathcal{T}_{\rm sym}[dA_{\rm tot}] + O\left[\left(\frac{s}{\hbar}\right)^3\right]. \tag{D16}$$

If we replace A by H_0 and $\mathcal{H}(t_1)$ by $\mathcal{L}_c$, $\mathcal{L}_h$, or $\mathcal{H}_w$, we immediately get the invariance of heat and work to symmetric rearrangement (up to s^3). If $|\tilde{\rho}[-(\tau/2)]\rangle$ is the same for all engines, then $|\tilde{\rho}(\tau/2)\rangle$ is also the same for all engine types up to $O(s^3)$. Consequently, for all stroke engines, the expressions for work and heat are

$$W = -2i\langle H_0|\int_{t\in t_w}\mathcal{H}_w(t)\frac{dt}{\hbar}\frac{|\tilde{\rho}(\frac{\tau}{2})\rangle + |\tilde{\rho}(-\frac{\tau}{2})\rangle}{2} + O\left[\left(\frac{s}{\hbar}\right)^3\right], \tag{D17}$$

$$Q_{c(h)} = -2i\langle H_0|\int_{t\in t_{c(h)}}\mathcal{L}_{c(h)}(t)\frac{dt}{\hbar}\frac{|\tilde{\rho}(\frac{\tau}{2})\rangle + |\tilde{\rho}(-\frac{\tau}{2})\rangle}{2} + O\left[\left(\frac{s}{\hbar}\right)^3\right]. \tag{D18}$$

Using the identity $|\tilde{\rho}(\tau/2)\rangle + |\tilde{\rho}[-(\tau/2)]\rangle = |\tilde{\rho}(t)\rangle + |\tilde{\rho}(-t)\rangle + O[(s/\hbar)^2]$ that follows from Eq. (D13), the integration over time of the energy flows $j_w = \langle H_0|(1/2\hbar)\mathcal{H}_w|\tilde{\rho}(t)\rangle$ and $j_{c(h)} = \langle H_0|(1/\hbar)\mathcal{L}_{c(h)}|\tilde{\rho}(t)\rangle$ for continuous engines yields expressions (D17) and (D18) once more. This implies that the SRT (D17) and (D18) holds even if the different operations $\mathcal{L}_c$, $\mathcal{L}_h$, and $\mathcal{H}_w$ overlap with each other.

We emphasize that all the above relations hold for any initial state and not only in the steady state where $|\tilde{\rho}(\tau/2)\rangle = |\tilde{\rho}[-(\tau/2)]\rangle$. The physical implication is that in the equivalence regime, different engines are thermodynamically indistinguishable when monitored at the end of each cycle, even when the system is not in its steady state.

[1] R. Alicki, *The Quantum Open System as a Model of the Heat Engine*, J. Phys. A **12**, L103 (1979).

[2] H. Spohn, *Entropy Production for Quantum Dynamical Semigroups*, J. Math. Phys. (N.Y.) **19**, 1227 (1978).

[3] M. Campisi, P. Talkner, and P. Hänggi, *Fluctuation Theorem for Arbitrary Open Quantum Systems*, Phys. Rev. Lett. **102**, 210401 (2009).

[4] M. Campisi, P. Hänggi, and P. Talkner, *Colloquium: Quantum Fluctuation Relations: Foundations and Applications*, Rev. Mod. Phys. **83**, 771 (2011).

[5] H. T. Quan and H. Dong, *Quantum Crooks Fluctuation Theorem and Quantum Jarzynski Equality in the Presence of a Reservoir*, arXiv:0812.4955.

[6] F. L. Curzon and B. Ahlborn, *Efficiency of a Carnot Engine at Maximum Power Output*, Am. J. Phys. **43**, 22 (1975).

[7] I. Novikov, *The Efficiency of Atomic Power Stations (A Review)*, J. Nucl. Energy **7**, 125 (1958).

[8] M. Esposito, K. Lindenberg, and C. Van den Broeck, *Universality of Efficiency at Maximum Power*, Phys. Rev. Lett. **102**, 130602 (2009).

[9] R. Uzdin and R. Kosloff, *Universal Features in the Efficiency at Maximal Work of Hot Quantum Otto Engines*, Europhys. Lett. **108**, 40001 (2014).

[10] P. Salamon, J. D. Nulton, G. Siragusa, T. R. Andersen, and A. Limon, *Principles of Control Thermodynamics*, Energy **26**, 307 (2001).

[11] B. Andresen, *Current Trends in Finite-Time Thermodynamics*, Angew. Chem., Int. Ed. Engl. **50**, 2690 (2011).

[12] R. Kosloff and T. Feldmann, *A Discrete Four Stroke Quantum Heat Engine Exploring the Origin of Friction*, Phys. Rev. E **65**, 055102 (2002).

[13] F. Plastina, A. Alecce, T. J. G. Apollaro, G. Falcone, G. Francica, F. Galve, N. L. Gullo, and R. Zambrini, *Irreversible Work and Inner Friction in Quantum Thermodynamic Processes*, Phys. Rev. Lett. **113**, 260601 (2014).

[14] A. del Campo, J. Goold, and M. Paternostro, *More Bang for Your Buck: Super-Adiabatic Quantum Engines*, Sci. Rep. **4**, 6208 (2014).

[15] R. Uzdin and R. Kosloff, *The Multilevel Four-Stroke Swap Engine and Its Environment*, New J. Phys. **16**, 095003 (2014).

[16] R. Kosloff, *A Quantum Mechanical Open System as a Model of a Heat Engine*, J. Chem. Phys. **80**, 1625 (1984).

[17] E. Geva and R. Kosloff, *A Quantum Mechanical Heat Engine Operating in Finite Time. A Model Consisting of Spin Half Systems as the Working Fluid*, J. Chem. Phys. **96**, 3054 (1992).

[18] T. Feldmann and R. Kosloff, *Performance of Discrete Heat Engines and Heat Pumps in Finite Time*, Phys. Rev. E **61**, 4774 (2000).

[19] Y. Rezek and R. Kosloff, *Irreversible Performance of a Quantum Harmonic Heat Engine*, New J. Phys. **8**, 83 (2006).

[20] R. Kosloff and A. Levy, *Quantum Heat Engines and Refrigerators: Continuous Devices*, Annu. Rev. Phys. Chem. **65**, 365 (2014).

[21] U. Harbola, S. Rahav, and S. Mukamel, *Quantum Heat Engines: A Thermodynamic Analysis of Power and Efficiency*, Europhys. Lett. **99**, 50005 (2012).

[22] A. E. Allahverdyan, K. Hovhannisyan, and G. Mahler, *Optimal Refrigerator*, Phys. Rev. E **81**, 051129 (2010).

[23] N. Linden, S. Popescu, and P. Skrzypczyk, *How Small Can Thermal Machines Be? The Smallest Possible Refrigerator*, Phys. Rev. Lett. **105**, 130401 (2010).

[24] M. J. Henrich, F. Rempp, and G. Mahler, *Quantum Thermodynamic Otto Machines: A Spin-System Approach*, Eur. Phys. J. Spec. Top. **151**, 157 (2007).

[25] P. Skrzypczyk, A. J. Short, and S. Popescu, *Work Extraction and Thermodynamics for Individual Quantum Systems*, Nat. Commun. **5**, 4185 (2014).

[26] D. Gelbwaser-Klimovsky, R. Alicki, and G. Kurizki, *Work and Energy Gain of Heat-Pumped Quantized Amplifiers*, Europhys. Lett. **103**, 60005 (2013).

[27] M. Kolář, D. Gelbwaser-Klimovsky, R. Alicki, and G. Kurizki, *Quantum Bath Refrigeration Towards Absolute Zero: Challenging the Unattainability Principle*, Phys. Rev. Lett. **109**, 090601 (2012).

[28] R. Alicki, *Quantum Thermodynamics: An Example of Two-Level Quantum Machine*, Open Syst. Inf. Dyn. **21**, 1440002 (2014).

[29] H. T. Quan, Y. x. Liu, C. P. Sun, and F. Nori, *Quantum Thermodynamic Cycles and Quantum Heat Engines*, Phys. Rev. E **76**, 031105 (2007).

[30] J. Roßnagel, O. Abah, F. Schmidt-Kaler, K. Singer, and E. Lutz, *Nanoscale Heat Engine Beyond the Carnot Limit*, Phys. Rev. Lett. **112**, 030602 (2014).

[31] F. Binder, S. Vinjanampathy, K. Modi, and J. Goold, *Quantum Thermodynamics of General Quantum Processes*, Phys. Rev. E **91**, 032119 (2015).

[32] L. A. Correa, J. P. Palao, D. Alonso, and G. Adesso, *Quantum-Enhanced Absorption Refrigerators*, Sci. Rep. **4**, 3949 (2014).

[33] R. Dorner, S. R. Clark, L. Heaney, R. Fazio, J. Goold, and V. Vedral, *Extracting Quantum Work Statistics and Fluctuation Theorems by Single-Qubit Interferometry*, Phys. Rev. Lett. **110**, 230601 (2013).

[34] L. A. Correa, J. P. Palao, G. Adesso, and D. Alonso, *Performance Bound for Quantum Absorption Refrigerators*, Phys. Rev. E **87**, 042131 (2013).

[35] R. Dorner, J. Goold, C. Cormick, M. Paternostro, and V. Vedral, *Emergent Thermodynamics in a Quenched Quantum Many-Body System*, Phys. Rev. Lett. **109**, 160601 (2012).

[36] D. Gelbwaser-Klimovsky, W. Niedenzu, and G. Kurizki, *Thermodynamics of Quantum Systems under Dynamical Control*, Adv. At. Mol. Opt. Phys. **64**, 329 (2015).

[37] A. S. L. Malabarba, A. J. Short, and P. Kammerlander, *Clock-Driven Quantum Thermal Engines*, New J. Phys. **17**, 045027 (2015).

[38] M. Perarnau-Llobet, K. V. Hovhannisyan, M. Huber, P. Skrzypczyk, N. Brunner, and A. Acín, *Extractable Work from Correlations*, arXiv:1407.7765v2.

[39] D. Segal and A. Nitzan, *Molecular Heat Pump*, Phys. Rev. E **73**, 026109 (2006).

[40] R. S. Whitney, *Most Efficient Quantum Thermoelectric at Finite Power Output*, Phys. Rev. Lett. **112**, 130601 (2014).

[41] M. Horodecki and J. Oppenheim, *Fundamental Limitations for Quantum and Nanoscale Thermodynamics*, Nat. Commun. **4**, 2059 (2013).

[42] L. del Rio, J. Aberg, R. Renner, O. Dahlsten, and V. Vedral, *The Thermodynamic Meaning of Negative Entropy*, Nature (London) **474**, 61 (2011).

[43] J. Gemmer, M. Michel, and G. Mahler, *Quantum Thermodynamics* (Springer, Berlin/Heidelberg, 2009).

[44] A. Riera, C. Gogolin, and J. Eisert, *Thermalization in Nature and on a Quantum Computer*, Phys. Rev. Lett. **108**, 080402 (2012).

[45] S. Trotzky, Y.-A. Chen, A. Flesch, I. P. McCulloch, U. Schollwöck, J. Eisert, and I. Bloch, *Probing the Relaxation Towards Equilibrium in an Isolated Strongly Correlated One-Dimensional Bose Gas*, Nat. Phys. **8**, 325 (2012).

[46] P. O. Boykin, T. Mor, V. Roychowdhury, F. Vatan, and R. Vrijen, *Algorithmic Cooling and Scalable NMR Quantum Computers*, Proc. Natl. Acad. Sci. U.S.A. **99**, 3388 (2002).

[47] W. S. Bakr, P. M. Preiss, M. Eric Tai, R. Ma, J. Simon, and M. Greiner, *Orbital Excitation Blockade and Algorithmic Cooling in Quantum Gases*, Nature (London) **480**, 500 (2011).

[48] J. Baugh, O. Moussa, C. A. Ryan, A. Nayak, and R. Laflamme, *Experimental Implementation of Heat-Bath Algorithmic Cooling Using Solid-State Nuclear Magnetic Resonance*, Nature (London) **438**, 470 (2005).

[49] L. J. Schulman, T. Mor, and Y. Weinstein, *Physical Limits of Heat-Bath Algorithmic Cooling*, Phys. Rev. Lett. **94**, 120501 (2005).

[50] F. Rempp, M. Michel, and G. Mahler, *Cyclic Cooling Algorithm*, Phys. Rev. A **76**, 032325 (2007).

[51] J. Goold, M. Huber, A. Riera, L. del Rio, and P. Skrzypzyk, *The Role of Quantum Information in Thermodynamics—A Topical Review*, arXiv:1505.07835.

[52] S. Vinjanampathya and J. Anders, *Quantum Thermodynamics*, arXiv:1508.06099.

[53] O. Abah, J. Rossnagel, G. Jacob, S. Deffner, F. Schmidt-Kaler, K. Singer, and E. Lutz, *Single-Ion Heat Engine at Maximum Power*, Phys. Rev. Lett. **109**, 203006 (2012).

[54] A. Dechant, N. Kiesel, and E. Lutz, *All-Optical Nanomechanical Heat Engine*, Phys. Rev. Lett. **114**, 183602 (2015).

[55] K. Zhang, F. Bariani, and P. Meystre, *Quantum Optomechanical Heat Engine*, Phys. Rev. Lett. **112**, 150602 (2014).

[56] A. Mari and J. Eisert, *Cooling by Heating: Very Hot Thermal Light Can Significantly Cool Quantum Systems*, Phys. Rev. Lett. **108**, 120602 (2012).

[57] D. Venturelli, R. Fazio, and V. Giovannetti, *Minimal Self-Contained Quantum Refrigeration Machine Based on Four Quantum Dots*, Phys. Rev. Lett. **110**, 256801 (2013).

[58] M. Lostaglio, K. Korzekwa, D. Jennings, and T. Rudolph, *Quantum Coherence, Time-Translation Symmetry, and Thermodynamics*, Phys. Rev. X **5**, 021001 (2015).

[59] M. Lostaglio, D. Jennings, and T. Rudolph, *Description of Quantum Coherence in Thermodynamic Processes Requires Constraints Beyond Free Energy*, Nat. Commun. **6**, 6383 (2015).

[60] P. Kammerlander and J. Anders, *Quantum Measurement and Its Role in Thermodynamics*, arXiv:1502.02673.

[61] M. T. Mitchison, M. P. Woods, J. Prior, and M. Huber, *Coherence-Assisted Single-Shot Cooling by Quantum Absorption Refrigerators*, arXiv:1504.01593.

[62] J. Åberg, *Catalytic Coherence*, Phys. Rev. Lett. **113**, 150402 (2014).

[63] F. C. Binder, S. Vinjanampathy, K. Modi, and J. Goold, *Quantacell: Powerful Charging of Quantum Batteries*, New J. Phys. **17**, 075015 (2015).

[64] K. Korzekwa, M. Lostaglio, J. Oppenheim, and D. Jennings, *The Extraction of Work from Quantum Coherence*, arXiv:1506.07875.

[65] S. Rahav, U. Harbola, and S. Mukamel, *Heat Fluctuations and Coherences in Quantum Heat Engines*, Phys. Rev. A **86**, 043843 (2012).

[66] M. O. Scully, M. S. Zubairy, G. S. Agarwal, and H. Walther, *Extracting Work from a Single Heat Bath via Vanishing Quantum Coherence*, Science **299**, 862 (2003).

[67] M. O. Scully, K. R. Chapin, K. E. Dorfman, M. Barnabas Kim, and A. Svidzinsky, *Quantum Heat Engine Power Can Be Increased by Noise-Induced Coherence*, Proc. Natl. Acad. Sci. U.S.A. **108**, 15097 (2011).

[68] M. Campisi, J. Pekola, and R. Fazio, *Nonequilibrium Fluctuations in Quantum Heat Engines: Theory, Example, and Possible Solid State Experiments*, New J. Phys. **17**, 035012 (2015).

[69] Other types of engines consist of small variations and a combination of these types.

[70] R. Alicki and M. Fannes, *Entanglement Boost for Extractable Work from Ensembles of Quantum Batteries*, Phys. Rev. E **87**, 042123 (2013).

[71] K. V. Hovhannisyan, M. Perarnau-Llobet, M. Huber, and A. Acín, *Entanglement Generation Is Not Necessary for Optimal Work Extraction*, Phys. Rev. Lett. **111**, 240401 (2013).

[72] M. Campisi, *Fluctuation Relation for Quantum Heat Engines and Refrigerators*, J. Phys. A **47**, 245001 (2014).

[73] G. Gennaro, G. Benenti, and G. Massimo Palma, *Entanglement Dynamics and Relaxation in a Few-Qubit System Interacting with Random Collisions*, Europhys. Lett. **82**, 20006 (2008).

[74] G. Gennaro, G. Benenti, and G. Massimo Palma, *Relaxation Due to Random Collisions with a Many-Qudit Environment*, Phys. Rev. A **79**, 022105 (2009).

[75] T. Rybár, S. N. Filippov, M. Ziman, and V. Bužek, *Simulation of Indivisible Qubit Channels in Collision Models*, J. Phys. B **45**, 154006 (2012).

[76] M. Ziman, P. Štelmachovič, and V. Bužek, *Description of Quantum Dynamics of Open Systems Based on Collision-like Models*, Open Syst. Inf. Dyn. **12**, 81 (2005).

[77] R. Kosloff, *Quantum Thermodynamics: A Dynamical Viewpoint*, Entropy **15**, 2100 (2013).

[78] J. Anders and V. Giovannetti, *Thermodynamics of Discrete Quantum Processes*, New J. Phys. **15**, 033022 (2013).

[79] H.-P. Breuer and F. Petruccione, *Open Quantum Systems* (Oxford University Press, Oxford, 2002).

[80] R. Kosloff and T. Feldmann, *Optimal Performance of Reciprocating Demagnetization Quantum Refrigerators*, Phys. Rev. E **82**, 011134 (2010).

[81] This is, of course, not true for the work repository.

[82] A. E. Allahverdyan, K. Hovhannisyan, and G. Mahler, *Optimal Refrigerator*, Phys. Rev. E **81**, 051129 (2010).

[83] H. E. D. Scovil and E. O. Schulz-DuBois, *Three-Level Masers as Heat Engines*, Phys. Rev. Lett. **2**, 262 (1959).

[84] E. Geva and R. Kosloff, *The Quantum Heat Engine and Heat Pump: An Irreversible Thermodynamic Analysis of the Three-Level Amplifier*, J. Chem. Phys. **104**, 7681 (1996).

[85] A. Levy and R. Kosloff, *The Local Approach to Quantum Transport May Violate the Second Law of Thermodynamics*, Europhys. Lett. **107**, 20004 (2014).

[86] G. Lindblad, *On the Generators of Quantum Dynamical Semigroups*, Commun. Math. Phys. **48**, 119 (1976).

[87] V. Gorini, A. Kossakowski, and E. C. G. Sudarshan, *Completely Positive Dynamical Semigroup of n-Level System*, J. Math. Phys. (N.Y.) **17**, 821 (1976).

[88] E. B. Davies, *Markovian Master Equations*, Commun. Math. Phys. **39**, 91 (1974).

[89] S. Mukamel, *Principles of Nonlinear Optical Spectroscopy* (Oxford University Press, New York, 1995), Vol. 29.

[90] H. O. R. N. Roger and R. J. Charles, *Topics in Matrix Analysis* (Cambridge University Press, Cambridge, England, 1994).

[91] T. F. Havel, *Robust Procedures for Converting Among Lindblad, Kraus and Matrix Representations of Quantum Dynamical Semigroups*, J. Math. Phys. (N.Y.) **44**, 534 (2003).

[92] E. Andersson, J. D. Cresser, and M. J. W. Hall, *Finding the Kraus Decomposition from a Master Equation and Vice Versa*, J. Mod. Opt. **54**, 1695 (2007).

[93] A. Rivas, A. D. K. Plato, S. F. Huelga, and M. B. Plenio, *Markovian Master Equations: A Critical Study*, New J. Phys. **12**, 113032 (2010).

[94] This can be seen by following the derivation in Ref. [79] and using the formalism introduced in Ref. [106].

[95] T. Jahnke and C. Lubich, *Error Bounds for Exponential Operator Splittings*, BIT Numerical Math. **40**, 735 (2000).

[96] M. D. Feit, J. A. Fleck, and A. Steiger, *Solution of the Schrödinger Equation by a Spectral Method*, J. Comput. Phys. **47**, 412 (1982).

[97] H. De Raedt, *Product Formula Algorithms for Solving the Time Dependent Schrödinger Equation*, Comput. Phys. Rep. **7**, 1 (1987).

[98] S. Blanes and F. Casas, *On the Necessity of Negative Coefficients for Operator Splitting Schemes of Order Higher than Two*, Applied Numerical Mathematics **54**, 23 (2005).
[99] A. E. Allahverdyan, R. Balian, and Th. M. Nieuwenhuizen, *Maximal Work Extraction from Finite Quantum Systems*, Europhys. Lett. **67**, 565 (2004).
[100] For simplicity, we think of a single-particle engine. Thus, entanglement and spin statistics are irrelevant quantum effects. In addition, in the weak system-bath coupling limit, the entanglement to the baths is negligible.
[101] T. Feldmann and R. Kosloff, *Quantum Lubrication: Suppression of Friction in a First-Principles Four-Stroke Heat Engine*, Phys. Rev. E **73**, 025107(R) (2006).
[102] This is very well known in the context of the Zeno effect.
[103] In the Lindblad framework, any thermalization is intrinsically associated with some dephasing. Yet, here we assume an additional controllable dephasing mechanism.
[104] E. Geva and R. Kosloff, *The Three-level Quantum Amplifier as a Heat Engine: A Study in Finite-Time Thermodynamics*, Phys. Rev. E **49**, 3903 (1994).
[105] A. O. Niskanen, Y. Nakamura, and J. P. Pekola, *Information Entropic Superconducting Microcooler*, Phys. Rev. B **76**, 174523 (2007).
[106] S. Machnes and M. B. Penio, *Surprising Interactions of Markovian Noise and Coherent Driving*, arXiv: 1408.3056v1.
[107] D. A. Lidar, P. Zanardi, and K. Khodjasteh, *Distance Bounds on Quantum Dynamics*, Phys. Rev. A **78**, 012308 (2008).
[108] R. Uzdin and O. Gat, *Time-Energy Trade-off in Unambiguous-State-Discrimination Positive Operator-Valued Measures*, Phys. Rev. A **88**, 052327 (2013).
[109] R. Uzdin, E. Lutz, and R. Kosloff, *Purity and Entropy Evolution Speed Limits for Open Quantum Systems*, arXiv:1408.1227.
[110] R. Uzdin, *Resources Needed for Non-unitary Quantum Operations*, J. Phys. A **46**, 145302 (2013).
[111] R. Uzdin, U. Günther, S. Rahav, and N. Moiseyev, *Time-Dependent Hamiltonians with 100% Evolution Speed Efficiency*, J. Phys. A **45**, 415304 (2012).

Appendix C

Quantum Heat Machines Equivalence, Work Extraction beyond Markovianity, and Strong Coupling via Heat Exchangers

entropy

MDPI

Article

Quantum Heat Machines Equivalence, Work Extraction beyond Markovianity, and Strong Coupling via Heat Exchangers

Raam Uzdin *, Amikam Levy and Ronnie Kosloff

Fritz Haber Research Center for Molecular Dynamics, Hebrew University of Jerusalem, Jerusalem 9190401, Israel; amikamlevy@gmail.com (A.L.); kosloff1948@gmail.com (R.K.)

* Correspondence: raam@mail.huji.ac.il

Academic Editor: Jay Lawrence

Received: 3 March 2016; Accepted: 31 March 2016; Published: 6 April 2016

Abstract: Various engine types are thermodynamically equivalent in the quantum limit of small "engine action". Our previous derivation of the equivalence is restricted to Markovian heat baths and to implicit classical work repository (e.g., laser light in the semi-classical approximation). In this paper, all the components, baths, batteries, and engines, are explicitly taken into account. To neatly treat non-Markovian dynamics, we use mediating particles that function as a heat exchanger. We find that, on top of the previously observed equivalence, there is a higher degree of equivalence that cannot be achieved in the Markovian regime. Next, we focus on the quality of the battery charging process. A condition for positive energy increase and zero entropy increase (work) is given. Moreover, it is shown that, in the strong coupling regime, it is possible to super-charge a battery. With super-charging, the energy of the battery is increased while its entropy is being reduced at the same time.

Keywords: quantum heat engines; quantum refrigerators; quantum thermodynamics; heat exchanger; engine equivalence; two-stroke; four-stroke; non-Markovian; strong coupling

1. Introduction

All heat engines, classical and quantum, extract work from heat flows between at least two heat baths. When the working fluid is very small and quantum , e.g., just a single particle, the dynamics of the engine can be very different from that of classical engines [1,2]. Nonetheless, some classical thermodynamic restrictions are still valid. For example, quantum heat engines are limited by the Carnot efficiency even when the dynamics is quantum. Today, it is fairly well understood why the Clausius inequality originally conceived for steam engines still holds for small quantum heat machines.

The field of quantum thermodynamics has been intensively studied in recent years. The main research directions are the study of quantum heat machines, thermodynamic resource theory, and the emergence of thermal states. See the recent reviews [3–5] and references therein for more information on these research directions.

The study of quantum heat machines dates back to [6] where it was shown that the lasing condition for a system pumped by two heat baths corresponds to the transition from a refrigerator to an engine. See [7,8] for a more detailed analysis of such systems. Since then, various types of heat machines have been studied: reciprocating, continuous, autonomous and non autonomous, four-stroke machines, two-stroke machines, Otto engines and Carnot engines in the quantum regime. See [9–45] for a partial list on heat machine studies in recent years.

Experimentally, a single ion heat engine [46] and an NMR refrigerator [36] have already been built. Suggestions for realizations in several other quantum systems include quantum dots [47,48], superconducting devices [49–52], cold bosons [53], and optomechanical systems [34,54,55]. For other related experiments and their theoretical studies, see [56–60].

The second law was found to be valid for heat machines [9] in the weak system-bath coupling, where the Markovian dynamics is described by the Lindblad equation. In fact, the second law is consistent with quantum mechanics regardless of Markovianity as long as proper thermal baths are used [61]. One of the main challenges in this field is to find "quantum signatures" [1] in the operation of heat machines—more accurately, to find quantum signatures in *thermodynamic* quantities such as work, heat, and entropy production. Clearly, the engine itself is quantum and as such it may involve quantum features such as coherences and entanglement. The question is whether by measuring only thermodynamic quantities such as average heat or work, it is possible to distinguish between a quantum engine and a classical one.

As it turns out, there are thermodynamic effects that are purely quantum, the most relevant to this work is the equivalence of heat machine types [1]. Other quantum thermodynamic effects include extraction of work from coherences [62], oscillation in cooling [2], and multiparticle statistics effects [63]. In resource theory, it seems that quantum coherences in the energy basis also play an important role and impose restrictions on the possible single shot dynamics [64,65].

The traditional models and analysis of quantum heat machines resemble that of laser physics in the semi classical approximation. The driving field is often modeled by a classical electromagnetic field. This field generates a time-dependent Hamiltonian so it is possible to extract pure work from the system. When the classical field is replaced by a work repository (battery) with quantum description, the dynamics become more complicated [66]. For example, for an harmonic oscillator battery, the initial state of the battery has to be fairly delocalized in energy to avoid entropy generation in the baths [30,67]. This is problematic since an oscillator always has a ground state. See [66] for a detailed account of this mechanism. In this work, we shall use multiple batteries to extract work by interacting with the engine via energy conserving unitary evolution. Interestingly, machines without classical fields have been previously studied [16,30,68]. However, the research goals in these studies are entirely different from those of the present study.

Another assumption that is almost always used in the analysis of heat machines is that of weak coupling to the bath. Weak coupling, initial product state assumption, and other approximations lead to the Lindblad equation for the description of the thermalization process. The Lindblad equation is widely used in open quantum systems and they describe very well the dynamics in many scenarios. In other scenarios, such as strong system-bath interactions, or for very short evolution times, the Lindblad equation fails [69]. In the scheme presented in this paper, we include heat exchangers. Their role is to enable non-Markovian engine dynamics while still using Markovian baths.

One of the goals of this paper is to show that heat machine equivalence goes beyond the classical field approximation, and also for very short times where the Markovian approximation does not hold.

A "stroke" of a quantum machine is defined in the following way [1]. It is an operation that takes place in a certain time segment. In addition, a stroke does not commute with the operations (strokes) that take place before or after it. This non commutativity is essential for thermodynamic machines. Without it, the system will reach a state that is compatible with all baths and batteries, and no energy flows will take place. Different machine types differ in the order of the non commuting operations. In a two-stroke machine, the first stroke generates simultaneous thermalization of two different parts of the machine (manifolds) to different temperatures. In the next stroke, a time dependent Hamiltonian couples the two manifolds and generates a unitary that reduces the energy of the system. The energy taken from the system is stored in a classical field or in a battery, and is referred to as work. In a four-stroke engine, the strokes are thermalization of the hot manifold, unitary evolution, thermalization of the cold manifold, and another unitary evolution. In the continuous machine, all terminals (baths and work repository) are connected simultaneously: hot bath, cold bath, and battery/classical field. In this paper, we shall refer to this machine as simultaneous and not continuous for reasons explained later on.

Due to the abovementioned non commutativity, different machines operate in a different manner, and, in general, their performances differ (even in cases where they have the same efficiency as in the

numerical examples in [1]) . Nonetheless, the thermodynamic equivalence principle presented in [1] states that in the quantum limit of small action, all machine types are thermodynamically equivalent. That is, they have the same work per cycle, and the same heat flows per cycle. This equivalence takes place where the operation of each stroke is very close to the identity operation. This regime is characterized by "engine action" that is small compared to $\hbar$. This does not mean low power since a small action cycle can be completed in a short time. Regardless of how close to identity the operations are, the different machine types exhibit very different dynamics (for example, the simultaneous machine does not have a pure unitary stage). Nevertheless, the equivalence principle states that all these differences disappear when looking at the *total heat or total work after an integer number of cycles*. The details of the equivalence principle will become clear as we present our results for the non-Markovian case.

The paper is organized as follows. Section 2 describes the engine and baths setup and introduces the heat exchangers. In Section 3.1, we derive the equivalence relation in the non-Markovian regime (short evolution time or strong couplings). The equivalence of heat machine types is valid when the "engine action" is small compared to $\hbar$. In Section 3.2, it is shown how to choose the initial state of the batteries in the weak action regime so that their entropy will not change in the charging process is shown. In addition, we find that, for large action, a different initial battery state is preferable. In the end of the section, it is shown that, for some initial states of the battery, the machine charges the battery with energy while reducing the entropy of the battery at the same time (super-charging). Section 3.3 shows that, in contrast to Markovian machines, it is possible to construct machines with a higher degree of equivalence. The emphasis is on the very existence of such machines, because their usefulness is presently unclear. In Section 4, we conclude the paper.

2. The Setup

We describe here the minimal model needed for extending the equivalence principle to short time dynamics beyond the Markovian approximation. However, the same logic and tools can be applied to more complicated systems with more levels or more baths. The setup studied in this paper is shown in Figure 1. Heat is transferred from the bath to the engine (black ellipse) via particles of the heat exchangers (circles on gears). In each engine cycle, the gears turn and a fresh particle enters the interaction zone (gray shaded area) where it stays until the next cycle. The engine can only interact with the particles in the interaction zone. The work repository is a stream of particles, or batteries, (green circles) that are "charged" with work by the engine. This interaction of the elements with the engine can be turned on and off as described by the periodic functions $f_k(t) = f_k(t + \tau_{cyc})$, where τ_{cyc} is the machine cycle time. Throughout the paper, we shall use the index "k" as a "terminal index" that can take the values "h", "c" or "w" that stand for hot, cold and work repository (battery), respectively. In what follows, we elaborate on the different elements in the scheme.

2.1. The Heat Exchanger and the Baths

The heat machine equivalence principle [1] calls for a small engine action, which reads in the present formalism $\|H_{ek}\|\,\tau \ll \hbar$. However, in the microscopic derivation of the Lindblad equation, a rotating wave approximation is made. The approximation is valid only if τ is large compared to the oscillation time. This implies that $\|H_{ek}\|$ has to be very small in the equivalence regime. Nevertheless, in principle, small action can be achieved with strong (or weak) coupling $\|H_{ek}\|$ and short evolution time as long as $\|H_{ek}\|\,\tau \ll \hbar$ holds. In this regime, which is the subject of this paper, the dynamics is highly non-Markovian. Non-Markovian bath dynamics is, in general, very complicated and strongly depend on the specific bath realization. Heat machines and the second law in the presence of strong coupling have been discussed in [70–72].

To overcome the complicated dynamics and *to obtain results that are universal and not bath-realization dependent, we add heat exchangers to our setup*. Heat exchangers are abundant in macroscopic heat machines. In house air conditioning, a coolant fluid is used to pump heat from the interior space to an

external cooling unit. Water in a closed system is used in car engines to transfer heat to the radiator where air can cool the water. Perhaps the simplest example is the cooling fins that are used to cool devices like computer chips. The metal strongly interacts with the chip and conduct the heat to the fins. Then, the weak coupling with the air cools the fins. The interaction with the air is weak but, due to the large surface, it accumulates into a large heat transfer that cools the chip.

In the quantum regime, heat exchangers enable the following simplifications. Firstly, they separate the system interaction scales from the bath interaction scales. The system can undergo non-Markovian dynamics with the heat exchangers while the baths can thermalize the heat exchangers using standard weak coupling Markovian dynamics. Secondly, they enable starting each engine cycle with a known environment state (the particles in the interaction zone). Most importantly, this environment state is in a product state with the system and contains no memory of previous cycles. Thirdly, it eliminates the dependence on all bath parameters except the temperature. This means that, from the point of view of the machine, all different bath realizations are equivalent. This bath parameter independence holds as long as the bath fully thermalizes the heat exchanger particles.

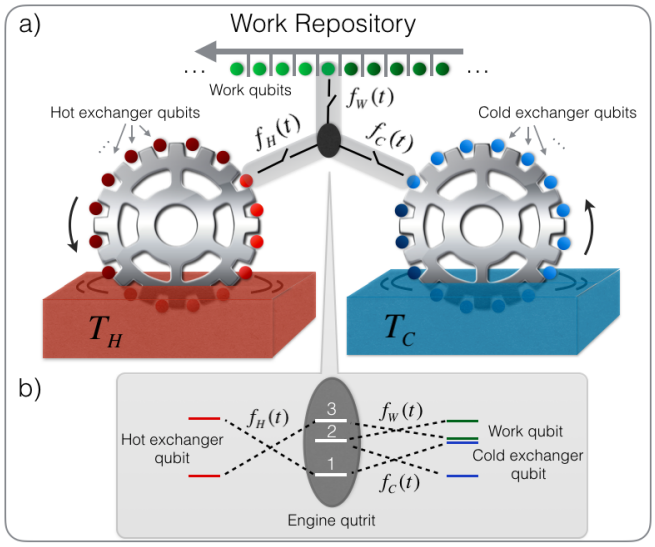

Figure 1. (**a**) heat machine scheme with heat exchangers (gears). Various engine types can be implemented in this scheme by controlling the coupling function $f_{c,h,w}(t)$ to the engine (ellipse). In each cycle, the gears turn and the work repository shifts so that new particles enter the interaction zone (gray shaded area). The heat exchangers enable the use of Markovian baths while having non-Markovian engine dynamics. This includes strong coupling and/or short time evolution. In this model, the work is stored in many batteries (work qubit in green); (**b**) the engine level diagram. This machine is based on two-body energy conserving unitaries. This is in contrast to other machines that employ three-body interaction.

In our scheme, the coolant fluids consist of N_c and N_h particles in each heat exchanger (particles around the gears in Figure 1a). The particles in the gear cyclically pass through the bath and the machine interaction zone (gray shaded area) with periods of $N_{c,h}\tau_{cyc}$. Note that the gears in Figure 1a are merely an illustration of the heat exchanger concept. The heat exchanger can be realized, for example, by adjacent superconducting qubit or by moving neutral atoms with light. The particles may interact strongly and in a non-Markovian way with the system. On the other hand, the particles interact *weakly* with the bath but for a sufficiently long time so that they fully thermalize when they leave the bath. After the exchanger particles exit the bath, they are in a thermal state and in a product state with the system (the bath removes all correlation to the machine). In each cycle of the engine, a different exchanger particle interacts with the system. $N_{c,h}$ are analogous to the size of the "cooling

fin". Their number is chosen so that within the Markovian, weak-coupling limit to the baths, for all practical purposes, they have sufficient time to fully thermalize.

Under the assumptions above, it does not matter what the exact details of the Markovian bath are (e.g., its thermalization time and correlation time). It only needs to induce thermal state via weak coupling (to avoid strong interaction issues). In this regime, the thermalization can be described by the Lindblad equation [69]. However, because of the heat exchanger full thermalization assumption, there is no need for an explicit solution.

The work repository is basically a heat exchanger without a bath. It may have a conveyor belt geometry as shown in Figure 1a, or it may be cyclic like the heat exchanger. The considerations of choosing the initial state of the batteries particles (work repository) will be discussed later.

The model can be extended by letting the system interact with more than one heat exchanger particle at a time, or by not fully thermalizing the particles. However, it seems like these types of extensions eliminate the advantages of using heat exchangers to begin with. The simple setup described above is sufficient to exemplify the equivalence principle in short time non-Markovian dynamics.

2.2. The Engine

The engine core shown in Figure 1b is a three-level system. Levels 1 and 3 constitute the hot manifold with an energy gap E_h, levels 1 and 2 constitute the cold manifold with a gap E_c, and the work manifold comprises levels 2 and 3. The more general notion of manifold separation in quantum heat machines is described in [1].

The hot (cold) manifold can interact only with the hot (cold) heat exchanger. This interaction can be switched on and off without any energetic cost as explained in the next section. The same holds for the work repository. If the engine qutrit interacts only with one heat exchanger, the hot for example, then the hot manifold of the system will eventually reach a Gibbs state at temperature T_h.

For the engine operating regime, we want the thermal strokes to create population inversion that would be used to excite the batteries to higher energies. This simple engine structure facilitates the construction of thermal machines using only two-body interactions rather than three-body interactions [16,30,68].

2.3. The Coupling of the Engine to the Heat Exchangers and to the Work Repository

In our model, the particles in the heat exchangers are all qubits. The energy gaps of the qubits in the heat exchangers are equal to the energy gaps of their corresponding manifold in the engine qutrit. As explained earlier, in each engine cycle, the heat exchanger dials turn and a new thermal particle is available to interact with the system. These exchanger particles are not initially correlated to the engine, so the initial state (in each cycle) of the particles in the engine interaction zone is $\rho_{tot}(t=0) = \rho_c \otimes \rho_h \otimes \rho_w \otimes \rho_e$ where ρ_e is the engine state and $\rho_{c,h,w}$ are the bath and work repository particles that are in the interaction zone of the system. The rest of the particles are not required until the next cycle of the machine.

The coupling between the engine and the hot bath particles has the form:

$$H_{int} = \sum_{k=c,h,w} f_k(t) H_{ek}, \tag{1}$$

where $f_k(t)$ are the controllable periodic scalar couplings (switches in Figure 1a and dashed lines in Figure 1b) introduced earlier. H_{ek} are energy conserving Hamiltonian: If H_k is the Hamiltonian of the exchanger particle and H_e is the qutrit engine Hamiltonian, then energy conserving interaction satisfies: $[H_{ek}, H_e + H_k] = 0$. This condition is the standard assumption in thermodynamic resource theory. It is used to define "thermal operations", and it ensures that energy is not exchanged with the controller that generates H_{ek}. The total energy in the exchangers, work repositories and the engine is not affected by H_{ek}. Thus, H_{ek} can only redistribute the total energy but not change it.

The simplest form of H_{int} is $H_{ek} = a_k a_{ek}^\dagger + a_k^\dagger a_{ek}$ where a_k is the annihilation operator for the k exchanger particle, and a_{ek} is the annihilation operator for hot manifold in the engine. These H_{ek} Hamiltonians generate a partial (or a full) swap between the k manifold in the machine and the terminal k. This operation is slightly more complicated than the standard partial swap as will be explained in the battery section.

In the beginning of each cycle, the engine starts in a product state with its immediate environment. This inserts a Markovianity scale to the model since there is no bath memory from cycle to cycle. Nonetheless, there are still important non-Markovian aspects in the intra-cycle dynamics. The full Markovian dynamics is obtained in the weak collision limit [73–77], where *in each thermal stroke*, the engine interacts weakly with *many particles of the heat exchanger*.

In the simultaneous machine, all the f_k are turned on and off together in order to couple the machine to different particles in the heat exchangers. Thus, the couplings are not fixed in time as in the Markovian continuous machine. While Markovian continuous machines do not have a cycle time, the simultaneous machines have a cycle time τ_{cyc} determined by the rate that particles of the heat exchangers enter the interaction zone.

2.4. The Work Repository

There are two major thermodynamic tasks: one is to produce work, and the other is to change the temperature of an object of interest. While cooling can be done either by investing work (power refrigerator) or by using only heat baths (absorption refrigerator), engines always involve the production of work. Often, the receiver of the work is not modeled explicitly. Instead, a classical field is used to drive the system and harvest the work. This is equivalent to a repository that is big and hardly changes its features due to the action of the engine.

When the work repository is modeled explicitly, various complications arise. First, the state of the battery may change significantly (especially if the battery starts close to its ground state) and therefore affect the operation of the engine (back action). Second, as entanglement starts to form between the battery and the system, the reduced state of the battery gains entropy. The energy exchange can no longer be considered as pure work. In an ideal battery, the energy increases without any accompanying entropy change. This feature is captured by the entropy pollution measure: $\Delta S / \Delta \langle E \rangle$ [78,79]. In a good battery, this number is very small and can even be negative as will be shown later.

To avoid the back action problem we will use multiple batteries. In the present scheme, it is sufficient to use qubits or qutrits. That is, instead of raising one weight by a large amount, we raise many weights just a little. In some cases, this is indeed the desired form of work. For example, an engine whose purpose is to prepare many particles with population inversion that are later used as a gain medium for a laser.

As with the heat exchanger, the batteries will be connected to the engine sequentially, one in each cycle (the $k =' \omega'$ in Equation (1)). The reduced state of a terminal particle k (may belong to the heat exchanger or to the battery) after the engine operated on it, will be denoted by $\rho_k' = tr_{\neq j}[\rho_{tot}']$. In general, after the cycle, the terminal particle may be strongly correlated to the engine.

The initial state of the battery is a key issue that dramatically affects the entropy pollution and the quality of charging the battery with work. Nevertheless, it is not directly related to the issue of heat machine equivalence so we will discuss the battery initial state only in Section 3.

2.5. Heat and Work

The heat that flows into the cold (hot) bath in one cycle is given by the change in the energy of the heat exchanger particle after one cycle:

$$Q_{c(h)}^{cycle} = tr[(U_{cyc}\rho_{tot}(0)U_{cyc}^\dagger - \rho_{tot}(0))H_{c(h)} \otimes \mathbb{1}_{else}], \tag{2}$$

where U_{cyc} is the evolution operator generated by H_{int} over one cycle of the machine. Writing this in terms of the state of the whole system, rather than using the reduced state of the bath, is very useful. To evaluate the total change in the bath energy, we need to know the global transformation over one cycle U_{cyc}. The internal dynamics, which are machine dependent, have no impact on the total heat. All engines that have the same U_{cyc} will have the same amount of heat per cycle. This is in contrast to the equivalence in the Markovian Lindblad formalism [1]. There, a symmetric rearrangement theorem had to be applied to show that the total heat per cycle is the same for different machines. In the present case, when the one cycle evolution is equivalent for different types of machines, Equation (2) immediately implies equivalence of heat and work per cycle. Equivalence of all heat and work energy flows implies that the efficiency W/Q_h is the same as well for different machine types in the equivalence regime.

As for energy exchanges with the work repository $\Delta \langle H_w \rangle$, we replace $H_{c(h)}$ by H_w in Equation (2). In order to identify it with work, it is required that no entropy is generated in the work repository.

3. Results

3.1. The Equivalence of Heat Machines in the Non-Markovian Regime

The construction of various heat machine types in the same physical system was studied in [1], and it is based on operator splitting techniques. In particular, the Strang splitting [80–82] for two non commuting operators A and B is $e^{(A+B)dt} = e^{\frac{1}{2}Adt}e^{Bdt}e^{\frac{1}{2}Adt} + O(dt^3)$. Starting with the simultaneous machine operator where all terminals are connected simultaneously:

$$\begin{aligned} \tilde{U}_{cyc}^{simul} &= e^{-i[\mathcal{H}_e + \sum\limits_{k=c,h,w} \mathcal{H}_k + \mathcal{H}_{ek}]\tau_{cyc}}, \\ &= U_0 U_{cyc}^{simul}, \qquad (3) \\ U_{cyc}^{simul} &= e^{-i[\mathcal{H}_{ec} + \mathcal{H}_{eh} + \mathcal{H}_{ew}]\tau_{cyc}}, \qquad (4) \end{aligned}$$

where $U_0 = e^{-i(\mathcal{H}_e + \mathcal{H}_c + \mathcal{H}_h + \mathcal{H}_w)\tau_{cyc}}$, the single-particle coherence evolution operator can be singled out from the total evolution operator since $[\mathcal{H}_e + \mathcal{H}_c + \mathcal{H}_h + \mathcal{H}_w, H_{int}] = 0$. All of the population change is generated by U_{cyc}^{simul} In fact, U_{cyc}^{simul} is the evolution operator in the interaction picture. Energy observables like heat look the same in the interaction picture ($U_0^\dagger H_{c,h,w} U_0 = H_{c,h,w}$). In practice, all states should be evolved with U_{cyc}^{simul} only. The bare Hamiltonians H_k are used only for calculating the energy observables. Thus, the single-particle coherences associated with interaction-free time evolution U_0 do not affect the population dynamics and observables like energy that are diagonal in the energy basis. The fact that U_0 commutes with U_{cyc}^{simul} means that outcome of the operation does not depend on the time the operation is carried out (time invariance).

This type of single-particle coherences should be distinguished from inter-particle coherences. Since the energy gaps in the machine and the terminal are matched, the inter-particle coherences are between degenerate states. For example, the states $|0_c 1_e\rangle$ and $|1_c 0_e\rangle$ are degenerate, and so are the pairs $\{|0_h 3_e\rangle, |1_h 0_e\rangle\}$ and $\{|0_w 3_e\rangle, |1_w 2_e\rangle\}$. The crossed lines in Figure 1b show the pairs of two-particle degenerate states. These inter-particle coherences are essential for the dynamics. Their complete suppression leads to a Zeno effect that halts all the dynamics in the engine. The inter-particle coherences are generated and modified by the interaction terms and hence cannot be separated from the rest of the evolution like the single-particle coherences. Note that changes in inter-particle coherence translate to population changes in the subspaces of individual particles.

When starting in a product state where the inter-particle coherences are zero, the energy transfer (population changes) is of order dt^2 while the coherence generation is of order dt. This is due to the fact that unitary transformation converts population to coherences and coherence to population (see Figure 8 in [1]). In thermodynamic resource theory, phases are often dismissed as non-essential, but we stress that this is true only for the single-particle coherences.

To study the relations between the simultaneous engine and the two-stoke engine, we apply the Strang decomposition which yields the following product form

$$\begin{aligned} U_{cyc}^{simul} &= e^{-i\mathcal{H}_{ew}\frac{\tau_{cyc}}{2}} e^{-i(\mathcal{H}_{ec}+\mathcal{H}_{eh})\tau_{cyc}} e^{-i\mathcal{H}_{ew}\frac{\tau_{cyc}}{2}} + O[(\frac{s}{\hbar})^3], \\ &= \mathcal{U}^{II\,stroke} + O[(\frac{s}{\hbar})^3], \end{aligned} \tag{5}$$

where s is the "engine norm action" $s = (\|\mathcal{H}_{ec}\|_{sp} + \|\mathcal{H}_{eh}\|_{sp} + \|\mathcal{H}_{ew}\|_{sp})\tau_{cyc}$ and $\|\cdot\|_{sp}$ is the spectral norm of the operator [1]. When this number is small compared to $\hbar$, $U_{cyc}^{II-stroke} \to U_{cyc}^{simul}$. Note that the first term and the third term in $U_{cyc}^{II-stroke}$ are two parts of the same stroke. The operator splits this way since the Strang splitting can only create symmetric units cells. A similar splitting can be done for the four-stroke engine exactly as shown in [1]. One immediate conclusion follows from the equivalence of the one cycle evolution operators: if different machine types *start in the same initial condition*, their state will coincide when monitored stroboscopically at $t_n = n\tau_{cyc}$. While at $t_n = n\tau_{cyc}$ the states of different machine types will differ by $O[(\frac{s}{\hbar})^3]$ at the most, at other times they will differ by $O[\frac{s}{\hbar}]$. This expresses the fact that the machine types are never identical at all times. They differ in the strongest order possible $O[\frac{s}{\hbar}]$, unless complete cycles are considered. Since the one cycle evolution operators are equivalent, it follows from Equation (2) that *for the same initial engine state*:

$$Q_{h(c)}^{simul} \cong Q_{h(c)}^{II\,stroke} \cong Q_{h(c)}^{IV\,stroke}, \tag{6}$$

where Q^{simul} refers to the heat transferred in time of τ_{cyc} in the particle machine. The $\cong$ stands for equality up to correction $\left\|H_{c(h)}\right\| O[(\frac{s}{\hbar})^4]$. Note that the cubic term does not appear in Equation (6). Due to lack of initial coherence, the $O[(\frac{s}{\hbar})^3]$ correction contributes only to the inter-particle coherence generation but not to population changes. Hence, the population changes differ only in order $O[(\frac{s}{\hbar})^4]$. In transients, the system energy changes from cycle to cycle so, in general, it is not correct to use energy conservation to deduce work equality from heat equality. Nevertheless, work equality follows from Equations (2) and (5) when using H_w instead of $H_{c(h)}$.

This establishes the equivalence of heat (and work) even very far away from steady state operation or thermal equilibrium *provided all engines start with the same state*. This behavior is very similar to the Markovian equivalence principle [1], but there is one major difference. Since each cycle starts in a product state, the leading order in heat and work is $O[(\frac{s}{\hbar})^2]$ and not $O[\frac{s}{\hbar}]$ as in the Markovian case. The linear term in the work originates from the single-particle coherence generated by the classical driving field. Without this coherence, the power scales as $(Q_h^{cyc} + Q_c^{cyc})/\tau_{cyc} \propto \tau_{cyc}$. Thus, as shown in Figure 2a, for small action, the power grows linearly with the cycle time. On the other hand, as explained earlier, the correction to the power is only of order $O[(\frac{s}{\hbar})^4]/\tau_{cyc} = O[(\frac{s}{\hbar})^3]$ since there is no cubic correction to the work.

Let us consider now the *steady state operation*. Despite Equation (6), it is not immediate that the heat will be the same for different machine types in steady state. In Equation (6), the initial density matrix is the same for all machine types. However, different types may have slightly different initial states, which may affect the total heat. To study equivalence in steady state operation, we first need to define what steady state means when the bath and batteries are included in the analysis. The whole system is in a continuous transient: the hot bath gets colder, the cold bath gets hotter, and the batteries are charged. Nonetheless, the reduced state of the engine relaxes to a limit cycle $\bar{\rho}_e(t) = \bar{\rho}_e(t+\tau)$ or explicitly $\bar{\rho}_e = tr_{\neq e}[U_{cyc}(\rho_c \otimes \rho_h \otimes \rho_w \otimes \bar{\rho}_e)U_{cyc}]$. To see the relation between steady states of different machines, we choose the steady state of one machine, for example $\bar{\rho}_e^{simul}$, and apply the two-stroke evolution operator to it:

$$\begin{aligned} \bar{\rho}_e' &= tr_{\neq e}[U_{cyc}^{II\,stroke}(\rho_c \otimes \rho_h \otimes \rho_w \otimes \bar{\rho}_e^{simul})U_{cyc}^{II\,stroke}] \\ &= \bar{\rho}_e^{simul} + O[(\frac{s}{\hbar})^4]. \end{aligned} \tag{7}$$

The cubic order is absent because, if there are no initial inter-particle coherences, then the cubic term only generates inter-particle coherences. Hence, the reduced state of the system is not modified by the cubic correction of the two-stroke evolution operator. From Equation (7), we conclude that the steady states are equal for both machines up to quartic corrections in the engine action. From Equation (6), it follows that heat and work in steady state are also equal in all machine types, up to quartic correction. Figure 2a shows the power in steady state for the three main types of machines as well as for a higher order six-stroke machine that will be discussed in the last section. Let the power of the machine (work per cycle divided by cycle time) be denoted by P. In Figure 2b, we plot the normalized power P/P^{simul} where it is easier to see that the correction in the power of one machine *with respect to the other* is quadratic. This graph shows that the equivalence of non-Markovian machines is actually similar to that of Markovian machines. The difference is that the reference simultaneous power is constant (in action) in the Markovian case and linearly growing (small action) in the present case. Figure 2b shows that the equivalence is a phenomenon that takes place in a regime and not only at the (ill defined) point $\tau_{cyc} = 0$. The same holds for the Markovian case.

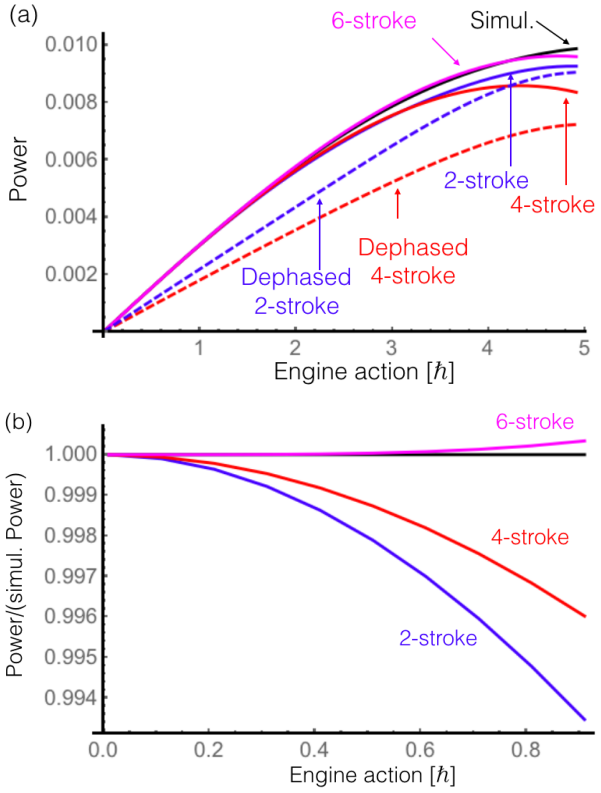

Figure 2. (**a**) In the non-Markovian regime the main machine types: four-stroke, two-stroke and simultaneous machine, have the same power when the engine action is small compared to $\hbar$. In contrast to the Markovian case here the power is not constant but grows linearly for small action. The action is increased by increasing the time duration of each stroke. The red and blue dashed curves show how the 4-stroke and 2-stroke engines are modified when a dephasing stroke is included. This demonstrates that the thermodynamic equivalence is a quantum coherence effect; (**b**) The equivalence become more visible when plotting the relative power of each machine with respect to the simultaneous machine. The 6-stroke machine, based on the Yoshida decomposition, is unique to the non-Markovian case and has a wider range of equivalence.

At this point, we wish to discuss the quantumness of the equivalence principle in the current setup. In [1], it was suggested to use dephasing in the energy basis to see if the machine is stochastic or quantum. If a dephasing stroke is carried out before the unitary stroke and the result is not affected,

then the machine operates as a stochastic machine. In the four-stroke engine and in the two-stroke engine described in Equation (5), the battery is accessed twice during the cycle. The first interaction with the battery creates some inter-particle coherence between the battery and the engine. As a result, the next interaction with the battery (the second work stroke) starts with nonzero inter-particle coherence. Thus, adding dephasing after the first work stroke will affect the power gained in the next work stroke. This is shown by the red and blue dashed curves in Figure 2a. The power of the simultaneous engine is zero if we continuously dephase the system (Zeno effect). We conclude that, although there is no coherence that carries over from one cycle to the next, as in the Markovian case, coherence is still needed for the equivalence principle to hold. This time, the coherence is an inter-particle coherence between degenerate states.

So far, we ignored the nature of the energy transferred to the battery, *i.e.*, if it is heat or work. If it is pure work, the device is an engine, whilst if it is heat, the device functions as an absorption machine (only heat bath terminals). However, the equivalence principle is indifferent to this distinction. If the action is small, two-stroke, four-stroke, and simultaneous machines will perform the same. In the next section, however, we study the conditions under which the entropy of the batteries is not increased and the device performs as a proper engine.

3.2. Work Extraction

3.2.1. The Initial State of the Battery in Strong and Weak Coupling

So far, we have not explicitly addressed the question of work extraction and whether the energy transferred to the batteries is actually pure work or heat. For engines, the goal is to make the entropy pollution $\Delta S_w / \Delta \langle H_w \rangle$ as small a possible. Figure 3 shows the well known expression for the entropy of a qubit as a function of the excited state population p_w. The von Neumann entropy and the Shannon entropy of single particles are identical since there are no single-particle coherences. The energy of the battery is proportional to the excited state population, so the x axis also indicates the energy of the battery. If the battery starts with a well defined energy state, that is the ground state $p_w = 0$, then a small increase in the energy will result in a large entropy generation in the battery. In fact, for small changes, this is the worst starting point (the origin in Figure 3). However, if we choose to start with a very hot battery at $p_w = 1/2$, ($T_w \to \infty$), the entropy increase will be very small if Δp_w is small. Thus, by using many batteries in a fully mixed state where each is only slightly changed ($\Delta p_w \ll 1$), it is possible to reach the $\Delta S_w / \Delta \langle H_w \rangle \to 0$ limit. This is in accordance with the claims that $T_w \to \infty$ limit of an absorption refrigerator, is analogous to a power refrigerator [83]. The price for this choice of the initial state of the battery is that the number of batteries diverges as $\Delta S_w / \Delta \langle H_w \rangle \to 0$.

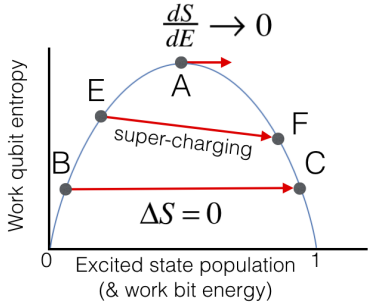

Figure 3. For infinitesimal changes (weak coupling), it is preferable to start with a battery qubit that is close to the fully mixed state (point A) where $dS/dE = 0$. For larger changes, it is preferable to generate a permutation that conserves the entropy and creates population inversion ($B \to C$ line). While $\Delta S = 0$ for the battery is analogous to classical field work repositories, in two-level batteries, it is possible to super-charge the batteries ($E \to F$) so that their energy is increased while their entropy is reduced (see also Figure 4).

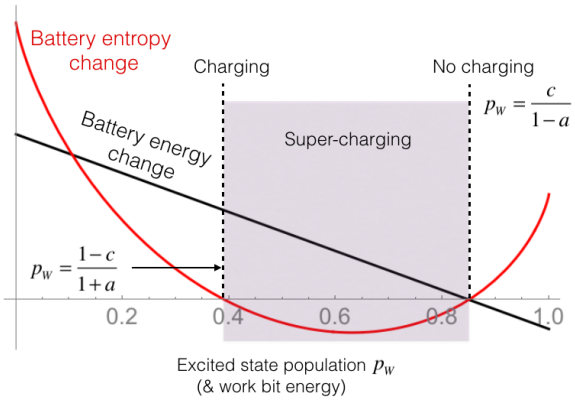

Figure 4. For a given engine, the changes in energy (**black**) and entropy (**red**) of the battery are plotted as a function of the initial excited state probability p_w of the battery. a, b and c are the population of levels 1–3 of the engine just before the interaction with the battery starts. The shaded area shows the super-charging regime where the battery is not only charged but also purified. This can only be done by strong interaction between the engine and the battery. The left border corresponds to regular charging where the energy is increased but the entropy of the battery remains the same.

In the semi-classical field approximation, the field generates a unitary operation that does not change the entropy of the system. This is often addressed as pure work as there is no entropy change in the system. However, when modeling the classical field explicitly, one finds that the source of the classical field actually gains some entropy. To counter this effect, the battery has to be prepared in a special state [30,67] or a feedback scheme must be applied [84]. Here, we suggest doing the exact opposite and applying an interaction that will generate a unitary transformation on the battery but will generate some entropy in the engine. Consider Point B in Figure 3, a full swap to Point C will increase the energy but will leave the entropy fixed. In general, this will *increase the entropy of the machine*. Let the initial state of the engine be $\rho_e = diag\{a, b, c\}$ and the initial state of the work qubit be $\rho_w = diag\{1 - p_w, p_w\}$. After a *full swap* interaction we get:

$$\begin{pmatrix} a & & \\ & b & \\ & & c \end{pmatrix}_e, \begin{pmatrix} 1-p_w & \\ & p_w \end{pmatrix}_w \rightarrow \begin{pmatrix} a & & \\ & (1-a)(1-p_w) & \\ & & (1-a)p_w \end{pmatrix}_e, \begin{pmatrix} b+a(1-p_w) & 0 \\ 0 & c+ap_w \end{pmatrix}_w. \quad (8)$$

If $a = 0$, a regular full swap takes place between levels 2 and 3 of the engine and levels 1 and 2 of the battery. If $a = 1$, there is no population in level 2&3 so nothing happens and levels 1&2 of the battery remain unchanged. This rule follows from the condition that guarantees energy conservation $\rho'_e - \rho_e = -(\rho'_w - \rho_w)$. Any population change in one particle must be compensated by an opposite change in the other particle (the energy levels are equal in our model). Now, we demand that this transformation of the battery will generate a full swap, that is $\rho'_w = diag\{p_w, 1 - p_w\}$. This leads to the condition $c + ap_w = 1 - p_w$ or

$$p_w = \frac{1-c}{1+a}. \quad (9)$$

Note that p_w defines a temperature through the Gibbs factor: $p_w/(1-p_w) = exp(-E_w/T_w)$. After the full swap, the temperature of levels 2&3 of the engine, is now T_w. It is simple to show from the positivity of the quantum mutual information that the entropy of the engine has increased. This entropy increase is associated with the formation of correlation (for the full swap it is strictly classical). When the total population on the subspace of interest on both sides is not equal (e.g., $a \neq 0$ in the example above), classical correlation forms. If the engine is measured, the marginal distribution of the battery changes. Another way to see the presence of correlation is the following. The unitary conserves the total entropy. However, the entropy of the reduced state of the battery does not change while the reduced entropy of the engine does change. This implies that the mutual information is larger than zero. This classical correlation formation can be avoided by replacing the qubit batteries with qutrit batteries whose initial state is $\rho_w = diag\{a, c, b\}$ (note the flip of b and c). In this case, the full swap operation will not generate any correlation between the engine and the battery.

The full swap is a strong coupling operation. Here, strong coupling was used to make a more efficient battery charging mechanism compared to the $T_w \to \infty$ alternative in the weak coupling limit.

3.2.2. Beyond the Semi-Classical Limit of the Driving Field

When the work repository can be described by a classical field, no entropy accounting is carried out for the work repository. However, for an explicit battery the possible changes in the entropy of the battery have to be studied. In this subsection, it is shown that these changes can actually be useful. As illustrated in the $E \to F$ trajectory in Figure 3, it is possible to increase the energy while reducing the entropy. We name this process "super-charging". In a *regular* charging, the energy increases but the entropy of the battery remains fixed. This corresponds to executing a unitary operation on the battery. In sub-charging, the energy is increased but so is the entropy. Heat flow to a thermal bath in the weak system-bath coupling limit is an example of sub-charging. Strictly speaking, in super-charging, the machine does not exactly correspond to an engine, since the energy change in the battery is associated with an entropy change as well. Nevertheless, this change in entropy is a welcomed one, as entropy reduction is hard to achieve and often requires some additional resources. In Figure 4, we show an explicit example for an initial engine state with populations $\{a, b, c\} = \{0.056, 0.074, 0.4\}$ as a function of the initial exited state population of the battery p_w. The shaded area corresponds to super-charging. The left boundary of the shaded regime corresponds to regular charging and is given by the $dS = 0$ condition Equation (9). The right boundary is given by the condition $\Delta E = 0$. Using Equation (8) $\Delta E = 0$ leads to the right boundary condition $p_w = c/1 - a = c/(b + c)$. This condition means that population ratio in the engine qutrit and in the battery is the same. Hence, nothing happens when the swap is carried out. This zero change in population also leads to $\Delta S = 0$ at this point.

3.3. Higher Order Splittings

The regime of equivalence studied in Section 3.1 and in [1] is determined by the use of the Strang decomposition for the evolution operator. Although higher order decompositions do exist, they involve coefficients with alternating signs [85]. In the Markovian case, this is not physical since a bath that generates evolution of the form $\exp(-\mathcal{L}t)$ is not physical (where $\exp(+\mathcal{L}t)$ is the standard Lindblad evolution). In the present paper, instead of non unitary evolution of the reduced state of the engine, we consider the global evolution operator of all the components. The global evolution is unitary and its generators, the interaction Hamiltonian, are all Hermitian. Hence, there is no problem to have for example $\exp(+iH_{ec}t)$ instead of $\exp(-iH_{ec}t)$. It simply means an interaction term with opposite sign. This facilitates the use of higher order decompositions in order to make machines with more strokes and a larger regime of equivalence.

In [86], Yoshida introduced a very elegant method to construct higher order decompositions. Let $U_{s^2}(t) = U^{simul}(t) + O[(\frac{s}{\hbar})^4]$ stand for an evolution operator that has a correction of order s^3 with

respect to $U^{simul}(t)$. It can be, for example, a four-stroke or two-stroke engine. As shown in [86], a fourth order evolution operator $U_{s^4}(t)$ can be constructed from $U_{s^2}(t)$ in the following way:

$$\begin{aligned} U_{s^4}(t) &= U_{s^4}(x_1 t) U_{s^4}(x_0 t) U_{s^4}(x_1 t), \\ \{x_0, x_1\} &= \{\frac{-2^{1/3}}{1-2^{1/3}}, \frac{1}{1-2^{1/3}}\}, \end{aligned} \tag{10}$$

where $U_{s^4}(t) = U^{simul}(t) + O[(\frac{s}{\hbar})^5]$. By applying the same arguments as before, when the cycle starts with fresh uncorrelated bath and battery particles, the correction to the work and heat are $O[(\frac{s}{\hbar})^6]$. The Yoshida method is powerful since it can be repeated, with different x_0, x_1 coefficients, to gain operators that are even closer to the simultaneous machine. Physically, Equation (10) can be interpreted as a regular $U_{s^2}(t)$ machine where the stroke durations alternate every cycle. Figure 2b shows the ratio of the power of various engines with respect to the simultaneous engine. While in the Strang four-stroke and two-stroke machine, the *power* deviation from the simultaneous machine is second order in the action, the power of the Yoshida engine of order four deviates from the simultaneous machine only in the fourth order in the action.

Two-stroke and four-stroke engines naturally emerge from practical considerations. Two-stroke engines emerge when it is easier to thermalize simultaneously the hot and cold manifolds. Four-stroke engines emerge when it is easier to thermalize one manifold at a time. In contrast, the Yoshida decomposition Equation (10) does not split the simultaneous engine into more basic or simpler operations compared to the two-stroke and four-stroke machines. Thus, the practical motivation for actually constructing Yoshida-like higher order machines is not obvious at all at this point. Nevertheless, our main point in this context is that higher order machines are forbidden in Markovian dynamics and are allowed in the non-Markovian machines studied here.

4. Conclusions

It has been demonstrated that the principle of thermodynamic equivalence of heat machine types is valid beyond Markovianity. We find higher order equivalence relations that do not exist in the Markovian regime. In addition, it was shown that the strong coupling limit enables delivery of finite work to the battery without increasing its entropy. It also enables charging and reducing the entropy of the battery at the same time. In our setup, we introduced heat exchangers to mediate between the machine and the baths. Heat exchangers significantly simplify the analysis, but they also have a significant practical value. They remove the strong dependence on the finer properties of the baths and allow more flexible machine operating regimes while still using a simple Markovian bath.

Acknowledgments: This work was supported by the Israeli science foundation. Part of this work was supported by the COST Action MP1209 "Thermodynamics in the quantum regime". Raam Uzdin cordially thanks the support of the Kenneth Lindsay trust fund.

Author Contributions: All authors contributed equally. All authors have read and approved the final manuscript.

Conflicts of Interest: The authors declare no conflict of interest.

References

1. Uzdin, R.; Levy, A.; Kosloff, R. Equivalence of Quantum Heat Machines, and Quantum-Thermodynamic Signatures. *Phys. Rev. X* **2015**, *5*, 031044.
2. Mitchison, M.T.; Woods, M.P.; Prior, J.; Huber, M. Coherence-assisted single-shot cooling by quantum absorption refrigerators. *New J. Phys.* **2015**, *17*, 115013, doi:10.1088/1367-2630/17/11/115013.
3. Goold, J.; Huber, M.; Riera, A.; del Rio, L.; Skrzypczyk, P. The role of quantum information in thermodynamics—A topical review. *J. Phys. A Math. Theor.* **2016**, *49*, 143001.
4. Vinjanampathy, S.; Anders, J. Quantum Thermodynamics. **2013**, doi:10.3390/e15062100.
5. Millen, J.; Xuereb, A. Perspective on quantum thermodynamics. *New J. Phys.* **2016**, *18*, 011002.
6. Scovil, H.E.D.; Schulz-DuBois, E.O. Three-Level Masers as Heat Engines. *Phys. Rev. Lett.* **1959**, *2*, 262–263.

7. Geva, E.; Kosloff, R. The Three-Level Quantum Amplifier as a Heat Engine: A Study in Finite-Time Thermodynamics. *Phys. Rev. E* **1994**, *49*, 3903–3918.
8. Geva, E.; Kosloff, R. The Quantum Heat Engine and Heat Pump: An Irreversible Thermodynamic Analysis of the Three-Level Amplifier. *J. Chem. Phys.* **1996**, *104*, 7681–7698.
9. Alicki, R. The quantum open system as a model of the heat engine. *J. Phys A Math. Gen.* **1979**, *12*, L103, doi:10.1088/0305-4470/12/5/007.
10. Kosloff, R. A Quantum Mechanical Open System as a Model of a Heat Engine. *J. Chem. Phys.* **1984**, *80*, 1625–1631.
11. Feldmann, T.; Kosloff, R. Performance of Discrete Heat Engines and Heat Pumps in Finite Time. *Phys. Rev. E* **2000**, *61*, 4774–4790.
12. Rezek, Y.; Kosloff, R. Irreversible performance of a quantum harmonic heat engine. *New J. Phys.* **2006**, *8*, 83, doi:10.1088/1367-2630/8/5/083.
13. Kosloff, R.; Levy, A. Quantum Heat Engines and Refrigerators: Continuous Devices. *Annu. Rev. Phys. Chem.* **2014**, *65*, 365–393.
14. Harbola, U.; Rahav, S.; Mukamel, S. Quantum heat engines: A thermodynamic analysis of power and efficiency. *Euro. Phys. Lett.* **2012**, *99*, 50005, doi:10.1209/0295-5075/99/50005.
15. Allahverdyan, A.E.; Hovhannisyan, K.; Mahler, G. Optimal refrigerator. *Phys. Rev. E* **2010**, *81*, 051129.
16. Linden, N.; Popescu, S.; Skrzypczyk, P. How Small Can Thermal Machines Be? The Smallest Possible Refrigerator. *Phys. Rev. Lett.* **2010**, *105*, 130401.
17. Henrich, M.J.; Rempp, F.; Mahler, G. Quantum thermodynamic Otto machines: A spin-system approach. *Eur. Phys. J.* **2005**, *151*, 157–165.
18. Skrzypczyk, P.; Short, A.J.; Popescu, S. Work extraction and thermodynamics for individual quantum systems. *Nat. Commun.* **2014**, *5*, 4185, doi:10.1038/ncomms5185.
19. Gelbwaser-Klimovsky, D.; Alicki, R.; Kurizki, G. Work and energy gain of heat-pumped quantized amplifiers. *Europhys. Lett.* **2013**, *103*, 60005, doi:10.1209/0295-5075/103/60005.
20. Kolář, M.; Gelbwaser-Klimovsky, D.; Alicki, R.; Kurizki, G. Quantum Bath Refrigeration towards Absolute Zero: Challenging the Unattainability Principle. *Phys. Rev. Lett.* **2012**, *109*, 090601.
21. Alicki, R. Quantum Thermodynamics: An Example of Two-Level Quantum Machine. *Open Syst. Inf. Dyn.* **2014**, *21*, 1440002, doi:10.1142/S1230161214400022.
22. Quan, H.; Liu, Y.X.; Sun, C.; Nori, F. Quantum thermodynamic cycles and quantum heat engines. *Phys. Rev. E* **2007**, *76*, 031105.
23. Roßnagel, J.; Abah, O.; Schmidt-Kaler, F.; Singer, K.; Lutz, E. Nanoscale Heat Engine Beyond the Carnot Limit. *Phys. Rev. Lett.* **2014**, *112*, 030602.
24. Binder, F.; Vinjanampathy, S.; Modi, K.; Goold, J. Quantum thermodynamics of general quantum processes. *Phys. Rev. E* **2015**, *91*, 032119.
25. Correa, L.A.; Palao, J.P.; Alonso, D.; Adesso, G. Quantum-enhanced absorption refrigerators. *Sci. Rep.* **2014**, *4*, 3949, doi:10.1038/srep03949.
26. Dorner, R.; Clark, S.; Heaney, L.; Fazio, R.; Goold, J.; Vedral, V. Extracting quantum work statistics and fluctuation theorems by single-qubit interferometry. *Phys. Rev. Lett.* **2013**, *110*, 230601.
27. Correa, L.A.; Palao, J.P.; Adesso, G.; Alonso, D. Performance bound for quantum absorption refrigerators. *Phys. Rev. E* **2013**, *87*, 042131.
28. Dorner, R.; Goold, J.; Cormick, C.; Paternostro, M.; Vedral, V. Emergent thermodynamics in a quenched quantum many-body system. *Phys. Rev. Lett.* **2012**, *109*, 160601.
29. Del Campo, A.; Goold, J.; Paternostro, M. More bang for your buck: Super-adiabatic quantum engines. *Sci. Rep.* **2014**, *4*, 6208, doi:10.1038/srep06208.
30. Malabarba, A.S.; Short, A.J.; Kammerlander, P. Clock-Driven Quantum Thermal Engines. *New J. Phys.* **2015**, *17*, 045027.
31. Gelbwaser-Klimovsky, D.; Niedenzu, W.; Kurizki, G. Chapter Twelve—Thermodynamics of Quantum Systems Under Dynamical Control. In *Advances In Atomic, Molecular, and Optical Physics*; Academic Press: Salt Lake City, UT, USA, 2015; Volume 64, pp. 329–407.
32. Whitney, R.S. Most efficient quantum thermoelectric at finite power output. *Phys. Rev. Lett.* **2014**, *112*, 130601.
33. Allahverdyan, A.E.; Hovhannisyan, K.; Mahler, G. Optimal refrigerator. *Phys. Rev. E* **2010**, *81*, 051129.

34. Mari, A.; Eisert, J. Cooling by Heating: Very Hot Thermal Light Can Significantly Cool Quantum Systems. *Phys. Rev. Lett.* **2012**, *108*, 120602.
35. Bakr, W.S.; Preiss, P.M.; Tai, M.E.; Ma, R.; Simon, J.; Greiner, M. Orbital excitation blockade and algorithmic cooling in quantum gases. *Nature* **2011**, *480*, 500–503.
36. Baugh, J.; Moussa, O.; Ryan, C.A.; Nayak, A.; Laflamme, R. Experimental implementation of heat-bath algorithmic cooling using solid-state nuclear magnetic resonance. *Nature* **2005**, *438*, 470–473.
37. Boykin, P.O.; Mor, T.; Roychowdhury, V.; Vatan, F.; Vrijen, R. Algorithmic cooling and scalable NMR quantum computers. *Proc. Natl. Acad. Sci. USA* **2002**, *99*, 3388–3393.
38. Rempp, F.; Michel, M.; Mahler, G. Cyclic Cooling Algorithm. *Phys. Rev. A* **2007**, *76*, 032325.
39. Segal, D.; Nitzan, A. Molecular heat pump. *Phys. Rev. E* **2006**, *73*, 026109.
40. Schulman, L.J.; Mor, T.; Weinstein, Y. Physical limits of heat-bath algorithmic cooling. *Phys. Rev. Lett.* **2005**, *94*, 120501.
41. Oscar Boykin, P.; Mor, T.; Roychowdhury, V.; Vatan, F.; Vrijen, R. Algorithmic cooling and scalable NMR quantum computer. *Proc. Nat. Acad. Sci.* **2002**, *99*, 3388–3393.
42. Skrzypczyk, P.; Brunner, N.; Linden, N.; Popescu, S. The smallest refrigerators can reach maximal efficiency. *J. Phys. A Math. Theor.* **2011**, *44*, 492002.
43. Brandner, K.; Bauer, M.; Schmid, M.T.; Seifert, U. Coherence-enhanced efficiency of feedback-driven quantum engines. *New J. Phys.* **2015**, *17*, 065006.
44. Bulnes Cuetara, G.; Engels, A.; Esposito, M. Stochastic thermodynamics of rapidly driven quantum systems. *New J. Phys.* **2015**, *17*, 055002.
45. Perarnau-Llobet, M.; Hovhannisyan, K.V.; Huber, M.; Skrzypczyk, P.; Brunner, N.; Acín, A. Extractable Work from Correlations. *Phys. Rev. X* **2015**, *5*, 041011.
46. Roßnagel, J.; Dawkins, S.T.; Tolazzi, K.N.; Abah, O.; Lutz, E.; Schmidt-Kaler, F.; Singer, K. A single-atom heat engine. Available online: http://arxiv.org/abs/1510.03681 (accessed on 23 March 2016).
47. Venturelli, D.; Fazio, R.; Giovannetti, V. Minimal self-contained quantum refrigeration machine based on four quantum dots. *Phys. Rev. Lett.* **2013**, *110*, 256801.
48. Bergenfeldt, C.; Samuelsson, P.; Sothmann, B.; Flindt, C.; Büttiker, M. Hybrid microwave-cavity heat engine. *Phys. Rev. Lett.* **2014**, *112*, 076803.
49. Niskanen, A.; Nakamura, Y.; Pekola, J. Information entropic superconducting microcooler. *Phys. Rev. B* **2007**, *76*, 174523.
50. Brask, J.B.; Haack, G.; Brunner, N.; Huber, M. Autonomous quantum thermal machine for generating steady-state entanglement. *New J. Phys.* **2015**, *17*, 113029.
51. Campisi, M.; Pekola, J.; Fazio, R. Nonequilibrium fluctuations in quantum heat engines: Theory, example, and possible solid state experiments. *New J. Phys.* **2015**, *17*, 035012.
52. Pekola, J.P. Towards quantum thermodynamics in electronic circuits. *Nat. Phys.* **2015**, *11*, 118–123.
53. Fialko, O.; Hallwood, D. Isolated quantum heat engine. *Phys. Rev. Lett.* **2012**, *108*, 085303.
54. Zhang, K.; Bariani, F.; Meystre, P. Quantum optomechanical heat engine. *Phys. Rev. Lett.* **2014**, *112*, 150602.
55. Dechant, A.; Kiesel, N.; Lutz, E. All-Optical Nanomechanical Heat Engine. *Phys. Rev. Lett.* **2015**, *114*, 183602.
56. Thierschmann, H.; Sánchez, R.; Sothmann, B.; Arnold, F.; Heyn, C.; Hansen, W.; Buhmann, H.; Molenkamp, L.W. Three-terminal energy harvester with coupled quantum dots. *Nat. Nanotechnol.* **2015**, *10*, 854–858.
57. Sánchez, R.; Büttiker, M. Optimal energy quanta to current conversion. *Phys. Rev. B* **2011**, *83*, 085428.
58. Roche, B.; Roulleau, P.; Jullien, T.; Jompol, Y.; Farrer, I.; Ritchie, D.; Glattli, D. Harvesting dissipated energy with a mesoscopic ratchet. *Nat. Commun.* **2015**, *6*, 6383, doi:10.1038/ncomms7738.
59. Hartmann, F.; Pfeffer, P.; Höfling, S.; Kamp, M.; Worschech, L. Voltage fluctuation to current converter with coulomb-coupled quantum dots. *Phys. Rev. Lett.* **2015**, *114*, 146805.
60. Sothmann, B.; Sánchez, R.; Jordan, A.N.; Büttiker, M. Rectification of thermal fluctuations in a chaotic cavity heat engine. *Phys. Rev. B* **2012**, *85*, 205301.
61. Sagawa, T. Second law-like inequalities with quantum relative entropy: An introduction. *Lect. Quantum Comput. Thermodyn. Stat. Phys.* **2012**, *8*, 127. Available online: http://arxiv.org/abs/1202.0983 (accessed on 2 April 2016).
62. Kammerlander, P.; Anders, J. Quantum measurement and its role in thermodynamics. Available online: http://arxiv.org/abs/1502.02673 (accessed on 29 March 2016).

63. Jaramillo, J.; Beau, M.; del Campo, A. Quantum Supremacy of Many-Particle Thermal Machines. Available online: http://arxiv.org/abs/1510.04633 (accessed on 3 April 2016).
64. Lostaglio, M.; Jennings, D.; Rudolph, T. Description of quantum coherence in thermodynamic processes requires constraints beyond free energy. *Nat. Commun.* **2015**, *6*, 6383, doi:10.1038/ncomms7383.
65. Ćwikliński, P.; Studziński, M.; Horodecki, M.; Oppenheim, J. Limitations on the Evolution of Quantum Coherences: Towards Fully Quantum Second Laws of Thermodynamics. *Phys. Rev. Lett.* **2015**, *115*, 210403.
66. Korzekwa, K.; Lostaglio, M.; Oppenheim, J.; Jennings, D. The extraction of work from quantum coherence. Available online: http://arxiv.org/abs/1506.07875 (accessed on 22 February 2016).
67. Åberg, J. Catalytic coherence. *Phys. Rev. Lett.* **2014**, *113*, 150402.
68. Levy, A.; Kosloff, R. Quantum absorption refrigerator. *Phys. Rev. Lett.* **2012**, *108*, 070604.
69. Breuer, H.-P.; Petruccione, F. *Open Quantum Systems*; Oxford University Press: New York, NY, USA, 2002.
70. Gallego, R.; Riera, A.; Eisert, J. Thermal machines beyond the weak coupling regime. *New J. Phys.* **2014**, *16*, 125009, doi:10.1088/1367-2630/16/12/125009.
71. Esposito, M.; Ochoa, M.A.; Galperin, M. Quantum Thermodynamics: A Nonequilibrium Green's Function Approach. *Phys. Rev. Lett.* **2015**, *114*, 080602.
72. Gelbwaser-Klimovsky, D.; Aspuru-Guzik, A. Strongly coupled quantum heat machines. *J. Phys. Chem. Lett.* **2015**, *6*, 3477–3482.
73. Uzdin, R.; Kosloff, R. The multilevel four-stroke swap engine and its environment. *New J. Phys.* **2014**, *16*, 095003.
74. Rybár, T.; Filippov, S.N.; Ziman, M.; Bužek, V. Simulation of indivisible qubit channels in collision models. *J. Phys. B At. Mol. Opt. Phys.* **2012**, *45*, 154006.
75. Ziman, M.; Štelmachovič, P.; Bužek, V. Description of quantum dynamics of open systems based on collision-like models. *Open Syst. Inf. Dyn.* **2005**, *12*, 81–91.
76. Gennaro, G.; Benenti, G.; Palma, G.M. Relaxation due to random collisions with a many-qudit environment. *Phys. Rev. A* **2009**, *79*, 022105.
77. Gennaro, G.; Benenti, G.; Palma, G.M. Entanglement dynamics and relaxation in a few-qubit system interacting with random collisions. *Europhys. Lett.* **2008**, *82*, 20006, doi:10.1209/0295-5075/82/20006.
78. Woods, M.P.; Ng, N.; Wehner, S. The maximum efficiency of nano heat engines depends on more than temperature. Available online: http://arxiv.org/abs/1506.02322 (accessed on 1 April 2016).
79. Uzdin, R. Coherence recycling, collective operation, and coherence induced reversibility in quantum heat engines. Available online: http://arxiv.org/abs/1509.06289 (accessed on 1 April 2016).
80. De Raedt, H. Product formula algorithms for solving the time dependent Schrödinger equation. *Comput. Phys. Rep.* **1987**, *7*, 1–72, doi:10.1016/0167-7977(87)90002-5.
81. Feit, M.; Fleck, J.; Steiger, A. Solution of the Schrödinger equation by a spectral method. *J. Comput. Phys.* **1982**, *47*, 412–433.
82. Jahnke, T.; Lubich, C. Error bounds for exponential operator splittings. *BIT Numer. Math.* **2000**, *40*, 735–744.
83. Levy, A.; Alicki, R.; Kosloff, R. Quantum refrigerators and the third law of thermodynamics. *Phys. Rev. E* **2012**, *85*, 061126.
84. Levy, A.; Diósi, L.; Kosloff, R. Quantum Flywheel. Available online: http://arxiv.org/abs/1602.04322 (accessed on 21 March 2016).
85. Blanes, S.; Casas, F. On the necessity of negative coefficients for operator splitting schemes of order higher than two. *Appl. Numer. Math.* **2005**, *54*, 23–37.
86. Yoshida, H. Construction of higher order symplectic integrators. *Phys. Lett. A* **1990**, *150*, 262–268.

Appendix D

Open quantum systems

where Z is the normalization factor (or the partition function from statistical mechanics), $Z = \mathrm{Tr}(\exp(-\beta\hat{H}))$, and $\beta \stackrel{\mathrm{def}}{=} 1/k_B T$ is the inverse temperature. Let the dynamics of the system be generated by the Hamiltonian $\hat{H}$, then we have $[\hat{\rho}_{th}, \hat{U}(t)] = 0$ where $\hat{U}(t) = \exp(-i\hat{H}t)$. The expectation value of two operators acting on the Hilbert space of the system satisfies the relation,

$$\left\langle \hat{A}(t)B \right\rangle = \left\langle B\hat{A}(t+i\beta) \right\rangle \quad \text{with} \quad \hat{A}(t) = \hat{U}^\dagger(t)A\hat{U}(t). \tag{D.2}$$

This relation follows immediately from the cyclic property of the trace and from Eq.(D.1). Applying this relation to the bath correlation functions we obtain,

$$\left\langle \hat{R}^\dagger(t)\hat{R}(0) \right\rangle = \left\langle \hat{R}(0)\hat{R}^\dagger(t+i\beta) \right\rangle. \tag{D.3}$$

The function $F(t) = \left\langle \hat{R}^\dagger(t)\hat{R}(0) \right\rangle$ is of a positive type and according to the Bochner's theorem it follows that its Fourier transform is also positive,

$$\gamma(\omega) = \int_{-\infty}^{\infty} e^{i\omega t} F(t) \geq 0. \tag{D.4}$$

This gives the proof that the rates $\gamma(\omega)$ are non-negative. Furthermore, the Fourier transform of Eq.(D.3) implies the relation,

$$\gamma(-\omega) = e^{-\beta\omega}\gamma(\omega). \tag{D.5}$$

D.2 Liouville space representation

Quantum dynamics is traditionally described in Hilbert space. However, it is convenient, in particular, for open quantum systems, to introduce an extended space where density operators are vectors and time evolution is generated by a Schrödinger-like equation. This space is usually referred to as the Liouville or Hilbert-Schmidt space. Suppose the density operator $\hat{\rho}$ is represented by an $n \times n$ matrix. The set of all $n \times n$ matrices form a linear space of dimension n^2. Under appropriate conditions this linear space can have a Hilbert space construction using the scalar product defined as,

$$(\hat{\rho}_1, \hat{\rho}_2) = \mathrm{Tr}\left\{\hat{\rho}_1^\dagger \hat{\rho}_2\right\}. \tag{D.6}$$

With such a construction we consider $\hat{\rho}$ as an n^2 vector, $|\rho\rangle \in \mathbb{C}^{1\times n^2}$. Similarly, we consider the super-operator $\mathcal{L}$, which is an operator that operates on elements in this linear space, as an $n^2 \times n^2$ matrix, $\hat{L} \in \mathbb{C}^{n^2\times n^2}$. The one to one mapping of two matrix indexes into a single vector index $\{i, j\} \to \alpha$ is arbitrary but has to be used consistently. The equation of motion of the density vector in Liouville space follows from

$$\frac{d}{dt}\hat{\rho}_\alpha = \sum_\beta \hat{\rho}_\beta \frac{\partial}{\partial \hat{\rho}_\beta}\left(\frac{d}{dt}\hat{\rho}_\alpha\right). \tag{D.7}$$

It is now easy to verify that the dynamics in the Liouville space is governed by a Schrödinger-like equation,

$$\frac{d}{dt}|\rho\rangle = -i\hat{L}|\rho\rangle, \tag{D.8}$$

with

$$\hat{L}_{\alpha\beta} = \hat{\rho}_\beta \frac{\partial}{\partial \hat{\rho}_\beta}\left(\frac{d}{dt}\hat{\rho}_\alpha\right). \tag{D.9}$$

A particularly useful index mapping is known as the vec-ing mapping [Roger 1994, Machnes 2014]. Here the $n \times n$ density matrix is flattened into an n^2 vector. The flattening is done by ordering the columns of $\hat{\rho}$ one below the other, so the $\{i, j\}$

entry of the matrix $\hat{\rho}$ is the $(j-1)n+i$ entry of the vector $|\rho\rangle$. The corresponding map for the super operators are the following: For the commutator

$$\left[\hat{H},\hat{\rho}\right] \rightarrow \left(\hat{I}\otimes\hat{H}-\hat{H}^{\mathsf{T}}\otimes\hat{I}\right)|\rho\rangle\,. \tag{D.10}$$

For the dissipative part

$$\hat{V}\hat{\rho}\hat{V}^{\dagger} \rightarrow \left(\left(\hat{A}^{\dagger}\right)^{\mathsf{T}}\otimes\hat{V}\right)|\rho\rangle \tag{D.11}$$

$$\hat{V}^{\dagger}\hat{V}\hat{\rho} \rightarrow \left(\hat{I}\otimes\hat{V}^{\dagger}\hat{V}\right)|\rho\rangle \tag{D.12}$$

$$\hat{\rho}\hat{V}^{\dagger}\hat{V} \rightarrow \left(\left(\hat{V}^{\dagger}\hat{V}\right)^{\mathsf{T}}\otimes\hat{I}\right)|\rho\rangle\,. \tag{D.13}$$

Here T is the transpose operation. Finally we obtain,

$$\hat{L}=\hat{I}\otimes\hat{H}-\hat{H}^{\mathsf{T}}\otimes\hat{I}+\left(\hat{V}^{\dagger}\right)^{\mathsf{T}}\otimes\hat{V}-\frac{1}{2}\left(\hat{I}\otimes\hat{V}^{\dagger}\hat{V}+\left(\hat{V}^{\dagger}\hat{V}\right)^{\mathsf{T}}\otimes\hat{I}\right). \tag{D.14}$$

For more details and additional matrix-vector representations, see [Am-Shallem 2015].

Appendix E

Stochastic differential equations

$[t_0, t]$ to n subintervals such that $t_0 \leq t_1 \leq ..t_{n-1} \leq t$ and $t_{i-1} \leq \tau_i \leq t_i$. The stochastic integral is defined as the limit of partial sums,

$$S_n = \sum_{i=1}^{n} G(\tau_i) \left(W(t_i) - W(t_{i-1})\right). \tag{E.1}$$

Note that S_n depends on the choice of τ_i. For the Itô stochastic integral we chose $\tau_i = t_{i-1}$ (this is no longer the Riemann-Stieltjes integral) and we finally have,

$$\int_{t_0}^{t} G(t')dW(t') = \text{ms} \lim_{n\to\infty} \sum_{i=1}^{n} G(t_{i-1}) \left(W(t_i) - W(t_{i-1})\right). \tag{E.2}$$

Here we defined the mean square limit, $\text{ms} \lim_{n\to\infty} X_n = X$ as the convergence of X_n to X in the mean square, i.e.

$$\lim_{n\to\infty} \int d\omega p(\omega) \left(X_n(\omega) - X(\omega)\right)^2 \equiv \lim_{n\to\infty} \left\langle (X_n - X)^2 \right\rangle = 0. \tag{E.3}$$

Alternative to the Itô integral is the Stratonovich integral. In this case the function $W(t)$ in the integrand is evaluated at the point $\left(W(t_i) + W(t_{i-1})\right)/2$,

$$S \int_{t_0}^{t} W(t')dW(t') \equiv \text{ms} \lim_{n\to\infty} \sum_{i} \frac{W(t_i) + W(t_{i-1})}{2} \Delta W_i = \frac{1}{2} \left(W(t)^2 - W(t_0)^2\right) \tag{E.4}$$

E.2 The Itô stochastic differential equation

The most satisfactory interpretation of the Langevin equation (2.61) is the stochastic integral equation

$$x(t) - x(0) = \int_0^t dt' a\left(x(t'), t'\right) + \int_0^t dW(t') b\left(x(t'), t'\right) \tag{E.5}$$

The Itô integral is mathematically and technically more convenient to use and prove theorems but not always gives the best physical interpretation. The Stratonovich integral is the better candidate for physical interpretation since it assumes that $\xi(t)$ is real noise with a finite correlation time. After calculating measurable quantities this time can be taken as infinitesimally small. Additionally, the Stratonovich integral allows us to use ordinary calculus. A stochastic quantity obeys the Itô SDE,

$$dx(t) = a\left(x(t), t\right) dt + b\left(x(t), t\right) dW(t) \tag{E.6}$$

if for all t and t_0,

$$x(t) = x(0) + \int_0^t dt' a\left(x(t'), t'\right) + \int_0^t dW(t') b\left(x(t'), t'\right). \tag{E.7}$$

The discrete version of the SDE takes the form

$$x_{i+1} = x_i + a(x_i, t_i)\Delta t_i + b(x_i, t_i)\Delta W_i \qquad t_0 < t_1 < ... < t_n = t. \tag{E.8}$$

In order to calculate x_{i+1} we add a deterministic term $a(x_i, t_i)\Delta t_i$ and a stochastic term $b(x_i, t_i)\Delta W_i$ to x_i. Note that ΔW_j is independent of x_i for all $j \geq i$.

The conditions for the existence and uniqueness in time interval $[t_0, T]$ are:

1. Lipschitz condition: $\forall\ x, y$ and $t \in [t_0, T]$ $\exists K$ such that $|a(x,t) - a(y,t)| + |b(x,t) - b(y,t)| \leq K\,|x - y|$

2. Growth condition: $\forall\ t \in [t_0, T]$ $\exists K$ such that $|a(x,t)|^2 + |b(x,t)|^2 \leq K^2\left(1 + |x|^2\right)$

E.3 The Stratonovich stochastic differential equation

The solution of the Itô SDE (E.6) can be represented using the Stratonovich integral,

$$x(t) = x(t_0) + \int_{t_0}^{t} dt' \alpha\left(x(t'), t'\right) + S\int_{t_0}^{t} dW(t')\beta\left(x(t'), t'\right) \tag{E.9}$$

where we have,

$$S\int_{t_0}^{t} dW(t')G\left(x(t'), t'\right) = \text{ms}\lim_{n\to\infty}\sum_i G\left(\frac{x(t_i)+x(t_{i-1})}{2}, t_{i-1}\right)\Delta W_i$$

Next, we show the relation between α, β and a, b. We note that,

$$S\int_{t_0}^{t} dW(t')\beta\left(x(t'), t'\right) \simeq \sum_i \beta\left(\frac{x(t_i)+x(t_{i-1})}{2}, t_{i-1}\right)\Delta W_i.$$

Using the Itô SDE (E.6) and the Itô formula Eq.(2.65), and defining $\beta(t_i) \equiv \beta\left(x(t_i), t_i\right)$ we can write,

$$\begin{aligned}
\beta\left(\frac{x(t_i)+x(t_{i-1})}{2}, t_{i-1}\right) &= \beta\left(x(t_{i-1}) + \frac{1}{2}dx(t_{i-1}), t_{i-1}\right) \\
&= \beta(t_{i-1}) + \frac{1}{2}\left(a(t_{i-1})\partial_x\beta(t_{i-1}) + \frac{1}{2}b(t_{i-1})^2\right)(t_i - t_{i-1}) \\
&+ \frac{1}{2}b(t_{i-1})\partial_x\beta(t_{i-1})\left(W(t_i) - W(t_{i-1})\right).
\end{aligned}$$

Plugging this relation into Eq.(E.9) and keeping terms up to dW^2 we obtain the relation between Itô and Stratonovich integrals (where $x(t)$ is the solution of the Itô

SDE).

$$S\int_{t_0}^{t} dW(t')\beta\left(x(t'),t'\right) = \int_{t_0}^{t} dW(t')\beta\left(x(t'),t'\right) + \frac{1}{2}\int_{t_0}^{t} dt' b\left(x(t'),t'\right)\partial_x\beta(x(t'),t'). \tag{E.10}$$

This relation is not general for an arbitrary function.

If we set $\alpha(x,t) = a(x,t) - \frac{1}{2}b(x,t)\partial_x b(x,t)$ and $\beta(x,t) = b(x,t)$ then,

$$\begin{cases} dx = adt + bdW(t) & \text{Ito SDE} \\ dx = (a - \frac{1}{2}b\partial_x b)dt + bdW(t) & \text{Stratonovich SDE} \end{cases} \tag{E.11}$$

or conversely,

$$\begin{cases} dx = \alpha dt + \beta dW(t) & \text{Stratonovich SDE} \\ dx = (\alpha + \frac{1}{2}\beta\partial_x\beta)dt + \beta dW(t) & \text{Ito SDE} \end{cases} \tag{E.12}$$

Appendix F

Entropy properties

where $0 \leq \lambda \leq 1$ and $x, y \in C$. The function is strictly convex if the equality is only attained for $x = y$ or $\lambda = 0$ or 1. Integrating Eq.(F.1) we obtain for a convex function

$$f\left(\sum_j \lambda_j x_j\right) \leq \sum_j \lambda_j f(x_j), \quad 0 \leq \lambda_j, \quad \sum_j \lambda_j = 1. \tag{F.2}$$

If μ is a probability and f is convex then Jensen's inequality holds

$$\int_C f(x)\mu(dx) \geq f\left(\int_C x\mu(dx)\right). \tag{F.3}$$

If f is twice continuously differentiable in C then convexity is equivalent to $0 \leq \frac{\partial^2 f}{\partial x_i \partial x_j}$. If f is once continuously differentiable then convexity can be expressed as,

$$f(y) \geq f(x) + (y - x)\nabla f(x)$$

thus f remains above every tangent plane. A function f is **concave** if $-f$ is **convex**.

Some Lemmas:

- If f and g are convex and g is non-decreasing, then $h(x) = g(f(x))$ is also

convex.

- If f is concave and g is convex and g is non-increasing, then $h(x) = g(f(x))$ is also convex.

- For a self-adjoint operator $\hat{A}$ acting on Hilbert space $\mathcal{H}$ and for a convex function f we have,

$$f\left(\langle\varphi|\,\hat{A}\,|\varphi\rangle\right) \leq \langle\varphi|\,f(\hat{A})\,|\varphi\rangle\,.$$

- For $\hat{A}$ and $\hat{B}$ Hermitian matrices such that $[a, b]$ contains the eigenvalues of the matrices and for convex $f \in [a, b]$ and $0 \leq \lambda \leq 1$ we have ,

$$Tr\left[f\left(\lambda\hat{A} + (1-\lambda)\hat{B}\right)\right] \leq \lambda Tr\left[f(\hat{A})\right] + (1-\lambda)Tr\left[f(\hat{B})\right].$$

- (Klein) For $\hat{A}$ and $\hat{B}$ Hermitian matrices such that (a, b) contains the eigenvalues of the matrices and for $f \in (a, b)$ which is once continuously differentiable we have,

$$Tr\left[f(\hat{B})\right] \geq Tr\left[f(\hat{A}) + (\hat{B} - \hat{A})f'(\hat{A})\right],$$

If f is strictly convex equality holds if $\hat{A} = \hat{B}$.

Lieb's theorem: For $\hat{A}$ and $\hat{B}$ positive operators, $\hat{X}$ arbitrary fixed operator and $0 \leq \lambda \leq 1$ the functional

$$f_\lambda(\hat{A}, \hat{B}) = -Tr\left[\hat{X}^\dagger \hat{A}^\lambda \hat{X} \hat{B}^{1-\lambda}\right]$$

is jointly convex in its arguments.

Using this theorem one can prove strong subaddivity of the von Neumann entropy. Also by taking $\hat{A} = \hat{B} = \hat{\rho}$ we get the convex functional $f_\lambda(\hat{\rho}) = -Tr\left[\hat{X}^\dagger \hat{\rho}^\lambda \hat{X} \hat{\rho}^{1-\lambda}\right]$. Taking the derivative with respect to λ at $\lambda = 0$ we obtain the convex functional $-Tr\left[\left(\hat{X}\hat{\rho}\hat{X}^\dagger - \hat{X}^\dagger \hat{X}\hat{\rho}\right)\ln\hat{\rho}\right]$.

F.2 The von Neumann entropy

The von Neumann entropy is defined as,

$$S(\hat{\rho}) \stackrel{\text{def}}{=} -Tr\left[-\hat{\rho}\ln\hat{\rho}\right] = -\sum_i p_i \ln p_i \quad p_i \geq 0 \quad \sum_i p_i = 1 \tag{F.4}$$

Properties:

- For any density matrix$\hat{\rho}$ and unitary operator $\hat{U}$ on $\mathbb{C}^d$ we have $S(\hat{\rho}) = S(\hat{U}\hat{\rho}\hat{U}^\dagger)$.

- For any density matrix $\hat{\rho}$ on $\mathbb{C}^d$ we have $0 \leq S(\hat{\rho}) \leq \ln d$.

- $S(\hat{\rho})$ is a concave function on the space of density matrices. Thus any collection of densities $\hat{\rho}_i$and for $0 \leq \lambda_i$, $\sum_i \lambda_i = 1$ we have

$$\sum_i \lambda_i S(\hat{\rho}_i) \leq S\left(\sum_i \lambda_i \hat{\rho}_i\right)$$

  equality holds if and only if all $\hat{\rho}_i$ are equal to each other.

- $S(\hat{\rho}_1 \otimes \hat{\rho}_2) = S(\hat{\rho}_1) + S(\hat{\rho}_2)$.

- $S(\lambda\hat{\rho}_1 \oplus (1-\lambda)\hat{\rho}_2 = \lambda S(\hat{\rho}_1) + (1-\lambda)S(\hat{\rho}_2) + \eta(\lambda) + \eta(1-\lambda)$.

- Subadditivity - $S(\hat{\rho}_{12}) \leq S(\hat{\rho}_1) + S(\hat{\rho}_2)$.

- Strong subadditivity - $S(\hat{\rho}_{123}) + S(\hat{\rho}_2) \leq S(\hat{\rho}_{12}) + S(\hat{\rho}_{23})$.

- Triangle inequality - $|S(\hat{\rho}_1) - S(\hat{\rho}_2)| \leq S(\hat{\rho}_{12})$.

- Bistochastic completely positive maps Λ are entropy increasing $S(\Lambda\sigma) \geq S(\sigma)$. A completely positive unital preserving transformation (meaning the adjoint map preserves the unity) is bistochastic if it preserves the trace.

F.3 Relative entropy

The relative entropy is defined as,

$$S(\hat{\rho}|\hat{\sigma}) \stackrel{\text{def}}{=} Tr\left[\hat{\rho}\ln\hat{\rho}\right] - Tr\left[\hat{\rho}\ln\hat{\sigma}\right] \tag{F.5}$$

For the canonical Gibbs state $\sigma = \exp(-\beta\hat{H})/Z$ we have,

$$S(\hat{\rho}|\hat{\sigma}) = Tr\left[\hat{\rho}\beta\hat{H}\right] - S(\hat{\rho}) + \ln z = \beta F(\hat{\rho}) - \beta F(\hat{\sigma}) \tag{F.6}$$

here $F(\hat{\rho})$ is the nonequilibrium free energy $F(\hat{\rho}) \stackrel{\text{def}}{=} Tr\left[\hat{\rho}\beta H\right] - \frac{S(\hat{\rho})}{\beta}$.

The entropy of a combined system with respect to its corresponding uncorrelated state is given by,

$$S(\hat{\rho}|\hat{\rho}_1 \otimes \hat{\rho}_2) = S(\hat{\rho}_1) + S(\hat{\rho}_2) - S(\hat{\rho}) \tag{F.7}$$

Properties:

- Positivity- $S(\hat{\rho}|\sigma) \geq 0$ equality holds only for $\hat{\rho} = \sigma$.
- Invariant under unitary transformation.
- Additivity- $S(\hat{\rho}_1 \otimes \hat{\rho}_2|\sigma_1 \otimes \hat{\sigma}_2) = S(\hat{\rho}_1|\hat{\sigma}_1) + S(\hat{\rho}_2|\hat{\sigma}_2)$.
- Jointly convexity- $S(\lambda\hat{\rho}_1 + (1-\lambda)\hat{\rho}_2|\lambda\hat{\sigma}_1 + (1-\lambda)\hat{\sigma}_2) = \lambda S(\hat{\rho}_1|\sigma_1) + (1-\lambda)S(\hat{\rho}_2|\hat{\sigma}_2)$.
- Lower bound- $S(\hat{\rho}|\hat{\sigma}) \geq \frac{1}{2}\|\hat{\rho} - \hat{\sigma}\|_1^2$.
- Decreasing under partial trace- $S(\hat{\rho}_1|\hat{\sigma}_1) \leq S(\hat{\rho}|\hat{\sigma})$.
- Under the CPTP map $S(\Lambda(t)\hat{\rho}|\hat{\rho}_o) \leq S(\hat{\rho}|\hat{\rho}_o)$, where $\hat{\rho}_o$ is a stationary state.
- For the dynamical semigroup $\Lambda(t) = \exp(\mathcal{L}t)$, the entropy production is non-negative, $-\frac{d}{dt}S(\Lambda(t)\hat{\rho}|\hat{\rho}_o) \geq 0$, where $\hat{\rho}_o$ is a stationary state.

Appendix G

List of publications

- Amikam Levy, Robert Alicki and Ronnie Kosloff. *Quantum refrigerators and the third law of thermodynamics.* **Phys. Rev. E**, vol. 85, page 061126, 2012.
- Amikam Levy, Robert Alicki and Ronnie Kosloff. *Comment on "Cooling by Heating: Refrigeration Powered by Photons".* **Phys. Rev. Lett.**, vol. 109, page 248901, 2012.
- Amikam Levy and Ronnie Kosloff. T*he local approach to quantum transport may violate the second law of thermodynamics.* **EPL (Europhysics Letters)**, vol. 107, no. 2, page 20004, 2014.
- Kosloff, R. and Levy, A. *Quantum Heat Engines and Refrigerators: Continuous Devices.* **Annual Review of Physical Chemistry**, vol. 65, pages 365–393, 2014.
- Raam Uzdin, Amikam Levy and Ronnie Kosloff. *Equivalence of Quantum Heat Machines, and Quantum-Thermodynamic Signatures.* **Phys. Rev. X**, vol. 5, page 031044, 2015.
- Raam Uzdin, Amikam Levy and Ronnie Kosloff. *Quantum heat machines equivalence, work extraction beyond markovianity, and strong coupling via heat exchangers.* **Entropy**, vol. 18, no. 4, page 124, 2016.
- Amikam Levy, Lajos Diósi and Ronnie Kosloff. *Quantum flywheel.* **Phys. Rev. A**, vol. 93, no. 5, page 052119, 2016.

ורעש פאסוני ואף מקשרים תוצאות אלו למדידה קוונטית חלשה ולהשפעתו של אמבט בטמפרטורה גבוהה כגורם המניע תהליך קירור.

בכדי לווסת התקנים קוונטים תרמים אנו מציגים לראשונה שימוש במדידה קוונטית חלשה ובקרה באמצעות משוב. באופן זה אנו משפרים את יעילות הטעינה של התקן אחסון האנרגיה הקוונטי באופן ניכר ומייצבים את הפלקטואציות ההרסניות במערכת. אנו מראים כי יחס בין אינפורמציה המתקבלת ממדידת המערכת לאינפורמציה המוזנת חזרה למערכת באמצעות המשוב ממקסמת את יעילות הטעינה. דינמיקה זו מתוארת באמצעות משוואות מסטר סטוכסטיות.

בנוסף אנו מציגים את התפקיד של קוהרנטיות בתרמודינמיקה של התקנים קוונטים. בתחום של פעולה חלשה של ההתקנים, המצאות קוהרנטיות במערכת מגדילה באופן משמעותי את כמות העבודה שניתן לחלץ מההתקן. בנוסף, בתחום פעולה זה, מנועים קוונטים שונים מציגים מדדים תרמודינמיים זהים. על ידי גילוי של חסמים על פעולת מנוע סטוכסטי קלאסי אנו מציגים חתימות תרמו-קוונטיות אשר מעידות על שימוש במשאבים קוונטים בתהליכים תרמודינמיים.

תקציר

עבודת מחקר זו מתמקדת בהבטיים תרמודינמים של התקנים קוונטים במטרה ללמוד את הקשר בין תרמודינמיקה ומכניקת הקוונטים. תרמודינמיקה היא אחת מאבני היסוד של הפיסיקה בימינו. התאוריה עוסקת בתהליכים אנרגטיים ואנטרופיים במערכות מקרוסקופיות תחת אילוצים. באמצעות מספר פרמטרים מצומצם ניתן לאפיין תרמודינמית מערכות בשיווי משקל. מכניקת הקוונטיסת לעומת זאת, עוסקת בדינמיקה ובתכונות של מערכות מיקרוסקופיות. בהתבסס על הנחות ספורות התאוריה חוזה את הדינמיקה המלאה של מערכות פיסיקליות, גם מחוץ לשיווי משקל. תרמודינמיקה קוונטית הינו תחום מחקר המבקש לחשוף את הקשר האינטימי בין שתי התאוריות.

הגישה של עבודת מחקר זו היא ניתוח פעולתם של התקנים קוונטים תרמים, באופן זה ניתן ללמוד על הקשר בין תרמודינמיקה ומכניקת הקוונטים. דוגמאות להתקנים אלו הם: מנועים קוונטים, מקררים קוונטים והתקנים קוונטים לאחסון אנרגיה. התקנים אלו מתארים מערכות קוונטיות מחוץ לשיווי משקל תרמודינמי שמתקבלות באמצעות צימוד המערכת למספר אמבטים פסיביים או אקטיביים במקביל. כלים מהתאוריות של מערכות קוונטיות פתוחות, מדידה קוונטית ובקרה באמצעות משוב משמשים לניתוח המודלים. התמקדות בגדלים כגון יעילות ההתקן, זרימת אנרגיה והקשר שלהם לתופעות קוונטיות כגון קורלציות קוונטיות וקוהרנטיות חושף היבטים יסודיים וטכנולוגים של התאוריות.

ההיבט המהותי של המחקר מתייחס לאופן בו חוקי התרמודינמיקה מתגלמים בתחום הקוונטי וביצירת שפה משותפת לתיאור תרמודינמי-קוונטי של המערכות. בפרט, אנו מציגים תיאור של הולכת אנרגיה בין שני אמבטי חום דרך מערכות קוונטיות. עבודה זו מעידה על טעות נפוצה בספרות המדעית שנעשית בתיאור מערכות שכאלה באמצעות משוואות מסטר. אנו מוכיחים כי הפורמליזם שאנו מציגים עולה בקנה אחד עם החוק השני של התרמודינמיקה, ויתרה מכן מבטא את האופי הגלובלי של מכניקת הקוונטים. כמו כן אנו מציעים הגדרות לגדלים תרמודינמיים כגון חום ועבודה עבור מערכות קוונטיות מורכבות ומוכיחים עקביות עם חוקי התרמודינמיקה. מערכות אלו מצמודות באופן חזק לשדה מחזורי חיצוני ובו זמנית למספר אמבטים בטמפרטורות שונות.

אנו מציעים ניסוח דינאמי של החוק השלישי של התרמודינמיקה שמאפשר לכמת את מהירות הקירור האופטימלית כאשר שואפים לטמפרטורת האפס המוחלט. אנו מראים כי ניסוח זה עליון לניסוחים אחרים של החוק, באופן זה אנחנו מציעים פתרון לסוגיה ארוכת שנים בנושא. בהקשר זה אנו גם מציגים התנהגות אוניברסלית של מקררים קוונטים כאשר הטמפרטורה שואפת לאפס המוחלט.

היבט נוסף של עבודת מחקר זו הוא לגלות משאבים ופרוטוקולים חדשים להניע תהליכים תרמודינמיים במשטר הקוונטי. אנו מציגים רעיון חדשני של מקרר קוונטי סופג אשר מנצל מקור רעש או מקור חום כדי להניע תהליך קירור. מקרר זה פעול באופן אוטונומי ואינו דורש בקרה חיצונית אקטיבית. בפרט, אנו בחנים את השפעתם של רעש גאוסי

עבודה זו נעשתה בהדרכתו של

פרופסור רוני קוזלוב

תֶּרְמוֹדִינָמִיקָה שֶׁל הֶתְקֵנִים קְוַנְטִים

חיבור לשם קבלת תואר דוקטור לפילוסופיה

מאת

עמיקם לוי

הוגש לסנט האוניברסיטה העברית בירושלים

חשוון ה'תשע"ז

נובמבר 2016